

Synthesis of Biologically Active Iminosugars and Strategies Towards the Preparation of Chiral Quinoline Derivatives

by

Marianne Bore Haarr

Thesis submitted in fulfilment of
the requirements for the degree of
PHILOSOPHIAE DOCTOR
(PhD)



Faculty of Science and Technology
Department of Chemistry, Biosciences, and Environmental Engineering
2021

University of Stavanger
NO-4036 Stavanger
NORWAY
www.uis.no

©2021 Marianne Bore Haarr

ISBN:978-82-8439-043-7

ISSN:1890-1387

PhD: Thesis UiS No. 614

Acknowledgements

I would like to express my very great appreciation to my supervisor, Prof. Magne Olav Sydnes for his valuable guidance and encouragement during this research work. My grateful thanks are also extended to Dr. Emil Lindbäck, whose expertise in iminosugar chemistry has been invaluable to the project. I would like to thank Dr. Kåre Jørgensen for operating and maintaining the NMR instrument, and for offering me a fume hood in his lab during the COVID distance regulations.

I wish to give a special thanks to all our technical staff, including Hans Kristian Brekken, Erling Berge Monsen, Liv Margareth Aksland, Lyudmyla Nilsen, Xiaoping Zhang, and Hong Lin, for all the help with technical issues, ordering of chemicals, and maintenance of lab facilities. I also wish to thank collaborators Dr. Óscar L. Lopéz at the Universidad de Sevilla, Spain, for performing the glycosidase inhibition assays and Dr. Bjarte Holmelid at the University of Bergen for providing the HRMS analysis.

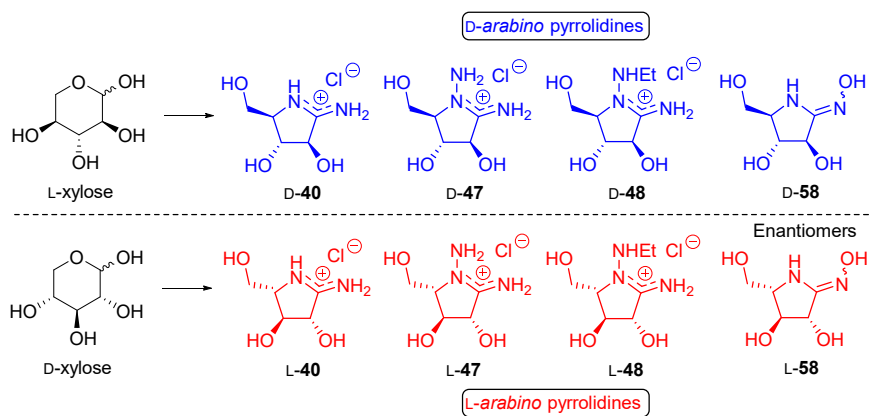
I am very grateful to the Vincent group at the University of Oxford, for having me as a visiting student. I wish to give a special thanks to Prof. Kylie Vincent, Dr. Holly Reeve, Dr. Sarah Cleary, and Dr. Jack Rowbotham for an inspiring trip to enzyme-land. Along this line, I gratefully acknowledge the support and training provided by BioCat, the Norwegian national graduate school in Biocatalysis.

A special thanks goes to my lab colleagues over the years: Dr. Utsav R. Dotel, Dr. Susana E. Duran, and PhD students Vebjørn Eikemo, Katja Håheim, I. Caroline Vaaland, Tereza C. Evangelista, Sindhu Kancherla, Hiwot Tiruye, and Ida T. Helgeland, for years of interesting conversations. I also wish to thank my colleagues at the department, especially the members of the Unofficial Coffee Group, for valuable scientific and non-scientific input.

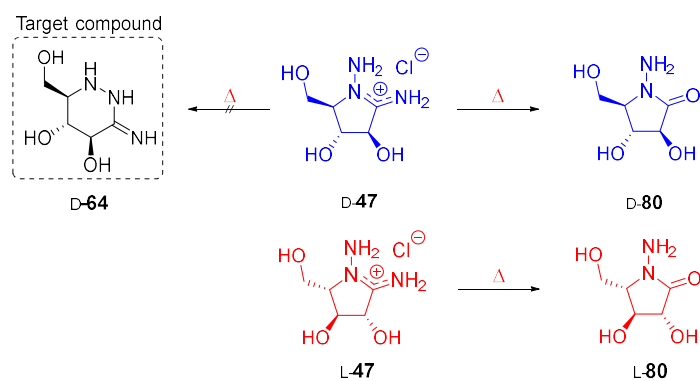
Finally, I wish to thank my family, including my three kids Samuel, Anne and John, my parents Anne Beth and John Martin, my brothers and extended family, and my family-in-law for having my back and cheering me on. A special thanks goes to my husband, Per Arne, for always helping me find the door.

Graphical Abstract

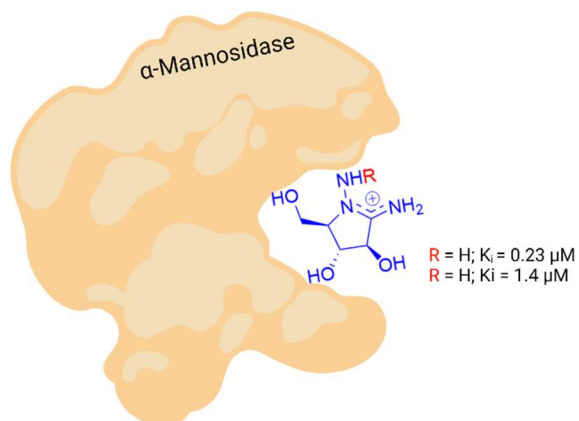
Chapter 3. Synthesis of the Functionalized *Arabino*-Amidines



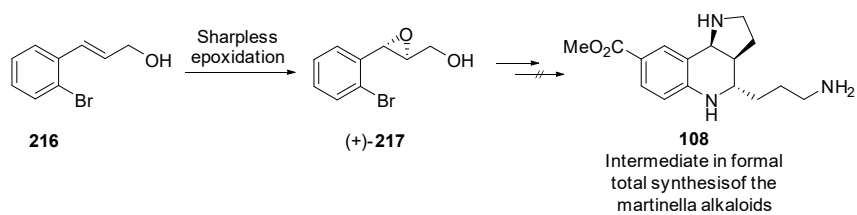
Chapter 4. Towards the *Glucono*-Hydrazide Imide



Chapter 5. Biological Evaluation of the Pyrrolidine Iminosugars



Chapter 6. Towards the Martinella Alkaloids



Abstract

Design and preparation of novel bioactive compounds for development of new drug leads is a challenging task. Chirality plays a key role in all biological systems, including drug targets, and stereoisomeric compounds often have very different pharmacological properties. Chirality is thus an important factor when designing and preparing novel bioactive molecules.

The intention of the first project was to create a library of novel iminosugar antipodes from optically active hexoses for the purpose of glycosidase inhibition testing. The aim of the second project was to synthesize the biologically active martinella alkaloids from prochiral building blocks by installing the stereochemistry with a chiral catalyst, and subsequently create analogues of the alkaloids by altering the side chains connected to the martinella tricyclic scaffold.

In the preparation towards the martinella alkaloids, the governing stereocenter was installed by asymmetric Sharpless epoxidation of a cinnamyl alcohol. The resulting epoxide was successfully obtained in 76% *ee*. However, upon an ineffective reaction step and numerous efforts to circumvent the problem, the progress towards the martinella alkaloids came to a full stop.

The library of novel iminosugars, namely the functionalized D- and L-*arabino*-pyrrolidines, were prepared and evaluated as glycosidase inhibitors. The D-*arabino*-hydrazide imide and its *N*-ethyl congener displayed selective α -mannosidase inhibition in the micromolar range, with inhibition constants $K_i = 0.23 \mu\text{M}$ and $K_i = 1.4 \mu\text{M}$, respectively. Selective α -mannosidase inhibitors are interesting lead molecules for development of therapeutic compounds, such as anticancer and antiviral agents.

Table of Contents

Acknowledgements.....	iii
Graphical Abstract.....	v
Abstract.....	vii
Abbreviations.....	x
Science Communication	xiv
1 Introduction.....	1
2 Glycosidase Inhibitors -A General Introduction	5
2.1 Glycosidases as Targets for Drug Design	8
2.2 Iminosugars.....	11
2.2.1 The Origin of Iminosugars	11
2.2.2 Properties of Iminosugars as Glycosidase Inhibitors.....	14
3 Synthesis of the Functionalized <i>Arabino</i> -Amidines	23
3.1 Results and Discussion.....	24
3.1.1 Preparation of D/L-Xylono-Nitriles	25
3.1.2 Synthesis of D/L-Arabino-Amidines.....	29
3.1.3 Synthesis of D/L-Arabino-Hydrazide Imides	31
3.1.4 Synthesis of D/L-Arabino-Amide Oximes	37
3.2 Conclusion	44
4 Towards the <i>Glucono</i> -Hydrazide Imide.....	46
4.1 Results and Discussion.....	47
4.1.1 Strategy with an N-Protecting Group	47
4.1.2 Attempted Formation of a Thermodynamic Product.....	51
4.1.3 Strategy via Nitrile Activation.....	55
4.1.4 Strategy via the Hydrazide Amide.....	63
4.2 Conclusion	66
5 Biological Evaluation of the Pyrrolidine Iminosugars	68
6 Towards the Martinella Alkaloids.....	71
6.1 Previous Synthetic Preparations of the Martinella Alkaloids.....	72
6.1.1 Guanidinylation of Ma's Intermediate (108).....	73
6.1.2 Assembly of the Tricyclic Core Structure	77

6.1.3	Objectives.....	93
6.2	Results and Discussion.....	95
6.2.1	Initial Retrosynthetic Plan	95
6.2.2	Attempted Synthesis from 2-Nitrocinnamic Ester.....	98
6.2.3	Revised Retrosynthetic Strategy.....	101
6.2.4	Attempted Synthesis from 2-Bromo Cinnamic acid.....	102
6.2.5	Conclusion	110
7	Experimental Methods	113
7.1	General Methods.....	113
7.2	Synthesis of the Arabino-Amidines	114
7.3	Synthesis Towards the Glucono-Hydrazide Imide.....	147
7.4	Synthesis Towards the Martinella Alkaloids	164
	References.....	187
	Paper I.....	206
	Paper II.....	207
	Paper III	208

Abbreviations

(DHQ) ₂ PHAL	Hydroquinine 1,4-phthalazinediyl diether
(S)-(+)-MTPA-Cl	(S)-(+)- α -Methoxy- α -(trifluoromethyl)phenylacetyl chloride
Ac	Acetyl
Ac ₂ O	Acetic anhydride
AcOH	Acetic acid
ATR	Attenuated total reflection
Bn	Benzyl
Boc	<i>tert</i> -Butyloxycarbonyl
Bz	Benzoyl
CAZymes	Carbohydrate-Active enzymes
COSY	Correlated Spectroscopy
COVID	Corona Virus Disease
DAB	1,4-dideoxy-1,4-imino-D-arabinitol
DCE	Dichloroethane
DCM	Dichloromethane
DGJ	1-deoxygalactonojirimycin
DIBAL	Diisobutylaluminium hydride
DMAP	4-Dimethylaminopyridine

DMF	<i>N,N</i> -dimethylformamide
DMJ	1-deoxymannojirimycin
DMP	Dess Martin Periodinane
DMPD	2,5-dideoxy-2,5-imino-D-mannitol
DMSO	Dimethyl sulfoxide
DNJ	1-deoxynojirimycin
EC	Enzyme Commission
ER	Endoplasmic Reticulum
ERAD	Endoplasmic Reticulum Associated Degradation
ERT	Enzyme Replacement Therapy
ESI	Electrospray ionization
Et	Ethyl
Et ₂ O	Diethylether
EtOAc	Ethyl acetate
EtOH	Ethanol
FDA	United States Federal Drug Administration
GH	Glycoside Hydrolase
h	hours
HMBC	Heteronuclear Multiple Bond Correlation
HRMS	High Resolution Mass Spectrometry

HSQC	Heteronuclear Single Quantum Coherence
Hz	Hertz
<i>i</i> -Pr	<i>iso</i> -Propyl
IR	Infrared
IUBMB	International Union of Biochemistry and Molecular Biology
IUPAC	International Union of Pure and Applied Chemistry
LAB	1,4-dideoxy-1,4-imino-L-arabinitol
LRMS	Low Resolution Mass Spectrometry
LSD	Lysosomal Storage Disorder
<i>m/z</i>	mass-to-charge ratio
Me	Methyl
MeCN	Acetonitrile
MeOH	Methanol
min	minutes
mp	melting point
MS	Molecular Sieves
Ms	Methane sulfonyl (Mesyl)
MW	Microwave
NJ	Nojirimycin

NMO	<i>N</i> -methylmorpholine- <i>N</i> -oxide
NMR	Nuclear Magnetic Resonance
NOESY	Nuclear Overhauser Effect Spectroscopy
PC	Pharmacological Chaperone
PCT	Pharmacological Chaperone Therapy
Pet. ether	Petroleum ether
<i>p</i> -TsOH	<i>para</i> -Toluenesulfonic acid
RCM	Ring Closing Metathesis
rt	room temperature
SRT	Substrate Replacement Therapy
TBDMS	<i>Tert</i> -Butyl Dimethyl Silyl
TBDPS	<i>Tert</i> -Butyl Diphenyl Silyl
<i>t</i> -BuOH	<i>tert</i> -Butanol
TFA	Trifluoroacetic acid
THF	Tetrahydrofuran
TLC	Thin Layer Chromatography

Science Communication

Publications

1. Haarr, M. B., & Sydnes, M. O. Synthesis of the Hexahydropyrrolo-[3,2-*c*]-quinoline Core Structure and Strategies for Further Elaboration to Martinelline, Martinellic Acid, Incargranine B, and Seneciobipyrrolidine. *Molecules*, **2021**, *26*, 341.
2. Haarr, M. B., López, O., Pejov, L., Fernández-Bolaños, J. G., Lindbäck, E., & Sydnes, M. O. 1, 4-Dideoxy-1, 4-imino-D-arabinitol (DAB) Analogues Possessing a Hydrazone Imide Moiety as Potent and Selective α -Mannosidase Inhibitors. *ACS omega*, **2020**, *5*, 18507-18514.

Presentations

1. Haarr, M. B. Preparation of Chiral Drugs using Redox Enzymes, BioCat Kickoff Event, 2021. **Scientific presentation.**

Awarded “Most Visually Appealing Presentation”

2. Haarr, M.B., Nilsen, M. M. Forsker på utvikling av mer treffsikre medisiner / Researching How to Make More Accurate Drugs. Labsnakk / Lab talk, 2021. **Podcast episode (Norwegian)**

3. Haarr, M. B. Hvordan få mer treffsikre medisiner / How to Make More Accurate Drugs. Forsker Grand Prix / Researcher Grand Prix, 2020. **Popular science presentation (Norwegian)**

Awarded 2nd place in the regional final, and advancement to the national final

-
4. Haarr, M. B., Lindbäck, E., Lopez, O., Tobiesen, Å., Fernández-Bolaños, J. G., Sydnes, M.O. Sugar Analogues as Glycosidase Inhibitors. BioCat conference, Hurdal, 2018. **Poster.**
5. Haarr, M. B., Lindbäck, E., Lopez, O., Tobiesen, Å., Fernández-Bolaños, J. G., Sydnes, M.O. Glycosidase Inhibitors –Sugar Analogues Containing a Hydrazide Imide Moiety. Leiv K. Sydnes symposium on Organic Chemistry, Bergen, 2018. **Poster.**
6. Haarr, M. B., Lindbäck, E., Lopez, O., Tobiesen, Å., Fernández-Bolaños, J. G., Sydnes, M.O. A New Family of Glycosidase Inhibitors – Sugar Analogues Containing a Hydrazide Imide Moiety. 33rd Organic Chemistry Winter Meeting, Skeikampen, 2018. **Scientific presentation and poster.**
7. Haarr, M. B. Årets Nobelpris i Kjemi -Kryoelektronmikroskopi / This Year's Nobel Prize in Chemistry –Cryoelectronmicroscopy. Annual meeting in Norwegian Chemical Society, division of Chemistry Education, 2017. **Scientific presentation.**
8. Haarr, M. B. Oppskriften på antibiotika / The Recipe for Antibiotics. Forsker stand-up / Researcher Stand-Up, 2017. **Popular science presentation.**
9. Haarr, M. B., Lindbäck, E., Sydnes, M. O. Synthetic Approach Towards the Martinella Alkaloids. 32nd Organic Chemistry Winter Meeting, Skeikampen, 2017. **Poster.**

1 Introduction

This thesis includes the descriptions of two main projects. Chapters 3 and 4 cover the synthetic preparation of biologically active iminosugars. The biological evaluation of the synthesized iminosugars as glycosidase inhibitors is then presented in chapter 5. The second project includes synthetic strategies towards preparation of the biologically active martinella alkaloids, presented in chapter 6. A common feature for both projects has been the aspect of how chirality affects a compound's biological properties. The aim of this chapter is therefore to provide a general introduction to the concept of chirality in biologically active molecules.

Chirality plays a key role in all biological systems.^{1,2} All natural proteins and carbohydrates are chiral compounds, that is, compounds that are non-identical to their mirror image. Figure 1 illustrates the concept of chirality by displaying chiral and achiral objects, such as hands and coffee cups and molecules, such as ibuprofen (**1**) and paracetamol (**2**). Because biological systems are composed of chiral compounds, including chiral drug receptors, the activity of biologically active compounds is mostly chirality dependent (Figure 2).^{3,4} This implies that two stereoisomers (e.g. enantiomers) of the same compound can have substantially different pharmacological profiles. One example of this is ibuprofen (**1**), a well-known anti-inflammatory drug, in which the *S* enantiomer is over 100-fold more potent inhibitor of cyclooxygenase 1 (COX 1) than the *R* enantiomer (Figure 1).⁵ Before 1994 ibuprofen (**1**) was distributed as a racemic mixture. In 1992 the United States Food and Drug Administration (FDA) issued a policy statement concerning stereoisomeric drugs, in which chirality was officially included in the pharmacological profile of a drug.^{6,7} Consequently, racemate drugs were considered to be mixtures of two compounds. The production of several racemate drugs, including ibuprofen (**1**), was thus switched to the preparation of the single-enantiomer.^{8,9}

Introduction

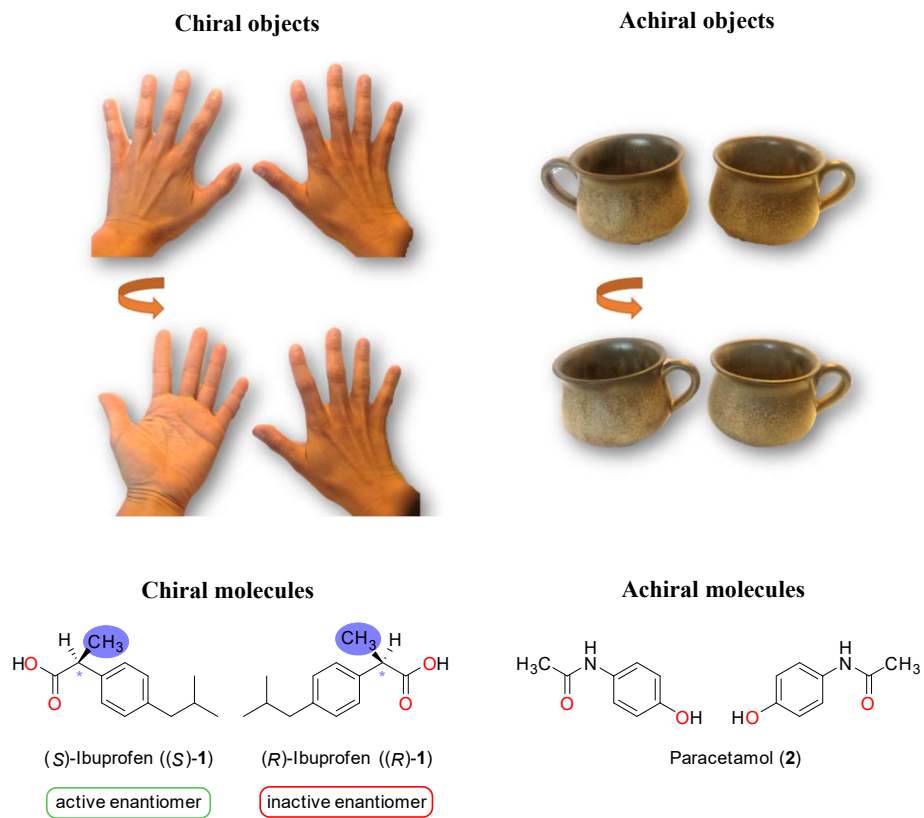


Figure 1. Concept of chirality.

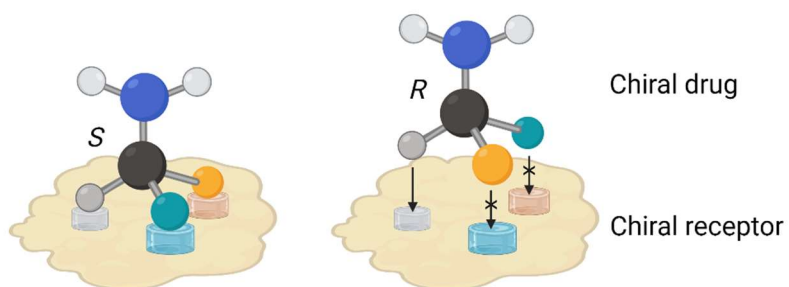


Figure 2. Chiral biological receptors interact with chiral compounds. (Created with BioRender.com)

Today, production of single-enantiomer versions is the standard in the pharmaceutical industry.¹⁰ Synthetic preparation of single enantiomers generally fall into one of three categories:¹¹ 1) Chiral pool, in which the chiral product is synthesized from optically active building blocks, 2) Chiral resolution, in which the desired enantiomer is isolated from the racemic mixture by co-crystallization with a chiral resolving agent, such as D- or L-tartaric acid, or 3) Stereoselective synthesis, in which the chiral product is obtained from a non-chiral/prochiral substrate by treatment with an enantiopure reagent in either stoichiometric (auxiliary) or catalytic amount. In the projects described in this thesis we have synthesized chiral iminosugars from chiral building blocks (chapters 3 and 4) and prepared a chiral epoxide from a prochiral alkene by asymmetric synthesis with a chiral catalyst (chapter 6).

The specific spatial arrangement of the groups connected to a compound's chiral centre is referred to as a compound's absolute configuration. Following the International Union of Pure and Applied Chemistry (IUPAC) nomenclature, the resulting stereochemical description is then specified using the Cahn-Ingold-Prelog (CIP) rules, in which stereocenters with opposite chirality are labelled *R* and *S*, respectively (Figure 3).^{1,12} According to the CIP rules, the four different groups attached to a chiral (carbon) centre are assigned priority, based on atomic number. When the lowest priority group is faced away from the viewer, the orientation of the residual groups determines the stereochemical description. If the priority ascends clockwise (to the right), the centre is annotated *R*. Equivalently, a centre with counter-clockwise (to the left) priority is labelled *S*.

The description of molecules with several chiral centres are often named by the direction in which the molecule rotates the plane of light, *viz.* optical rotation, annotated (+) or (-) for rotation to the right and left, respectively (Figure 3).¹³ For identification of monosaccharides and amino acids, the Fischer-Rosanoff convention from 1906 is frequently used, with descriptors D and L.^{13,14} In a Fischer-projection of the

molecule, with atom number one (C1, carbonyl) place at the top of the chain, the chiral atom furthest away from C1 determines the overall stereochemical description. For glucose (**3**), a hydroxyl group on the right-hand side at C5, gives D-glucose (D-**3**). In L-glucose (L-**3**) the C5 hydroxyl group is positioned on the left-hand side in the Fischer projection. The example illustrated in figure 3, shows that (+)-glucose ((+)-**3**) can also be termed D-glucose (D-**3**). In fact, the compound is most often referred to as D-(+)-glucose (D-(+)-**3**).

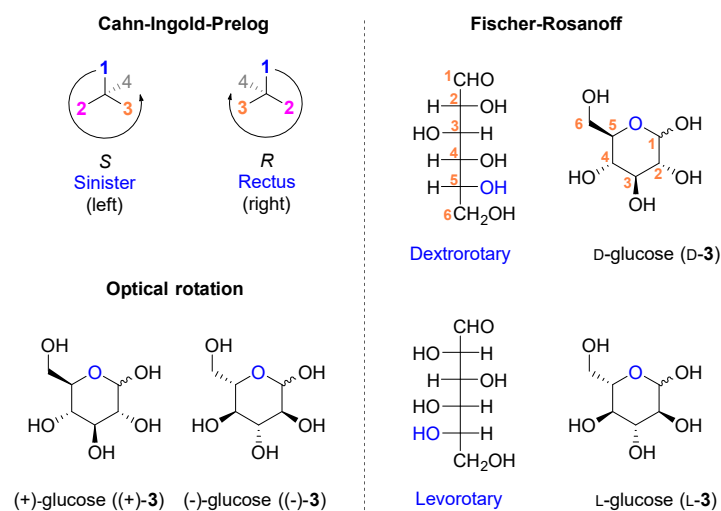


Figure 3. Stereochemical description following the Cahn-Ingold-Prelog rules apply for all organic compounds. Molecules with several stereocenters are often annotated by the molecule's optical rotation. The Fischer-Rosanoff nomenclature is specifically used for identifying monosaccharides and amino acids.

In chapters 3, 4 and 5 the D and L descriptors are used for most compounds, and opposite chirality is verified by the $[\alpha]_D$ optical rotation values. The chiral molecules in chapter 6 are described by their specific optical rotation (+/-).

2 Glycosidase Inhibitors -A General Introduction

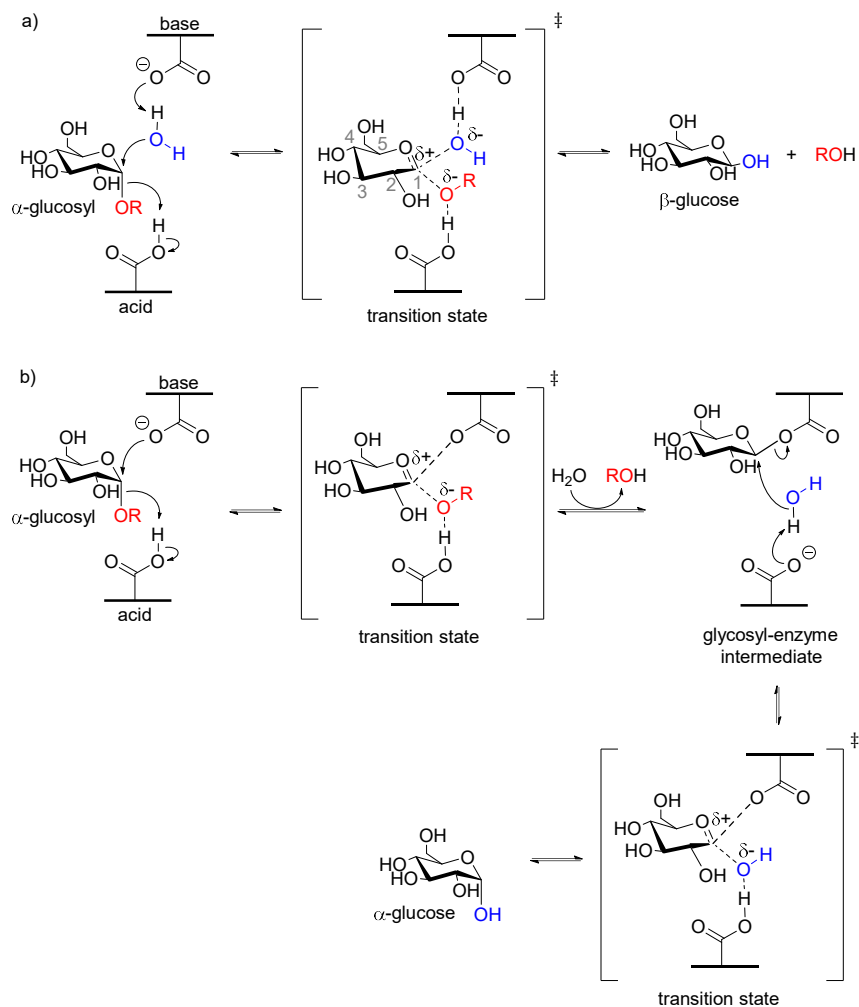
The group of enzymes that display activity towards glycosidic bonds are known as carbohydrate-active enzymes (CAZymes). These biomolecules catalyse the transfer of a glycosyl group to an acceptor substrate. According to the Enzyme Commission (EC) of the International Union of Biochemistry and Molecular Biology (IUBMB), CAZymes that use water as acceptor substrate are classified as glycoside hydrolases (GH) (EC 3.2),¹⁵ also known as glycosidases. In 1991 Henrissat and co-workers established a classification system of CAZymes, where the enzymes are grouped into families based on amino acid sequence similarity.¹⁶ The IUBMB nomenclature of glycosidases are, however, still linked to substrate specificity and enzymes with equal specificity but dissimilar structural features are found in different GH families in the CAZy classification system (<http://www.cazy.org/>).

A common feature for the majority of glycosidases are the two carboxylic amino acids (aspartate or glutamate) in the active site of the enzyme.^{17,18} These acid/base catalytic residues play a central role in the two main glycosidase hydrolysis mechanisms, in which the substrate is hydrolysed with either inversion or retention of the anomeric configuration. Scheme 1 illustrates both mechanisms of hydrolysis for α -glucosidases. Inverting glycosidases catalyze the direct attack of water on the anomeric carbon (C1) (Scheme 1a). The water is activated by the carboxylate residue that accepts a proton from the water molecule. The hydrolysis is promoted by a second carboxylic acid residue which donates a proton to the leaving group. In contrast to the single displacement mechanism of the inverting glycosidases, retaining glycosidases follow a double displacement mechanism which includes two inversions of the anomeric configuration and a covalent glycosyl-enzyme intermediate (Scheme 1b).^{19,20} Common for both mechanisms is

the shape and charge distribution of the glycoside in the transition state(s).

Mimicry of the glycoside shape and charge in the transition state has been an important lead in the design of glycosidase inhibitors.²¹ In the transition state the anomeric carbon holds a positive charge which is stabilized by the endocyclic oxygen. This oxocarbenium character allows for a coplanar arrangement across the C5-O5-C1-C2 atoms (Scheme 1a).²² From this planarity, the glycoside may adopt a limited number of conformations in its transition state, roughly grouped into half-chair conformations (³H₄ or ⁴H₃ or the closely related envelopes ⁴E or ³E) and boat conformations (^{2,5}B or B_{2,5}).²² The design and synthesis of oxocarbenium charge analogues and/or conformational analogues of the transition state glycosides has resulted in a number of potent and specific glycosidase inhibitors.^{23,24}

Glycosidase Inhibitors – A General Introduction



Scheme 1. Mechanism of hydrolysis for a) inverting α -glucosidases and b) retaining α -glucosidases. The transition state glycosides are here depicted in the 4H_3 half-chair conformation.

Although certain non-glycosidic compounds can inhibit glycosidases, the sugars mimics, including carbasugars, thiosugars, and iminosugars, is the major class of glycosidase inhibitors currently in use or under development. The study of sugar mimics as glycosidase inhibitors has

provided valuable insight into the mechanism of catalysis within the different enzyme families.^{25,26} The composition of mammalian glycans biosynthesized by a given cell is driven by enzyme activity rather than derived from a template such as proteins are derived from their genetic code. Glycosidase inhibitors have thus also served as a tool in understanding the roles of mammalian glycosides.²⁷ This has been done by regulating the enzymes responsible for formation and breakdown of the relevant glycans. The use of glycosidase inhibitors as research tools has further enabled the discovery of specific glucosidases as targets in the treatment of various diseases. In the pharmaceutical industry iminosugars and thiosugars, in which the endocyclic oxygen is replaced with a nitrogen or a sulfur, respectively, are currently the most promising compound classes due to their oral bioavailability.²⁸ This part of the thesis focuses on the inhibitory properties of iminosugars, and design and synthesis of new iminosugars as glycosidase inhibitors.

2.1 Glycosidases as Targets for Drug Design

Carbohydrates are essential biomolecules for all living organisms. In addition to operating as storage and source of energy, glycans cover all cellular surfaces and are thus important mediators of many biological processes such as protein folding,²⁹ cell signaling,³⁰ fertilization, embryogenesis, cell differentiation, and proliferation.³¹ Additionally, glycans influence disease development by playing a part in pathogen recognition,³² cancer metastasis,³³ the innate immune response,³⁴ and inflammation.³⁵ Furthermore, many diseases are directly caused by defects in the glycosylation machinery, and these are collectively termed congenital disorders of glycosylation.³⁶ Due to the ubiquity of carbohydrates, glycan metabolizing enzymes are valuable biomarkers and targets for the treatment of diseases and hence for the design of potent drugs.^{37,38}

Perhaps the most intuitive association to glycan metabolism is the degradation of carbohydrates and absorption of the resulting sugars for the purpose of energy uptake. Disruptions in this system can trigger metabolic disorders such as type 2 diabetes, a chronic disease which is characterized by insufficient levels of insulin and resulting disturbances in the sugar metabolism.³⁹ Low insulin levels are caused by low secretion of insulin by target cells and/or by cellular resistance to the produced insulin. Both processes cause elevated levels of blood sugar and patients that suffer from type 2 diabetes are at a risk of developing further complications such as cardiovascular diseases and neuropathy. One strategy to manage type 2 diabetes is to delay the absorption of glucose by manipulation of enzymes that degrade carbohydrates to sugars, such as the intestinal α -glucosidases.⁴⁰ Inhibition of the α -glucosidases bound to the intestinal epithelium cells slow down the rate of carbohydrate digestion and thereby postpone the absorption of glucose to the blood.⁴¹

Another vital role for glycosidases is the trimming of the glycoconjugates that are presented on the eukaryotic cell surface.^{42,43} Most glycoconjugates are biosynthesized stepwise in the Endoplasmic reticulum (ER) and Golgi apparatus and are transported to the cell surface by the secretory pathway.⁴⁴ The glycosylation pattern on cancer cell surfaces can distinguish them from normal cells. Furthermore, the distinct and aberrant combination of *N*-linked oligosaccharides on cancer cell surfaces can influence tumour progression and mitosis.⁴⁵ The biosynthesis of the glycoproteins include trimming of the glycan moiety by a set of glucosidases and mannosidases. Inhibitors of these enzymes may slow down cancer progression.⁴⁵

The biosynthesis of glycoproteins through the mammalian secretory pathway is also exploited by enveloped viruses.⁴⁶ The host glycosylation machinery is hijacked by the virus and used in viral replication. Inhibitors of α -glucosidase I and α -glucosidase II in the ER lumen are thought to interfere with the viral glycopeptide folding, and hence obstruct the assembly of the virus.⁴⁷⁻⁴⁹ It is worth mentioning that this

strategy for treatment of viral infections was researched as a potential treatment for COVID-19 during the (current) pandemic.⁴⁷

Glucosidases are also targeted in the lysosomal storage disorders (LSDs), such as Gaucher's, Fabry and Pompe disease. Symptoms of this group of genetic disorders vary greatly, but can include developmental delay, respiratory failure, blindness, deafness etc.⁵⁰ Though more than 50 different lysosomal disorders exist, the most common of these include the anomalous storage of glycosphingolipids.⁵¹ This group of biomolecules function as structural membrane components and are involved in processes such as cell adhesion and recognition and modulation of signal transduction.⁵² The catabolism of glycosphingolipids occurs mostly in lysosomes and endosomes. Disruptions in the lysosomal catabolism cause accumulation of glycosphingolipids, resulting in the lysosomal storage disorders.

For Gaucher's disease, generally considered to be the most prevalent of the LSDs, mutations in the *GBA1* gene encoding the lysosomal glucocerebrosidase cause improper folding of this enzyme. Though the enzyme's catalytic activity normally is intact, the misfolded enzyme is recognized by an ER quality control system and degraded by the ER Associated Degradation (ERAD) machinery.⁵³ Conventional strategies for treatment of Gaucher's disease include reducing levels of glycosphingolipids (substrate reduction therapy, SRT) or increasing levels of glucocerebrosidase (enzyme replacement therapy, ERT). Supplementary to this is pharmacological chaperone therapy (PCT).⁵³ In this strategy a misfolded enzyme is stabilized by a small molecule and may thus avoid ERAD degradation. The saved enzyme can then hydrolyse the glycosphingolipids and avoid accumulation of these. Since the glucocerebrosidase functions as a retaining β -glucosidase, glucosidase inhibitors have been accessed for their ability to function as pharmacological chaperones (PC) in Gaucher's disease.⁵⁴ PC therapy targeting glucosidases have also been investigated for other LSDs, such as the misfolded α -galactosidase in Fabry disease.^{55,56}

2.2 Iminosugars

Iminosugars are carbohydrate mimetics in which the endocyclic oxygen is replaced by a nitrogen.⁵⁷ They share many features with carbohydrates, such as size, water solubility, and oral bioavailability. Iminosugars are however not metabolized by carbohydrate degrading enzymes and are normally excreted unchanged by the kidneys.⁵⁸ Moreover, iminosugars have shown to be potent inhibitors of carbohydrate modifying enzymes, and have also displayed many biological effects other than glycosidase inhibition.⁵⁹ All these properties make iminosugars valuable drug candidates, as is further discussed in chapter 2.2.2.

Based on ring size and number of rings, naturally occurring iminosugars can be grouped into five classes, namely piperidines, pyrrolidines, indolizidines, pyrrolizidines, and nortropanes (Figure 4). Within the five classes, more than 200 iminosugars have been isolated from natural sources and their biological profiles have been evaluated.^{60,61}

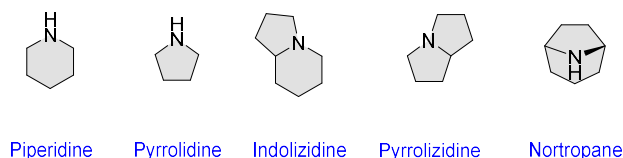


Figure 4. Most common ring structures of the naturally occurring iminosugars.

2.2.1 The Origin of Iminosugars

The idea of replacing the endocyclic oxygen in sugars with other heteroatoms was explored before iminosugars were isolated from natural sources.^{62,63} The first synthesis of 1-deoxynojirimycin (DNJ, **4**) (Figure 5) was performed by Paulsen and co-workers at the University of Hamburg in 1966.^{64,65} Later that year nojirimycin (NJ, **5**) (Figure 5) was

isolated from *Streptomyces roseochromogenes* R-468 and *S. lavendulae* SF-425, and was described as an antibiotic.^{66,67} It was also shown to be a potent inhibitor of α - and β -glucosidases from different sources.⁶⁸ A major drawback of the NJ (**5**) natural alkaloid was, however, its instability in solution. This instability may be explained by the unstable *N,O*-acetal present in the compound, which prevented its use as a pharmaceutical drug. Reduction of NJ (**5**) with sodium borohydride could provide the more stable DNJ (**4**), free from the anomeric hydroxyl group.⁶⁷ A decade after its first synthesis, DNJ (**4**) was isolated from the roots of Mulberry trees (*Morus* spp.).⁶⁹

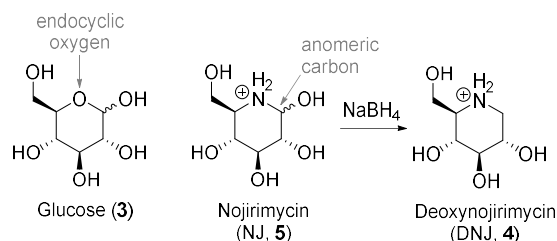


Figure 5. Nojirimycin (NJ, **5**), a glucose analogue with a nitrogen in place of the endocyclic oxygen. The hydroxyl group in the anomeric position can be removed by reduction of NJ (**5**) to the corresponding 1-deoxy-NJ (DNJ, **4**).

Mulberry trees have been used in traditional Chinese herbal medicine for treatment of a number of ailments, including diabetes, inflammations, coughing, fever, and high blood pressure.⁵⁷ All these properties can be ascribed to different iminosugars. With improved purification methods, more iminosugars were isolated from the *Morus* species in 1994,^{70,71} such as fagomine (**6**),⁷² *N*-methyl DNJ (**7**),^{73,74} and 1,4-dideoxy-1,4-imino-D-arabinitol (DAB, **8**) (Figure 6). The latter was originally isolated from fruits of *Angylocalyx boutiqueanus* in 1985.⁷⁵ In 1976 2,5-dideoxy-2,5-imino-D-mannitol (DMDP, **9**) was isolated from the leaves of the legume *Derris elliptica*,⁷⁶ and has later been found in other natural sources, such as a species of *Streptomyces* bacteria.⁷⁷ Castanospermine

(**10**) was first isolated in 1981 from *Castanospermum austral*.⁷⁸ The alkaloid **10** inhibits lysosomal α -glucosidase,⁷⁹ and disturbs the lysosomal catabolism of glycogen.⁸⁰ Together with other similar iminosugars, such as Australine (**11**),⁸¹ Castanospermine (**10**) was found to be the cause of toxicity in the legume *C. austral* for livestock.

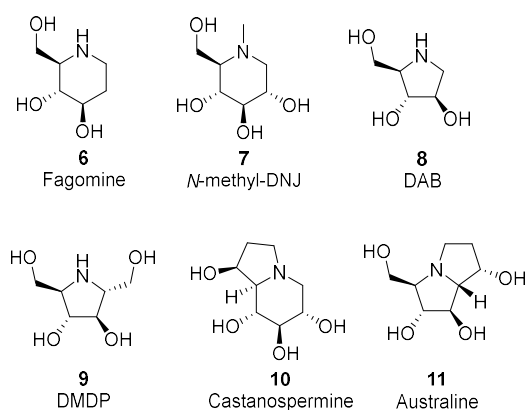


Figure 6. Natural iminosugars.

Iminosugars are today assumed to be widespread in plants and microorganisms.^{82,83} Moreover, many natural iminosugars display a broad inhibitory spectrum towards mammalian glycosidases. This broad activity is likely beneficial to the plants and microorganisms in which they are produced, as protection against digestion.⁵⁹ However, if the natural iminosugars were to be used for therapeutic purposes, they would give many side effects from off target activity. These sugars thus generally provide a basis for preparation of more selective pharmaceutical compounds. The specific physicochemical properties of the iminosugars that give them the ability to inhibit glycosidases have therefore been extensively studied.

2.2.2 Properties of Iminosugars as Glycosidase Inhibitors

The glycosidase inhibitory effect of iminosugars is believed to arise from their resemblance to the transition state species presented in Scheme 1.^{21,84} The sugar traits that the iminosugars mimic, can roughly be grouped into three categories, namely shape (conformation), charge and chirality (Figure 7).

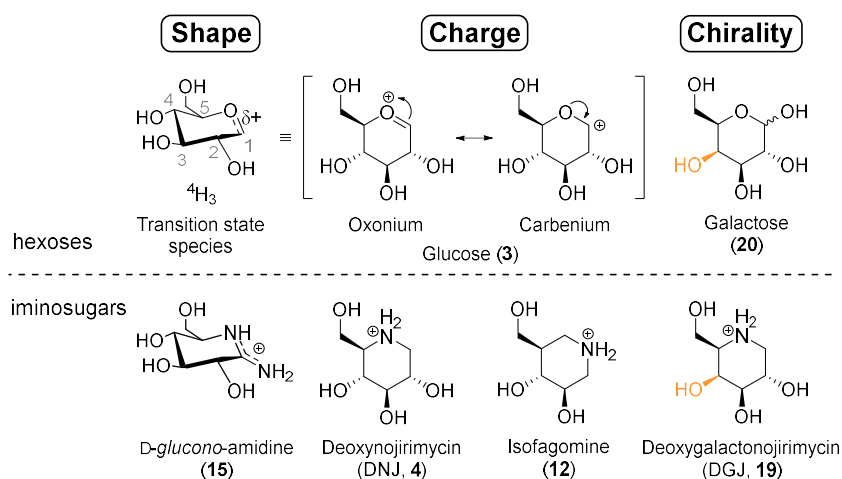


Figure 7. Iminosugars as glycoside transition state mimics, and their inhibitory profiles.⁸⁵⁻⁸⁸

Due to their inherent pKa, iminosugars have the ability to be protonated at physiological pH.⁸⁹ In its protonated form,⁹⁰ these sugars mimic the oxocarbenium character of the transition state glycoside (Figure 7). Furthermore, the position of the protonated nitrogen plays a part in the glycosidase inhibition selectivity between α and β glycosidases (Figure 8). One example of this is the difference in selectivity between deoxynojirimycin (DNJ, 4) and the iso-iminosugar isofagomine (12). DNJ (4), the standard D-glucono-iminosugars with a nitrogen in the place

of the endocyclic oxygen, favours inhibition of α -glucosidases.⁸⁵ On the other hand, isofagomine (**12**),⁹¹ with a nitrogen in the D-*glucono*-anomeric position has displayed high affinity for β -glucosidases.⁸⁶

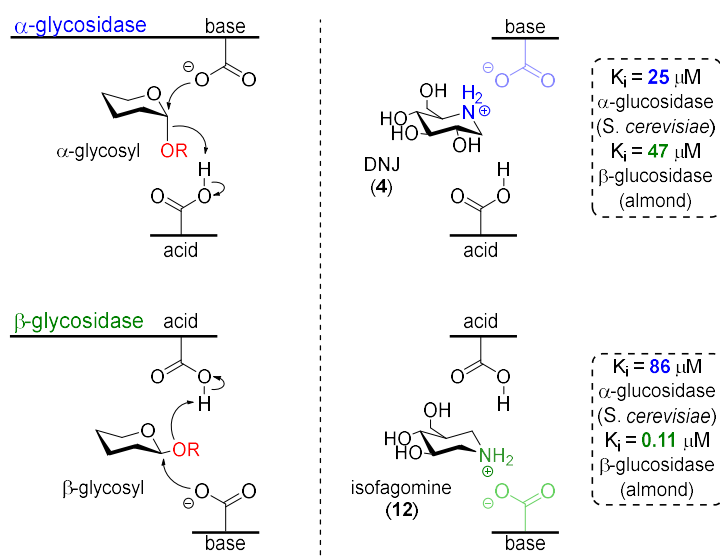


Figure 8. The position of the nitrogen in iminosugars influences glycosidase inhibition selectivity.

The influence that the position of the endocyclic nitrogen has on an iminosugar's biological activity has further been verified upon the synthesis of azafagomine (**13**) (Figure 9).⁸⁷ This D-*glucono*-iminosugar, with two nitrogens in the place of both the endocyclic oxygen and the anomeric carbon is a potent inhibitor of both yeast α -glucosidase and almond β -glucosidase.⁹² The study also concluded that the L-*glucono*-azafagomine (L-**13**) was a very poor inhibitor of the glucosidases.⁹²

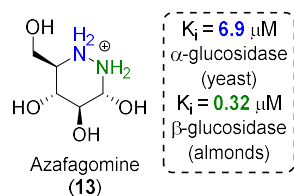


Figure 9. Azafagomine (D-13), a potent α - and β -glucosidase inhibitor.

Another feature that has provided valuable insight into glycosidase inhibition potency and selectivity, is the study of charge distribution across the endocyclic C-N bond by introduction of an amidine moiety into the D-*glucono*-iminosugars.^{24,93-95} The introduction of a double bond into the six-membered ring also influences the piperidine conformation, giving it a closer resemblance to the half-chair transition state species.²⁴ Similar conformation is also found in the natural iminosugar Kifunensine (14), which is a selective plant α -mannosidase inhibitor.⁹⁶ The amidine 15 introduced by Ganem and co-workers displayed a broad inhibitory profile, including the inhibition of α -glucosidase, β -glucosidase, β -galactosidase, and α -mannosidase (Figure 10).⁹³ On the contrary, isofagomine amidine analogue 16, reported by Lindbäck *et al.*,⁹⁵ showed a much narrower window of activity, more specifically, selective inhibition of α -mannosidase. Moreover, *N*-arming of Ganem's endocyclic amidine nitrogen to form hydrazide imide 17 also resulted in inhibition of several glycosidases.⁹⁴ The methylated analogue 18, on the other hand, displayed selective affinity for α -mannosidase.

Glycosidase Inhibitors – A General Introduction

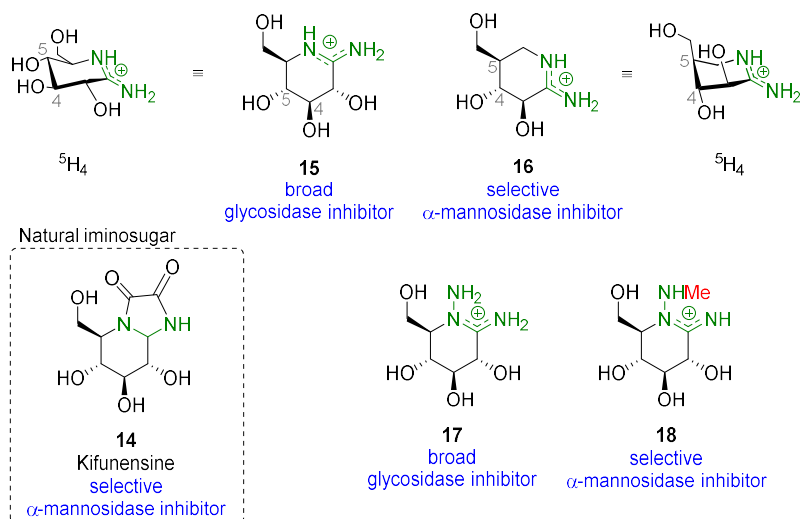


Figure 10. Synthetic functionalized D-glucono-amidines are potent glycosidase inhibitors that mimic both the shape and charge of the glycoside transition state.

The relative stereochemistry of the piperidine iminosugar hydroxyl groups generally determine their selectivity as glucosidase inhibitors. For instance, naturally occurring DNJ (**4**), with a D-glucono-configuration inhibits α -glucosidase, while deoxygalactonojirimycin (DGJ, **19**), the galactosidase (**20**) iminosugars analogue, inhibits α -galactosidase and deoxymannojirimycin (DMJ, **21**) inhibits α -mannosidase (Figure 11).^{97,98} This is, however, not always the case for pyrrolidine iminosugars. For instance, DMDP (D-**9**) inhibits both glucosidases and galactosidase.⁹⁹ In several instances the pyrrolidine iminosugars, such as DAB (D-**8**), are more potent glycosidase inhibitors than their piperidine derivatives, such as DNJ (D-**4**). This has been rationalized by the fact that the pyrrolidine envelope conformation resembles the half-chair conformation in a higher degree than what the piperidine conformation does.¹⁰⁰

Because an enzyme can normally distinguish between its desired substrate and its enantiomer, the unnatural L-iminosugars have been

given much less attention than their natural D-enantiomers. For instance, the L-enantiomers of DNJ (**4**) and isofagomine (**5**) have displayed 100-4000 fold less potency than their D-enantiomers.^{101,102} However, the furanose mimicking L-iminosugars LAB (L-**8**), L-DMDP (L-**9**) have proven to be even more potent inhibitors of mammalian and plant α -glucosidases than their D-antipodes.¹⁰²⁻¹⁰⁴ Furthermore, L-DMDP (L-**9**) is a more specific inhibitor of mammalian α -glucosidases than the natural product DMDP (D-**9**).¹⁰⁵ The four L-iminosugars mentioned were further suggested to be non-competitive inhibitors of the D-glycosidases. This means that the L-iminosugars inhibit the enzyme at an allosteric site, which gives the L-series an advantage over the D-series in terms of selective inhibition, namely less off target hits. It has therefore recently become more common to include the L-iminosugars in biological assays.¹⁰⁶⁻¹⁰⁸

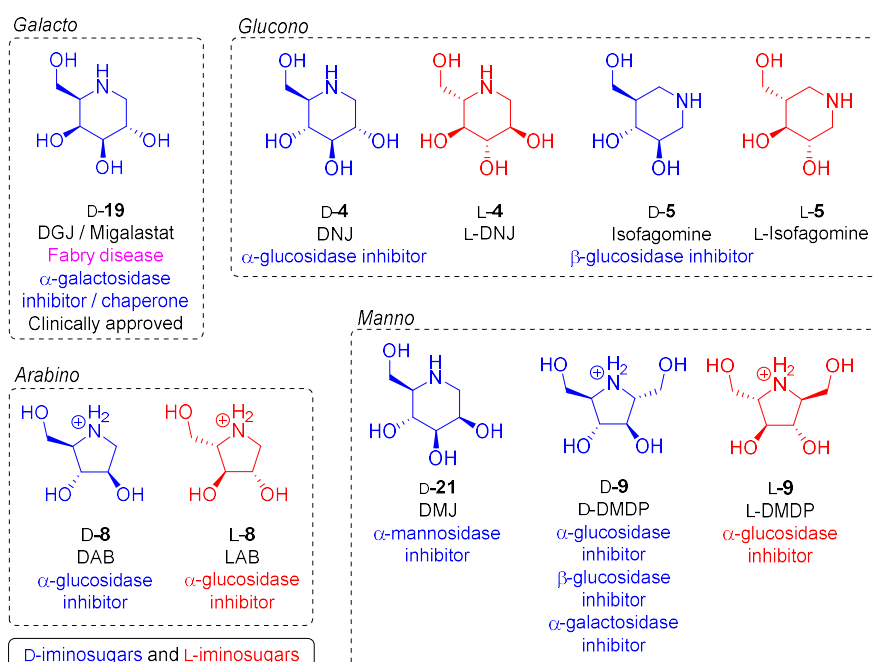


Figure 11. D- and L-iminosugars as glycosidase inhibitors.

L-Miglustat (*N*-butyl-L-deoxynojirimycin, L-24), which selectively enhances lysosomal α -glucosidase levels in Pompe disease fibroblasts.¹⁰⁶ L-Miglustat (L-24) has also shown anti-inflammatory response to *Pseudomonas aeruginosa* infections and is investigated for application in Cystic Fibrosis lung disease.¹¹⁹

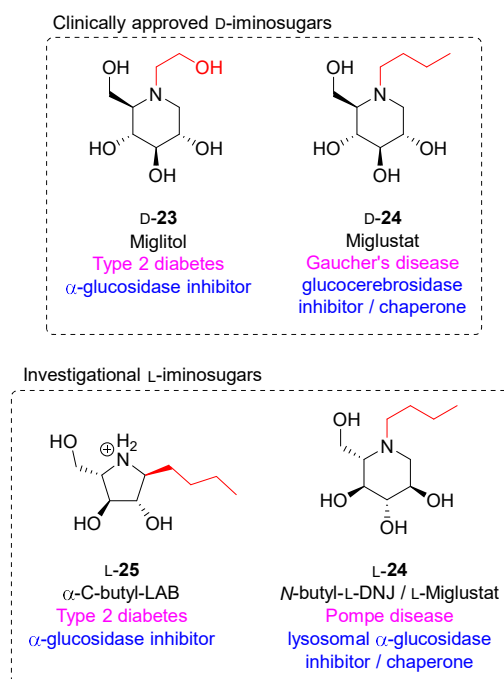


Figure 12. Example of alkylated iminosugars and their biological activity.

In conclusion, this chapter demonstrates that much is known about the correlation between the traits of iminosugars and their glycosidase inhibition activity. Iminosugars have many intrinsic properties that are desirable in a potential drug candidate, such as water solubility, chemical stability, and the ability to be readily absorbed through biological

membranes.¹²⁰ Moreover, the diverse roles of glycan processing enzymes in interaction with the variation of structures displayed by carbohydrates, provides a great opportunity for the identification of new and valuable chemotherapies. This motivates for further research on sugar mimetics, and much is yet to be explored within synthetic preparation of natural and unnatural iminosugars and examination of their biological activity. This project has aimed at contributing to the development of novel selective glycosidase inhibitors for the purpose of exploring the chemical attributes required in an iminosugars for potent and selective glycosidase inhibition.

The nomenclature of iminosugars normally follows the naming of monosaccharides with an endocyclic oxygen. Figure 13 shows the hexose and pentoses used for the naming of the iminosugars presented in this thesis, namely D/L-glucose (D/L-**3**), D/L-arabinose (D/L-**26**), D/L-xylose (D/L-**27**), D/L-ribose (D/L-**28**), and D/L-lyxose (D/L-**29**). Enantiomers are distinguished from one another by the D- or L-prefix. It can here be emphasized that C3-C5 in arabinose shares the same stereochemistry as the glucose C4-C6. Chapter 3 covers our synthesis of amidine iminosugars with an *arabino* configuration. Moreover, our synthetic work towards hydrazide imide iminosugars with a *glucono* configuration is presented in chapter 4.

Glycosidase Inhibitors – A General Introduction

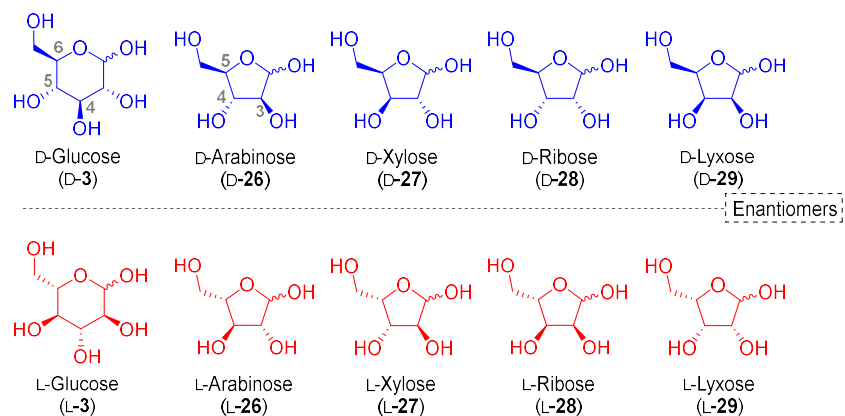


Figure 13. Hexoses and pentoses that are used for naming of iminosugars in this project.

3 Synthesis of the Functionalized Arabino-Amidines

The broad inhibitory profile of pyrrolidines, such as DAB (D-**8**) has been ascribed to its conformational flexibility (Figure 14).¹²¹ As described in chapter 2, chemical modifications of DAB (D-**8**), such *N*- and *C*-alkylation, has been one strategy for preparing more selective glycosidase inhibitors.^{107,122} Additionally, conformational rigidity of the pyrrolidines has been explored. For instance, the conformationally rigid diazole arabinoses D-**30** and D-**31** are selective α -mannosidase inhibitors (Figure 14).^{123,124} In this case, the diazole L-enantiomers L-**30** and L-**31** did not show any glycosidase inhibition. On the other hand, triazole L-**32** has proven to be a potent and selective inhibitor of α -glucosidase.¹²⁵ Though the heterocyclic aromatic ring fused to the pyrrolidine scaffold in compounds **30-32** induced conformational rigidity, the element of charge was absent. In this project, the element of charge has been added to the conformationally rigid pyrrolidines by the introduction of functionalized amidines to the five-membered ring.

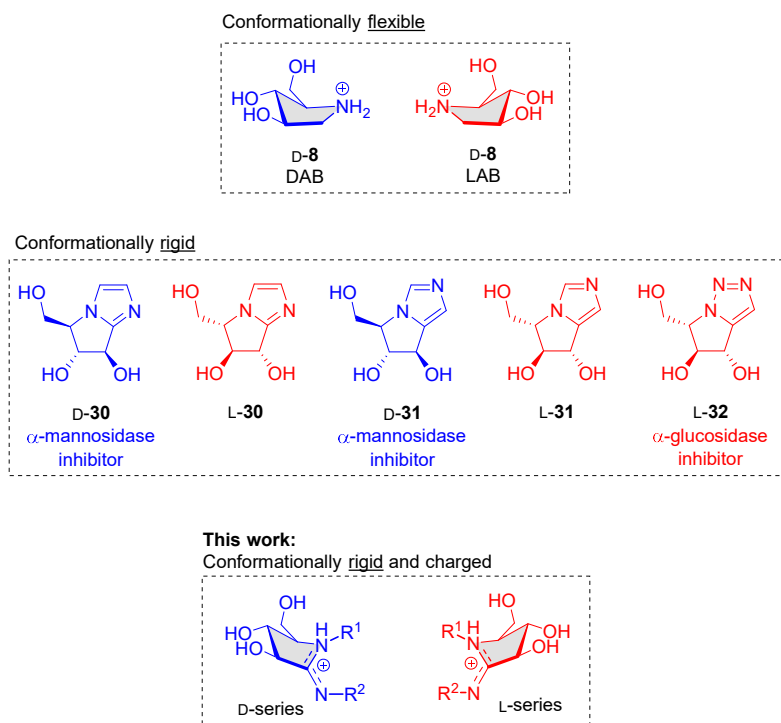
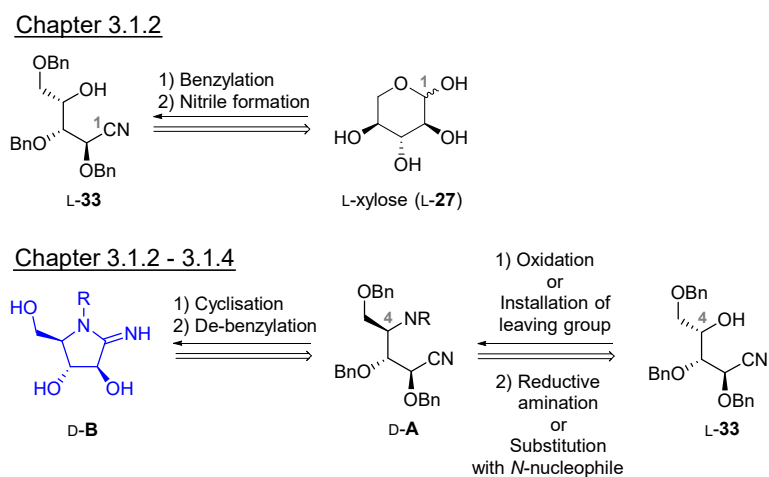


Figure 14. Introduction of conformational rigidity into the pyrrolidine iminosugars.

3.1 Results and Discussion

The synthetic plan for the formation of the *arabino*-amidines presented in Figure 14, is depicted in Scheme 3. The first part of the strategy was conversion of L-xylose (L-27) to nitrile L-33. Benzylation of L-xylose (L-27)¹²⁶ was to be followed by nitrile formation at C1, employing the method of Ermert and Vasella.¹²⁷ In the second part, the *arabino*-pyrrolidines were to be prepared from nitrile L-33. Inversion of C4 in L-*xylono*-nitrile L-33 would then provide the corresponding D-*xylono*-nitrile D-A, upon treatment with a suitable *N*-nucleophile. Activation of

the C4 hydroxyl moiety could be obtained by either oxidation to the corresponding ketone or installation of an appropriate leaving group. Promotion of a nucleophilic attack by the C4 nitrogen onto the C1 nitrile moiety would presumably provide a cyclized product containing the desired functionality. The final *arabino*-pyrrolidine sugars **D-B** could then be obtained from de-benzylation of the cyclization product. The same strategy was also planned for the preparation of the **L-B** enantiomers from D-xylose (**D-27**).



Scheme 3. Retrosynthetic strategy for preparation of the *arabino*-amidines **D-B** from L-xylose (**L-27**). Equivalent strategy was planned for the preparation of the **L-B** enantiomer from D-xylose (**D-27**).

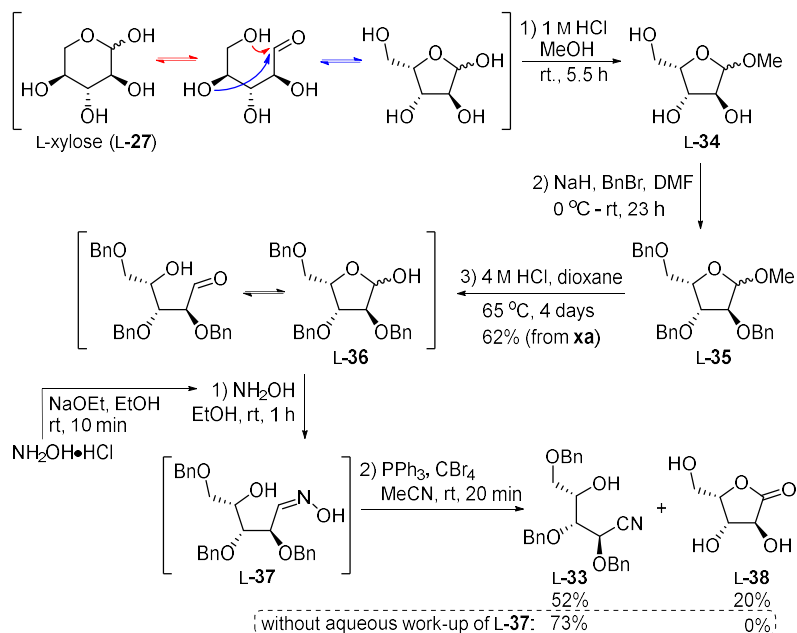
3.1.1 Preparation of D/L-Xylono-Nitriles

The synthesis of the *xylono*-nitriles **L-33** and **D-33** commenced with benzylation of L-xylose (**L-27**) in a three-step reaction procedure, previously reported by former group member T. Evangelista *et al.*

(Scheme 4).¹²⁶ The method included methylation of the anomeric hydroxyl group in L-xylose (L-27) followed by treatment of the resulting compound L-34 with benzyl bromide and sodium hydride to form the corresponding benzylated *O*-methyl xylose L-35. Acid promoted demethylation finally furnished tri-*O*-benzyl-L-xylose (L-36) from compound L-27 in 62% yield over three steps.

The ring-opened tautomer of xylose L-36 was further condensed with hydroxyl amine to provide aldoxime L-37, which was used directly in the next step without purification by column chromatography. Aldoxime L-37 was subjected to Appel conditions to provide L-*xylono*-nitrile L-33 in 52% yield, accompanied by substantial formation of the known lactone L-38.¹²⁸ This protocol was previously reported by Ermert and Vasella for the synthesis of 2,3,4,5-tetra-*O*-benzyl-D-*glucono*-nitrile.¹²⁷ They did not, however, report the formation of a lactone by-product. Lactone L-38 was presumably formed from a hydrolysed intermediate. We therefore repeated the two-step reaction from xylose L-27 to nitrile L-33, but omitted the aqueous work-up of the step 1 aldoxime product L-37. Instead, the residue from step 1 was dissolved in toluene and evaporated to dryness before it was subjected to the step 2 Appel conditions. This method afforded nitrile L-33 in 73% yield without formation of lactone L-38.

Synthesis of the Functionalized Arabino-Amidines



Scheme 4. Synthesis of nitrile **L-33** from L-xylose (**L-27**).

The IR analysis of nitrile **L-33** did not show the expected CN-stretch which should have been evident at approx. 2200 cm^{-1} . However, the ^{13}C NMR signal at 116.7 ppm confirmed the presence of a nitrile moiety in compound **L-33** (Figure 15). Also, the ^{13}C NMR spectrum of nitrile **L-33** exhibited the expected number of signals, including the multiplet of aromatic CH carbons at $129\text{--}127\text{ ppm}$, the three quaternary aromatic carbons at $138\text{--}135\text{ ppm}$, and the seven aliphatic carbon peaks between 80 ppm and 60 ppm . The structure of nitrile **L-33** was further evidenced by the presence of a molecular ion at $m/z\ 440.1827$ in the HRMS spectrum, which proved consistent with the molecular formula, *viz.* $\text{C}_{26}\text{H}_{27}\text{NO}_4$.

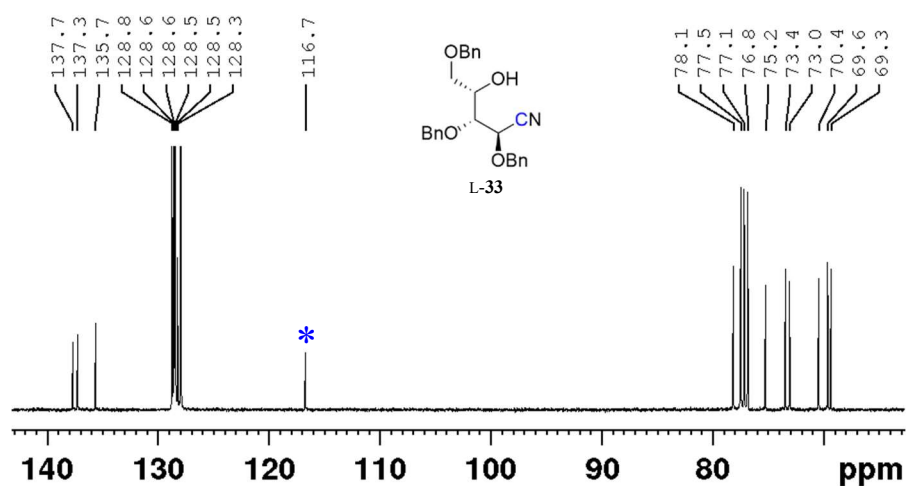
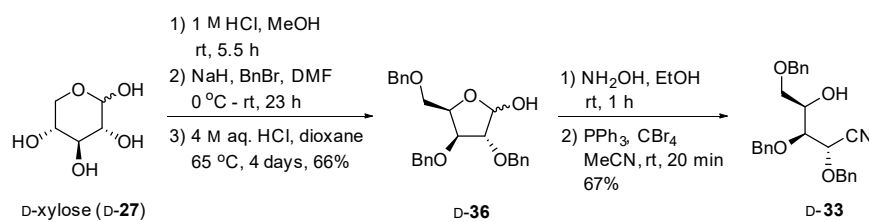


Figure 15. Section of the nitrile L-33 ^{13}C NMR spectrum. The blue star marks the nitrile carbon in compound L-33.

The D-enantiomer of nitrile L-33, namely D-33, was prepared under equivalent conditions from D-xylose (D-27) (Scheme 5). The spectroscopic data were in full accord with the data for nitrile L-33. Optical rotation measurements could also confirm that the two compounds L-33 and D-33 were mirror images of each other, in which $[\alpha]_D = -29$ and $+32$, respectively.

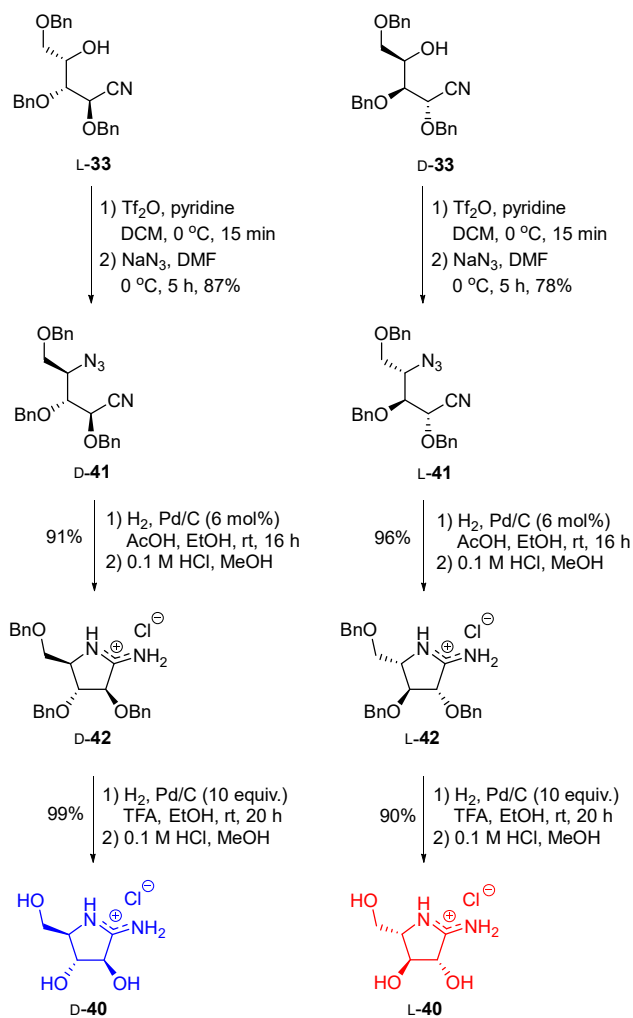


Scheme 5. Synthesis of nitrile D-33 from D-xylose.

3.1.2 Synthesis of D/L-Arabino-Amidines

The preparation of amidines **D-40** and **L-40** from nitriles **L-33** and **D-33** commenced with a triflation-azidation sequence (Scheme 6). The azide functionality in the resulting compounds **D-41** and **L-41** was confirmed by a strong IR stretch at 2100 cm^{-1} . Hydrogenation of azide **D-41** with a catalytic amount of Pd/C, in the presence of acetic acid, provided amidine **D-42** in 91% yield upon conversion to the corresponding HCl salt. A second hydrogenation reaction was then conducted with 10 equivalents of Pd/C, in the presence of TFA, to remove the benzyl groups from compound **D-42**. *D-Arabino*-amidine **D-40** was thus isolated as the HCl salt in 99% yield. *L-Arabino*-amidine **L-40** was then prepared in two steps from azide **L-41**. Palladium catalyzed hydrogenation of azide **L-41** provided amidine **L-42** upon treatment with HCl in methanol. This was followed by the palladium promoted hydrogenolysis of benzyl groups and formation of *L-arabino*-amidine **L-40**.

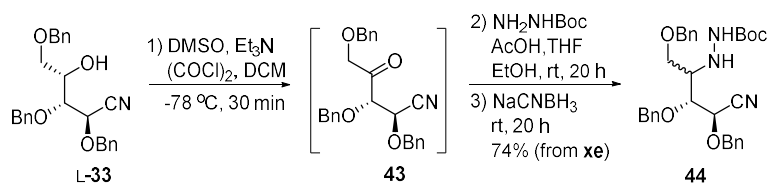
Synthesis of the Functionalized Arabino-Amidines



Scheme 6. Preparation of D- and L-arabino-amidines D-40 and L-40 from nitriles L-33 and D-33, respectively.

3.1.3 Synthesis of D/L-Arabino-Hydrazide Imides

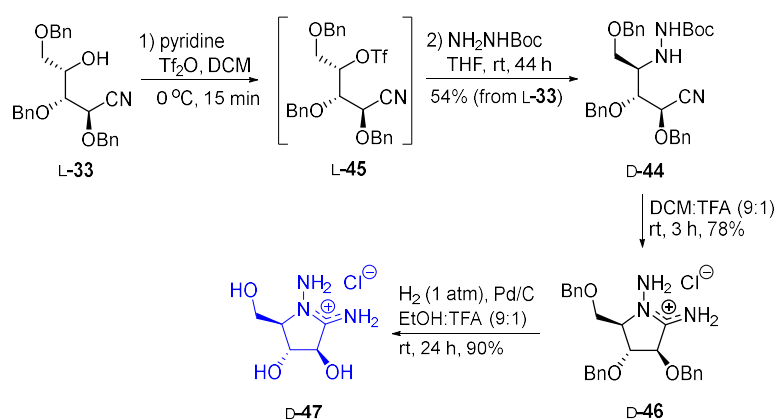
As presented in chapter 2.2.2, *N*-arming of Ganem's amidine **15** had provided hydrazide imide piperidine **17** with an interesting glycosidase inhibition profile (Figure 10). We thus wanted to do the same with *arabino*-amidines D/L-**40**. Nitrile L-**33** was therefore subjected to Swern oxidation to afford ketone **43**, which was used directly in the next step without purification (Scheme 7). The residue was thus stirred with *tert*-butyl carbazate for 20 hours before addition of sodium cyanoborohydride. After 20 hours reaction time, the reductive amination procedure provided hydrazide **44** in 74% yield as a mixture of stereoisomers.



Scheme 7. Formation of hydrazide **44** by oxidation of alcohol L-**33** followed by reductive amination with *tert*-butyl carbazate, employing sodium cyanoborohydride as reducing agent.

The two *D*-*glucono*- and *L*-*xylono*-hydrazide **44** stereoisomers could unfortunately not be separated by silica gel column chromatography. To obtain only one stereoisomer, the alcohol moiety in nitrile L-**33** was instead converted to a triflate leaving group by treatment with triflic anhydride and pyridine (Scheme 8). TLC analysis of the triflation reaction showed a spot-to-spot reaction. Therefore, triflate L-**45** was used directly in the next step without further purification. It can be mentioned that no decomposition or alteration of the triflate was observed.

Treatment of the triflate L-45 with *tert*-butyl carbazate further provided D-*glucono*-hydrazide D-44 in 54% yield from nitrile L-33. TFA mediated removal of the Boc group facilitated cyclization to hydrazide imide D-46. The benzyl groups were then removed by palladium promoted hydrogenolysis in ethanol to provide the target compound, namely D-*arabino*-hydrazide imide D-47.



Scheme 8. Preparation of D-*arabino* hydrazide imide D-47 from L-*glucono*-nitrile L-33.

The NMR analysis of compound D-47 was best conducted in D₂O, which gave the best resolved spectra for both ¹H and ¹³C NMR. The characteristic feature of the *arabino*-pyrrolidines with an endocyclic double bond presented in this thesis is the apparent H3 triplet, which implies equal *J*³ coupling constants between protons H3-H4 and H2-H3 (Figure 16). This feature was also observed in the ¹H NMR analysis of the *O*-benzyl *arabino*-pyrrolidines described in this thesis.

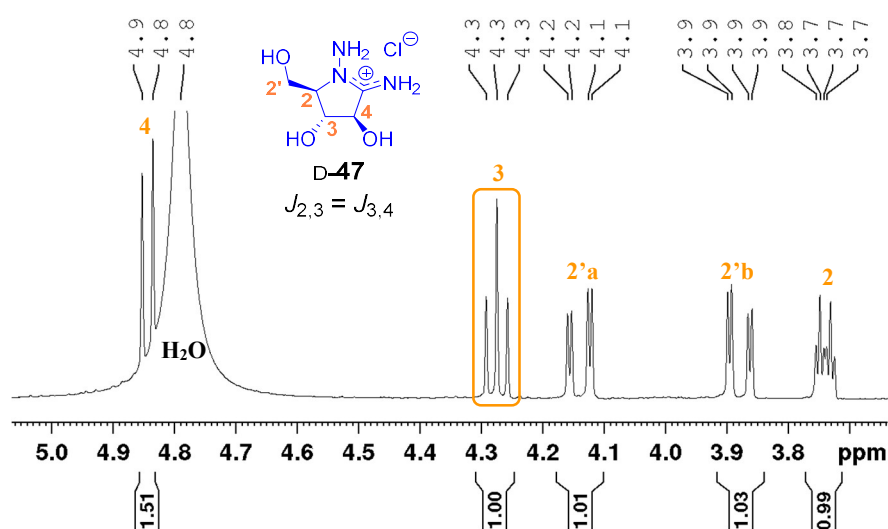


Figure 16. A section of the ^1H NMR section of D-arabino hydrazide imide D-47 showing the characteristic triplet for proton H3.

The structure of hydrazide imide D-47 was supported by the presence of a molecular ion at m/z 162.0871 in the HRMS spectrum, which proved consistent with the molecular formula of compound D-47, *viz.* $\text{C}_5\text{H}_{12}\text{O}_3\text{N}_3$. 2D NMR analysis was further conducted to verify the position of the hydrazide imide moiety and suggest the conformation of compound D-47 (Figure 17). To detect exchangeable protons in compound D-47, the ^1H - ^{13}C HMBC NMR analysis was run in DMSO-d_6 . ^1H - ^{13}C HMBC correlations were observed from the exocyclic NH_2 protons as well as from H4 the OH proton at C4 to the iminium carbon C5. Moreover, correlations from protons H2', H3 and H4 to the endocyclic nitrogen were detected in ^1H - ^{15}N HMBC NMR analysis of D-47 in D_2O .

For the conformational analysis, the assumption was made that the sp^2 character of N1 and C5 in hydrazide imide D-47 would afford a coplanar arrangement across C2-N1-C5-C4. This planarity left the two conformational options for compound D-47, namely the ^4E or the E_4

enveloped conformation. Observed ^1H - ^1H NOESY correlations between H2'-H3 and H2-H4 indicated that D-*arabino*-hydrazide imide D-47 holds an ^4E enveloped conformation. This was also consistent with the J^{β} coupling constants observed by ^1H NMR analysis between H2-H3 and H3-H4, which were both 7.0 Hz. By comparison, the ^1H NMR analysis of the benzylated D-*arabino*-hydrazide imide D-46 showed the smaller J^{β} coupling constant value of 3.4 Hz between protons H2-H3 and H3-H4 (Figure 17). This indicated that the benzylated compound D-46 held a different conformation than its debenzylated congener D-47. Moreover, the lack of an observed ^1H - ^1H NOESY correlation between H2-H4 indicated that compound D-46 holds an E_4 enveloped conformation.

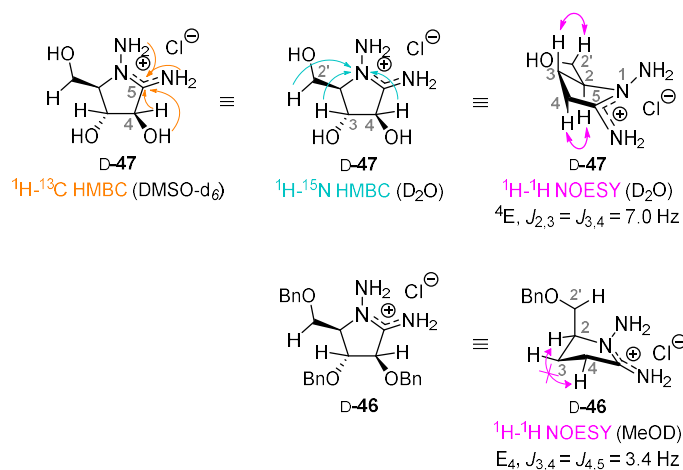
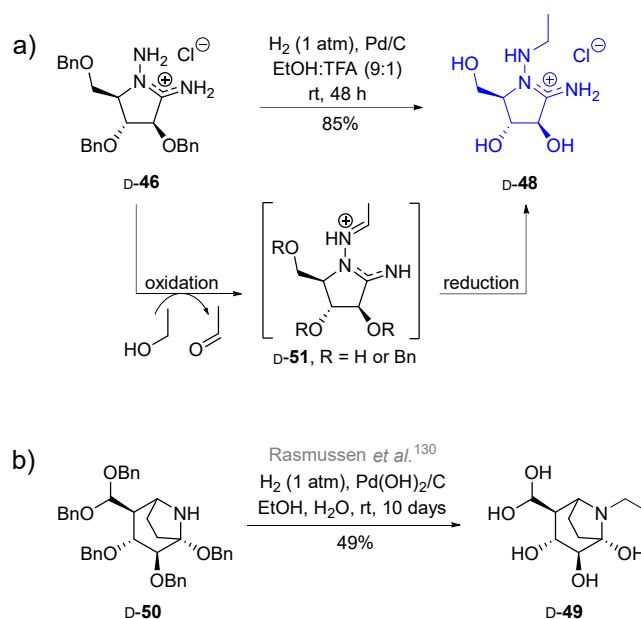


Figure 17. Conformational analysis of D-*arabino*-hydrazide imide D-47 and *O*-benzyl hydrazide imide D-46, from 2D NMR analysis. In the conformational analysis OCBn and OH groups at C3 and C4 have been omitted for clarity.

When hydrazide imide D-46 was subjected to palladium promoted hydrogenation for 48 hours, alkylation of the exocyclic nitrogen gave *N*-ethyl hydrazide imide D-48 in 85% yield (Scheme 9a). Similar *N*-alkylation during hydrogenolysis of benzyl groups has been encountered

by others.^{129,130} For instance, Rasmussen *et al.* obtained *N*-ethyl nortropine D-49 when employing (an old batch of) Pearlman's catalyst (Pd(OH)₂/C) for hydrogenolysis of benzyl groups from nortropine D-50 (Scheme 9b).¹³⁰ *N*-alkylation has also been observed in other palladium catalyzed hydrogenation reactions, such as reduction of nitrobenzenes.¹³¹ In all these cases it has been suggested that the alkylating agent is the corresponding aldehyde of the alcohol used as solvent. The aldehyde species is most likely formed by palladium catalyzed oxidation of the alcohol.¹³² Thus, the *N*-alkylation presumably occurs through a reductive amination reaction, forming imine intermediate D-51, with hydrogen over a palladium species as the reducing agent.



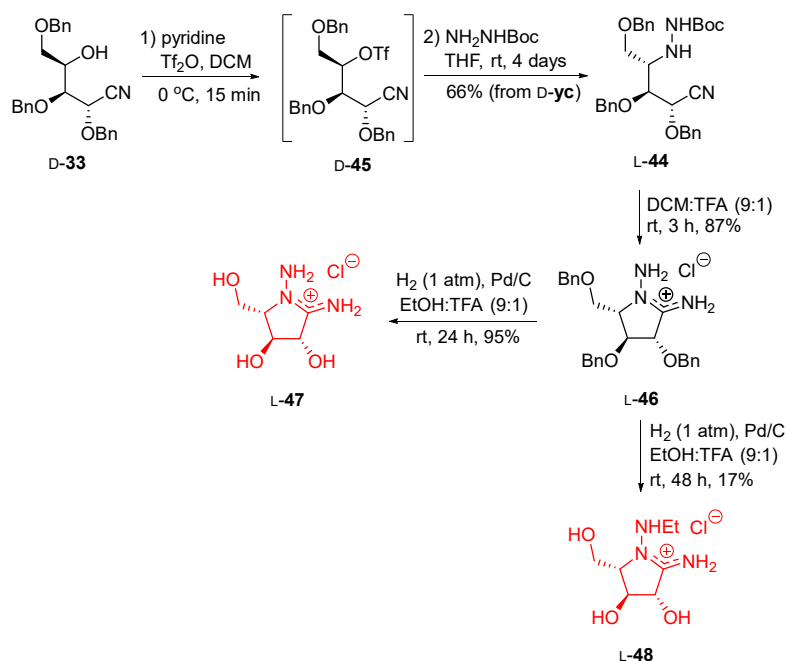
Scheme 9. a) Debenzylation and simultaneous *N*-alkylation of hydrazide imide D-46. b) Formation of *N*-ethyl nortropine D-49 from the corresponding *O*-benzyl compound D-50 reported by Rasmussen *et al.*¹³⁰

Equivalent to the preparation of D-*arabino*-hydrazide imides D-**47** and D-**48** from L-*glucono*-nitrile L-**33**, L-*arabino*-hydrazide imides L-**47** and L-**48** were prepared from D-*glucono*-nitrile D-**33** (Scheme 10). TLC analysis showed full conversion of the hydroxyl nitrile D-**33** to the corresponding triflate. However, the following substitution reaction with *tert*-butyl carbazate was very slow and provided the hydrazide L-**44** in 20-30% yield. Running the reaction at elevated temperatures did not enhance the yield, but instead led to formation of several unidentified side-products. TLC analysis indicated that the conversion from triflate D-**45** to hydrazide L-**44** stopped after approx. 24 hours. Addition of *tert*-butyl carbazate to the reaction mixture after 24 hours did not appear to enhance the turnover of the starting material.

Since *tert*-butyl carbazate is hygroscopic, it was likely that water was interfering with the reaction. Indeed, by stirring *tert*-butyl carbazate with 4 Å molecular sieves in THF for 24 hours before addition of triflate D-**45**, hydrazide L-**44** was obtained in 66% yield after stirring at room temperature for 4 days. TFA mediated removal of the Boc group facilitated cyclization to hydrazide imide L-**46**. The benzyl groups were then removed by palladium promoted hydrogenolysis over Pd/C in ethanol to provide L-*arabino* hydrazide imide L-**47** after 24 hours.

As presented in Scheme 9a, *N*-ethyl D-*arabino*-hydrazide imide D-**48** was obtained in 85% yield from the corresponding benzylated hydrazide imide D-**46** by extending the reaction time for the hydrogenation to 48 hours. Replicating the reaction for the conversion of compound L-**46** to *N*-ethyl D-*arabino*-hydrazide imide L-**48** was unfortunately not as straightforward as expected, even though the same batch of Pd/C was used for both reactions. After 48 hours TLC analysis indicated that the major product formed was L-**47**, and only 17% of product L-**48** was isolated from the reaction. Nevertheless, this provided enough of compound L-**48** for biological testing, and no further attempts were made to enhance the yield of this reaction.

Synthesis of the Functionalized Arabino-Amidines

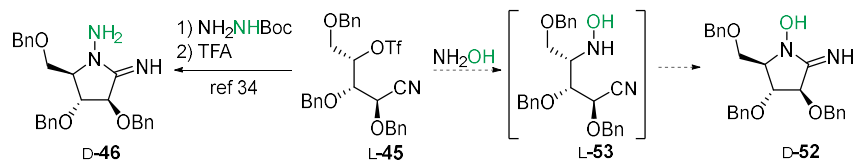


Scheme 10. Preparation of L-arabino hydrazide imides L-47 and L-48 from nitrile D-33.

3.1.4 Synthesis of D/L-Arabino-Amide Oximes

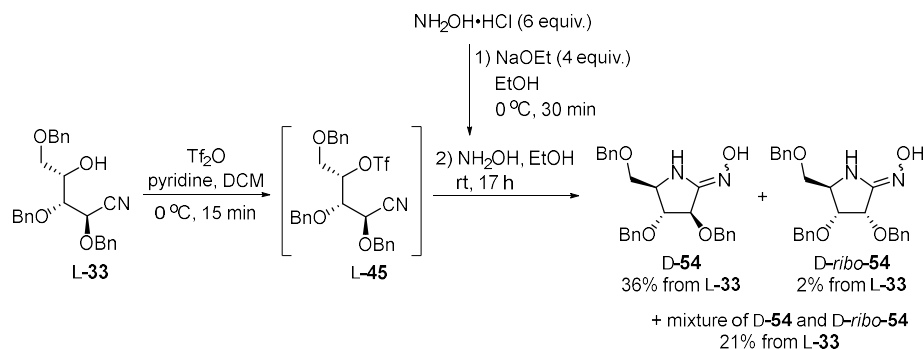
Analogous to the preparation of the hydrazide imide D-46 from triflate L-45, we initially assumed that the imino hydroxyl amine D-52 could be obtained from a reaction in which the hydroxylamine nitrogen first substituted the triflate moiety (Scheme 11). The assumed hydroxyl amine nitrile intermediate L-53 would then spontaneously cyclize to afford imino hydroxyl amine D-52 with the hydroxyl group connected to the endocyclic nitrogen.

Synthesis of the Functionalized Arabino-Amidines



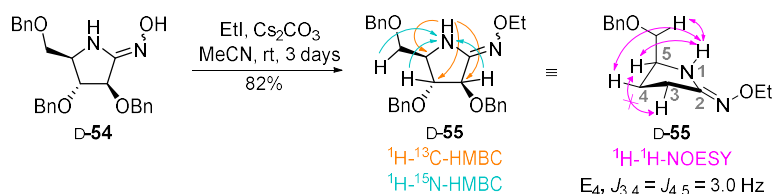
Scheme 11. Proposed formation of imino hydroxylamine **D-52** by treatment of triflate **L-45** with hydroxylamine, equivalent to the assembly of hydrazide imide **D-46**.

Triflate **L-45**, prepared from nitrile **L-33**, was therefore treated with hydroxyl amine in ethanol (Scheme 12). The hydroxyl amine was liberated from the corresponding HCl salt by treatment with sodium ethoxide. *D-arabino*-amide oxime **D-54** was isolated in 36% yield from a tight separation by silica gel column chromatography. Furthermore, the *D-ribo* isomer *D-ribo-54* was obtained in 2% yield, and a mixture of the isomers **D-54** and *D-ribo-54* was provided in 21% yield. The isomer *D-ribo-54* was presumably formed by racemization of the amide oxime α -carbon by residual sodium ethoxide in the reaction mixture, even though the hydroxyl amine HCl salt was employed in excess.



Scheme 12. Preparation of amidoxime **D-54** using excess of hydroxylammonium chloride over sodium ethoxide as base.

The structure of product D-54 was expectedly equal to imino hydroxylamine D-52 (Scheme 11). IR analysis of compounds D-54 showed the presence of a hydroxyl group, signified by a clear OH-stretch at 3100 cm^{-1} . However, from NMR analysis of the amide oxime D-54, the position of the *N*-hydroxyl group could not be ascertained. Due to solubility issues, the only solvent that would provide us with a descent NMR spectrum of compound D-54 was deuterated methanol, in which exchangeable protons are not observed. IR analysis could still confirm the presence of a hydroxyl group. We envisaged that 2D NMR analysis of a derivatized amide oxime could help us to determine the correct structure of compound D-54. Amide oxime D-54 was therefore alkylated with ethyl iodide in the presence of cesium carbonate to provide *O*-ethyl amide oxime D-55 in 82% yield (Scheme 13).

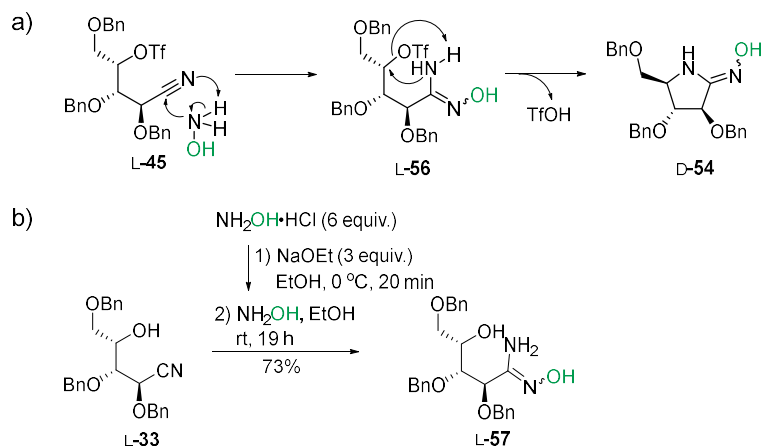


Scheme 13. Alkylation of amide oxime D-54 and consequent formation of *O*-ethyl amide oxime D-55. 2D NMR analysis of the reaction product D-55 accompanied by the proposed conformation of *O*-ethyl amide oxime D-55. OCBn groups at C3 and C4 have been omitted for clarity.

Surprisingly, NMR analysis of *O*-ethyl amide oxime showed that the *N*-ether moiety in compound D-55 was attached to the exocyclic nitrogen, and not to the endocyclic nitrogen, as anticipated. The most convincing evidence of this, was the presence of an NH proton attached to the endocyclic nitrogen in amide oxime ether D-55. This proton would have been absent if the ether oxygen in compound D-55 had been connected to the endocyclic nitrogen. Analysis of $^1\text{H}-^{13}\text{C}$ HMBC, $^1\text{H}-^{15}\text{N}$ -HMBC,

and ^1H - ^1H NOESY correlations confirmed the presence and position of the endocyclic NH moiety (Scheme 13). The ring conformation of pyrrolidine D-55 could also be estimate from analysis of the ^1H - ^1H NOESY correlations. The sp^2 character of N1 and C2 in compound D-55 was assumed to afford a coplanar arrangement across C5-N1-C2-C3. This planarity left the two configurational options for compound D-55, namely the ^4E or the E_4 enveloped configuration. Thus, the lack of an observed ^1H - ^1H NOESY correlation between H3 and H5 indicated that the amide oxime ether D-55 holds an E_4 enveloped conformation.

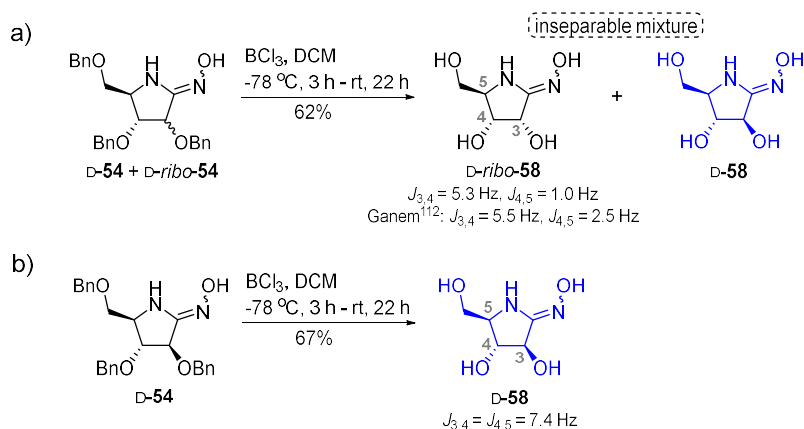
From structure elucidation of the *O*-ethyl amide oxime D-55, the *N*-hydroxyl group was most likely connected to the exocyclic nitrogen in compound D-54. Formation of compound D-54 from triflate L-45 must therefore have commenced by a nucleophilic attack by the hydroxyl amine onto the nitrile carbon to afford the amide oxime intermediate L-56 (Scheme 14a). A subsequent substitution of the protonated triflate moiety by the amide oxime primary nitrogen presumably gave the cyclization product D-54. The proposed mechanism for formation of the aldoxime D-54 was further validated by the treatment of hydroxyl nitrile L-33 with hydroxyl amine (Scheme 14b). In this reaction the nitrile L-33 was converted to the corresponding amide oxime L-57 in 73% yield, interestingly, without formation of unwanted stereoisomers when employing sodium ethoxide for the liberation of hydroxyl amine from its corresponding HCl salt.



Scheme 14. a) Proposed mechanism for formation of amide oxime **D-54** from treatment of nitrile **L-56** with hydroxylamine. b) Formation of amide oxime **L-57** from treatment of nitrile **L-33** with hydroxylamine.

The structure of compounds *D-ribo-54* and **D-54** was demonstrated by the presence of a molecular ion at m/z 455.1940 in the HRMS spectrum, which proved consistent with the molecular formula, *viz.* $C_{26}H_{28}O_4N_2$. Though the suggested mode of formation for compound *D-ribo-54* was reasonable, formation of other isomers could not be dismissed at this point. In 1994 Ganem and coworkers prepared the *ribo*-amide oxime *D-ribo-58* for its evaluation as a nucleoside hydrolase inhibitor.¹³³ To confirm the *ribo*-configuration of compound *D-ribo-54* we therefore treated the stereomeric mixture of amide oximes **D-54** and *D-ribo-54* with boron trichloride (BCl_3) to afford an inseparable mixture of the amide oximes **D-58** and *D-ribo-58* (Scheme 15a). BCl_3 was employed instead of palladium promoted hydrogenolysis to eliminate the possibility of reducing the amide oxime functionality. The difference in the observed ring proton-proton coupling constants in the isomers **D-58** and *D-ribo-58* substantiated that the two compounds are stereoisomers rather than regioisomers. The NMR analysis of the stereomeric mixture (**D-58** and *D-ribo-58*) was thus compared to that of Ganem and co-

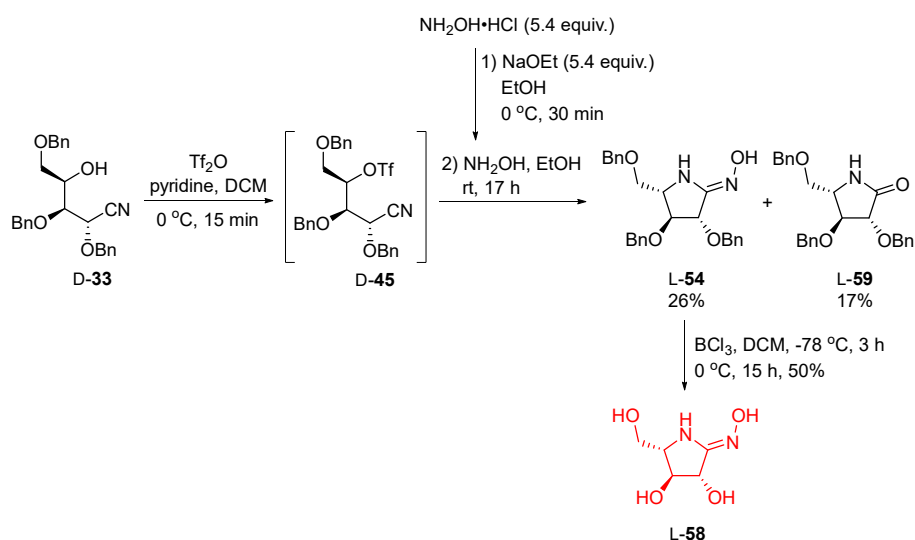
workers' product (D-ribo-**58**).¹³³ Despite the slight difference in H4-H5 coupling constant, the full NMR analysis of the *ribo*-compound D-ribo-**58** presented by the Ganem group supported our suggested *ribo*-configuration for the pyrrolidine D-ribo-**58** prepared by us, and thus also its benzylated congener D-ribo-**54**. Removal of benzyl groups from pyrrolidine D-**54** with BCl₃ further provided D-*arabino*-amide oxime D-**58** (Scheme 15b).



Scheme 15. Boron trichloride mediated removal of benzyl groups from a) the stereomeric mixture consisting of D-**54** and D-ribo-**54**, and consequent formation of D-ribo-**58** and D-**58** as an inseparable mixture, and b) compound D-**54** and formation of amide oxime D-**58**.

The L-*arabino*-amide oxime L-**58** was further prepared from nitrile D-**33** (Scheme 16). Triflation of nitrile D-**33** followed by treatment of the resulting triflate D-**45** with hydroxyl amine provided L-*arabino*-amide oxime L-**54** in 26% yield. To avoid formation of a *ribo*-conformer by racemization of the amide oxime α -carbon, hydroxyl amine was liberated from the corresponding HCl salt by treatment with triethyl amine instead of sodium ethoxide, which had been used in the preparation of amide oxime D-**58**. From the range of minor products that TLC analysis indicated had been formed in the reaction, the *ribo*-conformer was not

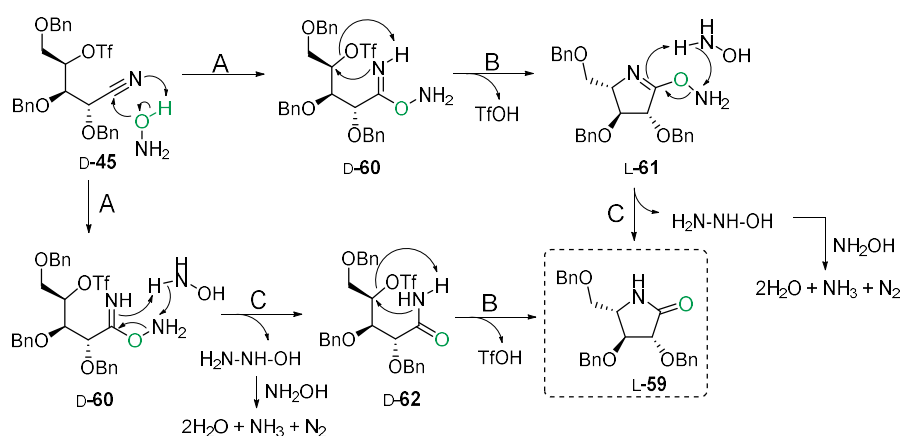
observed. In addition to compound L-54, the known lactam L-59 was isolated from the complex mixture of products.¹³⁴ The formation of lactam L-59 is presumably caused by the primary attack on the nitrile moiety in compound D-45 by the hydroxyl amine oxygen.



Scheme 16. Treatment of triflate D-45 with hydroxylamine provided amidoxime L-54 and amide L-59 as major compounds.

Based on the previous mechanistic studies presented by Stephenson *et al.* in 1969,¹³⁵ and by Vörös *et al.* in 2013,¹³⁶ the mechanism depicted in Scheme 17 was proposed for the formation of lactam L-59. The mechanistic pathway from nitrile D-45 to lactam L-59 is most likely initiated by the attack of the hydroxylamine oxygen onto the nitrile moiety and the resulting formation of *O*-amino amide intermediate D-60 (step A). The next two steps (B and C) may presumably occur in either order. *O*-amino amide L-61 could be formed in a cyclization reaction (step B) from intermediate D-60. The cyclization product L-61 could then

react with excess hydroxylamine *via* the nitrogen (step C), to form amide L-59, along with water, ammonia, and nitrogen. Alternatively, *O*-amino amide intermediate D-60 reacted directly with excess hydroxyl amine (step C) to form amide D-62, followed by a spontaneous cyclization reaction (step B) and the consequent formation of lactam L-59.



Scheme 17. Proposed mechanism for formation of amide L-59 via routes A, B, and C.

With both amide oxime enantiomers D-58 and L-58 in hand, a glycosidase inhibition assay was to be conducted before a potential optimization study for the amide oxime synthesis would be initiated.

3.2 Conclusion

The functionalized *arabino*-amidine enantiomers D-40, D-47, D-48, and D-58 and L-40, L-47, L-48, and L-58 have been prepared from L-xylose (L-27) and D-xylose (D-27), respectively (Figure 18). Key transformations included nitrile formation at C1 of tri-*O*-benzyl xylose

D/L-**36**, followed by inversion of C4 by appropriate *N*-nucleophiles. Cyclization and concomitant formation of the desired functionality finally provided the functionalized *arabino*-amidines **D-40**, **D-47**, **D-48**, and **D-58** and **L-40**, **L-47**, **L-48**, and **L-58**, upon appropriate removal of benzyl groups. The functionalized *arabino*-amidines **D-40**, **D-47**, **D-48**, and **D-58** and **L-40**, **L-47**, **L-48**, and **L-58** were further tested as glycosidase inhibitors by collaborator Óscar L. López at the Universidad de Sevilla in Spain.¹³⁷ The biological data is discussed in chapter 5.

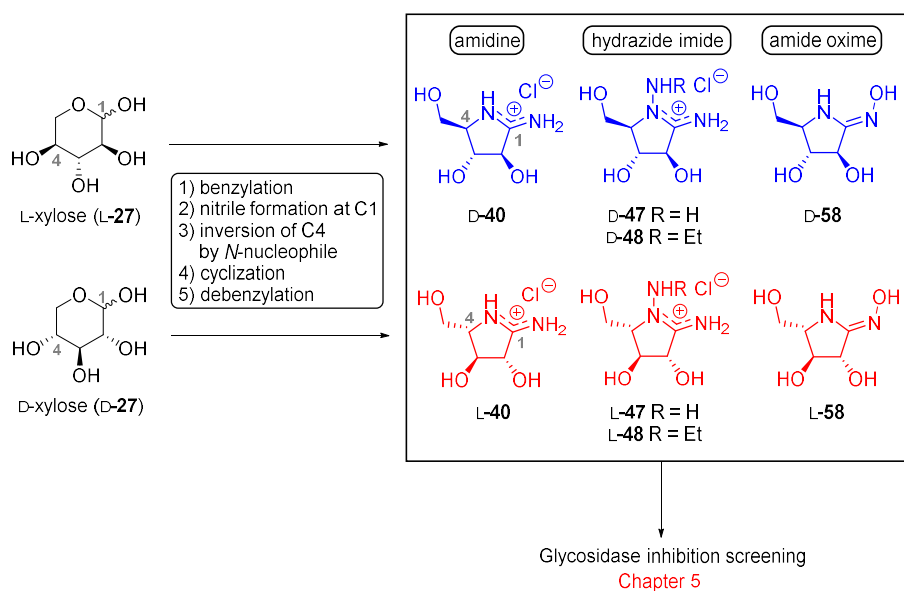


Figure 18. The functionalized *arabino*-amidine enantiomers **D-40**, **D-47**, **D-48**, and **D-58** and **L-40**, **L-47**, **L-48**, and **L-58** synthesized from L-xylose (L-27) and D-xylose (D-27), respectively.

4 Towards the *Glucono*-Hydrazide Imide

In 2000 Ramana and Vasella prepared *glucono*-hydrazide D-63, by introducing a carbonyl group in the 6 position of azafagomine (D-13) (Figure 19).¹³⁸ Hydrazide D-63 exhibited inhibition activity in the micromolar range against β -glucosidase, α -mannosidase, and β -mannosidase. The strong activity against the β -glucosidase was hypothesized to arise from favourable interaction of the lactam moiety in compound D-63 and the catalytic acid of the β -glucosidase.

Instead of the lactam moiety in hydrazide D-63, isofagomidine D-16, prepared by Lindbäck *et al.* possesses a basic amidine moiety in the 1,2-position. Isofagomidine D-16 was a selective α -mannosidase inhibitor, and thus exhibits a very different inhibition profile compared to hydrazide D-63.

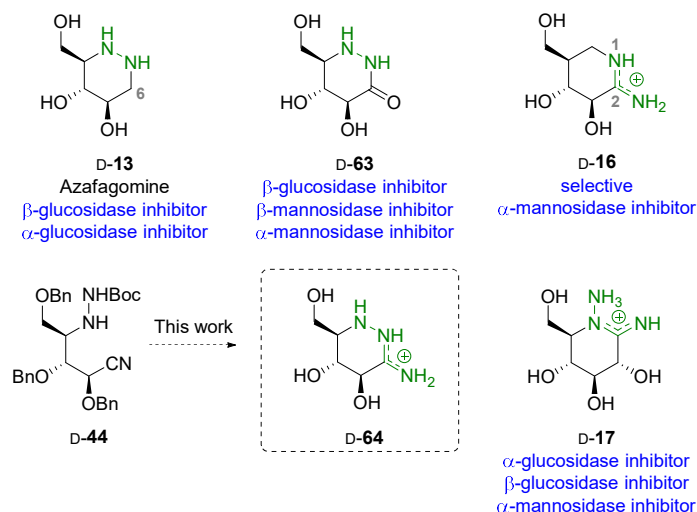


Figure 19. *Glucono*-hydrazide imide D-64 presumably combines the basic hydrazide element of amidine D-16 and the flattened conformation of hydrazide D-63.

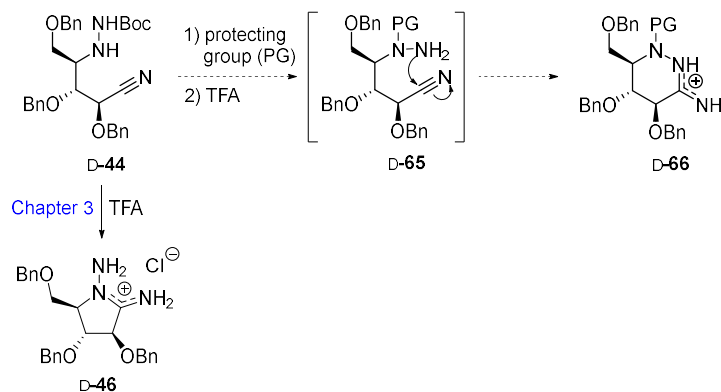
Glucono-iminosugar D-17 with a hydrazide imide moiety has previously been prepared in our group and evaluated as glycosidase inhibitors (Figure 19).⁹⁴ Hydrazide imide D-17 displayed a relatively broad inhibitory profile, with inhibition activity in the micromolar range against α -glucosidase, β -glucosidase, and α -mannosidase. Following up on this, we considered compounds of type D-64, which includes the inhibitory motifs found in compounds D-17 and D-16, *viz.* the basic nitrogen exocyclic nitrogen and the basic amidine moiety, respectively, to be a highly interesting type of compound to investigate as a glycosidase inhibitor. Also, we expected that the combination of the basic hydrazide element of D-16 and the flatten conformation of D-63 would provide interesting glycosidase inhibition.

4.1 Results and Discussion

4.1.1 Strategy with an N-Protecting Group

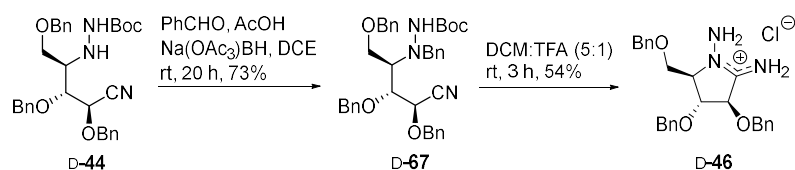
As presented in chapter 3, treatment of hydrazide D-44 with TFA facilitated cyclization to the corresponding pyrrolidine containing a hydrazide imide moiety (Scheme 18). By attaching an acid stable protecting group to the sp^3 hydrazide nitrogen, we hypothesized that treatment with TFA would provide intermediate D-65 which would spontaneously cyclize to the six-membered ring D-66.

Towards the Glucono-Hydrazide Imide



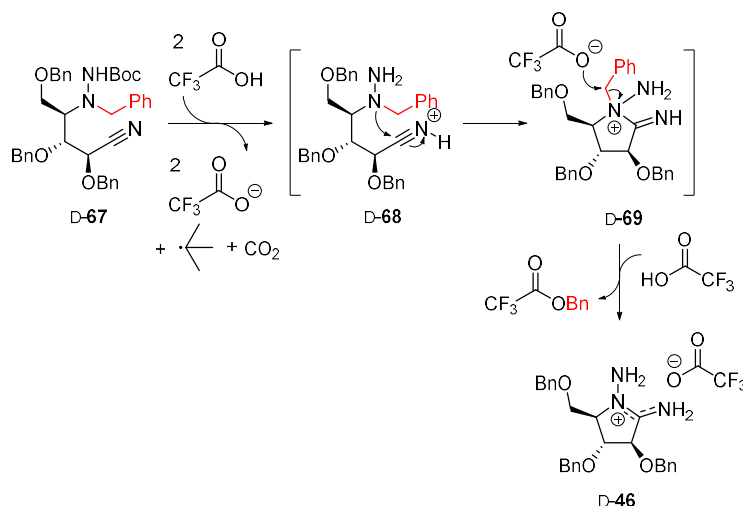
Scheme 18. First strategy for preparation of piperidazine D-66 from hydrazide D-44, via intermediate D-65: attaching a protection group to the sp^3 nitrogen in compound D-44.

Hydrazide D-44 was therefore converted to *N*-benzyl hydrazide D-67 in a reductive amination reaction with benzaldehyde, employing sodium triacetoxyborohydride ($\text{Na}(\text{OAc})_3\text{BH}$) as the reducing agent (Scheme 19). The benzyl group was chosen as protecting group because the *N*-benzyl and *O*-benzyl groups presumably could be removed from piperidazine D-66 simultaneously. Treatment of hydrazide D-67 with TFA for 3 hours effectively removed the Boc group, but piperidazine D-66 was not formed. Instead, hydrazide imide D-46 was obtained in 53% yield, in which the *N*-benzyl group had also been removed.



Scheme 19. Benzylation of hydrazide D-44 followed by acid promoted Boc removal and concomitant cyclization to pyrrolidine D-46.

A mechanism for formation of hydrazide imide **D-46** from *N*-benzyl hydrazide **D-67** was further proposed (Scheme 20). The Boc group was probably first removed by TFA to provide the corresponding hydrazine **D-68**. Nucleophilic attack by the tertiary hydrazine nitrogen onto the nitrile moiety then most likely formed hydrazide imide **D-69** with the benzyl group still attached to the endocyclic quaternary nitrogen. The *N*-benzyl group was presumably removed from hydrazide imide **D-69** by trifluoroacetate present in the reaction mixture. This resulted in the formation of hydrazide imide **D-46** and benzyl trifluoroacetate.

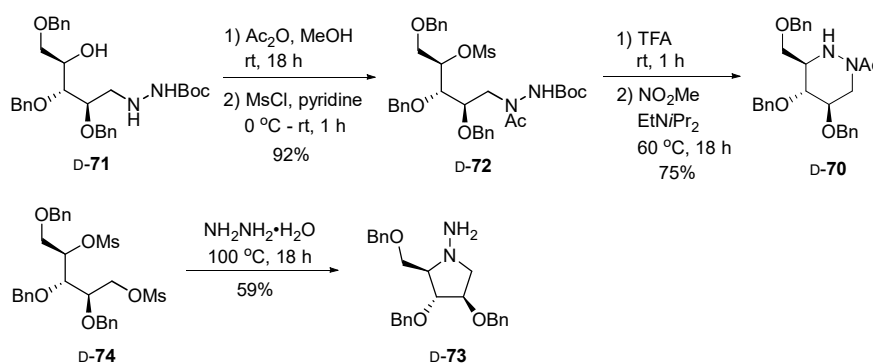


Scheme 20. Proposed mechanism for debenzylation during TFA promoted cyclization.

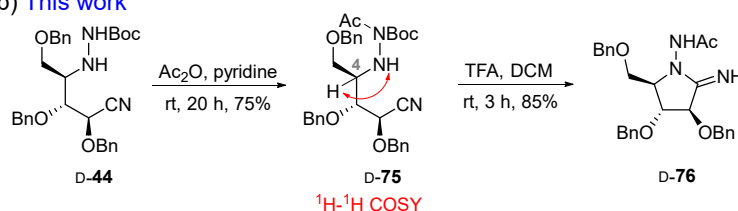
In an attempt to prevent cyclization to the five-membered ring by converting the sp^3 nitrogen in hydrazide **D-44** to a less nucleophilic sp^2 hybridized nitrogen, the protecting group was changed from benzyl to acetyl. The Bols group had previously used the Boc/Acetyl combination of protecting groups for the synthesis of azafagomine **D-70** from hydrazide **D-71**, via the *N*-Boc-*N*-Acetyl hydrazine **D-72** (Scheme 21a).⁸⁷

In the absence of protecting groups, Bols and co-workers obtained the undesired pyrrolidine D-73 from dimesylate D-74. Hydrazide D-44 was thus treated with acetic anhydride and pyridine to obtain the corresponding *N*-acetyl hydrazide D-75 (Scheme 21b). The NMR spectrum of compound D-75 clearly showed the presence of both the Boc and the acetyl group. The ¹H-¹H COSY NMR correlations observed between H4 and the proton on the adjacent amine, however, indicated that the Boc and acetyl groups were both attached to the same nitrogen. Indeed, treatment of *N*-acetyl hydrazide D-75 with TFA afforded pyrrolidine D-76 in 85% yield.

a) Bols and co-workers⁸⁷



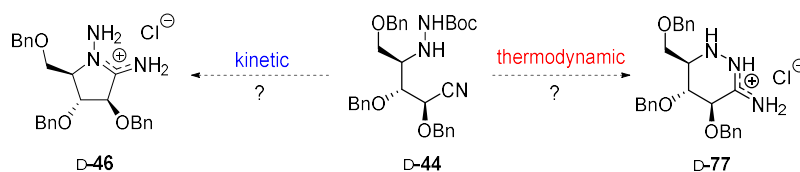
b) This work



Scheme 21. a) Synthesis of *O*-benzyl-*N*-acetyl azafagomine D-70 from hydrazide D-71 conducted by the Bols group.⁸⁷ b) Acetylation of hydrazide D-44 followed by TFA promoted Boc removal and concomitant cyclization to pyrrolidine D-76.

4.1.2 Attempted Formation of a Thermodynamic Product

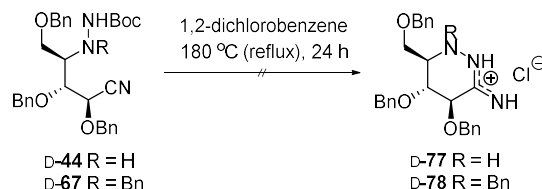
In Bols and co-workers' preparation of *O*-benzyl azafagomine D-70 removal of the Boc group from mesylate D-72 did not facilitate spontaneous formation of the corresponding six-membered ring D-70 (Scheme 21a).⁸⁷ Instead, cyclization was promoted by treating the *N*-acetyl hydrazine intermediate with Hünigs base (EtN*i*Pr₂) in nitromethane (NO₂Me) at 60 °C for 18 hours. Contrary to this, cyclization of hydrazide D-44 to the pyrrolidines, described in chapter 3, occurred spontaneously upon removal of the Boc group, at room temperature. As presented in Scheme 21a, Bols and coworkers also obtained a five-membered ring (D-73) by treatment of dimesylate D-74 with hydrazine hydrate.⁸⁷ With this information at hand, we hypothesized that the five-membered rings, such as D-46, were kinetic products, and that its constitutional isomer, namely the six-membered ring D-77, could be a thermodynamic product (Scheme 22).



Scheme 22. Proposed hypothesis: the six-membered ring D-77 was a thermodynamic cyclization product and the five-membered ring D-46 was a kinetic cyclization product.

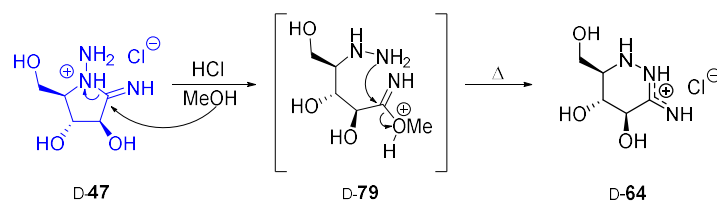
Thermal Boc-deprotection was thus attempted by refluxing hydrazides D-44 and D-67 in dichlorobenzene for 24 hours (Scheme 23). However, neither piperidazines D-77 nor D-78 could be obtained from the complex mixture of unidentified products formed in the reaction.

Towards the Glucono-Hydrazide Imide



Scheme 23. Attempted thermal deprotection of the Boc-group in hydrazides D-44 and D-67 to promote cyclization to the proposed thermodynamic products D-77 and D-78.

We next postulated that the six-membered ring D-64 could be obtained by recyclization of *arabino*-pyrrolidine D-47 under thermodynamic conditions. This could be executed by applying heat to imidate intermediate D-79, formed from acid catalyzed ring opening of hydrazide imide D-47 with methanol (Scheme 24).



Scheme 24. Mechanistic scheme for a proposed recyclization reaction from pyrrolidine D-47 to piperidazine D-64.

Hydrazide imide D-47 was thus dissolved in methanolic HCl and subjected to conventional heating of the solution in a sealed tube (Table 1). The reaction was followed by ^1H NMR analysis of the crude mixture, which turned black over the course of the reaction. Conversion of starting material D-47 was not observed upon heating at 70 °C or 100 °C for 17 hours. However, after running the reaction at 200 °C for 4.5 hours, crude NMR analysis showed the presence of a new product (D-80) in approx. 1:1 mixture with the starting material D-47. Full consummation of the starting material was observed upon turning to microwave irradiation of the reaction, at 150 °C for 90 minutes (Figure 20).

Towards the Glucono-Hydrazide Imide

Table 1. Conversion of hydrazide imide D-47 to hydrazide amide D-80. Reaction conditions: Compound D-47 (8mg), MeOH (1 mL), 0.05 M HCl (AcCl + MeOH)

Entry	Method	Time	Temp	Result ^a
1	Sealed tube	17 h	70 °C	D-47 (no rxn)
2	Sealed tube	17 h	100 °C	D-47 (no rxn)
3	Sealed tube	4.5 h	200 °C	D-47: D-80~1:1
4	Microwave	15 min	100 °C	D-47 (no rxn)
5	Microwave	15 min	150 °C	D-47: D-80 ~4:1
6	Microwave	90 min	150 °C	D-80 ^b

^a Based on ¹H NMR integration of the crude reaction mixture. ^bNo observed starting material.

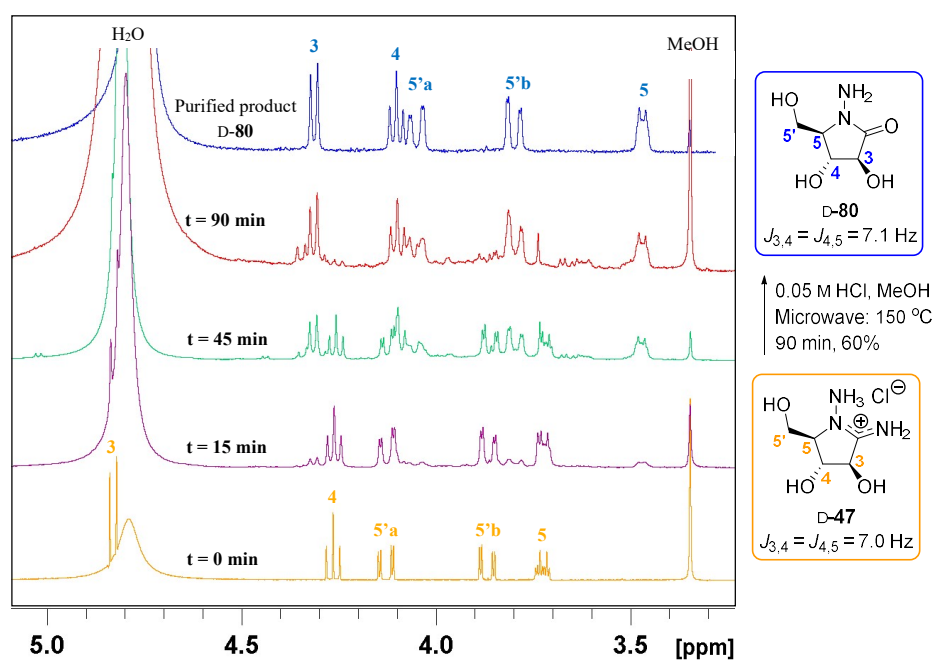
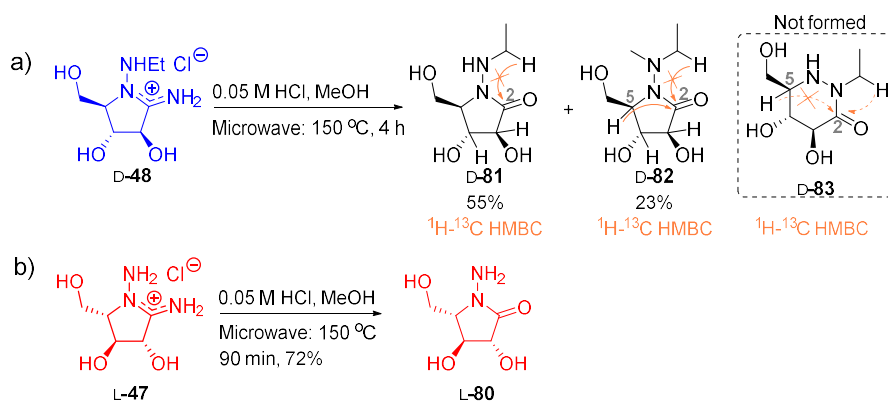


Figure 20. Stacked section of the ¹H NMR spectra that display the conversion of hydrazide imide D-47 to hydrazide amide D-80.

The isolated product from the attempted recyclization reaction was not identified as piperidine D-64. Instead, the presence of a molecular ion at m/z 163.0721 in the HRMS spectrum, proved consistent with the molecular formula of hydrolysis product D-80, *viz.* C₅H₁₁O₄N₂. Moreover, the $J_{3,4}$ and $J_{4,5}$ coupling constants extrapolated from the ¹H NMR spectrum were almost equal to those of pyrrolidine D-47, which indicated that the reaction product was the five-membered ring hydrazide amide D-80. To confirm that product D-80 in fact was a five-membered ring and not a six-membered ring, *N*-ethyl hydrazide imide D-48 was subjected to microwave irradiation under similar reaction conditions as for the conversion of compound D-47 to amide D-80 (Scheme 25a). After 4 hours *N*-ethyl hydrazide amide D-81 and the corresponding methylated compound D-82, were obtained. A ¹H-¹³C HMBC correlation between the ethyl protons and the carbonyl carbon (C2) in compounds D-81 and D-82 should have been evident in the six-membered ring D-83. The absence of said correlation confirmed that both products were five-membered rings. Furthermore, the ¹H-¹³C HMBC correlation observed between H5 and C2 in compound D-82 supported that the six-membered ring D-83 had not been formed.

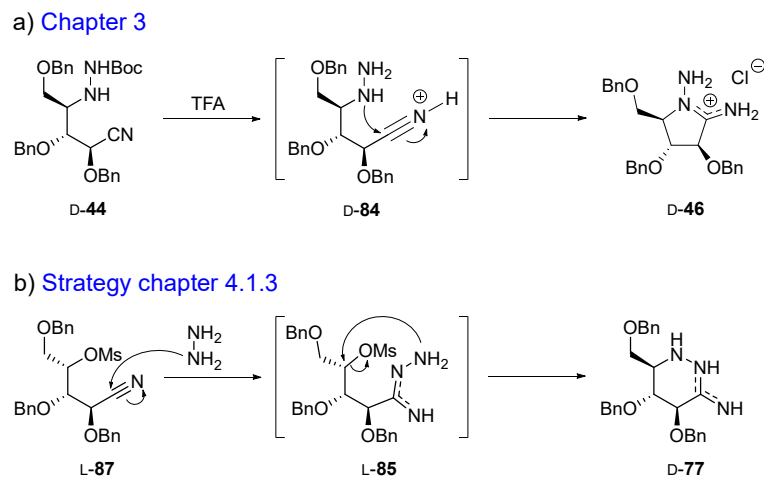


Scheme 25. Treatment with methanolic HCl and subsequent formation of a) amides D-81 and D-82 from hydrazide imide D-48, b) hydrazide amide L-80 from hydrazide imide L-47.

In any case, the hydrolysis product **D-80** was an interesting analogue of the *arabino*-hydrazide imide **D-47** (presented in chapter 3) for the glycosidase inhibition assay. To complete the series, the mirror image of pyrrolidine **D-80**, namely **L-80**, was prepared from the *L-arabino* hydrazide imide **L-47** (Scheme 25b). Microwave irradiation of compound **L-47** in methanolic HCl for 90 minutes provided hydrolysis product **L-80** in 72% yield.

4.1.3 Strategy via Nitrile Activation

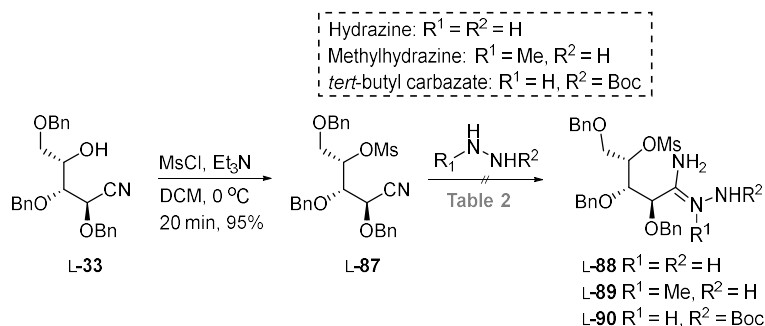
In this project intramolecular nucleophilic attack on the nitrile group by the hydrazine moiety in compound **D-44** and its derivatives, have provided five-membered rings, such as pyrrolidine **D-46**, via intermediate **D-84** (Scheme 26a). We further suggested that cyclization to the six-membered ring **D-77**, could be achieved by intramolecular nucleophilic substitution of a leaving group by a preformed amidrazone moiety (Scheme 26b). The amidrazone intermediate **L-85** could presumably be formed by treatment of nitrile **L-87** with a hydrazine species.¹³⁹ A mesylate was chosen as the leaving group, instead of the more reactive triflate, to avoid an intermolecular substitution of the leaving group by the hydrazine species.



Scheme 26. a) Ring closing of hydrazide D-44 provided pyrrolidine D-46. b) Proposed formation of the six-membered ring D-77 upon treatment of mesylate L-87 with hydrazine.

Nitrile L-33 was therefore converted to the corresponding mesylate L-87 by treatment with mesyl chloride (MsCl) and triethylamine (Et₃N) in dichloromethane (DCM) (Scheme 27). As predicted, substitution of the mesyl group was not observed upon treatment of nitrile L-87 with hydrazine, methyl hydrazine or Boc-protected hydrazine (*tert*-butyl carbazate). However, TLC analysis showed no conversion of the nitrile starting material L-87 in any of the attempted reaction procedures presented in Table 2. Amidrazones L-88-L-90 were thus not obtained under these reaction conditions.

Towards the Glucono-Hydrazide Imide



Scheme 27. Treatment of mesylate L-87 with different hydrazines did not provide the desired hydrazide imides L-88-L-90.

Table 2. Reaction conditions for attempted amidrazone formation (Scheme 27)

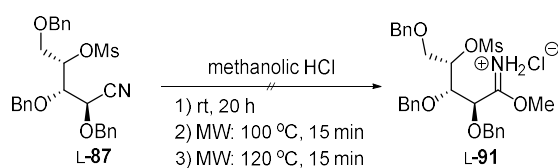
Entry	Nucleophile	Solvent	Promoter	Temperature	Time
1	NH ₂ NHBoc	THF	-	rt	20 h
2	NH ₂ NHBoc	EtOH	CuCl	rt	20 h
3	NH ₂ NH ₂	EtOH	CuCl	rt	20 h
4	NH ₂ NH ₂	EtOH	-	rt	20 h
5	NH ₂ NH ₂	THF	AcOH	rt	20 h
6	NH ₂ NH ₂	THF	TFA	rt	20 h
7	NH ₂ NH ₂	THF	TFA	100 °C (MW)	15 min
8	NH ₂ NH ₂	EtOH	TFA + CuCl	rt	20 h
9	NH ₂ NHMe ^a	MeCN	-	rt	20 h
10	NH ₂ NHMe ^b	MeCN	-	rt	20 h
11	NH ₂ NHMe ^b	MeCN	-	100 °C (MW)	15 min

Towards the Glucono-Hydrazide Imide

12	NH ₂ NHMe ^b	MeCN	-	100 °C (MW)	15 min
13	NH ₂ NHMe ^b	MeCN	TFA	rt	20 h
14	NH ₂ NHMe ^b	MeCN	TFA	100 °C (MW)	15 min
15	NH ₂ NHMe ^b	MeCN	AcOH	rt	20 h
16	NH ₂ NHMe ^b	MeCN	AcOH	100 °C (MW)	15 min
17	NH ₂ NHMe ^b	MeCN	CuCl	rt	20 h
18	NH ₂ NHMe ^b	MeCN	CuCl	100 °C (MW)	15 min

^a5 equiv. ^b10 equiv.

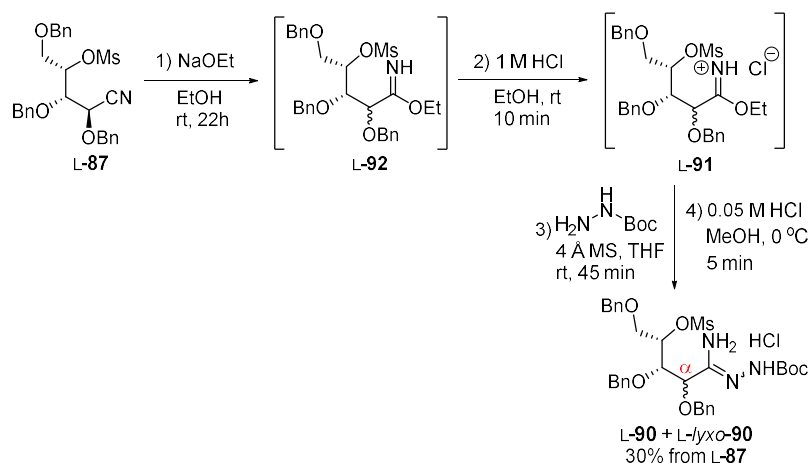
Since the reactivity of nitrile L-87 did not seem sufficient for a direct conversion to the corresponding hydrazide imide we wanted to transform the nitrile L-87 to the corresponding imidate, *viz.* Pinner salt L-91 (Scheme 28). As shown in Scheme 28 compound L-91 was not formed upon treatment of nitrile L-87 with methanolic HCl. No conversion of starting material was observed at room temperature or after subjecting the methanolic solution to microwave irradiation at 100 °C. After running the reaction for 15 minutes at 120 °C NMR analysis of the crude product indicated no conversion of the nitrile moiety, but substantial deprotection of benzyl groups.



Scheme 28. Attempts to form the Pinner salt L-91 from nitrile L-87 was unsuccessful.

Instead of using acidic conditions, nitrile L-87 was treated with sodium ethoxide in ethanol to form imidate L-92 (Scheme 29). However, imidate L-92 could not be isolated due to decomposition of the compound during

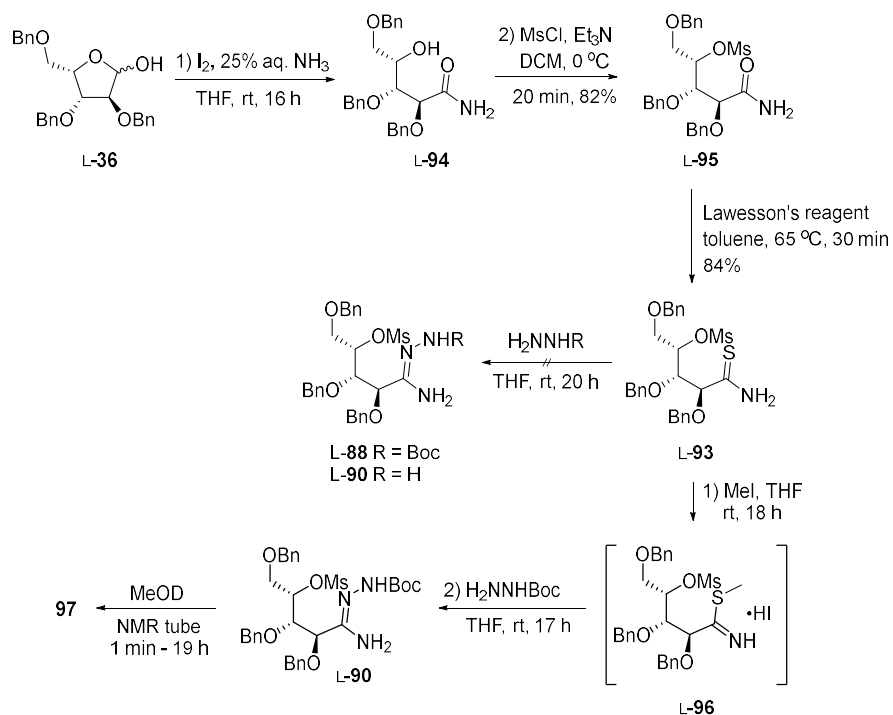
evaporation of the reaction solvent. Before removing the ethanol, the reaction solution was therefore added ethanolic HCl. The resulting Pinner salt **L-91**, identified by low resolution mass spectrometry (LRMS), was then treated with Boc-protected hydrazine that had been pre-treated with 4 Å molecular sieves in THF for 24 hours. Amidrazone **L-90** was finally afforded from nitrile **L-87**, upon treatment with 0.05 M HCl in methanol which presumably provided the corresponding HCl salt. Unsurprisingly, the amidrazone **L-90** α -carbon had epimerized during the reaction, and the product constituted a mixture of *L-xylo*no-amidrazone **L-90** and the *L-lyxo*no-amidrazone **L-lyxo-90**. Most likely, this was caused by sodium ethoxide as seen in chapter 3.1.4 for the preparation of amide oxime **D-54**.



Scheme 29. Formation of the pinner salt **L-91** by treatment of the nitrile **L-87** with NaOEt followed by and acid quench. The pinner salt was treated with *t*-butyl carbazate to provide amidrazone **L-90**.

To avoid epimerization the next approach was to obtain amidrazone **L-90** via thioamide **L-93** (Scheme 30). Furanose **L-36** was first treated with iodine and aqueous ammonia to afford amide **L-94**, as previously reported by Wang *et al.*¹⁴⁰ Product **L-94** was then converted to the corresponding mesylate **L-95**, which was further subjected to Lawesson's reagent to afford thioamide **L-93**. TLC analysis showed no

conversion of compound L-93 upon treatment with Boc protected hydrazine or with hydrazine. Thioamide L-93 was therefore converted to the more reactive thioimidate L-96, which was treated with Boc-protected hydrazine to afford the amidrazone L-90. During purification of compound L-90 by silica gel column chromatography, TLC analysis indicated formation of a new product 97. Compounds L-90 and 97 were isolated separately, but further TLC analysis of the purified amidrazone L-90 indicated that the compound L-90 was converted to compound 97 on the benchtop.



Scheme 30. Asymmetric synthesis of amidrazone L-90 from tribenzylated L-xylose L-36.

Subsequent NMR analysis in deuterated methanol showed that complete transformation of amidrazone L-90 to compound 97 had occurred after 19 hours (Figure 21). LRMS analysis indicated that compound 97 was a hydrolysis product, in which an NH group had been replaced by an oxygen. However, the composition of the suggested hydrolysis product 97 was unclear.

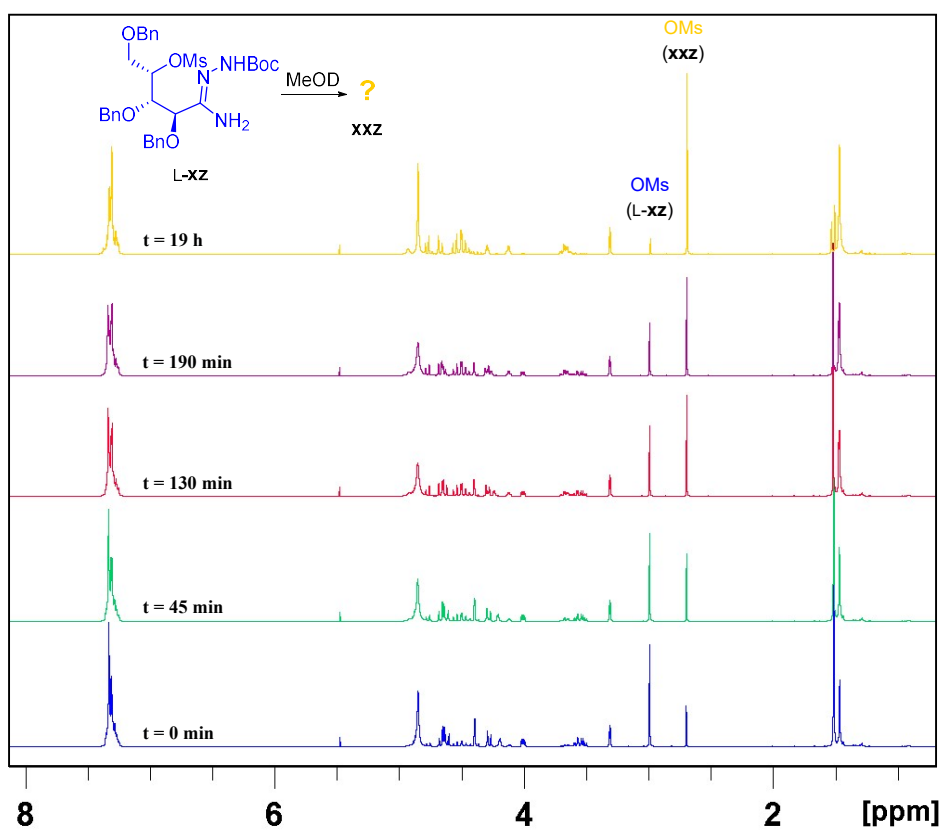
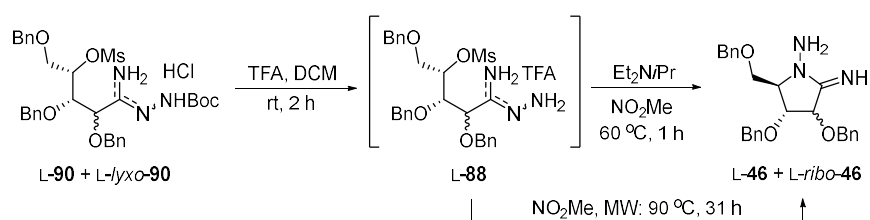


Figure 21. Stacked ¹H NMR spectra showing the conversion of amidrazone L-90 in MeOD, in the NMR tube to an unidentified product 97.

As presented in Scheme 29, amidrazone L-90 + L-lyxo-90 was treated with 0.05 M HCl before purification. Conversion to a corresponding salt

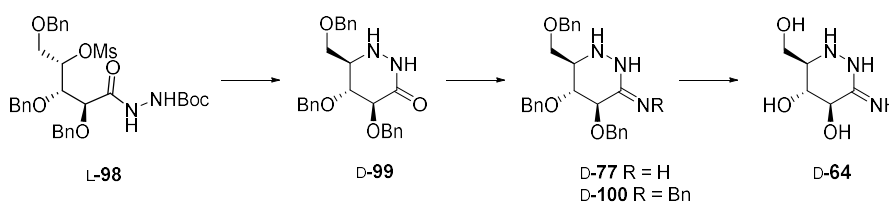
was evidently a good way to avoid hydrolysis of amidrazone L-90 + L-lyxo-90, as described by Ganem and co-workers for the preparation of D-glucono-amidrazones (even though these were not Boc protected).⁸⁸ Before repeating the synthesis of L-90 to provide the unhydrolyzed product, we wanted to verify that the six-membered ring could be obtained from cyclization of amidrazone L-90. The unhydrolyzed amidrazone L-90 + L-lyxo-90 in hand was thus treated with TFA for Boc removal, which gave the intermediate L-88, according to TLC and LRMS analysis (Scheme 31). To convert amidrazone L-88 to the corresponding six-membered cyclization product, intermediate L-88 was treated with Hünig's base in nitromethane at 60 °C, as conducted by the Bols group for formation of azafagomine D-70 (Scheme 21a).⁸⁷ After 1 hour TLC analysis indicated that the cyclization reaction was complete. However, NMR analysis of the crude showed that the undesired five-membered cyclization products L-46 + L-ribo-46 had been formed. Hünig's base was omitted in a second attempt at cyclization of the amidrazone TFA salt L-88 in nitromethane at elevated temperatures. When subjected to microwave irradiation, no reaction could be observed at lower temperatures than 90 °C. After 31 hours, the reaction was complete, as indicated by TLC analysis. However, once again, NMR analysis of the crude showed that the cyclization product was the undesired five membered ring L-46 + L-ribo-46.



Scheme 31. Cyclization of L-90/L-lyxo-90.

4.1.4 Strategy via the Hydrazide Amide

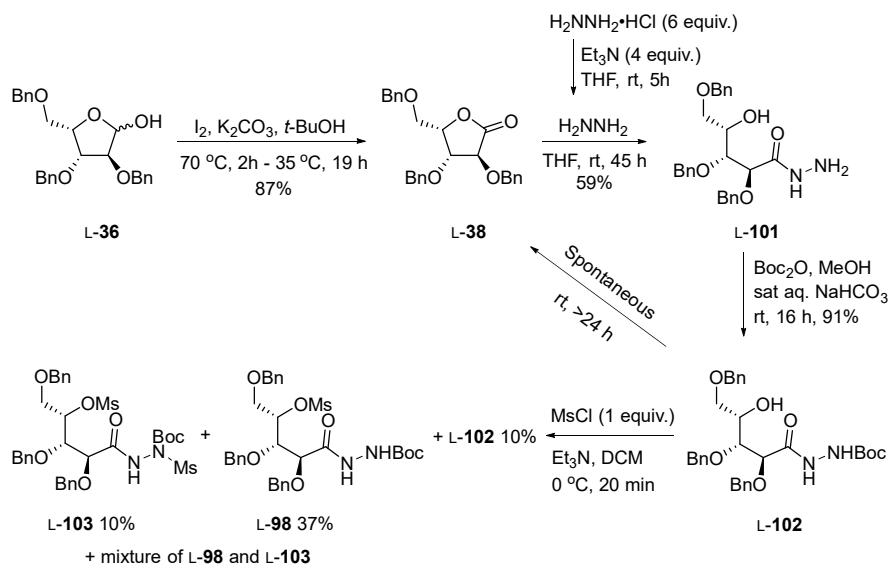
In our next strategy towards the desired six-membered ring, the imide nitrogen in compound L-88 was to be replaced with an oxygen to form compound L-98 (Scheme 32). Removal of the *N*-Boc group followed by a cyclization reaction would presumably provide piperidazine D-99. The hydrazide amide moiety could then be converted to the corresponding hydrazide thioamide, which could further be treated with an amine source such as ammonia or benzylamine to afford hydrazide imide D-77 or D-100, respectively. Removal of benzyl groups would finally afford the desired hydrazide imide D-64.



Scheme 32. Strategy for formation of hydrazide imide D-64 via hydrazide amide D-99.

Preparation of hydrazide L-98 commenced with oxidation of xylose L-36 with molecular iodine and potassium carbonate (Scheme 33).¹⁴¹ The resulting lactone L-38 was further converted to hydrazide L-101 by ring opening with hydrazine.¹²⁸ Selective *N*-Boc protection further provided compound L-102. To avoid the observed spontaneous lactonization of hydrazide L-102 to lactone L-38 occurring at room temperature, compound L-102 was stored at -80 °C (Figure 22). Similar lactonization was also experienced by Meng and Hesse.¹²⁸ The leaving group was then installed by *O*-mesylation with 1 equiv. of mesyl chloride. The desired *O*-mesylate L-98 was isolated in 37% yield from the reaction mixture.

The low yield was caused by formation of substantial amount of di-*N,O*-mesylate L-103.



Scheme 33. Synthesis of hydrazide L-98 via ring opening of lactone L-38 with hydrazine.

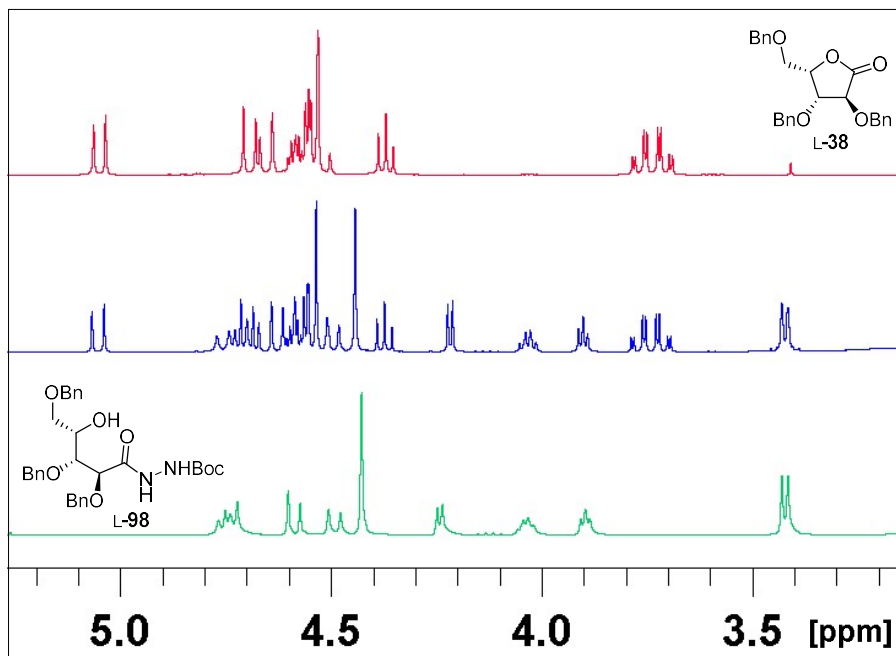
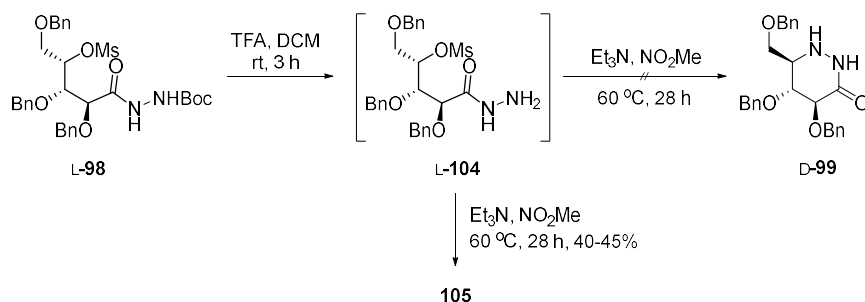


Figure 22. Stacked section of the ¹H NMR spectra showing lactonization of hydrazide L-98.

Mesylate L-98 was further treated with TFA to remove the Boc group (Scheme 34). The presence of a molecular ion at m/z 529 in the LRMS spectrum, proved consistent with the molecular formula of hydrazide L-104, viz. C₂₇H₃₂N₂O₇S. Intermediate L-104 was then treated with triethylamine in nitromethane. After stirring the reaction at 60 °C for 28 h, TLC analysis indicated full conversion of starting material L-104. However, several reaction products had been formed of which the major product (**105**) was afforded in approx. 40-45% yield. NMR analysis of compound **105** showed the presence of 18 aromatic carbons, 7 aliphatic carbons, one carbonyl carbon, two nitrogen, and no mesyl group, which could have been consistent with compound D-99. However, in the HRMS spectrum of compound **105** a molecular ion was observed at m/z 441.2345, which did not correspond with the molecular formula of hydrazide imide D-99. To clarify the structure of compound **105**,

attempts to form crystals for x-ray analysis is in progress at the time of the thesis submission.

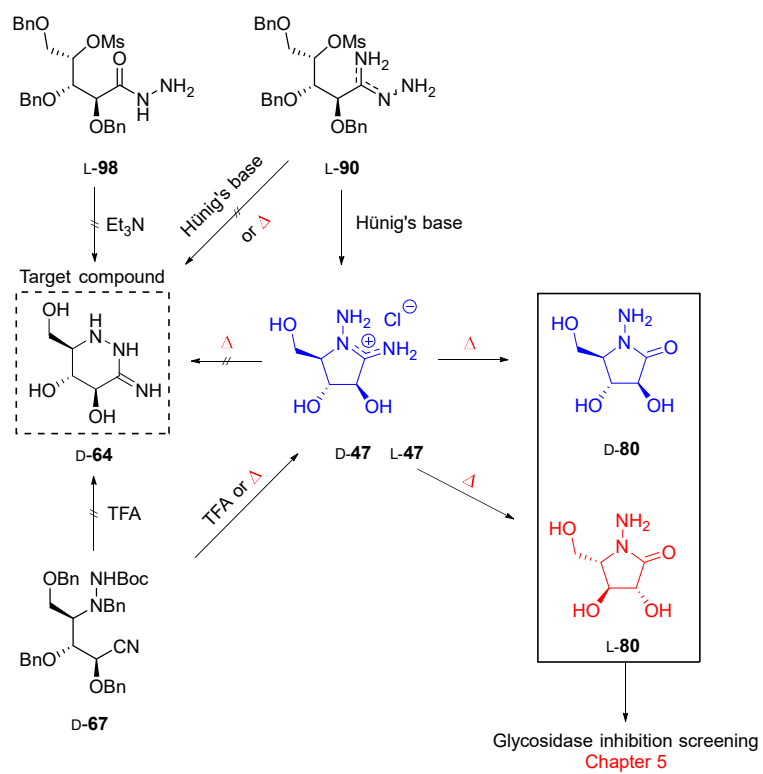


Scheme 34. Attempted formation of hydrazide amide L-99.

4.2 Conclusion

The attempted strategies towards the *glucono*-hydrazide imide target compound D-64 were described in this chapter (Scheme 35). Cyclization of both hydrazide D-67 and amidrazone L-90 afforded pyrrolidine D-47 instead of the desired piperidazine D-77. Moreover, a six-membered cyclization product was not obtained from the attempted ring closing of hydrazide L-98. Efforts to transform pyrrolidine D-47 to target compound D-64 in thermodynamic reaction conditions, resulted in formation of hydrazide amide D-80. Compound D-80 was an interesting analogue to the biologically active iminosugar D-47, and the L-antipode, *viz.* compound L-80, was thus prepared. Hydrazide amides D-80 and L-80 were included in the glycosidase inhibition screening described in chapter 5.

Towards the Glucono-Hydrazide Imide



Scheme 35. The attempted strategies towards hydrazide imide **D-64** described in this chapter.

5 Biological Evaluation of the Pyrrolidine Iminosugars

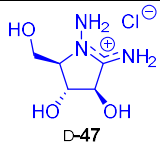
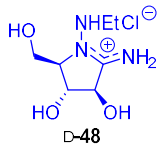
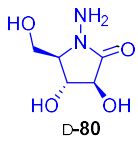

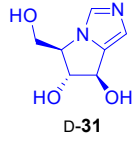
The synthetic iminosugars presented in chapters 3 and 4 were screened by Dr. Óscar L. López at the Universidad de Sevilla, Spain, for their glycosidase inhibition activity against a line of commercially available glycosidases including α -glucosidase (*Saccharomyces cerevisiae*), β -glucosidase (almonds), α -mannosidase (jack beans), β -mannosidase (*Helix pomatia*), α -galactosidase (green coffee beans), β -galactosidase (*Escherichia coli*) and β -galactosidase (*Aspergillus oryzae*).¹³⁷ A selection of the results from the screening are presented in Table 3. At the time for submission of this thesis, only the biological data for compounds D-47, D-48 and D-80 were available to us (Table 3, entry 1-3).

The inhibition data showed that hydrazide imide D-47 was a potent inhibitor of α -mannosidase and α -glucosidase, with a 22-fold selectivity towards α -mannosidase. Though, the corresponding *N*-ethyl hydrazide imide D-48 was a 6-fold weaker α -mannosidase inhibitor than hydrazide imide D-47, compound D-48 selectively inhibited α -mannosidase over α -glucosidase with a selectivity index of >400. In contrast to the selective inhibition displayed by the charged hydrazide imides D-47 and D-48, hydrazide amide D-80 was not active against any of the tested glycosidases.

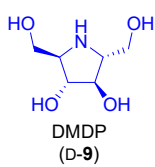
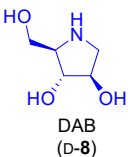
D-*arabino*-diazoles D-30 and D-31, with a rigid pyrrolidine conformation, also display selective α -mannosidase inhibition (Table 3, entries 4 and 5). Still, compound D-48, with a positively charged hydrazide imide moiety was more potent α -mannosidase inhibitor than diazoles D-30 and D-31, by a factor of 26 and 4, respectively. Moreover, in contrast to the natural pyrrolidine-D-iminosugars DAB (D-8) and DMDP (D-9) (Table 3, entries 6 and 7) hydrazide imides D-47 and D-48 showed no inhibition of the β -glycosidases.

Biological Evaluation of the Pyrrolidine Iminosugars

Table 3. Concentration of our synthetic D-arabino-iminosugars giving inhibition of various glycosidases compared to natural D-pyrrolidine iminosugars and synthetic D-arabino-diazoles.

Entry	Compound	α -gluc'ase	β -gluc'ase	α -manno'ase	β -galac'ase
1	 <p>D-47</p>	6.6/5.0 (<i>S.cerevisiae</i>)	NI (almonds)	0.23 (jack beans)	NI (<i>E. coli</i>) (<i>A. oryzae</i>)
2	 <p>D-48</p>	>100 (<i>S.cerevisiae</i>)	NI (almonds)	1.4 (jack beans)	NI (<i>E. coli</i>) (<i>A. oryzae</i>)
3	 <p>D-80</p>	>100 (<i>S.cerevisiae</i>)	NI (almonds)	NI (jack beans)	NI (<i>E. coli</i>) (<i>A. oryzae</i>)
4 ^a	 <p>D-30</p>	160 (yeast)	NI (almond)	36 (jack beans)	NI (<i>E. coli</i>)
5 ^b	 <p>D-31</p>	NI (yeast)	NI (almond)	10/5 (jack beans)	NI (<i>E. coli</i>)

Biological Evaluation of the Pyrrolidine Iminosugars

6	 DMDP (D-9)	1.1 ^d	10 ^c	NI ^c	3.3 ^c
		(yeast)	(almonds)	(jack beans)	(bovine liver)
		214 ^c	9.7 ^c		
		(rice)	(bovine liver)		
7	 DAB (D-8)	0.18 ^e	35 ^g	100 ^c	NI ^e
		(yeast)	(almonds)	(jack beans)	(<i>A. niger</i>)
		250 ^f			
		(rice)			

IC₅₀/K_i (μM), NI = No inhibition (at >100 μM concentration), ^aref.¹²⁴, ^bref.¹²³, ^cref.⁹⁹, ^dref.¹⁰⁵, ^eref.¹⁰³, ^fref.¹⁰², ^gref.¹⁰⁷.

The similarity between the biologically relevant mammalian α-mannosidases and the commercially available Jack bean α-mannosidase makes the latter a useful model enzyme for design of inhibitors.¹⁴² Human (golgi/lysosomal) α-mannosidases plays an important role in *N*-glycan catabolism of glycopeptides, and have been a target of interest in the development of pharmacologically relevant compounds, such as anticancer agents,¹⁴³ and antiviral agents.¹⁴⁴ Compounds that selectively inhibit Jack bean α-mannosidase, such as hydrazide imides D-47 and D-48 may thus be valuable lead compounds in the search for new and improved pharmaceuticals.

6 Towards the Martinella Alkaloids

The alkaloids martinelline (**106**) and martinellic acid (**107**) (Figure 23) were first isolated in 1995 from the roots of the Peruvian plant *Martinella iquitosensis*, by Witherup and co-workers at the Merck laboratories.¹⁴⁵ In 2016 the alkaloids were also identified in several other natural sources, such as the leaves of the Nigerian plant *Emilia coccinea* (Sims) G Dons,¹⁴⁶ skin from the Australian cane toad *Bufo marinus*,¹⁴⁷ and in the Australian plant *Elephantopus scaber*.¹⁴⁸ Extracts from both the martinella plants and the emilia plants have been used for treating eye infections.^{149,150} Witherup and co-workers therefore investigated the toxicity as well as the antimicrobial and anti-inflammatory activities of the isolated alkaloids. Although martinellic acid (**107**) did not display any significant biological activity, Witherup and co-workers found that martinelline (**106**) possessed moderate antimicrobial activity towards *E. coli* and *B. subtilis*.¹⁴⁵ Furthermore, martinelline (**106**) inhibited several G-protein coupled receptor systems, such as the bradykinin, adrenergic, muscarinic and histaminergic receptors, which could substantiate the inflammatory effect. Along with the low toxicity displayed by martinelline (**106**), Witherup and co-workers concluded that these effects were consistent with the properties needed for the treatment of eye infections.

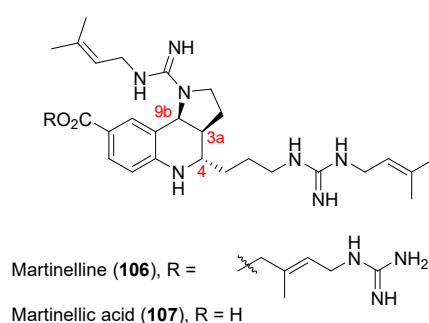


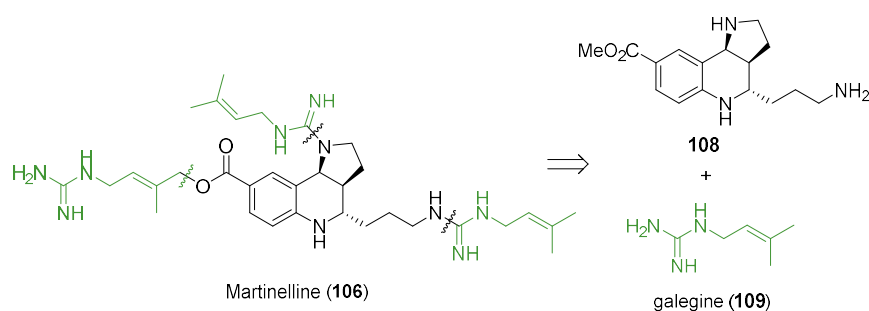
Figure 23. Martinelline (**106**) and Martinellic acid (**107**)

Martinelline (**106**) was the first naturally occurring non-peptidic bradykinin antagonist to be isolated from nature. In addition to their biological properties, the interesting structure of the alkaloids has inspired many chemists to take on the endeavours of synthesizing these natural products. The compounds contain a tricyclic core structure with three consecutive stereocenters. In the structural elucidation of the isolated martinella alkaloids, Witherup and co-workers, found that the proton H4 (Figure 23) was in *trans* position to H3a. Moreover, they identified a *cis*-relationship between protons H3a and H9b. Comparison of the measured optical rotation values between the isolated alkaloids,¹⁴⁵ and the corresponding synthetic enantiopure compounds,¹⁵¹ suggests that the isolated alkaloids in the Merck laboratory were comprised of an epimeric mixture of the two possible stereoisomers. All synthetic preparations of the martinella alkaloids and its partially reduced pyrrolo-[3,2-*c*]-quinoline core structure, since its discovery in 1995, have been summed up in three reviews.¹⁵²⁻¹⁵⁴ The predominant syntheses of the natural products and their tricyclic core structure, are presented in the following chapter.

6.1 Previous Synthetic Preparations of the Martinella Alkaloids

Martinelline (**106**) and martinellie acid (**107**) have been synthetically prepared in a variety of approaches. The common element in all the retrosynthetic strategies, has been a disconnection between the triamine **108** and the galegine side chains **109** (Scheme 36). Galegine (**109**) was identified as a toxic and antidiabetic component from *Galega officinalis* (Goat's Rue),¹⁵⁵ and have also been isolated from a handful of natural sources, such as *Verbesina encelioides* (Asteraceae), as and *Pterogyne nitens*.^{156,157}

The assembly of the triamine **108** was presented by Ma and coworkers in the first reported total synthesis of martinelliac acid (**107**).¹⁵⁸ The structure has since been referred to as Ma's intermediate (**108**), and has been a key target compound in a number of total and formal total syntheses of martinelline (**106**) and martinelliac acid (**107**).^{151,159-169} This section will briefly discuss methods for attachment of the galegine (**109**) side chains to the tricyclic core structure (**108**) to form the martinella alkaloids, followed by a more elaborate presentation of the main types of approaches towards Ma's intermediate (**108**), including its tricyclic scaffold.



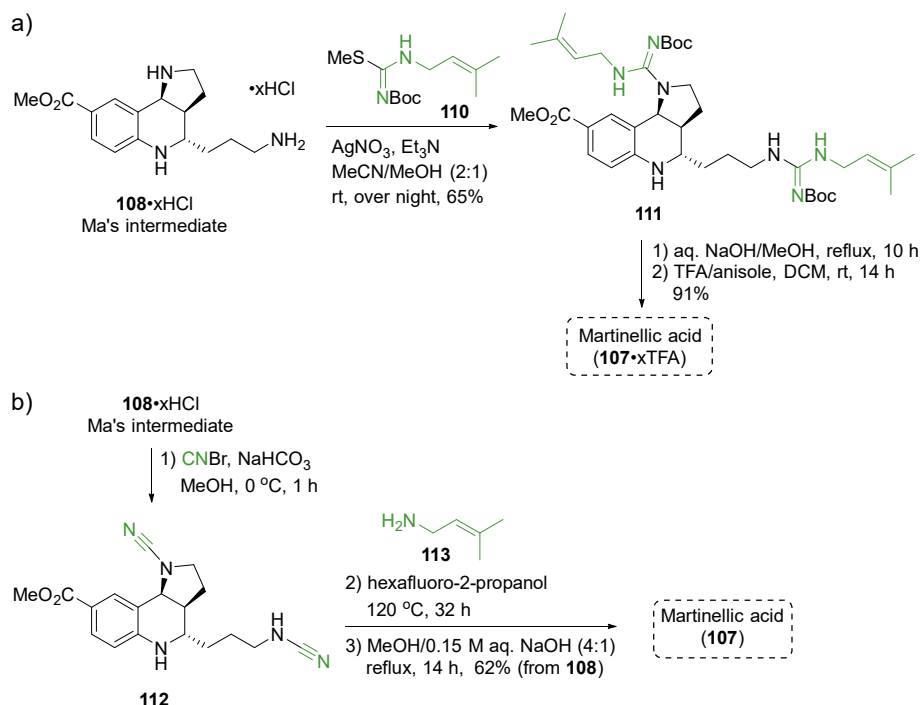
Scheme 36. Typical retrosynthetic chart for the endgame to martinelline (**106**) by disconnecting galegine (**109**) sidechains from the tricyclic scaffold **108**.

6.1.1 Guanidinylation of Ma's Intermediate (**108**)

In June 2001, Ma and co-workers presented the synthesis of the key intermediate **108** (see chapter 6.1.2) and the conversion of the triamine **108** to martinelliac acid (**107**) (Scheme 37a). The said conversion commenced with guanidinylation¹⁷⁰ of triamine **108** with *S*-methylthioisourea **110** in the presence of triethylamine, promoted by

silver nitrate, to provide the corresponding bis-guanidine **111**. The TFA salt of martinelllic acid (**107**) was then obtain from the base catalyzed hydrolysis of the methyl ester moiety in compound **111**, followed by TFA mediated Boc deprotection. A more in-depth model study of the guanidinylation reaction was presented by Ma and co-workers in 2003.¹⁷¹ Their silver nitrate promoted guanidinylation method was also employed by Ikeda *et al.* in 2007 and by Davies *et al.* in 2013 to finalize the syntheses of martinelllic acid (**107**) from Ma's intermediate (**108**).^{151,160}

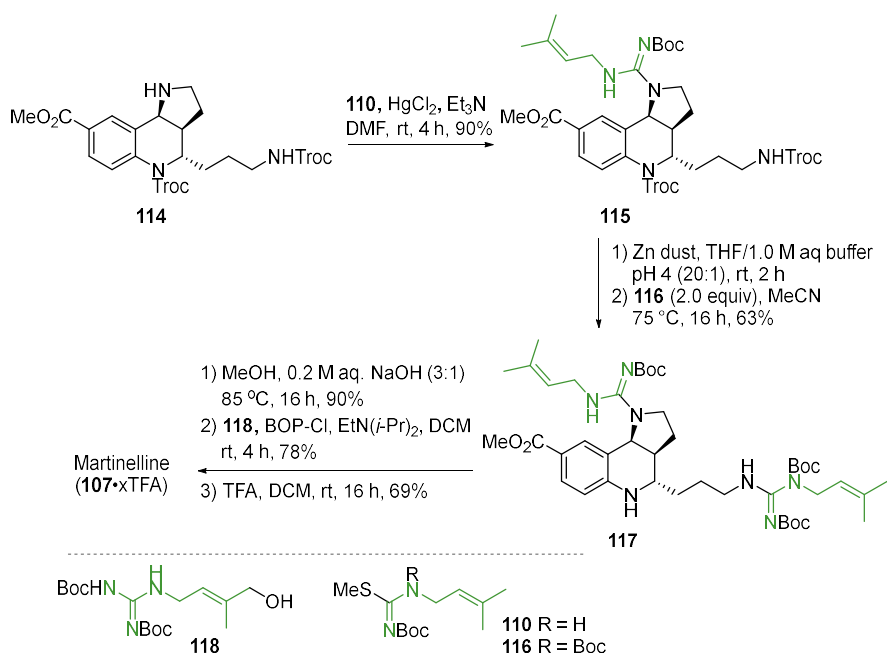
An alternative approach for the formation of martinelllic acid (**107**) from Ma's intermediate (**108**) was presented by Snider *et al.* in November 2001 (Scheme 37b).^{166,172} They converted the triamine **108** to the corresponding bis-cyanamide **112** by reaction with sodium bicarbonate and cyanogen bromide. The bis-cyanamide **112** was then treated with amine **113** in hexafluoro-2-propanol at 120 °C to afford the corresponding bis-guanidine. Final base catalyzed hydrolysis of the methyl ester moiety provided martinelllic acid (**107**) in 62% yield from Ma's intermediate (**108**).



Scheme 37. a) Ma and coworkers' coupling of galegine analogue **110** and Ma's intermediate **108** to form the guanylated product **111**. Subsequent base catalyzed hydrolysis of the methyl ester followed by TFA mediated deprotection of Boc groups provided martinelllic acid (**107**).¹⁵⁸ b) Formation of martinelllic acid (**107**) from Ma's intermediate as performed by Snider, Ahn and O'Hare.^{166,172}

In July 2002, Batey and Powell reported the first total synthesis of martinelline (**106**) (Scheme 38).¹⁶⁵ Due to encountered difficulties with preparing the bis-guanidine **111** in one step from triamine **108**, the guanidinylation protocol was reported by Batey and Powell as a two-step procedure, as presented in Scheme 38. A mercury chloride promoted coupling between the pyrrolidine amine in the di-Troc protected compound **114** and *S*-methylthioisourea **110**, provided guanidine **115**. The Troc groups were further removed by zinc dust in a pH 4 buffer before a second guanidinylation reaction was carried out, this time with the *S*-methylthioisourea **116** as the electrophile, to afford bis-guanidine

117. To finally attach the third galegine (**109**) side chain to compound **117**, Batey and Powell first performed a base catalyzed hydrolysis of the methyl ester moiety in compound **117**. The resulting carboxylic acid was then coupled with hydroxygalegine **118**, mediated by the phosphoric acid coupling agent BOP-Cl. The TFA salt of martinelline (**106**) was then obtained after a final TFA promoted deprotection of the Boc groups. In October 2002 Ma and co-workers also presented a total synthesis of martinelline (**106**) in which they used the carbodiimide EDCI to promote the final coupling of hydroxygalegine **118** to the bis-guanidine compound **117**.¹⁶⁸



Scheme 38. Batey and Powell's two step coupling of galegine electrophile analogues **110** and **116** to the triamine scaffolds **114** and **115**, respectively. The final coupling between hydroxygalegine **118** and methyl ester **117** followed by TFA mediated deprotection of Boc groups, provided martinelline (**106**).¹⁶⁵

6.1.2 Assembly of the Tricyclic Core Structure

As presented in Scheme 36, the martinella alkaloids are composed of a core structure flanked by the galegine (**109**) side chains. The core structure consists of a hexahydropyrrolo-[3,2-*c*]-quinoline (Figure 24a) and is referred to in this thesis as “the martinella scaffold”. This scaffold is a partially reduced derivative of the fused ring system pyrrolo-[3,2-*c*]-quinoline (Figure 24b), and thus named thereafter.¹⁷³ The three stereocenters (C9b, C3a, and C4, Figure 24a) give rise to eight possible stereoisomers of the martinella scaffold. However, in the isolated natural products the protons at C9b and C3a are in *cis* position to one another, leaving four possible stereoisomers.

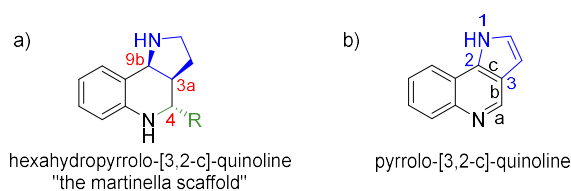


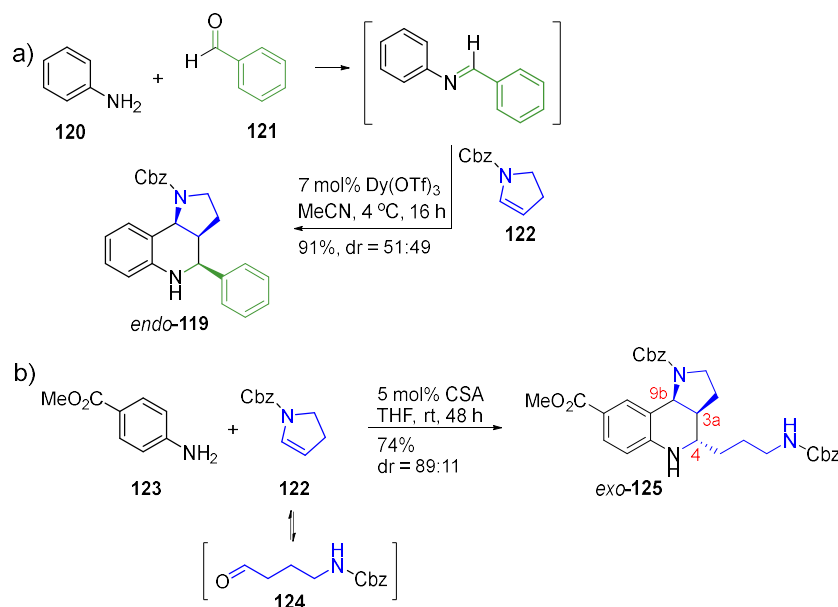
Figure 24. a) The hexahydropyrrolo-[3,2-*c*]-quinoline core structure found in the martinella alkaloids, referred to in this thesis as “the martinella scaffold”, including numbering of the stereocenters. b) The pyrrolo-[3,2-*c*]-quinoline structure with numbering for the nomenclature of fused ring systems.¹⁷³

Hetero Diels-Alder strategy

Batey *et al.* first assembled the hexahydropyrrolo[3,2-*c*]quinoline structure **119** in a three component reaction initiated by the condensation of aniline (**120**) and benzaldehyde (**121**) (Scheme 39a).¹⁷⁴ The resulting imine functioned as the diene in an aza Diels-Alder (DA) reaction with enamine **122**, catalyzed by the lanthanide triflate, Dy(OTf)₃. The DA product **119** was provided from this reaction in an approx. 1:1 mixture of diastereomers (*endo*-**119** and *exo*-**119**). Batey *et al.* further discovered

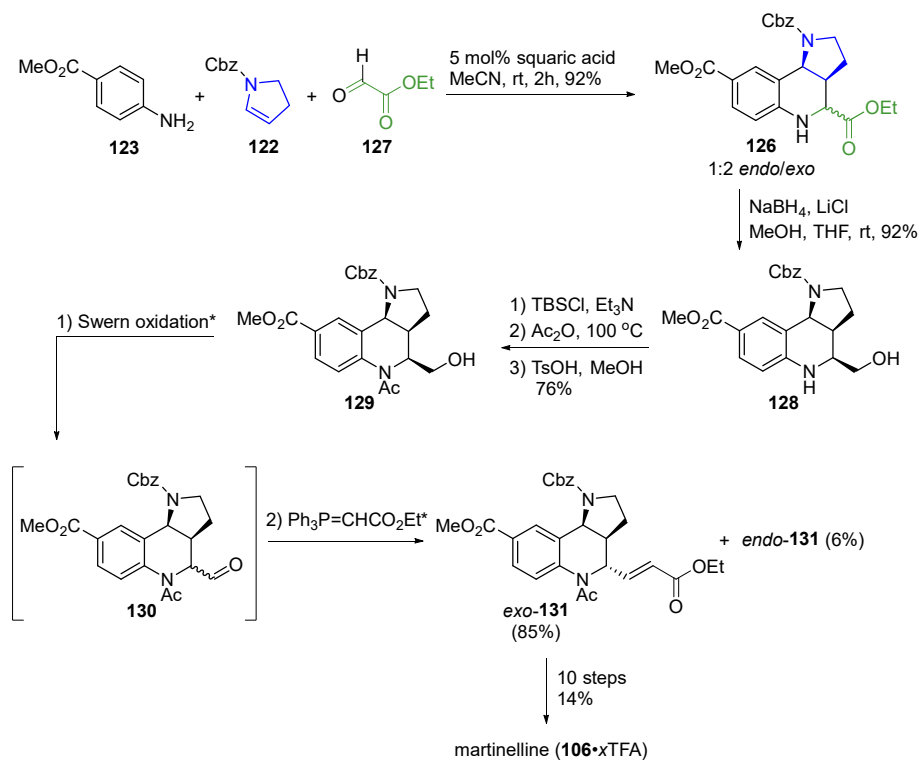
that in the absence of benzaldehyde (**121**), the aniline **120** coupled with two equivalents of the enamine **122** (Scheme 39b). They hypothesized that formation of a diene occurred by condensation of aniline **123** with the *in situ* hydrolyzed product of enamine **124**. The tricyclic product **125** was then obtained from an aza DA reaction between the resulting diene and a second equivalent of the enamine **122**.

The two-component Dy(OTf)₃ catalyzed reaction favoured formation of the *endo*-product (*endo*-**119**). In 2002 Batey and Powell presented a further study of the diastereoselective outcome of this two-component reaction by testing out different protic acids as reaction catalysts.¹⁶⁵ They found that in the presence of camphor sulfonic acid (CSA), the DA product **125** was obtained in 89:11 (*exo/endo*) diastereomeric ratio. The *exo*-product (*exo*-**125**) was further transformed into martinelline (**106**), as described in chapter 6.1.1 (Scheme 38). Though normally and specifically associated with products from the DA reactions, the *endo/exo* terminology has since Batey and Powell's work been widely used to describe the stereochemical relationship between the C4 sidechain and the ring juncture at C3a and C9b of the martinella scaffold (Scheme 39). The *endo/exo* terminology will therefore also be used further on in this thesis.



Scheme 39. Assembly of the tricyclic scaffold (**125**) by Batey and co-workers in a hetero Diels-Alder reaction. dr = diastereomeric ratio (*endo*/*exo* or *exo*/*endo*).

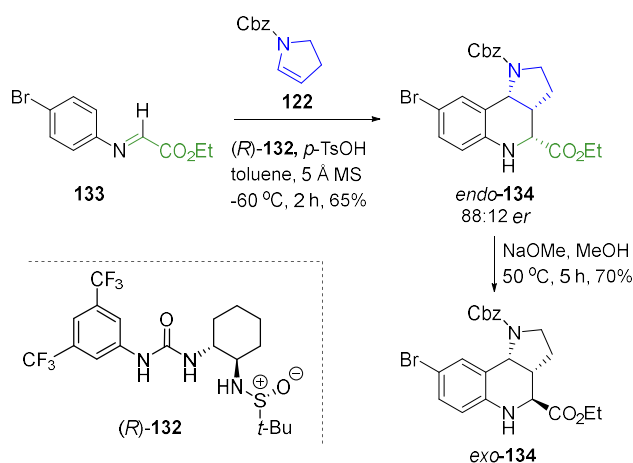
The hetero DA approach was also used by Ma and co-workers in their synthesis of martinelline (**106**).¹⁶⁸ An *endo*/*exo* mixture of the tricyclic core structure **126** was assembled in a three component aza DA reaction between compounds **122**, **123**, and **127**, catalyzed by squaric acid (Scheme 40). Reduction of the ethyl ester moiety in compound **126** provided the corresponding alcohol **128** with an *endo*-configuration. The quinoline nitrogen was then acetylated, and the resulting *N*-acetylated alcohol **129** was subjected to Swern oxidation to form intermediate **130**, followed by a Wittig reaction to yield the corresponding allyl ester **131**. The ethyl ester **131** was isolated as the *exo*-diastereomer in 85% yield, which indicated that the *endo*-aldehyde intermediate *endo*-**130** had been isomerized to its thermodynamically more stable isomer *exo*-**130** under the Swern oxidation conditions. In this approach, the stereochemistry in the DA product **126** could thus be considered irrelevant.



Scheme 40. Synthesis of the martinella scaffold in Ma and coworkers' synthesis of martinelline (**106**) employing a hetero Diels-Alder approach.¹⁶⁸ *Specific reactions conditions were not provided by the authors.

An additional number of publications have explored various conditions for the formation of the martinella core structure as a DA product with high diastereoselectivity.¹⁷⁵⁻¹⁸⁰ However, the first report of an asymmetric hetero DA approach to the martinella core structure was presented by the Jacobsen group.¹⁸¹ They used a chiral urea-based catalyst (*R*)-**132** in the hetero DA reaction between imine **133** and pyrrolidine **122** to obtain the tricyclic *endo*-scaffold **134** with a high enantiomeric ratio (er) (Scheme 41). The opposite enantiomer of the *endo*-compound **134** could be obtained by using the (*S*)-**132** catalyst. The corresponding more stable *exo*-isomer *exo*-**134** was formed upon racemization of the α -amino ester moiety in the *endo*-compound **134** with sodium methoxide. The four resulting enantiomers formed in the

urea catalyzed hetero DA reaction and the subsequent base promoted racemization reaction were further elaborated to a 2328-membered library used in a Stereo/Structure-Activity-Relationship (SSAR) study.¹⁸²

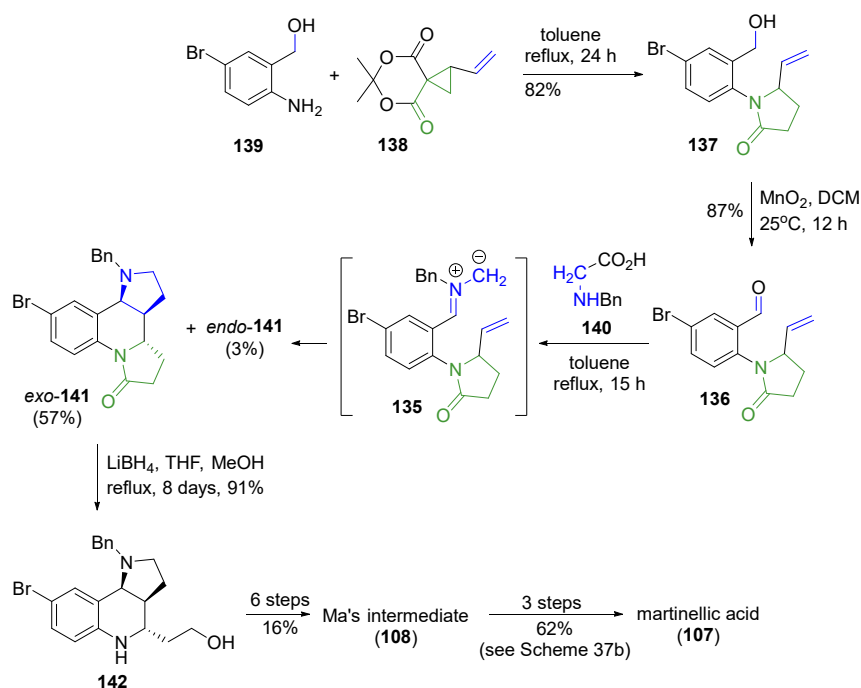


Scheme 41. Scaffold synthesis by Jacobsen, Marcaurelle and co-workers for the assembly of a 2328-membered library used in a Stereo/Structure-Activity-Relationship (SSAR) study.^{181,182}

Via an Imine at C9b

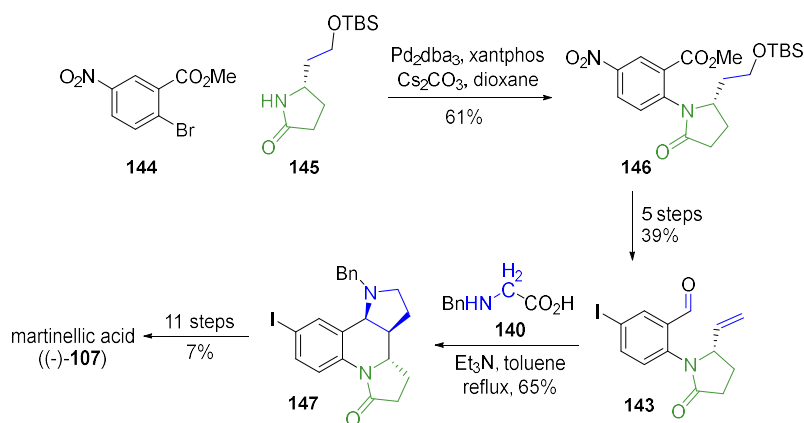
Another approach to martinellid acid (**107**), via an azomethine ylide intermediate **135** (Scheme 42), was presented by Snider *et al.* in 2001. The intermediate precursor, aldehyde **136**, was obtained from oxidation of the corresponding alcohol **137**, which was assembled in a reaction sequence including addition of Danishefsky's vinylcyclopropane **138**¹⁸³ to aniline **139** followed by cyclization to the corresponding pyrrolidinone by the loss of acetone and a final decarboxylation. Condensation of the aldehyde **136** with *N*-benzyl glycine (**140**) provided, upon decarboxylation, the azomethine ylide intermediate **135**, that instantaneously cyclized to the corresponding pyrrolidine **141**.

Reduction of the pyrrolidinone amide moiety in the major *exo*-diastereomer *exo*-**141** provided the tricyclic structure **142**, that was further used in the synthesis of martinelllic acid



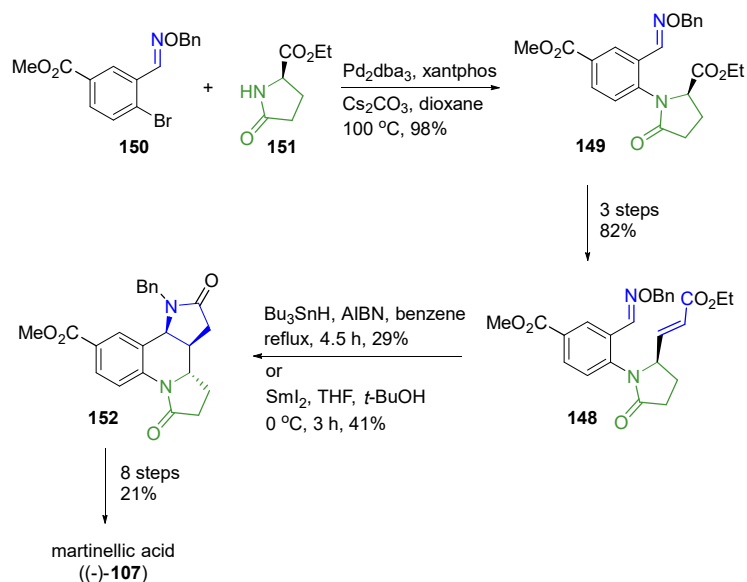
Scheme 42. Assembly of the martinella scaffold via azomethine ylide **135**, by Snider *et al.*¹⁶⁶

An asymmetric version of Snider's azomethine ylide-approach to martinelllic acid (**106**) was presented by Badarinarayana and Lovely in 2007 (Scheme 43).¹⁸⁴ The aldehyde precursor **143** of the azomethine ylide intermediate originated from the coupling reaction between bromoaryl **144** and the chiral pyrrolidinone **145** and consequent formation of compound **146**. The cyclized product **147** was further converted to martinelllic acid ((-)-**106**) in 11 steps.



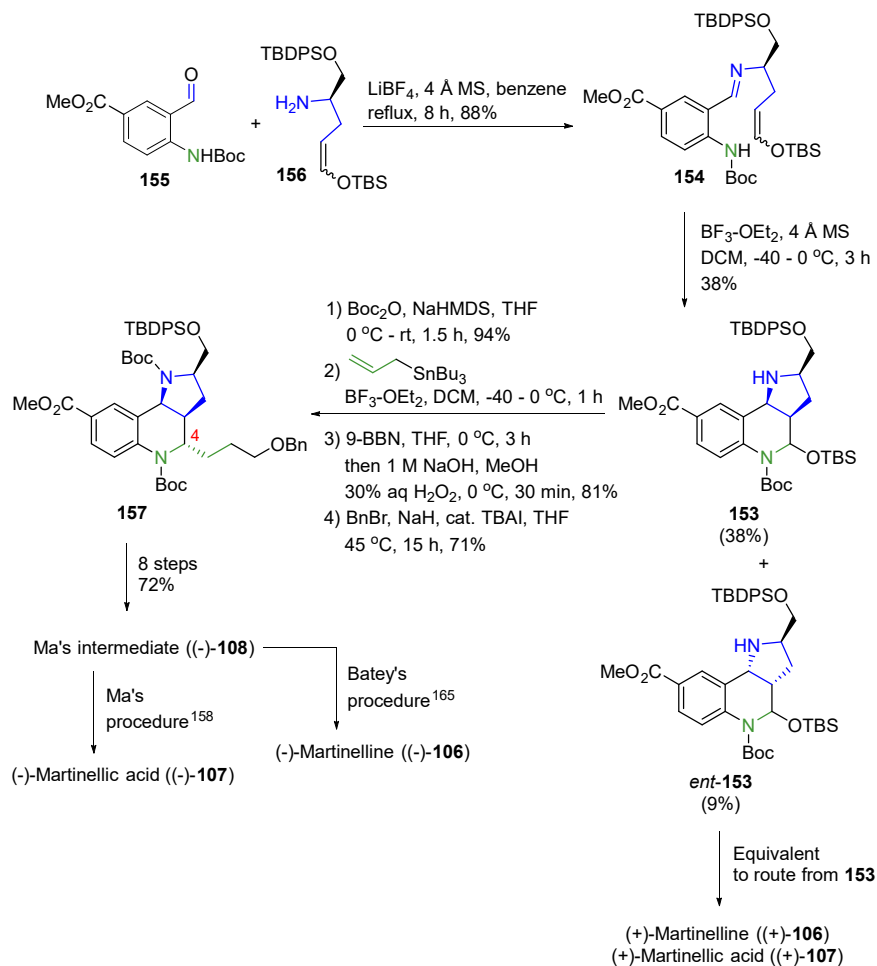
Scheme 43. Badarinarayana and Lovely's enantioselective synthesis of martinelic acid via the azomethine ylide obtained from the chiral amide **145** and bromide **144**.¹⁸⁴

The Naito group presented a radical cascade sequence for the cyclization of compound **148** (Scheme 44), comprised of a similar structure to the azomethine ylide precursors **136** and **143** (Schemes 42 and 43). The aldoxime ether **148** originated from the coupling product **149** generated from the cross coupling of bromoaryl **150** and the chiral pyrrolidinone **151**. The Naito group originally ran the RACE (radical addition-cyclization-elimination) reaction with Bu₃SnH as radical initiator but found that higher yield of the desired diastereomer **152** could be obtained with SmI₂ as presented in Scheme 44.



Scheme 44. RACE chemistry for the asymmetric assembly of the martinella scaffold by the Naito group.^{185,186}

In 2007 the Iwabuchi group presented the synthesis of all four stereoisomers of the martinella alkaloids (-)-**106**, (+)-**106**, (-)-**107**, and (+)-**107**. Assembly of the tricyclic scaffold **153** was obtained in a tandem Mukaiyama-Mannich reaction sequence from imino-alkene **154** (Scheme 45). The imine **154** was the condensation product from benzaldehyde **155** and the chiral amine **156**. The [4+2] cycloaddition provided a separable mixture of diastereomers **153** and *ent*-**153**, each of which were further elaborated to martinelline ((-)-**1** and (+)-**1**) and martinellinic acid ((-)-**2** and (+)-**2**). Diastereoselective installation of the side chain at C-4 was obtained by addition of the allyltributyltin to the *in situ* generated acyliminium ion, formed from treatment with $\text{BF}_3\text{-OEt}_2$. Hydroboration-oxidation of the resulting alkene provided the terminal hydroxyl group to the side chain, which was finally benzylated to form the martinella scaffold **157**.

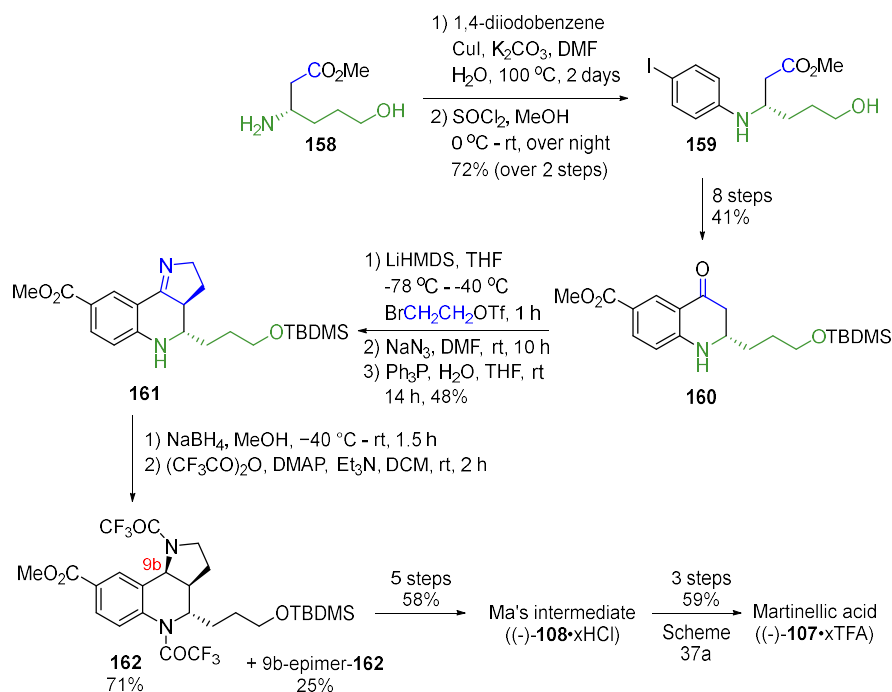


Scheme 45. Synthesis of the martinella enantiomers (-)-106, (+)-106, (-)-107, and (+)-107 presented by the Iwabuchi group.¹⁵¹

Initial Installation of the C4 Stereochemistry

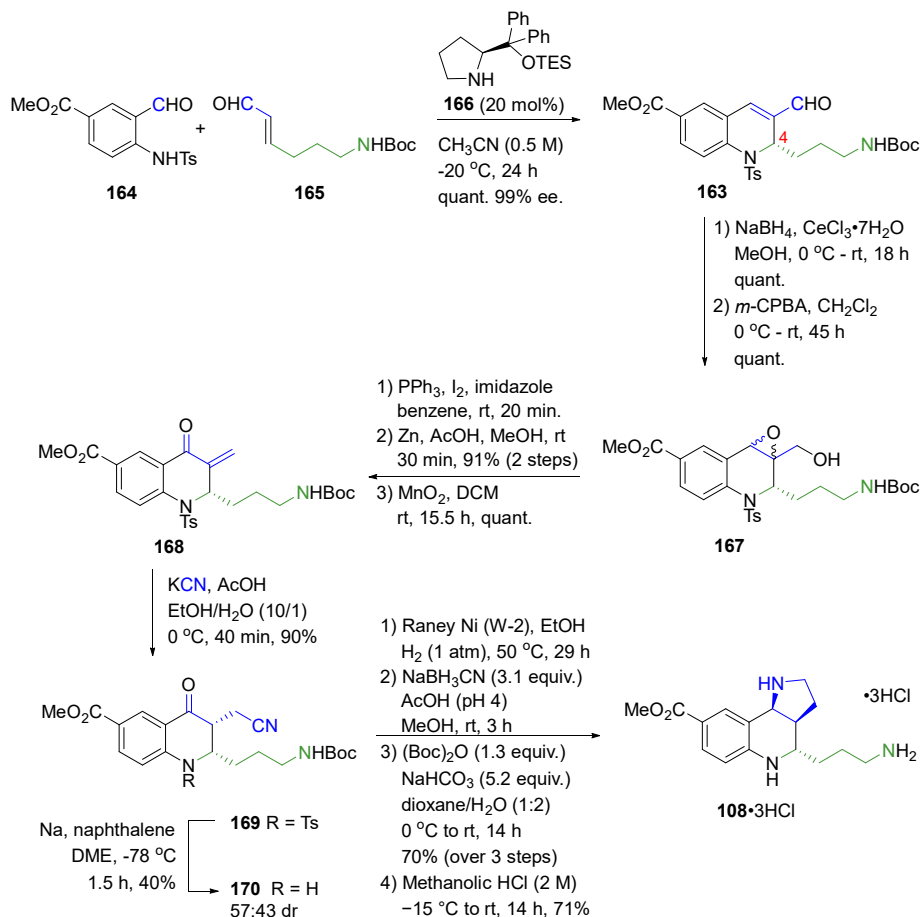
The first asymmetric synthesis of martinellic acid ((-)-107) was reported by Ma and co-workers (Scheme 46).¹⁵⁸ Their synthetic pathway commenced from the chiral β -amino ester **158** which was synthesized from 1,4-butandiol by following a procedure developed by Davies and

co-workers.¹⁸⁷ Methyl ester **159** was obtained from esterification of the corresponding acid, which was the coupling product of 1,4-diiodobenzene and β -aminoester **158**. The methyl ester **159** was converted to ketone **160** in 8 steps, including protection, deprotection and re-protection of amino- and hydroxyl groups, intramolecular acylation, and conversion of the iodo moiety to a methylester group by carbonylation. Stereoselective alkylation of the α carbon in ketone **160** by bromoethyltriflate, followed by azidation and azide reduction provided the condensation product **161**. Imine reduction of compound **161** with sodium borohydride followed by *N*-protection provided the tricyclic scaffold **162** and its 9b-epimer. Compound **162** was further transformed to Ma's intermediate ((-)-**108**·HCl) in 5 steps. The conversion from Ma's intermediate ((-)-**108**) to martinelllic acid ((-)-**107**) has been presented in Scheme 37a.



Scheme 46. Synthesis of (-)-martinellic acid ((-)-**107**) by Ma and co-workers.¹⁵⁸

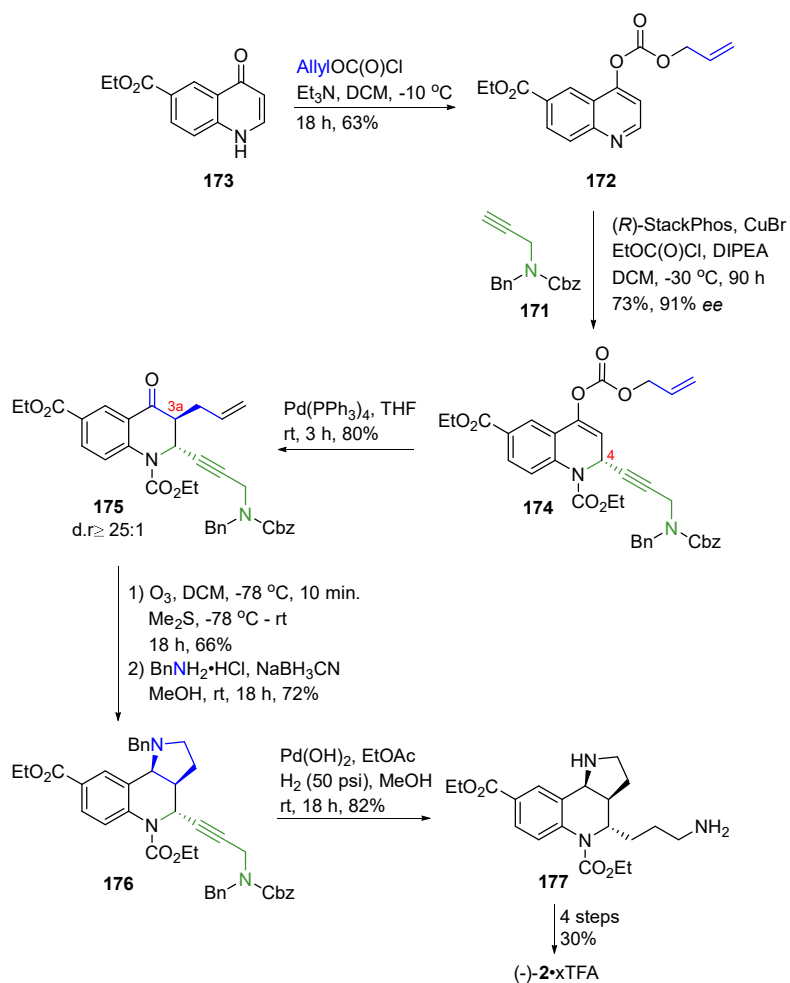
Another approach to the martinella scaffold that commenced with installation of the C-4 stereocenter was reported by the Hamada group (Scheme 47).¹⁶² They obtained the chiral quinoline **163** from an asymmetric Michael Aldol reaction between benzaldehyde **164** and alkenal **165**, catalyzed by organocatalyst **166**. With the C4 stereochemistry in place, the allyl aldehyde **163** was reduced to the corresponding allylic alcohol which was further treated with *m*-CPBA to form epoxide **167**. Iodination of alcohol **167** followed by reductive cleavage, provided the allylic alcohol, that was finally oxidized to the unsaturated ketone **168**. Hydrocyanation of the alkene moiety in compound **168** provided nitrile **169**. After elaborating the nitrile product **169** to Ma's intermediate **108**, the Hamada group realized that alkyl side chains in compound **169** held a *cis* relationship. The *cis* compound **169** proved to be stable under basic conditions and the attempted base-promoted racemization failed. The *N*-tosyl group was suspected to stabilize the *cis* conformer **169**, and *N*-deprotection successfully provided nitrile **170** as a mixture of diastereomers. The more stable *trans* conformer of Ma's intermediate ((-)-**108**•HCl) was finally obtained from the diastereomers **170** by reduction of the nitrile moiety, reduction of the resulting condensation product followed by immediate Boc protection of the triamine. Boc groups were finally removed in methanolic hydrochloric acid which simultaneously formed the HCl salt of Ma's intermediate ((-)-**108**•HCl).



Scheme 47. Synthesis of Ma's intermediate ((-)-**108**) by Hamada and co-workers.¹⁶²

Pappoppula and Apponick installed the C4 stereochemistry in a copper-catalyzed alkylation reaction with alkyne **171** using (*R*)-StackPhos (Scheme 48).¹⁸⁸ The aromatic enol **172**, obtained from treatment of quinolone **173** with Alloc chloride, was in this key step, stereoselectively converted to alkyne **174**. The *trans*-diastereomer **175** was further provided by decarboxylative α -allylation of the allyl carbonate **174**. The alkene moiety in compound **175** was subjected to ozonolysis followed

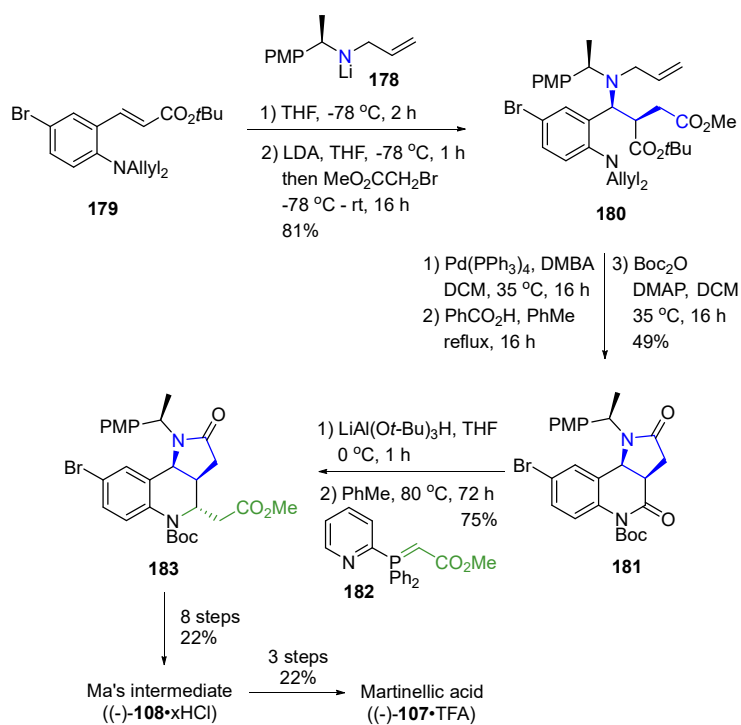
by a double reductive amination to provide the tricyclic scaffold **176**. Reduction of the sidechain alkyne in compound **176** gave compound **177**, which was further converted to martinellie acid ((-)-**107**) in 4 steps.



Scheme 48. Synthesis of martinellie acid ((-)-**2**) by Pappoppula and Aponick.¹⁸⁸

The method for preparation of chiral amines developed by Davies *et al.*,¹⁸⁷ was first used by Ma *et al.* to synthesize martinellie acid ((-)-**107**)

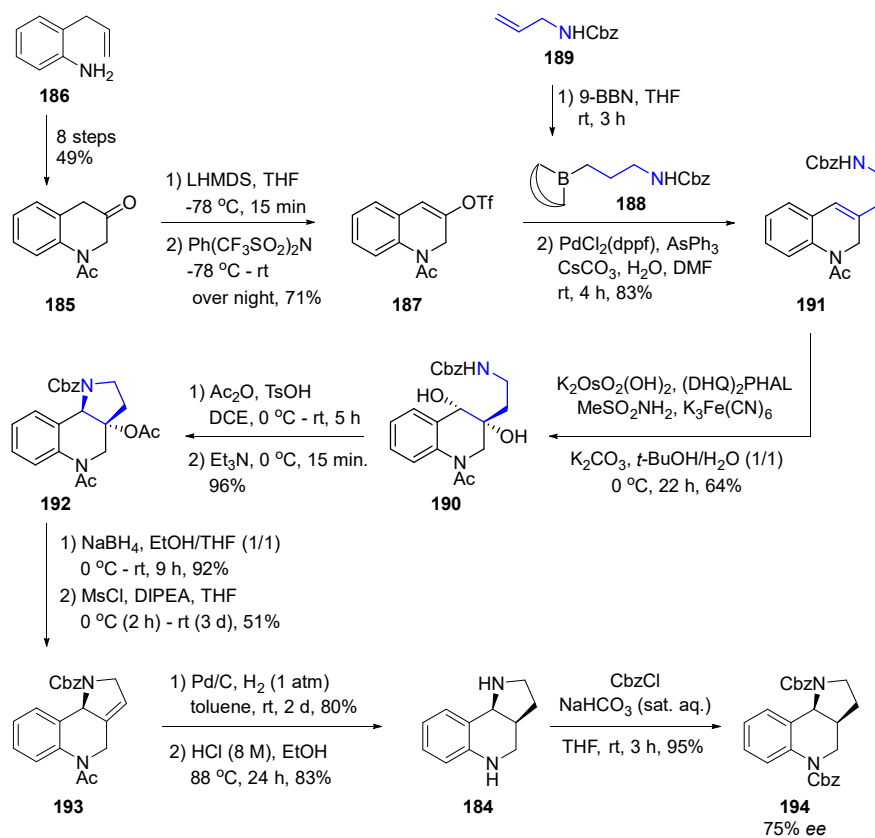
in 2001.¹⁵⁸ Davies and his group later developed their own synthetic route to martinelllic acid ((-)-**107**) from the chiral building block **178** (Scheme 49). Conjugate addition of the lithium amide **178** to the cinnamic ester **179** followed by alkylation with methyl bromoacetate provided the chiral compound **180**. Deprotection of allyl groups followed by a benzoic acid promoted double-cyclization and Boc protection gave the tricyclic compound **181**. With the C9b and C3a stereochemistry in place, the C4 carbonyl group was reduced to its corresponding hemiaminal and treated with phosphorane **182**. The resulting olefin instantly cyclized to the *trans* diastereomer **183** in an intramolecular aza Michael addition reaction. The tricyclic structure **183** was further converted to Ma's intermediate ((-)-**108**) in 8 steps, and finally to martinelllic acid ((-)-**107**).



Scheme 49. Synthesis of Martinelllic acid ((-)-**107**) by Davies *et al.*^{159,160}

Our group has previously explored the use of Sharpless dihydroxylation for installing the stereochemistry of the tricyclic structure **184** (Scheme 50).¹⁸⁹ Quinolone **185** was first obtained in 8 steps from commercially available aniline **186**. Base catalyzed enolization of quinolone **185** followed by triflation of the corresponding enol then provided enol triflate **187**. This was followed by a Suzuki–Miyaura cross-coupling of triflate **187** with boron **188**, which was formed from hydroboration of *N*-Cbz protected allylamine **189**. Diol **190** was then enantioselectively obtained from the Sharpless asymmetric dihydroxylation of quinoline **191**. The tricyclic structure **192** was afforded from acid catalyzed acetylation of diol **190** followed by an intramolecular substitution reaction. The ester moiety in compound **192** was reduced to the corresponding hydroxyl group, which then, upon treatment with mesyl chloride, was dehydrated via elimination of the mesylate to afford alkene **193**. The target compound **184** was finally obtained from hydrogenation of alkene **193** over Pd/C followed by acid mediated removal of the *N*-protecting groups. The tricyclic structure **184** was obtained in 75% *ee*, which was identified by HPLC analysis of the *N*-Cbz protected derivative **194**.

Towards the Martinella Alkaloids



Scheme 50. Our in-house assembly of the partially reduced pyrroloquinoline **184**.¹⁸⁹

6.1.3 Objectives

As described in our review paper,¹⁵⁴ the hexahydropyrrolo[3,2-*c*]quinoline core structure found in the martinella alkaloids is a valuable scaffold for preparation of biologically active molecules. For instance, the library compiled by Marcaurelle and coworkers (Scheme 41),¹⁸² which was assembled around the hexahydropyrrolo[3,2-*c*]quinoline scaffold, has been included in several biological studies for the identification of biologically active compounds, such as pyrroloquinolines **195** and **196** (Figure 25).^{190,191}

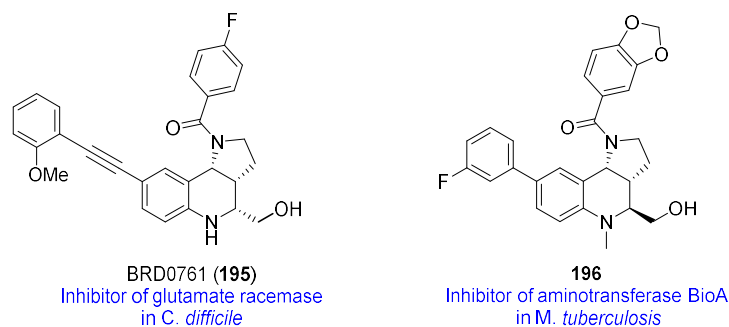


Figure 25. Biologically active compounds assembled around the hexahydropyrrolo-[3,2-*c*]quinoline scaffold.

In this project we wanted to develop an approach for the asymmetric synthesis of martinelline and martinellie acid from commercially available non-chiral building blocks. The purpose of the synthesis was 1) assaying the biological profile of the prepared martinella enantiomers and 2) preparation of analogues to the martinella alkaloids by attaching different side chains to the pyrroloquinoline scaffold. The biological testing, presented in Table 4, was to be conducted by internal and external collaborators.

Table 4. Planned external assays for screening the of the martinella natural products and analogues.

Assay category	Assay name/target	Type
Anti-microbial ^a	Growth inhibition curves (<i>E. coli</i> , <i>S. aureus</i> , <i>C. glutamicum</i> , <i>P. aereginosa</i> , <i>L. anguillarum</i>)	Cellular
	Antifungal test (<i>B. cinerea</i> , <i>S. cerevisiae</i> , <i>C. albicans</i>)	Cellular
Mechanisms of action	Cell viability assay (<i>E. coli</i> and gram-positive bacteria)	Cellular
-anti bacterial ^a	Membrane integrity assay	Cellular
	–test of membrane disruptive capacity	
	Replication inhibition	Cellular
	Protein expression inhibition	Cellular
Mechanism of action -anti fungal ^a	Chitin binding	Biochemical
Anti-cancer ^{b,c,d}	A range of targets are available	Cellular
Immunomodulatory ^b	Human TNF-a, IL-1b (ELISA), interleukins	Cellular
Antioxidants ^b	FRAP	Biochemical
	ORAC	Biochemical
	Cellular anti-oxidant activity	Cellular

Malaria ^c	Confocal imaging assay	Parasite growth
Trypanosomes (brucei and cruzi) ^c	Whole organism HTS	Whole-organism

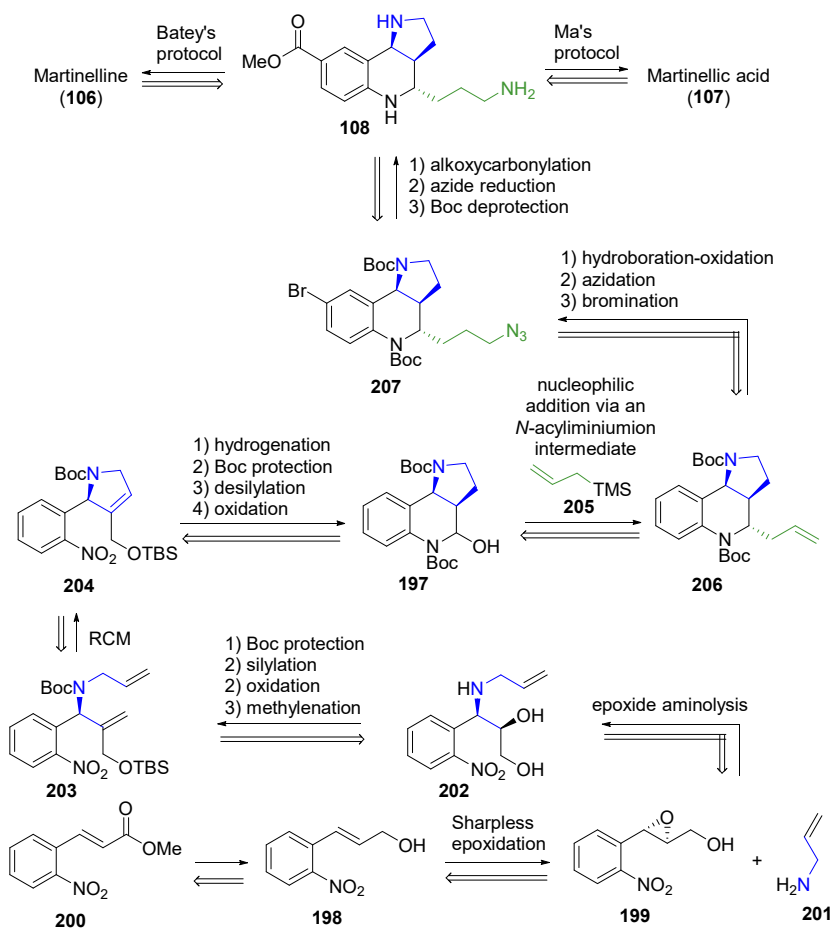
Tests conducted at ^aUniversity of Tromsø (UiT), ^bMarbio-UiT, ^cGriffith University, Australia, and ^dUniversity of Stavanger.

6.2 Results and Discussion

6.2.1 Initial Retrosynthetic Plan

Our synthetic plan for the formation of martinelline ((-)-**106** and (+)-**106**) and martinellic acid ((-)-**107** and (+)-**107**), presented in Scheme 51, included asymmetric assembly of the tricyclic structure **197** and further elaboration to Ma's intermediate (**108**). The triamine **108** could then be converted to the natural products using the series of steps developed by Ma *et al.* to form martinellic acid (**106**) and by Batey and Powell to form martinelline (**107**). The idea behind the stepwise build-up of the martinella alkaloids rather than a one-pot approach, was to enable the mid- and late-stage synthesis of a variety of analogues.

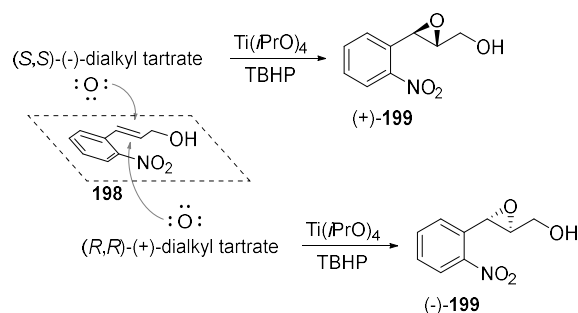
Towards the Martinella Alkaloids



Scheme 51. Our retrosynthetic strategy towards Ma's intermediate (**108**) from 2-nitrocinnamic ester **200**.

The key reaction planned for installation of the stereochemistry was the Sharpless asymmetric epoxidation of the 2-nitrocinnamyl alcohol (**198**) to the corresponding epoxide **199**.¹⁹² The allylic alcohol **198** could be obtained from the selective reduction of the allylic methyl ester **200** which was readily available from our in-house storage, prepared from commercially available 2-nitro benzaldehyde. In the asymmetric Sharpless epoxidation both epoxide enantiomers (-)-**199** and (+)-**199**

could be obtained by employing the two dialkyl tartrate ligand enantiomers (Scheme 52). The Sharpless asymmetric epoxidation of cinnamyl alcohols normally provides epoxides in high enantiomeric excess.^{193,194}



Scheme 52. Sharpless asymmetric epoxidation of 2-nitro cinnamyl alcohol **198**.

With the chiral epoxide **199** in hand, the next step would be to conduct an aminolysis of the epoxide **199** using allylamine (**201**) to form amino diol **202** (Scheme 51). Boc protection of the amine and selective silyl protection of the primary hydroxyl group followed by oxidation of the secondary hydroxyl group and final methylenation of the resulting ketone would provide the dialkene **203**. A ring closing metathesis (RCM) reaction with Grubbs catalyst would presumably generate the pyrrolidine ring fragment of the tricyclic structure and provide us with compound **204**.^{195,196}

We further envisioned that a standard hydrogenation reaction would reduce the pyrrolidine alkene and the nitro group to the corresponding 2-pyrrolidinyl aniline, in one-pot. Upon Boc protection of the aniline, we anticipated that removal of the silyl group and oxidation of the resultant alcohol to the corresponding aldehyde would facilitate spontaneous cyclization to the hemiaminal **197**. Diastereoselective alkylation at the C4 carbon with allyl trimethylsilane (**205**) would likely provide us with compound **206**. This nucleophilic addition reaction, via an *N*-

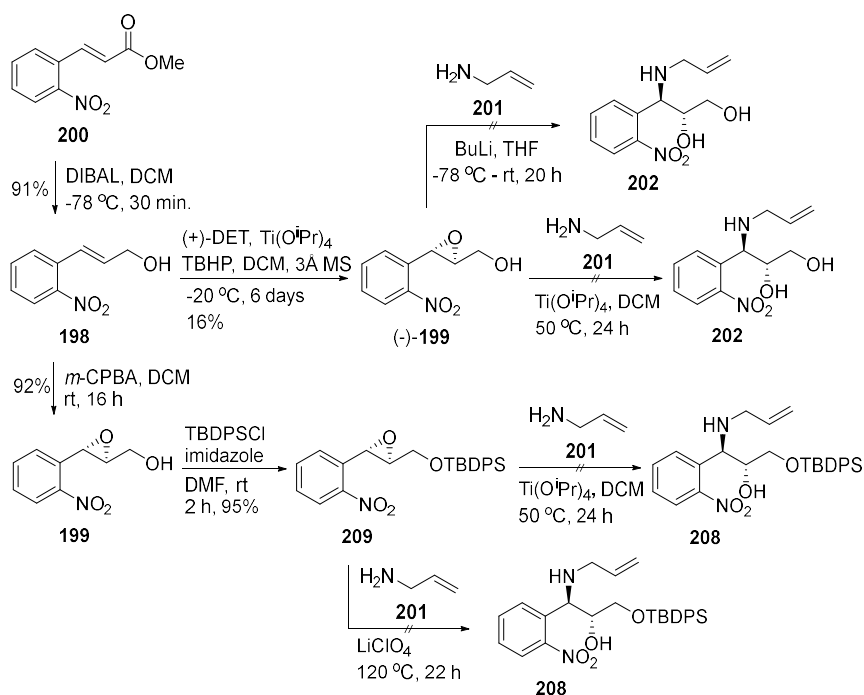
acyliminium intermediate, has previously been performed by Shaw and co-workers on similar compounds.¹⁹⁷

The planned endgame to Ma's intermediate (**108**) included a hydroboration-oxidation sequence of the alkene functionality in compound **206** followed by installation of an azide. Bromination of the aniline in *para* position was expected to provide us with bromo-compound **207**, which upon carbonylation would form the corresponding ester. Finally, reduction of the azide to the corresponding amine and deprotection of Boc groups would provide us with Ma's intermediate (**108**).

6.2.2 Attempted Synthesis from 2-Nitrocinnamic Ester

Nitro-cinnamic ester **200** was converted to the corresponding cinnamyl alcohol **198** in a DIBAL reduction reaction (Scheme 53). The cinnamyl alcohol **198** was treated with *m*-CPBA to provide epoxide **199** in an epimeric mixture as a reference for the stereochemistry of the Sharpless epoxidation product (-)-**199**. Though the epoxidation reaction with *m*-CPBA proceeded smoothly, the Sharpless epoxidation of the nitro-cinnamyl alcohol **198** progressed very slowly. After 6 days reaction time TLC analysis indicated that the mixture contained mostly unreacted starting material. Purification of the reaction mixture by flash column chromatography provided epoxide (-)-**199** in 16% isolated yield. The optical rotation value of epoxide (-)-**199** $\alpha_D = -86.6$ verified the absolute configuration of compound (-)-**199**, when compared to the literature value for the opposite enantiomer (+)-**199** $\alpha_D = +122.64$.¹⁹⁸ Epoxide **199** was further treated with allylamine in the presence of titanium (IV) tetraisopropoxide (Ti(O*i*Pr)₄). However, no conversion of the starting material **199** to amino diol **202** was observed. Efforts to open the epoxide

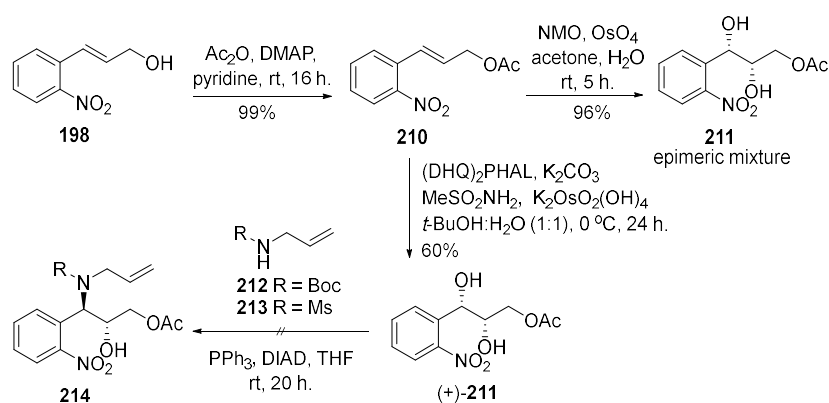
ring with allylamine in a BuLi promoted reaction was also unsuccessful. As was the attempted formation of aminoalcohol **208** by ring opening of the silyl-protected epoxide **209**.



Scheme 53. Epoxidation of nitrocinnamyl alcohol **198** and failed attempts to open the epoxide via aminolysis.

Since the Sharpless epoxidation gave disappointing results and the attempted insertion of allylamine was unsuccessful, we turned to the Sharpless asymmetric dihydroxylation reaction. We envisioned that the diol formed from the dihydroxylation reaction could be converted to the corresponding amino alcohol in a Mitsunobu substitution reaction that would simultaneously reverse the stereochemistry at the benzylic position.

With this strategy in mind, cinnamyl alcohol **198** was first converted to acetate **210** by treatment with acetic anhydride in pyridine (Scheme 54). The vicinal diol (+)-**211** was obtained from alkene **210** in 60% yield in the Sharpless asymmetric dihydroxylation reaction. Treatment of alkene **210** with osmium tetroxide in the presence of *N*-methyl morpholine *N*-oxide (NMO) provided an epimeric mixture of the *cis* vicinal diol **211**. This was used as a stereochemical reference to the Sharpless diol (+)-**211**. Compound (+)-**211** was then treated with triphenylphosphine, diisopropyl azodicarboxylate (DIAD), and an allylamine species (**212** or **213**) in an attempted formation of the amino alcohol **214**. However, no conversion of the starting material (+)-**211** was observed from the Mitsunobu reaction.



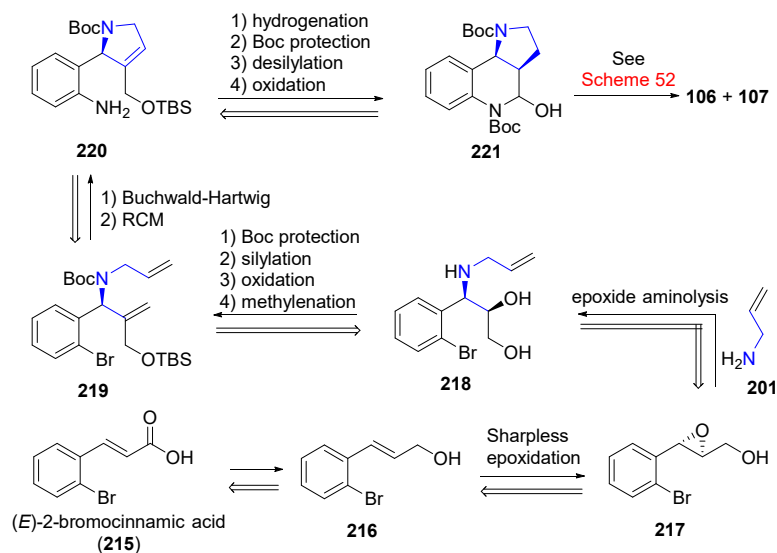
Scheme 54. Dihydroxylation of cinnamyl acetate **210** and failed attempt of a Mitsunobu substitution reaction with protected allylamine.

At this point we suspected that the low conversion from 2-nitrocinnamyl alcohol **198** to the corresponding Sharpless epoxide **199** along with the failed attempts to insert allylamine was caused by inductive effects from the electron withdrawing nitro group in *ortho* position. The

retrosynthetic strategy towards the martinella alkaloids was therefore revised.

6.2.3 Revised Retrosynthetic Strategy

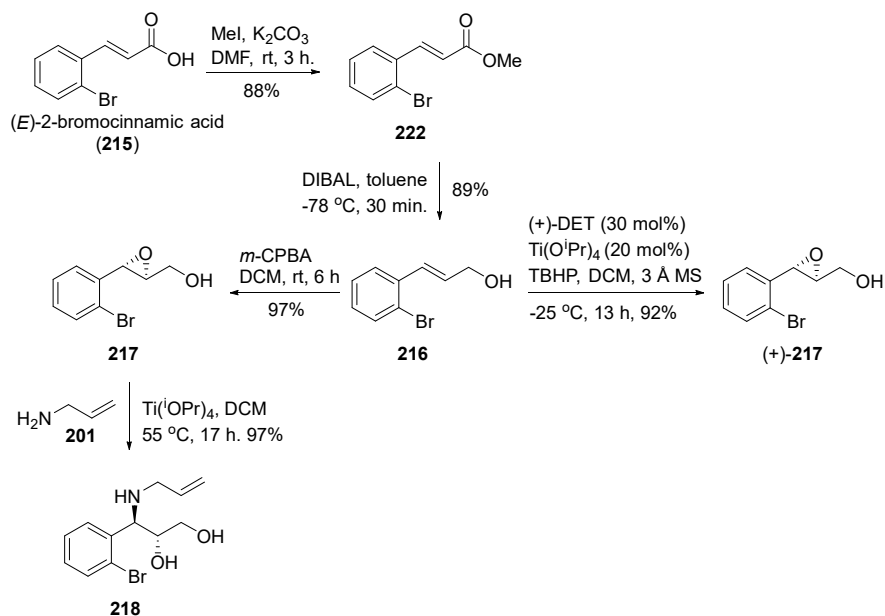
Since we assumed that the nitro group in the cinnamyl compounds was causing trouble, we decided to start the synthesis from commercially available (*E*)-2-bromo-cinnamic acid (**215**) (Scheme 55). Identical to the initial synthetic plan, the stereochemistry was to be installed with the Sharpless asymmetric epoxidation of cinnamyl alcohol **216** followed by aminolysis of the resulting epoxide **217** and formation of amino diol **218**. As before *N*- and *O*-protection followed by oxidation of the free secondary hydroxyl group and methylenation of the resulting ketone would provide a dialkene **219**. After the RCM reaction, we planned to install the aniline amine by a Buchwald-Hartwig amination to form compound **220** from the corresponding bromo compound. We still presumed that hydrogenation of the alkene moiety in compound **220** followed by *N*-Boc protection, removal of the silyl group and oxidation of the resulting free hydroxyl group would provide hemiaminal **221**. The remaining planned pathway towards martinelline (**106**) and martinellic acid (**107**) was kept as described in Scheme 51.



Scheme 55. Revised synthetic strategy towards the Martinella alkaloids, starting from 2-bromocinnamic acid (**215**).

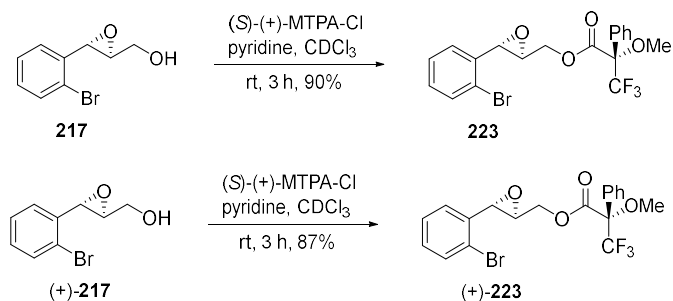
6.2.4 Attempted Synthesis from 2-Bromo Cinnamic acid

Esterification of 2-bromocinnamic acid (**215**) to methyl ester **222** followed by DIBAL reduction to cinnamyl alcohol **216** proceeded uneventfully (Scheme 56). The cinnamyl alcohol **216** was then subjected to the standard Sharpless asymmetric epoxidation reaction conditions, and the epoxide (+)-**217** could fortunately be isolated in 92% yield. The optical rotation values of Sharpless product (+)-**217** was $\alpha_D = +17.3$. The cinnamyl alcohol was also treated with *m*-CPBA to form epoxide **217** as a racemic reference. Regioselective aminolysis of epoxide **217**, mediated by Ti(*i*OPr)₄, provided the amino diol **218** in excellent yield.



Scheme 56. Formation of epoxide **217** from (*E*)-2-bromocinnamic acid followed by titanium isopropoxide mediate regioselective aminolysis to form amino diol **218**.

To determine the enantiomeric excess (*ee*) of compound (+)-**217** generated by the Sharpless asymmetric epoxidation, epoxide (+)-**217** was converted to the corresponding Mosher ester (+)-**223** (Scheme 57).^{199,200} Compound **223** was formed from epoxide **217** as a racemic reference. ¹H NMR analysis of the esters (+)-**223** and **223** displayed the Mosher ester diastereomers in an 88:12 ratio (Figure 26). This indicated that epoxide (+)-**217** was provided in 76% *ee* from the Sharpless asymmetric epoxidation reaction.



Scheme 57. Preparation of Mosher ester **223** for NMR analysis of the enantiomeric excess (*ee*) of epoxide **(+)-217**.

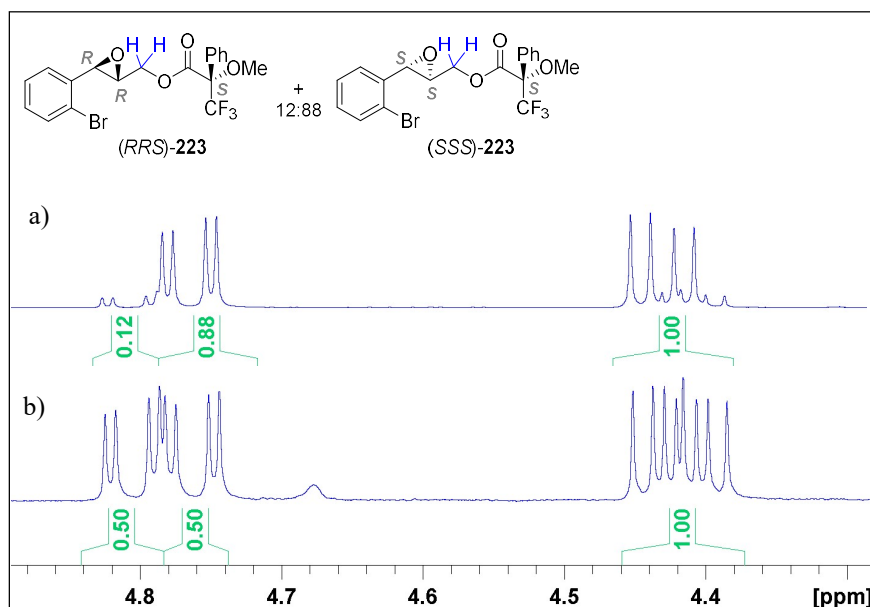
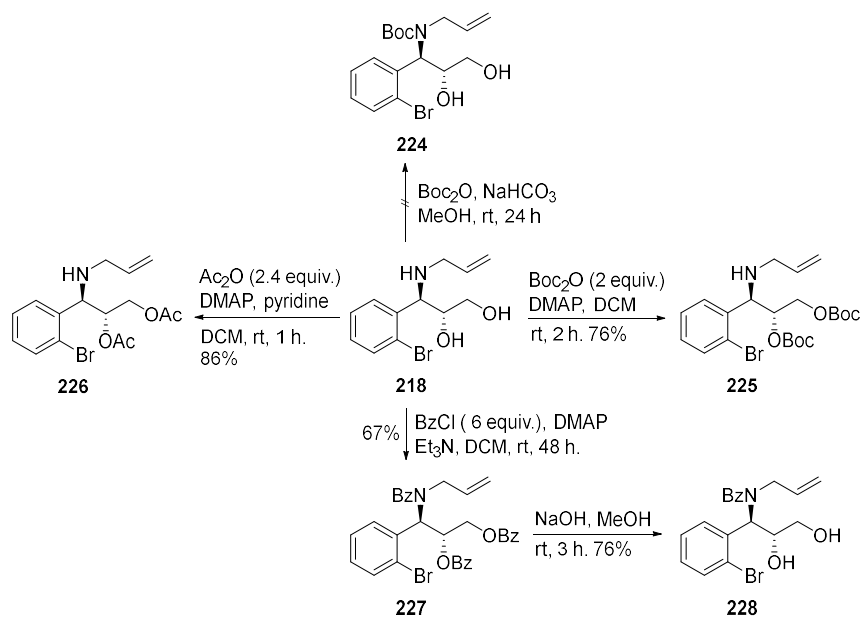


Figure 26. Projection of the 88:12 enantiomeric ratio of the epoxide **(+)-217** by ^1H NMR analysis of the CH_2 protons (in blue) in the corresponding Mosher ester diastereomers **(RRS)-223** and **(SSS)-223**. Epoxidation reaction conditions are a) Sharpless Asymmetric epoxidation, b) *m*-CPBA.

The amino diol **218** was further treated with Boc anhydride and sodium bicarbonate in methanol for the selective *N*-Boc protection (Scheme 58).

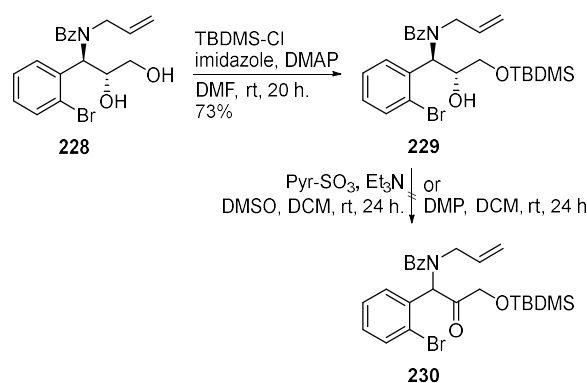
However, we observed no conversion of the starting material **218** to the corresponding *N*-Boc compound **224** in this reaction. Instead, we attempted DMAP promoted Boc protection of the amino diol **218** in dichloromethane. Unfortunately, these reaction conditions provided the *O*-Boc protected compound and left us with a free amine in compound **225**. Equally, acetylation of the amino diol **218** provided the *O*-acetylated compound **226**, with no trace of *N*-acetylation occurring. Selective *N*-protection was apparently not possible. Instead, amino diol **218** was treated with six equivalents of benzoyl chloride to form the tri-benzoylated compound **227**. The base-labile *O*-benzoyl groups were then carefully hydrolysed with sodium hydroxide in methanol to provide the diol **228**.



Scheme 58. *N*-protection of aminodiol **218**.

Silyl protection of the primary hydroxyl group in compound **228** proceeded smoothly (Scheme 59). Oxidation of the secondary hydroxyl group in compound **229** was however, unsuccessful. Neither treatment of alcohol **229** with freshly prepared Dess Martin Periodinane, nor

subjection to the conventional Parikh-Doering reaction conditions provided us with the desired ketone **230**. The reason for the failed oxidation was unclear to us. Still, we considered steric hinderance to possibly make the hydroxyl group inaccessible for an oxidant. Rather than employing the benzoyl protected compound **228**, we therefore returned to acetylation of amino diol **218**.

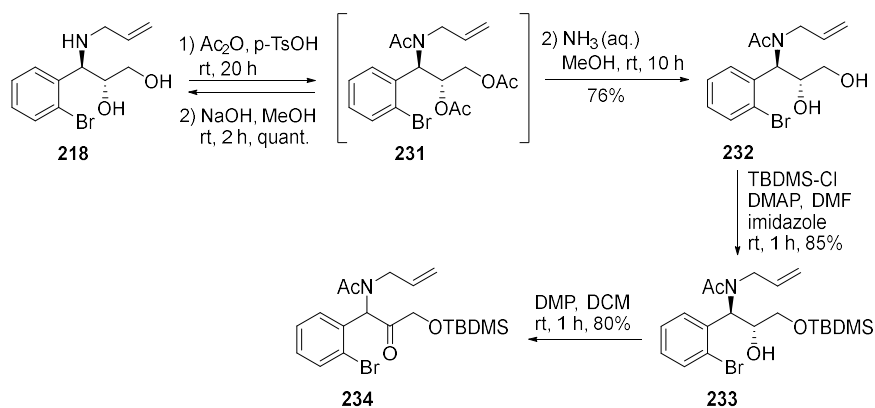


Scheme 59. Silyl-protection of the primary hydroxyl group in diol **228** followed by failed attempts to oxidize the secondary OH.

In our previous attempt to acetylate amino diol **218** with 2.4 equivalents of acetic anhydride, in the presence of DMAP and pyridine, only the hydroxyl groups had been protected (Scheme 58). Full acetylation of the amino diol **218** was however accomplished in a *para*-toluenesulfonic acid (*p*-TsOH) promoted reaction, run in acetic anhydride (Scheme 60). The resulting tri-acetylated compound **231** was then treated with sodium hydroxide in methanol, as the equivalent *N*-benzoyl diol **228** previously had been obtained. In this case, however, the base promoted hydrolysis effectively provided the amino diol starting material **218**.

Treatment of intermediate **231** with 25% aqueous ammonia in methanol ultimately provided, after continuous surveillance of the reaction by TLC analysis, the desired *N*-acetyl diol **232**. Selective silyl protection of the

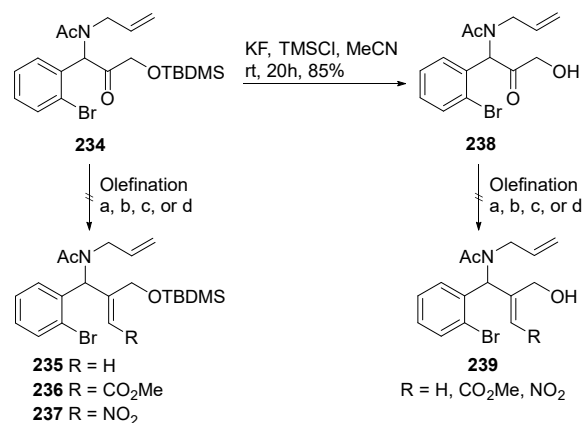
primary alcohol in the diol **232** efficiently provided compound **233**. The ketone **234** was finally obtained in 80% yield from oxidation of the secondary hydroxyl group in compound **233** with Dess Martin Periodinane.



Scheme 60. Acetylation of amino diol **218** followed by silyl protection and Dess Martin oxidation.

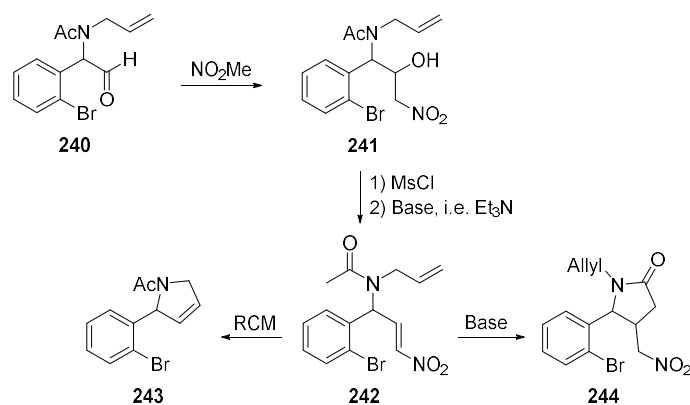
With ketone **234** in hand, the next step was to obtain the corresponding alkene **235** (Scheme 61). In our first attempt to form the alkene **235**, the ketone **234** was treated with methylenetriphenylphosphorane. However, after 24 h we did not observe any conversion of the starting material **234**. Equally, attempted olefination of ketone **234** with methyl(triphenylphosphoranylidene) acetate provided starting material **234**, and not compound **236**. We also observed no conversion of starting material **234** in an attempted Lombardo methylenation,²⁰¹ employing activated zinc, dibromomethane, and titanium (IV) chloride, either. Finally, we tried to obtain the nitroalkene **237** by treatment of ketone **234** in nitromethane and triethylamine. Once again, we detected no conversion of the starting material **234**.

We further attempted olefination of the silyl deprotected compound **238**, which was obtained from treatment of compound **234** with potassium fluoride and trimethylsilyl chloride in acetonitrile.²⁰² However, none of the olefination reactions provided the desired alkene **239**. We therefore left this strategy.



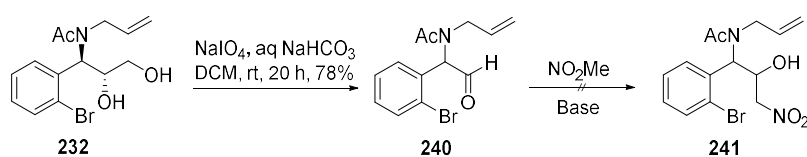
Scheme 61. Attempted alkene formation from ketones **234** or **238** using the following reaction conditions: a) *n*-BuLi, MePPh₃Br, THF, -78 °C – rt, 24 h. b) Me(PPh₃)Acetate, toluene, rt, 24 h. c) Zn, CH₂Br₂, TiCl₄, THF, 0 °C – rt, 24. d) NO₂Me, Et₃N, rt, 24 h – 45 °C, 24 h.

Since the attempted olefination of the *O*-silyl ketone **234** and α -hydroxy ketone **238** was unsuccessful, we wanted to see if removing the hydroxymethyl group in compound **238** entirely, could allow for further progression towards the target compounds. We envisioned that treatment of the corresponding aldehyde **240** with nitromethane could provide the nitro alcohol **241** (Scheme 62). From mesylation of the nitro alcohol **241** followed by base promoted elimination of the resulting mesoyl group we could obtain the nitro alkene **242**. Cyclization could then proceed via the planned RCM to form the pyrroline **243**. Another option could be a base-mediated cyclization to the pyrrolidone **244** via the Michael addition of the *N*-acetyl α -carbon to the nitro alkene moiety in compound **242**.



Scheme 62. Proposed plan for further synthesis via nitro alcohol **241**.

With this strategy in mind, oxidative cleavage of diol **232** with sodium periodate provided the aldehyde **240** in 78% yield (Scheme 63). Treatment of the aldehyde **240** with different bases in nitromethane failed to provide us with the nitro alcohol **241**. Microwave irradiation of the reaction mixture at temperatures up to 90 °C also failed to convert the aldehyde **240** to the desired product **241**.



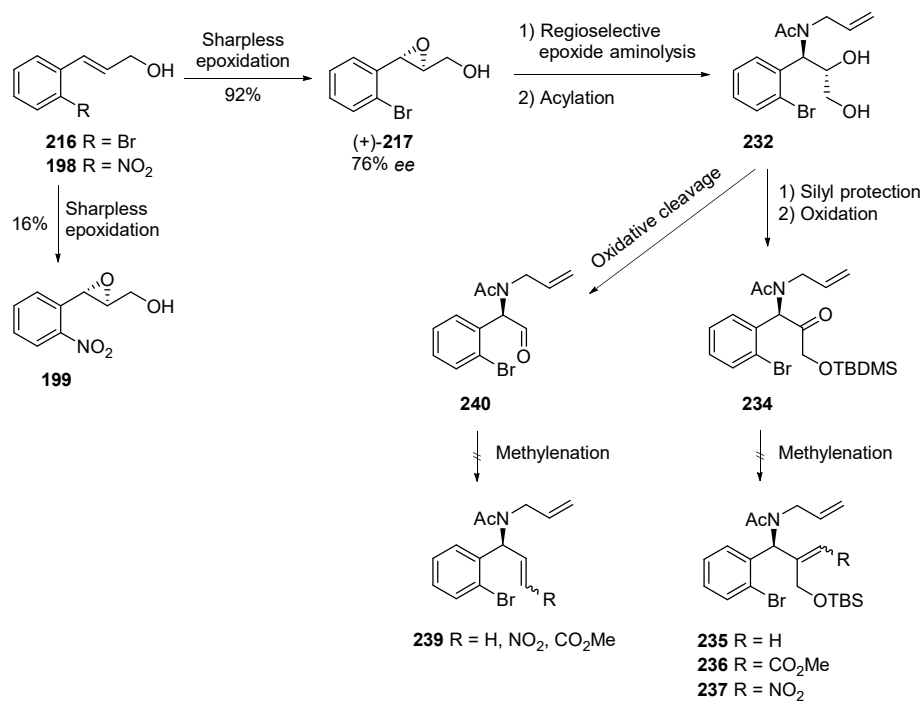
Scheme 63. Oxidative cleavage and attempted formation of nitro alcohol **241**. Bases used for the attempted formation of nitro alcohol **241**: Et₃N, K₂CO₃, and NH₄OAc.

Since all efforts to proceed towards the pyrroloquinoline scaffold from α -phenyl carbonyls **234** and **240** were ineffective, the synthetic strategy towards the martinella alkaloids was once again re-assessed.

6.2.5 Conclusion

In the attempted synthesis towards the martinella alkaloids, the stereochemistry was installed by the Sharpless asymmetric epoxidation of 2-bromo cinnamyl alcohol **216** (Scheme 64). The resulting epoxide **217** was obtained in 76% *ee*. The initial strategy commencing from 2-nitro cinnamyl alcohol **198** was quickly dismissed as a dead-end approach, presumably effected by the electron-withdrawing nitro group. Titanium catalyzed aminolysis regioselectively opened the epoxide ring which upon *N*-acylation provided amino diol **232**. After oxidation of the secondary alcohol in amino diol **232** to afford aldehyde **240** or ketone **234**, the progress towards the martinella alkaloids came to a full stop. Re-evaluation of the synthetic strategy finally led us to the conclusion that the suggested synthetic approach from amino diol **232** was ineffective.

Towards the Martinella Alkaloids



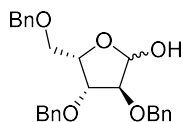
Scheme 64. Overview of the attempted synthesis towards the martinella alkaloid.

7 Experimental Methods

7.1 General Methods

All chemicals were obtained from Sigma Aldrich/Merck or VWR and used as supplied. When specified, solvents were dried by storing over 4 Å molecular sieves. For petroleum ether (PE), the 40-65 °C fraction was used. All reactions were carried out under a nitrogen or argon atmosphere, unless otherwise specified. TLC analyses were performed on Merck silica gel 60 F254 plates using UV light, KMnO₄, or heat for visualization. Silica gel NORMASIL 60® 40-63 μm was used for flash column chromatography. Nuclear magnetic resonance (NMR) spectra were recorded on a Bruker Ascend TM 400 series, operating at 400.13 MHz for ¹H and 100.61 MHz for ¹³C in CDCl₃, CD₃OD, D₂O, or DMSO-*d*₆. The assignment of signals in all NMR spectra was assisted by conducting ¹H-¹H correlation spectroscopy (COSY), ¹H-¹³C/¹H-¹⁵N heteronuclear single-quantum correlation spectroscopy (HSQC) and/or ¹H-¹³C/¹H-¹⁵N heteronuclear multiple bond correlation spectroscopy (HMBC). Chemical shifts (δ) are reported in ppm relative to an internal standard of residual chloroform (δ = 7.26 ppm for ¹H NMR; δ = 77.16 ppm for ¹³C NMR), residual methanol (δ = 3.31 ppm for ¹H NMR; δ = 49.00 ppm for ¹³C NMR), residual dimethyl sulfoxide (δ = 2.50 ppm for ¹H NMR; δ = 39.52 ppm for ¹³C NMR), or residual water (δ = 4.79 ppm for ¹H NMR). Infrared spectroscopy (IR) was performed on a Cary 360 FTIR spectrophotometer. High resolution mass spectra (HRMS) were recorded from MeOH solutions on a JMS-T100LC AccuTOFTM in positive electrospray ionization (ESI) mode. The microwave-assisted experiments were performed in a CEM Focused Microwave™ Synthesis System, model type Discover, operating at 0–300 W at a temperature of 150 °C, a pressure range of 0–290 psi, with reactor vial volumes of 10 mL.

7.2 Synthesis of the Arabino-Amidines



2,3,5-Tri-*O*-benzyl-L-xylofuranose (L-36)¹²⁶

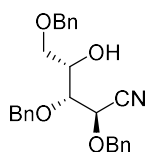
Step 1: To a solution of AcCl (0.58 mL, 8 mmol) in MeOH (80 mL) was added L-xylose (L-27) (6 g, 40 mmol) at room temp. The reaction was kept stirring at room temp. for 5.5 h. The reaction mixture was then cooled to 0 °C and pH was adjusted to ca. 9 with NaOH (1 M). The solvent was then removed under reduced pressure and the resulting residue was suspended in toluene (6 x 20 mL) and conc. to dryness.

Step 2: The residue from step 1 was dissolved in dry DMF (130 mL) and NaH (8.48 g, 5.3 equiv.) was added at room temp. The reaction mixture was then cooled to 0 °C prior to addition of BnBr (23.8 mL, 5 equiv.). The reaction mixture was stirred at room temp for 23 h before being extracted with EtOAc (2 x 150 mL). The combined extracts were dried over MgSO₄ and conc. by vacuo.

Step 3: The residue from step 2 was dissolved in dioxane (120 mL) and HCl (120 mL, 4 M) and stirred at 65 °C for 4 days. The reaction mixture was then extracted with EtOAc (2 x 150 mL) and the combined organic fractions were concentrated and subjected to flash column chromatography (Pet. ether/EtOAc 17:3 → 3:1). Collection of the appropriate fractions ($R_f = 0.25$; Pet. ether/EtOAc 3:1) provided compound L-36 (10.49 g, 62%) as a clear light-yellow oil, $[\alpha]_D^{26.6} = -10$ (c 1.2 in CHCl₃) (lit.¹²⁶ $[\alpha]_D^{26.0} = -12$ (c 1.2 in EtOAc)). The spectroscopic data were in full accord with the previously reported data.¹²⁶

¹H NMR (CDCl₃, 400 MHz): $\delta = 7.32$ -7.18 (m, 15 H, Ar-H), 5.43 (d, $J = 4.1$ Hz, 1Ha), 5.20 (br. s, 1Hb), 4.64-4.32 (m, 7H, CHPh + CH), 4.06 (dd, $J = 5.4, 3.0$ Hz, 1Hb), 3.99 (dd, $J = 4.4, 2.4$ Hz, 1Ha), 3.95 (dd, $J = 3.0, 1.0$ Hz, 1Hb), 3.89 (dd, $J = 4.2, 2.4$ Hz, 1Ha), 3.74-3.60 (m, 2H).

^{13}C NMR (CDCl_3 , 100 MHz): δ = 138.3 (ArCa), 137.8 (ArCa), 137.7 (ArCb), 137.6 (ArCb), 137.5 (ArCb), 136.9 (ArCa), 128.8-128.4 (Ar), 128.1-127.7 (Ar), 101.8 (CHb), 96.3 (CHa), 86.7 (CH), 81.4 (CHb), 81.2 (CHa), 80.0 (CH), 77.4 (CH), 73.8 (CH₂b), 73.6 (CH₂a), 73.2 (CH₂a), 72.8 (CH₂b), 72.5 (CH₂a), 72.0 (CH₂b), 68.8 (CH₂b), 68.4 (CH₂a).



2,3,5-Tri-*O*-benzyl-L-xylononitrile (L-33) ¹²⁷

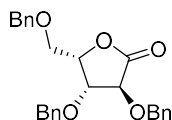
Method 1:

Step 1: To a solution of Na (315 mg, 13.7 mmol) dissolved in absolute EtOH (60 mL) was added $\text{NH}_2\text{OH}\cdot\text{HCl}$ (1.77 g, 27.5 mmol). The reaction mixture was stirred at room temp. for 5 min. before a solution of furanose L-36 (1.44 g, 3.42 mmol) in absolute EtOH (11 mL) was added. The resulting reaction mixture was stirred at room temp. for 1 h before volatiles were removed under reduced pressure. Water (50 mL) and EtOAc (50 mL) was then added to the residue. The two phases were separated, and the aq. phase was extracted with EtOAc (2 x 50 mL). The combined organic fractions were dried over MgSO_4 , filtered, and concentrated by vacuo. The residue (R_f = 0.4, Pet. ether/EtOAc 3:2) was dissolved in toluene, concentrated, and used directly in the following step.

Step 2: To a solution of PPh_3 (1.89 g, 6.84 mmol, 2 equiv.) in MeCN (27 mL) at room temp. was added the residue from step 1. The reaction mixture was stirred at room temp. for 20 min before a solution of CBr_4 (2.84 g, 8.55 mmol, 2.5 equiv.) in MeCN (11 mL) was added. The reaction was then stirred at room temp. for 20 min before adding a solution of PPh_3 (472 mg, 1.71 mmol, 0.5 equiv.) in MeCN:MeOH

(1:5.5, 45 mL). The reaction mixture was then stirred for an additional 15 min before the solvent was removed under reduced pressure. The residue was subjected to flash chromatography (silica, Pet. ether/EtOAc 1:0 \rightarrow 9:1). Collection of the first fraction ($R_f = 0.6$; Pet. ether/EtOAc, 3:1) provided lactone L-38 (286 mg, 20%) as a clear colorless oil. Collection of the appropriate fractions ($R_f = 0.4$, Pet. ether/EtOAc, 3:1) provided nitrile L-36 (741 mg, 52%) as a clear colorless oil; $[\alpha]_D^{26.6} = -28$ (c 0.5 in CHCl_3).

The spectroscopic data for lactone L-38 were in full accord with the previously reported data.¹²⁸



3,4,5-Tri-O-benzyl-L-xylonolactone (L-38)¹²⁸

¹H NMR (CDCl_3 , 400 MHz): $\delta = 7.36$ - 7.25 (m, 15 H), 5.05 (d, $J = 11.5$ Hz, 1 H), 4.60-4.50 (m, 5 H), 4.37 (t, $J = 7.1$ Hz, 1 H), 3.77 (dd, $J = 2.9$ Hz, $J = 10.8$ Hz, 1 H), 3.71 (dd, $J = 3.2$ Hz, $J = 10.8$ Hz, 1 H).

¹³C NMR (CDCl_3 , 100 MHz): $\delta = 173.5$, 137.8, 137.4, 137.2, 128.7-127.7, 79.5, 77.4 (2 \times C), 73.8, 72.8, 72.7, 67.3.

Method 2:

Step 1: A solution of Na (270 mg, 11.7 mmol) dissolved in absolute EtOH (40 mL) was added $\text{NH}_2\text{OH}\cdot\text{HCl}$ (1.63 g, 23.5 mmol). The reaction mixture was stirred at room temp. for 15 min. before a solution of furanose L-36 (1.23 g, 2.93 mmol) in absolute EtOH (10 mL) was added. The resulting reaction mixture was stirred at room temp. for 1.5 h before volatiles were removed under reduced pressure. The residue was

then added toluene, concentrated under reduced pressure, and used directly in the following step without further purification.

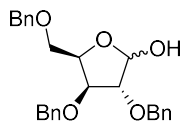
Step 2: A solution of PPh₃ (1.214 g, 1.5 equiv.) in MeCN (18 mL) at room temp. was added to the dried residue from step 1. The reaction mixture was stirred at room temp. for 20 min before a solution of CBr₄ (2.43 g, 7.33 mmol, 2.5 equiv.) in MeCN (6 mL) was added. The reaction was then stirred at room temp. for 20 min before adding a solution of PPh₃ (809 mg, 1 equiv.) in MeCN (12 mL) and MeOH (37 mL) simultaneously. The reaction mixture was then stirred for an additional 1 h before the solvent was removed under reduced pressure. The residue was subjected to flash chromatography (Pet. ether/EtOAc 5:1 → 4:1). Collection of the appropriate fractions ($R_f = 0.4$, Pet. ether/EtOAc 3:1) provided nitrile L-**33** (893 mg, 73%) as a clear colorless oil; $[\alpha]_D^{26.0} = -29.0$ (c 0.5 in CHCl₃).

¹H NMR (CDCl₃, 400 MHz): $\delta = 7.37$ - 7.24 (m, 15 H, Ar-H), 4.88 (d, $J = 11.5$ Hz, 1 H, CHPh), 4.82 (d, $J = 11.2$ Hz, 1 H, CHPh), 4.60 (d, $J = 11.2$ Hz, 1 H, CHPh), 4.55 (d, $J = 11.5$ Hz, 1 H, CHPh), 4.45 (d, $J = 1.5$ Hz, 2 H, CHPh), 4.43 (d, $J = 6.6$ Hz, 1 H, H-2), 4.11 (m, 1 H, H-4), 3.88 (dd, $J_{3,4} = 2.9$ Hz, $J_{3,2} = 6.6$ Hz, 1 H, H-3), 3.45 (ddd in 1:2:2:1 ratio, $J_{5a,4} = 6.0$ Hz, $J = 9.5$ Hz, $J_{5b,4} = 16.3$ Hz, 2H, H-5), 2.29 (d, $J = 7.2$ Hz, 1 H, OH).

¹³C NMR (CDCl₃, 100 MHz): $\delta = 137.7$ (ArC), 137.3 (ArC), 135.7 (ArC), 128.8-128.0 (ArCH), 116.8 (CN), 78.1 (C-3), 75.2 (CH₂Ph), 73.4 (CH₂Ph), 73.0 (CH₂Ph), 70.4 (C-5), 69.6 (C-4), 69.3 (C-2).

IR (ATR, cm⁻¹): 3470, 3065, 3032, 2920, 2870, 1955, 1882, 1812, 1554, 1497, 1455, 1398, 1353, 1250, 1210, 1096, 1028, 1002, 913, 821, 738.

HRMS (ESI): m/z [M+Na]⁺ calcd. for C₂₆H₂₇O₄NNa: 440.1832; found: 440.1827.



2,3,5-Tri-*O*-benzyl-D-xylofuranose (D-36)²⁰³

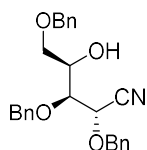
Step 1: To a solution of AcCl (0.29 mL, 4 mmol) in MeOH (40 mL) was added D-xylose (D-27) (3 g, 20 mmol) at room temp. The reaction was kept stirring at room temp. for 5.5 h. The reaction mixture was then cooled to 0 °C and pH was adjusted to ca. 9 with NaOH (1 M). The solvent was then removed under reduced pressure and the resulting residue was suspended in toluene (6 x 10 mL) and conc. to dryness.

Step 2: The residue from step 1 was dissolved in dry DMF (64 mL) and NaH (4.24 g, 5.3 equiv.) was added at room temp. The reaction mixture was then cooled to 0 °C prior to addition of BnBr (11.9 mL, 5 equiv.). The reaction mixture was stirred at room temp for 23 h before being extracted with EtOAc (2 x 75 mL). The combined extracts were dried over MgSO₄ and conc. by vacuo.

Step 3: The residue from step 2 was dissolved in dioxane (60 mL) and HCl (60 mL, 4 M) and stirred at 65 °C for 4 days. The reaction mixture was then extracted with EtOAc (2 x 75 mL) and the combined organic fractions were concentrated and subjected to flash column chromatography (PET. ETHER/EtOAc, 17:3 → 3:1). Collection of the appropriate fractions ($R_f = 0.25$; PE/EtOAc, 3:1) provided compound D-36 (5.536 g, 66 %) as a clear light-yellow oil. $[\alpha]_D^{26.6} = +10$ (c 1.2 in CHCl₃) (lit.¹²⁶ $[\alpha]_D^{26.0} = -12$ (c 1.2 in EtOAc) for opposite enantiomer). The spectroscopic data were in full accord with the previously reported data.^{126,203}

¹H NMR (CDCl₃, 400 MHz): $\delta = 7.32$ -7.18 (m, 15 H, Ar-H), 5.43 (d, $J = 4.1$ Hz, 1Ha), 5.20 (br. s, 1Hb), 4.64-4.32 (m, 7H, CHPh + CH), 4.06 (dd, $J = 5.4, 3.0$ Hz, 1Hb), 3.99 (dd, $J = 4.4, 2.4$ Hz, 1Ha), 3.95 (dd, $J = 3.0, 1.0$ Hz, 1Hb), 3.89 (dd, $J = 4.2, 2.4$ Hz, 1Ha), 3.74-3.60 (m, 2H).

^{13}C NMR (CDCl_3 , 100 MHz): δ = 138.3 (ArCa), 137.8 (ArCa), 137.7 (ArCb), 137.6 (ArCb), 137.5 (ArCb), 136.9 (ArCa), 128.8-128.4 (Ar), 128.1-127.7 (Ar), 101.8 (CHb), 96.3 (CHa), 86.7 (CH), 81.4 (CHb), 81.2 (CHa), 80.0 (CH), 77.4 (CH), 73.8 (CH_2b), 73.6 (CH_2a), 73.2 (CH_2a), 72.8 (CH_2b), 72.5 (CH_2a), 72.0 (CH_2b), 68.8 (CH_2b), 68.4 (CH_2a).



2,3,5-Tri-*O*-benzyl-D-xylofuranonitrile (D-33)

Step 1: To a solution of Na (460 mg, 20 mmol) dissolved in absolute EtOH (80 mL) was added $\text{NH}_2\text{OH}\cdot\text{HCl}$ (2.65 g, 38 mmol). The reaction mixture was stirred at room temp. for 10 min. before a solution of furanose D-36 (2.20 g, 5.23 mmol) in absolute EtOH (15 mL) was added. The resulting reaction mixture was stirred at room temp. for 1 h before volatiles were removed under reduced pressure. The residue was then added toluene and concentrated under reduced pressure.

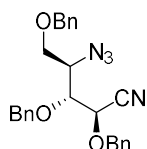
Step 2: To a solution of PPh_3 (2.89 g, 10.46 mmol, 2 equiv.) in MeCN (42 mL) at room temp. was added the dried residue from step 1. The reaction mixture was stirred at room temp. for 20 min before a solution of CBr_4 (4.38 g, 13.08 mmol, 2.5 equiv.) in MeCN (18 mL) was added. The reaction was then stirred at room temp. for 20 min before adding a solution of PPh_3 (720 mg, 2.61 mmol, 0.5 equiv.) in MeCN (10.5 mL) and MeOH (66 mL) simultaneously. The reaction mixture was then stirred for an additional 15 min before the solvent was removed under reduced pressure. The residue was subjected to flash chromatography (PE/EtOAc, 5:1 \rightarrow 4:1). Collection of the appropriate fractions (R_f = 0.40; Pet. ether/EtOAc, 3:1) provided nitrile D-33 (1.46 g, 67%) as a clear light yellow oil; $[\alpha]_D^{26.0} = +32$ (c 1.2 in CHCl_3).

¹H NMR (CDCl₃, 400 MHz): δ = 7.38-7.26 (m, 15H, ArH), 4.89 (d, *J* = 11.6 Hz, 1H, CHPh), 4.83 (d, *J* = 11.2 Hz, 1H, CHPh), 4.61 (d, *J* = 11.2 Hz, 1H, CHPh), 4.56 (d, *J* = 11.6 Hz, 1H, CHPh), 4.52-4.43 (m, 3H, CHPh and H-2), 4.13 (ddd, *J* = 13.0, 6.1, 2.9 Hz, 1H, H-4), 3.89 (dd, *J* = 6.6, 2.9 Hz, 1H, H-3), 3.49 (dd, *J* = 9.5, 6.0 Hz, 1H, H-5a), 3.43 (dd, *J* = 9.5, 6.0 Hz, H-5b), 2.37 (d, *J* = 7.2 Hz, 1H, OH).

¹³C NMR (CDCl₃, 100 MHz): δ = 137.8 (Ar), 137.3 (Ar), 135.7 (Ar), 128.9-127.9 (Ar), 116.8 (CN), 78.2 (C-3), 75.3 (CH₂), 73.5 (CH₂), 73.1 (CH₂), 70.5 (C-5), 69.7 (C-4), 69.4 (C-2).

IR (ATR, cm⁻¹): 3470, 3065, 3032, 2920, 2870, 1955, 1882, 1812, 1554, 1497, 1455, 1398, 1353, 1250, 1210, 1096, 1028, 1002, 913, 821, 738.

HRMS (ESI): *m/z* [M +Na]⁺ calcd for C₂₆H₂₇O₄NNa, 440.1838; found, 440.1835.



2,3,5-Tri-*O*-benzyl-4-azido-4-deoxy-D-arabinonitrile (D-41)

Step 1: To a solution of compound D-33 (676 mg, 1.62 mmol) in DCM (15 mL) at 0 °C was added pyridine (0.30 mL, 4.05 mmol, 2.5 equiv.). The reaction mixture was stirred for 10 min prior to dropwise addition of triflic anhydride (0.33 mL, 2.03 mmol, 1.25 equiv.). The reaction mixture was further stirred at 0 °C for 15 min. before being diluted with DCM (150 mL), washed with ice cold HCl (45 mL, 1 M), followed by sat. aq. NaHCO₃ (60 mL), dried over Na₂SO₄, and filtered. The residue (*R_f* = 0.71, Pet. ether/EtOAc 7:3) was concentrated under reduced pressure and used directly in the following step.

Experimental Methods

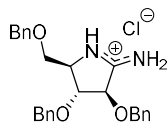
Step 2: To a solution of the residue from step 1 in DMF (10 mL) at 0 °C was added NaN₃ (160 mg, 2.46 mmol). The reaction was stirred at 0 °C for 5 h and then added water (100 mL) and extracted with EtOAc (150 mL). The organic fraction was concentrated under reduced pressure and the residue was subjected to flash column chromatography (Pet. ether/EtOAc 95:5). Collection of the appropriate fractions (*R_f* = 0.37, Pet. ether/EtOAc 9:1) provided azide D-**41** (620 mg, 1.40 mmol, 87%) as a clear colorless oil; $[\alpha]_D^{25.4} = -56$ (*c* 2.0 in CHCl₃).

¹H NMR (CDCl₃, 400 MHz): δ = 7.41-7.27 (m, 15H, ArH), 4.92 (d, *J* = 11.7 Hz, 1H, CHPh), 4.87 (d, *J* = 10.9 Hz, 1H, CHPh), 4.61 (d, *J* = 10.9 Hz, 1H, CHPh), 4.57 (d, *J* = 11.7 Hz, 1H, CHPh), 4.52 (br. s, 2H, CHPh), 4.41 (d, *J* = 2.7 Hz, H-2), 3.81-3.79 (m, 3H), 3.70-3.66 (m, 1H).

¹³C NMR (CDCl₃, 100 MHz): δ = 137.5 (ArC), 136.9 (ArC), 135.3 (ArC), 128.9-128.8 (ArCH), 128.64-128.56 (ArCH), 128.4 (ArCH), 128.1 (ArCH), 127.9 (ArCH), 117.0 (CN), 77.9 (C-3), 75.3 (CH₂Ph), 73.6 (CH₂Ph), 72.9 (CH₂Ph), 68.8 (C-2), 67.4 (C-5), 60.2 (C-4).

IR (ATR, cm⁻¹): 3065, 3030, 2923, 2870, 2100, 1497, 1455, 1398, 1362, 1315, 1269, 1210, 1094, 1028, 915, 820, 737.

HRMS (ESI): *m/z* [M+Na]⁺ calcd. for C₂₆H₂₆O₃N₄Na: 465.1902; found, 465.1898.



3,4,6-Tri-*O*-benzyl-2,5-deoxy- (3*R*,4*R*,5*R*)-3,4-bis(benzyloxy)-5-((benzyloxy)methyl)-2-iminopyrrolidine hydrochloride (D-42)

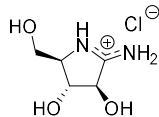
A suspension of compound D-41 (100 mg, 0.23 mmol), Pd/C (1.4 mg, 6 mol%) and acetic acid (2 drops) in EtOH (3 mL) was hydrogenated at 1 atm for 16 h at rt. The mixture was then filtered through Celite by the aid of MeOH. The filtrate was concentrated under reduced pressure and then added 0.5 M methanolic HCl (30 mL). Volatiles were removed under reduced pressure. The resulting HCl salt was subjected to flash column chromatography (95:5, CHCl₃/MeOH (0.1 M HCl)). Collection of the appropriate fractions ($R_f = 0.35$, CHCl₃/MeOH (0.1 M HCl) 9:1) provided amidine D-42 (95 mg, 0.21 mmol, 91%) as a clear, slightly yellow oil; $[\alpha]_D^{26.1} = +6$ (c 1.0 in MeOH).

¹H NMR (MeOD, 400 MHz): $\delta = 7.34$ -7.26 (m, 15H), 4.83 (d, $J_{3,4} = 4.6$ Hz, 1H, H-3), 4.76 (d, $J = 11.5$ Hz, 1H, CHPh), 4.67 (d, $J = 11.5$ Hz, 1H, CHPh), 4.56-4.48 (m, 4H, CHPh), 4.26 (t, $J = 4.4$ Hz, 1H, H-4), 3.98 (app. q, $J = 4.5$ Hz, 1H, H-5), 3.64 (dd, $J = 4.2, 10.3$ Hz, 1H, H-6), 3.53 (dd, $J = 5.0, 10.3$ Hz, 1H, H-6).

¹³C NMR (MeOD, 100 MHz): $\delta = 168.8$ (C=N), 138.9 (Ar), 138.6 (Ar), 138.1 (Ar), 129.6-129.0 (Ar), 84.0 (C-3), 81.7 (C-4), 74.39 (CH₂), 74.36 (CH₂), 73.5 (CH₂), 69.8 (C-6), 64.5 (C-5).

IR (ATR, cm⁻¹): 3029, 2929, 2866, 1701, 1496, 1453, 1395, 1359, 1204, 1092, 1027, 911, 732.

HRMS (ESI): m/z [M+H]⁺ calcd. for C₂₆H₂₉O₃N₂: 417.2178, found: 417.2172.



(2*R*,3*R*,4*R*)- 3,4-dihydroxy-2-(hydroxymethyl)-5-iminopyrrolidine hydrochloride (D-40)

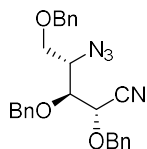
A solution of compound D-42 (65 mg, 0.16 mmol) and Pd/C (170 mg, 10 equiv.) in EtOH/TFA (5 mL, 9:1) was hydrogenated at 1 atm for 20 h at rt. The mixture was filtered through Celite with the aid of MeOH. The filtrate was concentrated under reduced pressure. The residue was added methanolic HCl and concentrated under reduced pressure. The resulting HCl salt was subjected to gravity column chromatography (MeCN/H₂O 97:3). Collection of the appropriate fractions ($R_f = 0.22$, MeCN/H₂O 8:2) provided compound D-40 (23.1 mg, 0.158, 99%) as a white wax; $[\alpha]_D^{26.2\text{ }^\circ\text{C}} = +15.1$ (c 0.53 in MeOH).

¹H NMR (D₂O, 400 MHz): $\delta = 4.88$ (d, $J_{4,3} = 7.8$ Hz, 1H, H-4), 4.23 (dd, $J_{3,4} = 7.8$ Hz, $J_{3,2} = 6.6$ Hz, 1H, H-3), 3.95-3.91 (m, 1H, H-2'a), 3.78-3.73 (m, 2H, H-2'b + H-2).

¹³C NMR (D₂O, 100 MHz): $\delta = 168.7$ (C=N), 75.9 (C-4), 74.8 (C-3), 62.3 (C-2), 59.2 (C-2').

IR (ATR, cm⁻¹): 3153, 1699, 1405, 1333, 1271, 1200, 1096, 1042, 990, 922, 886.

HRMS (ESI): m/z [M+H]⁺ calcd. for C₅H₁₀O₃N₂: 147.0769; found 147.0764.



2,3,5-Tri-O-benzyl-4-azido-4-deoxy-L-arabinonitrile (L-41)

Step 1: To a solution of alcohol D-**33** (222 mg, 0.53 mmol) in DCM (5 mL) at 0 °C was added pyridine (0.10 mL, 1.33 mmol, 2.5 equiv.). The reaction mixture was stirred for 10 min prior to dropwise addition of triflic anhydride (0.11 mL, 0.66 mmol, 1.25 equiv.). The reaction mixture was further stirred at 0 °C for 15 min. before being diluted with DCM (50 mL), washed with ice cold HCl (15 mL, 1 M), followed by sat. aq. NaHCO₃ (20 mL), dried over Na₂SO₄, and filtered. The residue (*R_f* = 0.71; Pet. ether/EtOAc, 7:3) was concentrated under reduced pressure and used directly in the following step.

Step2: To a solution of the residue from step 1 in DMF (5 mL) at 0 °C was added NaN₃ (58 mg, 0.89 mmol). The reaction was stirred for 1 h and then added water (50 mL) and extracted with EtOAc (100 mL). The organic fraction was concentrated under reduced pressure and the residue was subjected to flash column chromatography (Pet. ether/EtOAc 9:1). Collection of the appropriate fractions (*R_f* = 0.37, Pet. ether:EtOAc 9:1) provided azide L-**41** (182 mg, 78%) as a clear colorless oil; $[\alpha]_D^{25.6} = +53$ (*c* 2.0 in CHCl₃).

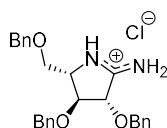
¹H NMR (CDCl₃, 400 MHz): δ = 7.41-7.27 (m, 15H, ArH), 4.92 (d, *J* = 11.7 Hz, 1H, CHPh), 4.87 (d, *J* = 10.9 Hz, 1H, CHPh), 4.61 (d, *J* = 10.9 Hz, 1H, CHPh), 4.57 (d, *J* = 11.7 Hz, 1H, CHPh), 4.52 (br. s, 2H, CHPh), 4.41 (d, *J* = 2.7 Hz, H-2), 3.81-3.79 (m, 3H), 3.70-3.66 (m, 1H).

¹³C NMR (CDCl₃, 100 MHz): δ = 137.5 (ArC), 136.9 (ArC), 135.3 (ArC), 128.9-128.8 (ArCH), 128.64-128.56 (ArCH), 128.4 (ArCH), 128.1 (ArCH), 127.9 (ArCH), 117.0 (CN), 77.9 (C-3), 75.3 (CH₂Ph), 73.6 (CH₂Ph), 72.9 (CH₂Ph), 68.8 (C-2), 67.4 (C-5), 60.2 (C-4).

Experimental Methods

IR (ATR, cm^{-1}): 3065, 3030, 2923, 2870, 2101, 1497, 1455, 1398, 1362, 1315, 1269, 1210, 1094, 1028, 915, 820, 737.

HRMS (ESI): m/z $[\text{M}+\text{Na}]^+$ calcd. for $\text{C}_{26}\text{H}_{26}\text{O}_3\text{N}_4\text{Na}$: 465.1902; found, 465.1900.



(3*S*,4*S*,5*S*)-3,4-bis(benzyloxy)-5-((benzyloxy)methyl)-2-iminopyrrolidine hydrochloride (L-42)

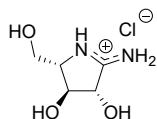
A suspension of Pd/C (1 mg, 6 mol%) and azide **L-41** (62 mg, 0.14 mmol) in EtOH (2 mL) was added acetic acid (2 drops) and hydrogenated at rt for 16 h. The reaction mixture was then filtered through Celite by the aid of MeOH. The residue was converted to the HCl salt by evaporation from methanolic HCl (0.5 M, 5 mL) and then subjected to flash column chromatography ($\text{CHCl}_3/\text{MeOH}$ (0.1 M HCl) 195:5). Collection of the appropriate fractions ($R_f = 0.35$, $\text{CHCl}_3/\text{MeOH}$ (0.1 M HCl) 9:1) provided amidine **L-42** (61 mg, 0.134 mmol, 96%) as a clear slightly yellow oil; $[\alpha]_D^{26.1} = -6$ (c 1.0 in MeOH).

^1H NMR (D_2O , 400 MHz): $\delta = 7.34\text{--}7.26$ (m, 15H), 4.83 (d, $J_{3,4} = 4.6$ Hz, 1H, H-3), 4.76 (d, $J = 11.5$ Hz, 1H, CHPh), 4.67 (d, $J = 11.5$ Hz, 1H, CHPh), 4.56–4.48 (m, 4H, CHPh), 4.26 (t, $J = 4.4$ Hz, 1H, H-4), 3.98 (app. q, $J = 4.5$ Hz, 1H, H-5), 3.64 (dd, $J = 4.2, 10.3$ Hz, 1H, H-6), 3.53 (dd, $J = 5.0, 10.3$ Hz, 1H, H-6).

^{13}C NMR (D_2O , 100 MHz): $\delta = 168.8$ (C=N), 138.9 (Ar), 138.6 (Ar), 138.1 (Ar), 129.6–129.0 (Ar), 84.0 (C-3), 81.7 (C-4), 74.39 (CH_2), 74.36 (CH_2), 73.5 (CH_2), 69.8 (C-6), 64.5 (C-5).

IR (ATR, cm^{-1}): 3029, 2929, 2866, 1701, 1496, 1453, 1395, 1359, 1204, 1092, 1027, 911, 732.

HRMS (ESI): m/z $[\text{M}+\text{H}]^+$ calcd. for $\text{C}_{26}\text{H}_{29}\text{O}_3\text{N}_2$: 417.2178; found: 417.2174.



(2S,3S,4S)-3,4-dihydroxy-2-(hydroxymethyl)-5-iminopyrrolidine hydrochloride (L-40)

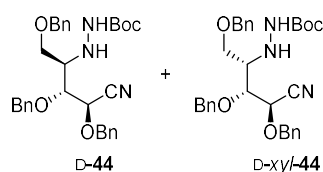
A solution of compound L-42 (59 mg, 0.13 mmol) and Pd/C (138 mg, 10 equiv.) in EtOH/TFA (5 mL, 9:1) was hydrogenated at rt for 18 h. The mixture was filtered through Celite with the aid of MeOH. The filtrate was added 0.5 M methanolic HCl (1 mL) and concentrated under reduced pressure. The resulting HCl salt was subjected to gravity column chromatography (MeCN/ H_2O 97:3). Collection of the appropriate fractions (R_f = 0.25-0.38, MeCN/ H_2O 8:2) provided compound L-40 (21.4 mg, 90%) as a white wax; $[\alpha]_D^{26.2}$ = -16 (c 0.50 in MeOH).

^1H NMR (D_2O , 400 MHz): δ = 4.89 (d, $J_{4,3}$ = 7.8 Hz, 1H, H-4), 4.24 (dd, $J_{3,2}$ = 6.6 Hz, $J_{3,4}$ = 7.8 Hz, 1H, H-3), 3.94 (ddd, $J_{2,2'}$ = 4.7 Hz, $J_{2,3}$ = 6.6 Hz, J = 12.6 Hz, 1H, H-2), 3.76 (ddd, $J_{2'a2'b}$ = 1.3 Hz, $J_{2'2}$ = 4.7 Hz, J = 12.6 Hz, 2H, H-2')

^{13}C NMR (D_2O , 100 MHz): δ = 168.6 (C=N), 75.9 (C-4), 74.7 (C-3), 62.2 (C-2), 59.2 (C-2').

IR (ATR, cm^{-1}): 3153, 1699, 1405, 1333, 1271, 1200, 1096, 1042, 990, 922, 886.

HRMS (ESI): m/z $[M+H]^+$ calcd. for $C_5H_{10}O_3N_2$: 147.0769.; found, 147.0766.



2,3,5-Tri-*O*-benzyl-4-(2-tert-butoxycarbonyl)hydrazinyl-4-deoxy-D-arabinonitrile (D-44) + 2,3,5-Tri-*O*-benzyl-4-(2-tert-butoxycarbonyl)hydrazinyl-4-deoxy-L-xylo-44

Step 1: To a solution of DMSO (1.56 mL, 21.9 mmol) in DCM (12 mL) at $-78\text{ }^{\circ}\text{C}$ under nitrogen was dropwise added oxalyl chloride (0.93 mL, 11.0 mmol). The resultant mixture was stirred for 10 min before a solution of alcohol L-33 (592 mg, 1.42 mmol) in DCM (12 mL) was dropwise added. The reaction mixture was further stirred at $-78\text{ }^{\circ}\text{C}$ for 2 h before slow addition of Et_3N (8.14 mL, 41.2 mmol). The mixture was stirred at $-78\text{ }^{\circ}\text{C}$ for 30 min and then at $0\text{ }^{\circ}\text{C}$ for 30 min before the reaction mixture was added water (70 mL) and the aqueous phase was extracted with DCM (70 mL x 3). Organic fractions were combined, dried (MgSO_4), filtered, and concentrated under reduced pressure.

Step 2: The residue from step 1 was dissolved in THF:EtOH (1:1, 8.5 mL) at $0\text{ }^{\circ}\text{C}$ under nitrogen and was added AcOH (0.49 mL) followed by *tert*-butylcarbazate (377 mg, 2.85 mmol). The resulting reaction was stirred at room temp. for 20 h. The mixture was then added AcOH (0.49 mL) followed by NaCNBH_3 (844 mg, 13.4 mmol). The resulting reaction mixture was then stirred at room temp. for another 20 h before adding sat. aq. NaHCO_3 (70 mL). The aq. phase was extracted with EtOAc (70 mL x 3) and the organic fractions were combined, dried (MgSO_4),

Experimental Methods

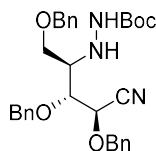
filtered, and concentrated under reduced pressure. The residue was subjected to flash chromatography (Pet. ether/EtOAc 95:5 → 9:1). Collection of the appropriate fractions (R_f = 0.28, Pet. ether/EtOAc 9:1) provided compound D-**44** and L-*xylo*-**44** as a mixture of diastereomers (2:3 by ^1H NMR analysis) (558 mg, 74%) as a clear slightly yellow oil.

^1H NMR (CDCl_3 , 400 MHz): δ = 7.38-7.30 (m, 30 H), 6.05 (br. s, 1H, NH, L-*xylo*-**44**), 5.84 (brs, 1H, NH, D-**44**), 4.94 (d, $J_{2,3}$ = 3.9 Hz, 1H, H-2, L-*xylo*-**44**), 4.91-4.86 (m, 4H, CHPh), 4.77 (d, $J_{2,3}$ = 3.7 Hz, 1H, H-2, D-**44**), 4.69-4.41 (m, 8H, CHPh), 4.26-4.22 (m, 2H, NH), 3.90 (dd, $J_{2,3}$ = 3.9 Hz, $J_{3,4}$ = 6.5 Hz, 1H, H-3, L-*xylo*-**44**), 3.85 (dd, $J_{2,3}$ = 3.7 Hz, $J_{3,4}$ = 7.0 Hz, 1H, H-3, D-**44**), 3.74 (dd, $J_{5a,4}$ = 4.4 Hz, $J_{5a,5b}$ = 9.7 Hz, 1H, H-5a, D-**44**), 3.64 (dd, $J_{5a,4}$ = 4.4 Hz, $J_{5a,5b}$ = 9.8 Hz, 1H, H-5a, L-*xylo*-**44**), 3.61-3.57 (m, 1H, H-5b, D-**44**), 3.54 (dd, $J_{5b,4}$ = 6.3 Hz, $J_{5b,5a}$ = 9.8 Hz, 1H, H-5b, L-*xylo*-**44**), 3.34-3.27 (m, 2H, H-4), 1.46 (s, 18H).

^{13}C NMR (CDCl_3 , 100 MHz): δ = 156.60 (CO), 156.57 (CO), 137.9 (ArC), 137.8 (ArC), 137.6 (ArC), 137.4 (ArC), 136.2 (ArC), 135.9 (ArC), 128.6-127.9 (ArCH), 117.7 (CN), 117.1 (CN), 80.5 (C), 78.0 (C-3 (L-*xylo*-**44**)), 77.95 (C-3 (D-**44**)), 74.8 (CH_2), 74.5 (CH_2), 73.4 (CH_2), 72.9 (CH_2), 71.4 (C-2 (L-*xylo*-**44**)), 68.3 (C-2 (D-**44**)), 67.8 (C-5 (L-*xylo*-**44**)), 67.7 (C-5 (D-**44**)), 60.6 (C-4), 28.3 (CH_3).

IR (ATR, cm^{-1}): 3339, 3014, 2979, 2929, 2870, 1718, 1497, 1454, 1393, 1367, 1249, 1216, 1157, 1088, 1073, 1028

HRMS (ESI): m/z $[\text{M}+\text{H}]^+$ calcd. for $\text{C}_{31}\text{H}_{38}\text{O}_5\text{N}_3$: 532.2806; found: 532.2802.



2,3,5-Tri-*O*-benzyl-4-(2-*tert*-butoxycarbonyl)hydrazinyl-4-deoxy-D-arabinonitrile (D-44)

Step 1: To a solution of alcohol L-33 (200 mg, 0.48 mmol) in DCM (4 mL) at 0 °C was added pyridine (0.1 mL, 1.24 mmol, 2.6 equiv.). The reaction mixture was stirred for 10 min prior to dropwise addition of triflic anhydride (0.1 mL, 0.60 mmol, 1.25 equiv.). The reaction mixture was further stirred at 0 °C for 15 min. before being diluted with DCM (20 mL), washed with cold HCl (10 mL, 1 M), sat. aq. NaHCO₃ (12 mL), dried over MgSO₄, and filtered. The residue (R_f = 0.71, Pet. ether/EtOAc 7:3) was concentrated under reduced pressure and used directly in the following step.

Step 2: To a solution of the triflate from step 1 in THF (1.5 mL) at 0 °C was added *tert*-butylcarbazate (320 mg, 2.42 mmol, 5 equiv.). The reaction was stirred at room temp. for 44 h before volatiles were removed under reduced pressure. The residue was subjected to flash column chromatography (Pet. ether/EtOAc 95:5 → 9:1). Collection of the appropriate fractions (R_f = 0.28, Pet. ether/EtOAc 9:1) provided hydrazide D-44 (138 mg, 54 %) as a clear white oil; $[\alpha]_D^{25.4^\circ C} = -8$ (c 1.0 in CHCl₃).

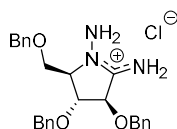
¹H NMR (CDCl₃, 400 MHz): δ = 7.36-7.28 (m, 15 H), 5.77 (br. s, 1H, NH), 4.88 (d, J = 11.5 Hz, 1H, CHPh), 4.84 (d, J = 11.1 Hz, 1H, CHPh), 4.73 (d, $J_{2,3}$ 3.7 Hz, 1H, H-2), 4.64 (d, J = 11.1 Hz, 1H, CHPh), 4.57 (d, J = 11.5 Hz, 1H, CHPh), 4.52 (d, J = 11.8 Hz, 1H, CHPh), 4.45 (d, J = 11.8 Hz, 1H, CHPh), 3.82 (dd, $J_{2,3}$ 3.7, $J_{3,4}$ 7.0 Hz, 1H, H-3), 3.71 (dd, $J_{5a,4}$ 4.4, $J_{5a,5b}$ 9.7 Hz, 1H, H-5a), 3.60 (dd, $J_{5b,4}$ 5.7, $J_{5b,5a}$ 9.7 Hz, 1H, H-5b), 3.27 (ddd, $J_{4,5a}$ 4.4, $J_{4,5b}$ 5.7, $J_{4,3}$ 7.0 Hz, 1H, H-4), 1.44 (s, 9H).

Experimental Methods

¹³C NMR (CDCl₃, 100 MHz): δ = 156.7 (CO), 137.9 (ArC), 137.5 (ArC), 136.0 (ArC), 128.8-128.0 (ArCH), 117.8 (CN), 80.6 (C), 78.1 (C-3), 74.9 (CH₂Ph), 73.5 (CH₂Ph), 72.9 (CH₂Ph), 68.3 (C-2), 67.8 (C-5), 60.5 (C-4), 28.4 (CH₃).

IR (ATR): 3339, 3014, 2979, 2929, 2870, 1718, 1497, 1454, 1393, 1367, 1249, 1216, 1157, 1088, 1073, 1028 cm⁻¹.

HRMS (ESI): *m/z* [M+H]⁺ calcd. for C₃₁H₃₈O₅N₃: 532.2806; found: 532.2802.



(2R,3R,4R)-1-Amino-3,4-bis(benzyloxy)-2-((benzyloxy)methyl)-5-iminopyrrolidine hydrochloride (D-46)

To a solution of nitrile D-44 (140 mg, 0.26 mmol) in DCM (10 mL) at rt was added TFA (2 mL) dropwise. The reaction mixture was stirred at rt for 3 h before toluene was added and the volatiles were removed in vacuo. The residue was then purified by flash column chromatography (DCM/MeOH (0.1 M HCl) 94:6). Collection of the appropriate fractions (*R_f* = 0.35, DCM/MeOH (0.1 M HCl) 9:1) provided compound D-46 (98.3 mg, 88%) as a clear colorless oil; [α]_D^{27.2 °C} = -11 (*c* 0.20 in MeOH).

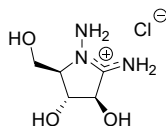
¹H NMR (MeOD, 400 MHz): δ = 7.34-7.25 (m, 15H, ArH), 4.82 (d, *J*_{4,3} = 3.9 Hz, 1H, H-4), 4.73 (d, *J* = 11.5 Hz, 1H, CHPh), 4.63 (d, *J* = 11.5 Hz, 1H, CHPh), 5.59 (d, *J* = 11.8 Hz, 1H, CHPh), 4.48 (bs, 2H, CHPh), 4.47 (d, *J* = 11.8 Hz, 1H, CHPh), 4.25 (t, *J* = 3.9 Hz, 1H, H-3), 3.96 (m, 1H, H-2), 3.89 (dd, *J*_{2'a,2} = 3.4 Hz, *J*_{2'a,2'b} = 10.9 Hz, 1H, H-2'a), 3.63 (dd, *J*_{2'b,2} = 3.2 Hz, *J*_{2'b,2'a} = 10.9 Hz, 1H, H-2'b).

Experimental Methods

¹³C NMR (MeOD, 100 MHz): δ = 166.7 (C=N), 138.9 (ArC), 138.4 (ArC), 138.1 (ArC), 129.6-129.1 (ArCH), 82.3 (C-2), 79.6 (C-3), 74.2 (CH₂Ph), 74.0 (CH₂Ph), 73.3 (CH₂Ph), 71.0 (C-4), 66.3 (C-4').

IR (ATR, cm⁻¹): 3029, 2929, 2110, 1953, 1882, 1811, 1702, 1624, 1495, 1453, 1362, 1261, 1209, 1121, 1099, 1063, 1028, 971, 915.

HRMS (ESI): m/z [M+H]⁺ calcd. for C₂₆H₃₀O₃N₃: 432.2282; found: 432.2276.



(2R,3R,4R)-1-Amino-3,4-dihydroxy-2-(hydroxymethyl)-5-iminopyrrolidine hydrochloride (D-47)

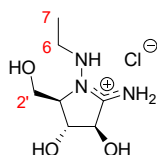
A degassed suspension of compound D-46 (98 mg, 0.23 mmol) and Pd/C (280 mg, 11.4 equiv.) in EtOH/TFA (10 mL, 9:1) was hydrogenated at 1 atm. at room temp for 19 h. The reaction mixture was then filtered through Celite by the aid of EtOH before the filtrate was concentrated by vacuo. The residue was dissolved in methanolic HCl (0.5 M) and evaporated to dryness to afford the HCl salt. The salt residue was purified by flash column chromatography (MeCN/H₂O 92:8). Collection of the appropriate fractions (R_f = 0.42, MeCN/H₂O (0.1 M HCl) 85:15) provided compound D-47 (40 mg, 90%) as yellow solids; mp 156.0-156.2 °C (decomposes). $[\alpha]_D^{27.2}$ = - 5.7 (*c* 0.35 in MeOH)

¹H NMR (D₂O, 400 MHz): δ = 4.83 (d, $J_{4,3}$ = 7.0 Hz, 1H, H-4), 4.27 (t, J = 7.0 Hz, 1H, H-3), 4.13 (dd, $J_{2'a,2}$ = 2.6 Hz, $J_{2'a,2'b}$ = 13.3 Hz, 1H, H-2'a), 3.87 (dd, $J_{2'b,2}$ = 2.5 Hz, $J_{2'b,2'a}$ = 13.3 Hz, 1H, H-2'b), 3.72 (app. dt, $J_{2,2'}$ = 2.5 Hz, $J_{2,3}$ = 7.0 Hz, 1H, H-2).

^{13}C NMR (D_2O , 100 MHz): $\delta = 167.4$ (C=N), 74.1 (C-4), 72.7 (C-3), 68.7 (C-2), 55.5 (C-6).

IR (ATR): 3369, 2125, 1724, 1624, 1205, 1109, 1063 cm^{-1} .

HRMS (ESI): m/z $[\text{M}+\text{H}]^+$ calcd. for $\text{C}_5\text{H}_{12}\text{O}_3\text{N}_3$: 162.0873; found: 162.0871.



**(2R,3R,4R)-1-(Ethylamino)-3,4-dihydroxy-2-(hydroxymethyl)-5-
iminopyrrolidine hydrochloride (D-48)**

A degassed suspension of compound D-46 (95 mg, 0.20 mmol) and Pd/C (235 mg) in EtOH/TFA (2 mL, 9:1) was hydrogenated at 1 atm at rt for 48 h. The reaction mixture was then filtered through Celite and washed with EtOH before the filtrate was concentrated in vacuo. The residue was dissolved in methanolic HCl (0.5 M) and evaporated to dryness to afford the HCl salt. The salt residue was purified by flash column chromatography (MeCN/ H_2O 88:12). Collection of the appropriate fractions ($R_f = 0.44$, MeCN/ H_2O , 9:1) provided compound D-48 (39 mg, 85%) as a yellow solid; mp 130.2–130.4 $^\circ\text{C}$ (decomposes); $[\alpha]_D^{25.2} = +12.0$ (c 0.17 in MeOH).

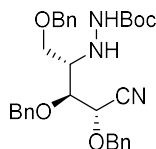
^1H NMR (D_2O , 400 MHz): $\delta = 4.90$ (d, $J_{4,3} = 6.9$ Hz, 1H, H-4), 4.31 (app. t, $J = 6.8$ Hz, 1H, H-3), 4.07 (dd, $J_{2'a,2'b} = 13.0$ Hz, $J_{2'b,2} = 2.6$ Hz, 1H, 2'a), 4.03 (dt, $J_{2,3} = 6.7$ Hz, $J_{2,2'b} = 2.7$ Hz, $J_{2,2'a} = 2.6$ Hz, 1H, H-2), 3.90 (dd, $J_{2'b,2'a} = 13.0$ Hz, $J_{2'b,2} = 2.7$ Hz, 1H, 2'b), 3.04 (dq, $J_{6a,6b} = 11.7$ Hz, $J_{6a,7} = 7.3$ Hz, 1H, H-6a), 2.91 (dq, $J_{6b,6a} = 11.7$ Hz, $J_{6b,7} = 7.1$ Hz, 1H, H-6b), 1.09 (app. t, $J = 7.2$ Hz, 3H, H-7).

Experimental Methods

^{13}C NMR (D_2O , 100 MHz): δ = 167.9 (C=N), 73.9 (C-4), 73.0 (C-3), 64.8 (C-2), 56.0 (C-2'), 42.0 (C-6), 11.8 (C-7).

IR (ATR, cm^{-1}): 3215, 2977, 2934, 2878, 2110, 1702, 1637, 1454, 1383, 1332, 1276, 1201, 1103, 1063, 905.

HRMS (ESI): m/z $[\text{M} + \text{H}]^+$ calcd for $\text{C}_7\text{H}_{16}\text{O}_3\text{N}_3$, 190.1186; found, 190.1184.



2,3,5-Tri-*O*-benzyl-4-(2-*tert*-butoxycarbonyl)hydrazinyl-4-deoxy-L-arabinonitrile (L-44)

Step 1: To a solution of alcohol D-**33** (334 mg, 0.8 mmol) in DCM (7 mL) at 0 °C was added pyridine (0.16 mL, 2.0 mmol, 2.5 equiv.). The reaction mixture was stirred for 10 min prior to dropwise addition of triflic anhydride (0.17 mL, 1.0 mmol, 1.25 equiv.). The reaction mixture was further stirred at 0 °C for 15 min. before being diluted with DCM (60 mL), washed with ice cold HCl (15 mL, 1 M), sat. aq. NaHCO_3 (20 mL), dried over Na_2SO_4 , and filtered. The residue (R_f = 0.71; Pet. ether/EtOAc, 7:3) was concentrated under reduced pressure and used directly in the following step.

Step 2: A suspension of *tert*-butylcarbazate (1.06 g, 8.0 mmol, 10 equiv.) and 4Å MS was stirred in THF (4.5 mL) for 24 hours. The suspension was then added a solution of the triflate from step 1 in THF (4.5 mL). The reaction was stirred at rt for 4 days before volatiles were removed under reduced pressure. The residue was subjected to flash column chromatography (Pet. ether/EtOAc 23:2 \rightarrow 17:3). Collection of the appropriate fractions (R_f = 0.39, Pet. ether/EtOAc 3:1) provided

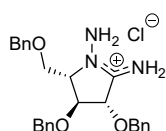
hydrazide L-44 (277 mg, 66 %) as a clear slightly white oil; $[\alpha]_D^{25.4^\circ\text{C}} = +8$ (*c* 1.0 in CHCl_3).

$^1\text{H NMR}$ (CDCl_3 , 400 MHz): $\delta = 7.37$ - 7.29 (m, 15 H), 5.83 (m, 1H, NH), 4.89 (d, $J = 11.5$ Hz, 1H, CHPh), 4.85 (d, $J = 11.1$ Hz, 1H, CHPh), 4.76 (d, $J_{2,3} 3.7$ Hz, 1H, H-2), 4.66 (d, $J = 11.1$ Hz, 1H, CHPh), 4.58 (d, $J = 11.5$ Hz, 1H, CHPh), 4.54 (d, $J = 11.8$ Hz, 1H, CHPh), 4.46 (d, $J = 11.8$ Hz, 1H, CHPh), 4.21 (br. s, 1H, NH), 3.84 (dd, $J_{2,3} 3.7$, $J_{3,4} 7.0$ Hz, 1H, H-3), 3.73 (dd, $J_{5a,4} 4.4$, $J_{5a,5b} 9.7$ Hz, 1H, H-5a), 3.62 (dd, $J_{5b,4} 5.7$, $J_{5b,5a} 9.7$ Hz, 1H, H-5b), 3.30 (ddd, $J_{4,5a} 4.4$, $J_{4,5b} 5.7$, $J_{4,3} 7.0$ Hz, 1H, H-4), 1.45 (2 br.s, 9H).

$^{13}\text{C NMR}$ (CDCl_3 , 100 MHz): $\delta = 156.7$ (C=O), 137.9 (Ar), 137.5 (Ar), 136.0 (Ar), 128.8-128.0 (Ar), 117.8 (CN), 80.6 (C), 78.1 (C-3), 74.9 (CH₂Ph), 73.5 (CH₂ Ph), 72.9 (CH₂ Ph), 68.3 (C-2), 67.8 (C-5), 60.5 (C-4), 28.4 (CH₃).

IR (ATR, cm^{-1}): 3339, 3014, 2979, 2929, 2870, 1718, 1497, 1454, 1393, 1367, 1249, 1216, 1157, 1088, 1073, 1028 cm^{-1} .

HRMS (ESI): m/z $[\text{M}+\text{Na}]^+$ calcd for $\text{C}_{31}\text{H}_{37}\text{O}_5\text{N}_3\text{Na}$: 554.2630; found: 554.2626.



(2S,3S,4S)-1-Amino-3,4-bis(benzyloxy)-2-((benzyloxy)methyl)-5-iminopyrrolidine hydrochloride (L-46)

To a solution of compound L-44 (165 mg, 0.31 mmol) in DCM at rt under argon was added TFA dropwise. The reaction was kept stirring for 2 h before volatiles were removed under reduced pressure. The residue was dissolved in methanolic HCl (0.2 M) and evaporated to afford the HCL-

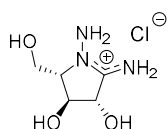
salt. The residue was subjected to flash column chromatography (CH₃Cl/MeOH (0.1 M HCl) 9:1). Collection of the appropriate fractions ($R_f = 0.25$, CH₃Cl/MeOH (0.1 M HCl) 9:1) provided compound L-46 (128 mg, 88%) as a clear slightly yellow oil; $[\alpha]_D^{27.0} = +10$ (c 0.20 in MeOH).

¹H NMR (MeOD, 400 MHz): $\delta = 7.36$ -7.25 (m, 15 H, ArH), 4.82 (d, $J_{4,3} = 3.8$ Hz, 1H, H-4), 4.73 (d, $J = 11.5$ Hz, 1H, CHPh), 4.63 (d, $J = 11.5$ Hz, 1H, CHPh), 4.59 (d, $J = 11.7$ Hz, 1H, CHPh), 4.48 (d, $J = 11.7$ Hz, 1H, CHPh), 4.48 (br. s, 2H, CHPh), 4.25 (t, $J = 3.8$ Hz, 1H, H-3), 3.97 (m, 1H, H-2), 3.89 (dd, $J_{6a,2} = 3.5$ Hz, $J_{6a,6b} = 10.8$ Hz, 1H, H-6a), 3.63 (dd, $J_{6b,2} = 2.8$, $J_{6a,6b} = 10.8$ Hz, 1H, H-6b).

¹³C NMR (MeOD, 100 MHz): $\delta = 166.6$ (C=N), 138.8 (Ar), 138.4 (Ar), 138.1 (Ar), 129.5-129.0 (Ar), 82.2 (C-4), 79.5 (C-3), 74.2 (CH₂), 74.0 (CH₂), 73.3 (CH₂), 70.9 (C-2), 66.3 (C-6).

IR (ATR, cm⁻¹): 3029, 2929, 2110, 1953, 1882, 1811, 1702, 1624, 1495, 1453, 1362, 1261, 1209, 1121, 1099, 1063, 1028, 971, 915.

HRMS (ESI): m/z [M+H]⁺ calcd for C₂₆H₃₀O₃N₃, 432.2287; found, 432.2283.



(2*S*,3*S*,4*S*)-1-Amino-3,4-dihydroxy-2-(hydroxymethyl)-5-iminopyrrolidine hydrochloride (L-47)

A suspension of compound L-46 (30 mg, 0.064 mmol) and Pd/C (84 mg, 0.79 mmol) in 9:1 EtOH/TFA (2.5 mL) was hydrogenated at rt for 18 h. The reaction mixture was then filtered through celite by the aid of methanol (10 mL). The filtrate was added a solution of methanolic HCl

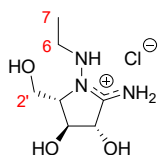
(10 mL) and evaporated to afford the HCl-salt. The residue was subjected to gravity column chromatography (MeCN/H₂O 97:3). Collection of the appropriate fractions ($R_f = 0.29$, MeCN/H₂O (0.1 M HCl) 8:2) provided compound L-47 (12 mg, 0.061 mmol, 95%) as a yellow solid; mp: 156-156.5 °C; $[\alpha]_D^{26.2^\circ\text{C}} = +5.4$ (c 0.37 in MeOH).

¹H NMR (D₂O, 400 MHz): $\delta = 4.83$ (d, $J_{4,3} = 7.0$ Hz, 1H, H-4), 4.27 (t, $J = 7.0$ Hz, 1H, H-3), 4.13 (dd, $J_{6a,2} = 2.6$ Hz, $J_{6a,6b} = 13.3$ Hz, 1H, H-6a), 3.87 (dd, $J_{6b,2} = 2.5$ Hz, $J_{6b,6a} = 13.3$ Hz, 1H, H-6b), 3.72 (app. dt, $J_{2,6} = 2.5$ Hz, $J_{2,3} = 7.0$ Hz, 1H, H-2).

¹³C NMR (D₂O, 100 MHz): $\delta = 167.4$ (C=N), 74.1 (C-4), 72.7 (C-3), 69.0 (C-2), 55.6 (C-6).

IR (ATR, cm⁻¹): 3369, 2125, 1724, 1624, 1205, 1109, 1063 cm⁻¹.

HRMS (ESI): m/z [M+H]⁺ calcd. for C₅H₁₂O₃N₃: 162.0878; found 162.0874.



(2S,3S,4S)-1-(Ethylamino)-3,4-dihydroxy-2-(hydroxymethyl)-5-iminopyrrolidine hydrochloride (L-48)

A suspension of compound L-46 (20 mg, 0.043 mmol) and Pd/C (70 mg, 0.65 mmol) in 9:1 EtOH/TFA (2.5 mL) was hydrogenated at rt for 47 h. The reaction mixture was then filtered through celite by the aid of methanol (10 mL). The filtrate was added a solution of methanolic HCl (10 mL) and evaporated to afford the HCl-salt. The residue was subjected to gravity column chromatography (MeCN/H₂O 97:3). Collection of the appropriate fractions ($R_f = 0.45$, MeCN/H₂O (0.1 M HCl) 4:1) provided

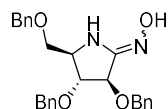
compound L-48 (1.7 mg, 7.5 μ mol, 17%) as a yellow solid; mp = 130.0-131.0 $^{\circ}$ C (decomposes); $[\alpha]_{\text{D}}^{25.2} = -12$ (*c* 0.17 in MeOH).

$^1\text{H NMR}$ (D_2O , 400 MHz): $\delta = 4.90$ (d, $J_{4,3} = 6.9$ Hz, 1H, H-4), 4.31 (app. t, $J = 6.8$ Hz, 1H, H-3), 4.07 (dd, $J_{2'a,2'b} = 13.0$ Hz, $J_{2'a,2} = 2.6$ Hz, 1H, 2'a), 4.03 (dt, $J_{2,3} = 6.7$ Hz, $J_{2,2'b} = 2.7$ Hz, $J_{2,2'a} = 2.6$ Hz, 1H, H-2), 3.90 (dd, $J_{2'b,2'a} = 13.0$ Hz, $J_{2'b,2} = 2.7$ Hz, 1H, 2'b), 3.04 (dq, $J_{6a,6b} = 11.7$ Hz, $J_{6a,7} = 7.3$ Hz, 1H, H-6a), 2.91 (dq, $J_{6b,6a} = 11.7$ Hz, $J_{6b,7} = 7.1$ Hz, 1H, H-6b), 1.09 (app. t, $J = 7.2$ Hz, 3H, H-7).

$^{13}\text{C NMR}$ (D_2O , 100 MHz): $\delta = 167.9$ (C=N), 73.9 (C-4), 73.0 (C-3), 64.8 (C-2), 56.0 (C-2'), 42.0 (C-6), 11.8 (C-7).

IR (ATR, cm^{-1}): 3215, 2977, 2934, 2878, 2110, 1702, 1637, 1454, 1383, 1332, 1276, 1201, 1103, 1063, 905.

HRMS (ESI): m/z $[\text{M} + \text{H}]^+$ calcd for $\text{C}_7\text{H}_{16}\text{O}_3\text{N}_3$, 190.1191; found, 190.1186.



(3R,4R,5R)-3,4-bis(benzyloxy)-5-((benzyloxy)methyl)pyrrolidin-2-one oxime (D-54)

Step 1: To a solution of alcohol L-33 (271 mg, 0.65 mmol) in DCM (10 mL) at 0 $^{\circ}$ C was added pyridine (0.13 mL, 1.63 mmol, 2.5 equiv.). The reaction mixture was stirred for 10 min prior to dropwise addition of triflic anhydride (0.13 mL, 0.81 mmol, 1.25 equiv.). The reaction mixture was further stirred at 0 $^{\circ}$ C for 15 min. before being diluted with DCM (60 mL), washed with ice cold HCl (20 mL, 1 M), followed by sat. aq. NaHCO_3 (30 mL), dried over Na_2SO_4 , and filtered. The residue ($R_f =$

0.71, Pet. ether/EtOAc 7:3) was concentrated under reduced pressure and used directly in the following step.

Step 2: To a solution of sodium (58 mg, 2.52 mmol) dissolved in EtOH (3 mL) was added $\text{NH}_2\text{OH}\cdot\text{HCl}$ (275 mg, 3.96 mmol) and 4 Å MS (5 mg) at rt. The heterogeneous mixture was stirred for 10 min before adding a solution of the residue from step 1 in EtOH (3 mL) at 0 °C. The resulting reaction mixture was stirred at rt for 24 h. Volatiles were then removed under reduced pressure and the residue was subjected to flash column chromatography ($\text{CHCl}_3/\text{MeOH}$ 95:5). Collection of the appropriate fractions ($R_f = 0.40$, $\text{CHCl}_3/\text{MeOH}$ 95:5) provided compounds D-ribo-**54** (6.3 mg, 2%), D-**54** (103 mg, 36%), and a mixture of D-ribo-**54** and D-**54** (57.5 mg, 21%) as clear colorless oils.

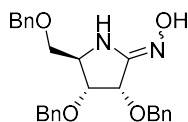
$$[\alpha]_{\text{D}}^{24.0\text{ }^\circ\text{C}} = -14 \text{ (} c \text{ 1.0 in } \text{CHCl}_3 \text{)}$$

^1H NMR (MeOD, 400 MHz): $\delta = 7.33\text{--}7.26$ (m, 15H, ArH), 4.77 (d, $J_{4,3} = 3.5$ Hz, 1H, H-4), 4.70 (d, $J = 11.4$ Hz, 1H, CHPh), 4.60 (d, $J = 11.4$ Hz, 1H, CHPh), 4.53 (d, $J = 12.0$ Hz, 2H, CHPh), 4.49 (d, $J = 12.0$ Hz, 2H, CHPh), 4.25 (t, $J = 3.5$ Hz, 1H, H-3), 3.96 (m, 1H, H-2), 3.62 (dd, $J_{2'a,2'b} = 10.2$ Hz, $J_{2'a,2} = 5.2$ Hz, 1H, H-2'a), 3.56 (dd, $J_{2'b,2'a} = 10.2$ Hz, $J_{2'b,2} = 4.7$ Hz, 1H, H-2'b).

^{13}C NMR (MeOD, 100 MHz): $\delta = 162.0$ (C=N), 139.0 (ArC), 138.6 (ArC), 138.1 (ArC), 129.5-128.9 (ArCH), 82.5 (C-3), 82.2 (C-4), 74.3 (CHPh), 73.9 (CHPh), 73.1 (CHPh), 70.0 (C-2'), 64.3 (C-2).

IR (ATR, cm^{-1}): 3152, 3032, 2868, 1707, 1496, 1454, 1364, 1281, 1223, 1164, 1103, 913, 735.

HRMS (ESI): m/z $[\text{M}+\text{Na}]^+$ calcd. for $\text{C}_{26}\text{H}_{28}\text{O}_4\text{N}_2\text{Na}$: 455.1946, found: 455.1940.



(3S,4R,5R)-3,4-bis(benzyloxy)-5-((benzyloxy)methyl)pyrrolidin-2-one oxime D-ribo-54

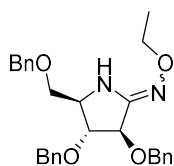
$$[\alpha]_{\text{D}}^{24.0\text{ }^{\circ}\text{C}} = +4 \text{ (} c \text{ 0.5 in CHCl}_3\text{)}$$

¹H NMR (MeOD, 400 MHz): δ = 7.32-7.27 (m, 15H, ArCH), 4.70 (d, J = 11.5 Hz, 1H, CHPh), 4.56-4.50 (m, 6H, CHPh + H-3), 4.12 (t, J = 2.8 Hz, 1H, H-4), 3.85 (ddd, $J_{5,4}$ = 2.8 Hz, $J_{5,5'b}$ = 5.5 Hz, $J_{5,5'a}$ = 5.9 Hz, 1H, H-5), 3.56 (dd, $J_{5'a,5}$ = 6.0 Hz, $J_{5'a,5'b}$ = 9.8 Hz, 1H, H-5'a), 3.53 (dd, $J_{5'b,5}$ = 5.6 Hz, $J_{5'b,5'a}$ = 9.8 Hz, 1H, H-5'b).

¹³C NMR (MeOD, 100 MHz): δ = 162.0 (C=N), 139.0 (ArC), 138.6 (ArC), 138.1 (ArC), 129.5-128.9 (ArCH), 82.5 (C-3), 82.2 (C-4), 74.3 (CHPh), 73.9 (CHPh), 73.1 (CHPh), 70.0 (C-2'), 64.3 (C-2).

IR (ATR, cm^{-1}): 3230, 3062, 3031, 2924, 2866, 1706, 1496, 1454, 1363, 1262, 1208, 1096, 1027, 736, 697.

HRMS (ESI): m/z $[M+\text{Na}]^+$ calcd. for $\text{C}_{26}\text{H}_{28}\text{O}_4\text{N}_2\text{Na}$: 455.1946, found: 455.1940.



(3R,4R,5R)-3,4-bis(benzyloxy)-5-((benzyloxy)methyl)pyrrolidin-2-one O-ethyl oxime (D-55)

A solution of compound D-54 (10 mg, 0.023 mmol), iodoethane (0.4 mL, 5 mmol), and Cs_2CO_3 (7.5 mg, 1 equiv.) in MeCN (1 mL) was stirred for

Experimental Methods

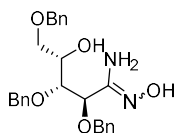
3 days until TLC analysis indicated full conversion from starting material to product. Volatiles were then removed under reduced pressure. The residue was subjected to flash column chromatography (Pet. ether/EtOAc 5:1). Collection of the appropriate fractions ($R_f = 0.52$, Pet. ether/EtOAc 3:1) provided compound D-55 (8.7 mg, 82%) as a clear colorless oil.

$^1\text{H NMR}$ (CDCl_3 , 400 MHz): $\delta = 7.34\text{-}7.25$ (m, 15H, ArH), 5.40 (br. s, 1H, NH), 4.93 (d, $J = 11.7$ Hz, 1H, CHPh), 4.60 (d, $J = 11.7$ Hz, 1H, CHPh), 4.57 (d, $J = 11.8$ Hz, 1H, CHPh), 4.52 (d, $J = 11.9$ Hz, 1H, CHPh), 4.51 (d, $J = 11.8$ Hz, 1H, CHPh), 4.48 (d, $J = 11.9$ Hz, 1H, CHPh), 4.36 (d, $J_{3,4} = 3.0$ Hz, 1H, H-3), 4.03 (dq, $J = 3.1, 7.0$ Hz, 2H, CH_2), 3.87 (t, $J = 3.0$ Hz, 1H, H-4), 3.75 (m, 1H, H-5), 3.56 (dd, $J_{5'a,5} = 5.2$ Hz, $J_{5'a,5'b} = 9.2$ Hz, 1H, H-5'a), 3.42 (dd, $J_{5'b,5} = 8.2$ Hz, $J_{5'b,5'a} = 9.2$ Hz, 1H, H-5'b), 1.26 (t, $J = 7.0$ Hz, 3H, CH_3).

$^{13}\text{C NMR}$ (CDCl_3 , 100 MHz): $\delta = 154.3$ (C=N), 137.89 (ArC), 137.85 (ArC), 137.5 (ArC), 128.5-127.7 (ArCH), 82.3 (C-4), 80.0 (C-3), 73.4 (CHPh), 72.2 (C-5'), 71.8 (CHPh), 71.6 (CHPh), 69.0 (CH_2), 60.2 (C-5), 14.8 (CH_3).

IR (ATR, cm^{-1}): 3062, 3032, 2925, 2857, 1735, 1668, 1496, 1454, 1377, 1362, 1314, 1287, 1207, 1090, 1055, 910, 869, 735, 697.

HRMS (ESI): m/z $[\text{M}+\text{H}]^+$ calcd. for $\text{C}_{28}\text{H}_{32}\text{O}_4\text{N}_2$: 461.2440; found 461.2438.



(2*R*,3*R*,4*S*)-2,3,5-tris(benzyloxy)-*N'*,4-dihydroxypentanimidamide (L-57)

Experimental Methods

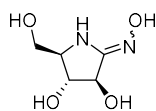
A suspension of $\text{NH}_2\text{OH}\cdot\text{HCl}$ (50 mg, 6 equiv.) and 0.43 M NaOEt in EtOH (0.84 mL, 3 equiv.) was stirred for 20 min before adding a solution of compound L-33 (50 mg, 0.12 mmol) EtOH (2 mL). The resulting reaction was stirred at rt under nitrogen for 19 h. Volatiles were then removed under reduced pressure and the residue was subjected to flash column chromatography (DCM/MeOH 95:5). Collection of the appropriate fractions ($R_f = 0.49$, DCM/MeOH 9:1) provided compound L-57 (39 mg, 73%) as a clear colorless oil; $[\alpha]_D^{25.5\text{ }^\circ\text{C}} = -10.7^\circ$ (c 1.5 in CHCl_3).

^1H NMR (CDCl_3 , 400 MHz): $\delta = 7.34\text{-}7.28$ (m, 15H, ArH), 4.92 (br. s, 2H, OH), 4.88 (d, $J = 11.2$ Hz, 1H, CHPh), 4.61 (d, $J = 11.4$ Hz, 1H, CHPh), 4.59 (d, $J = 11.2$ Hz, 1H, CHPh), 4.50 (d, $J = 12.0$ Hz, 1H, CHPh), 4.47 (d, $J = 11.4$ Hz, 1H, CHPh), 4.43 (d, $J = 12.0$ Hz, 1H, CHPh), 4.32-4.28 (m, 1H, H-2), 3.98-3.95 (m, 1H, H-4), 3.76-3.74 (m, 1H, H-3), 3.51 (dd, $J = 6.8, 9.3$ Hz, 1H, H-5a), 3.41 (dd, $J = 5.5, 9.3$ Hz, 1H, H-5b).

^{13}C NMR (CDCl_3 , 100 MHz): $\delta = 152.2$ (C=N), 138.4 (ArC), 137.9 (ArC), 137.5 (ArC), 128.6-127.9 (ArCH), 80.2 (C-3), 79.3 (C-2), 75.3 (CH_2Ph), 73.5 (CH_2Ph), 72.1 (CH_2Ph), 71.7 (C-5), 69.5 (C-4).

IR (ATR, cm^{-1}): 3479, 3354, 3063, 3030, 2920, 2865, 1785, 1664, 1575, 1496, 1453, 1364, 1209, 1089, 1073, 1027, 914, 821, 734.

HRMS (ESI): m/z $[\text{M}+\text{H}]^+$ calcd. for $\text{C}_{26}\text{H}_{30}\text{O}_5\text{N}_2$: 451.2233, found: 451.2229.



(3R,4R,5R)-3,4-dihydroxy-5-(hydroxymethyl)pyrrolidin-2-one oxime (D-58)

Experimental Methods

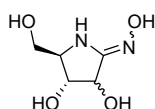
A solution of compound D-**54** (57 mg, 0.13 mmol) in DCM (10 mL) at -78 °C under argon was added a solution of 1 M BCl₃ in heptane (0.78 mL, 0.78 mmol). The reaction was stirred at -78 °C for 3 h and then stirred at rt for 22 h. The reaction was then quenched with EtOH (4 mL) at 0 °C. Volatiles were removed by reduced pressure and the residue was subjected to gravity column chromatography (MeCN/H₂O 98:2). Collection of appropriate fractions (*R*_f = 0.37, MeCN/H₂O 8:2) provided compound D-**58** (14.1 mg, 67%) as a clear white wax; $[\alpha]_D^{24.0} = -25.8$ (*c* 0.5 in MeOH).

¹H NMR (D₂O, 400 MHz): $\delta = 4.93$ (d, $J_{4,3} = 7.4$ Hz, 1H, H-4), 4.24 (t, $J = 7.2$ Hz, 1H, H-3), 3.91-3.87 (m, 1H, H-2'a), 3.77-3.73 (m, 2H, H-2+H-2'b).

¹³C NMR (D₂O, 100 MHz): $\delta = 162.7$ (C=N), 75.2 (C-3), 74.9 (C-4), 62.4 (C-2), 59.0 (C-2').

IR (ATR, cm⁻¹): 3162, 1701, 1405, 1333, 1271, 1200, 1096, 1042, 990, 922, 886.

HRMS (ESI): *m/z* [M+H]⁺ calcd. For C₅H₁₀N₂O₄: 163.0718; found 163.0713.



(4*R*,5*R*)-3,4-dihydroxy-5-(hydroxymethyl)pyrrolidin-2-one oxime (D-ribo-58** + D-**58**)**

A solution of compound D-ribo-**54** + D-**54** (50 mg, 0.11 mmol) in DCM (10 mL) at -78 °C under argon was added a solution of 1 M BCl₃ in heptane (0.66 mL, 0.66 mmol). The reaction was stirred at -78 °C for 3 h and then stirred at rt for 22 h. The reaction was then quenched with

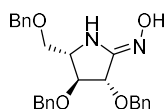
EtOH (4 mL) at 0 °C. Volatiles were removed by reduced pressure and the residue was subjected to gravity column chromatography (MeCN/H₂O 98:2). Collection of appropriate fractions ($R_f = 0.37$, MeCN/H₂O 8:2) provided a mixture of isomers *D-ribo-58* and *D-58* (11.0 mg, 62%) as a clear white wax.

¹H NMR (D₂O, 400 MHz): $\delta = 5.13$ (d, $J_{3,4} = 5.3$ Hz, 1H- H-3, *D-ribo-58*), 4.93 (d, $J_{3,4} = 7.4$ Hz, 1H, H-3, *D-58*), 4.39 (dd, $J_{4,3} = 5.3$ Hz, $J_{4,5} = 1.0$ Hz, 1H, H-4, *D-ribo-58*), 4.25 (t, $J = 7.2$ Hz, 1H, H-4, *D-58*), 3.94 (td, $J_{5,4} = 1.0$ Hz, $J_{5,5'} = 3.8$ Hz, 1H, H-5, *D-ribo-58*), 3.93-3.88 (m, 1H, H-5'a, *D-58*), 3.77-3.73 (m, 2H, H-5+H-5'b, *D-58* + 2H, H-5', *D-ribo-58*)

¹³C NMR (D₂O, 100 MHz): $\delta = 164.0$ (C=N, *D-ribo-58*), 162.7 (C=N, *D-58*), 75.3 (C-3, *D-58*), 74.9 (C-4, *D-58*), 71.1 (C-3, *D-ribo-58*), 70.9 (C-4, *D-ribo-58*), 67.0 (C-2, *D-ribo-58*), 62.5 (C-2, *D-58*), 60.6 (C-2', *D-ribo-58*), 59.0 (C-2', *D-58*)

IR (ATR, cm⁻¹): 3163, 1698, 1405, 1333, 1271, 1202, 1096, 1042, 990, 923, 886

HRMS (ESI): m/z [M+H]⁺ calcd. For C₅H₁₀N₂O₄: 163.0718; found 163.0712.



(3*S*,4*S*,5*S*)-3,4-bis(benzyloxy)-5-((benzyloxy)methyl)pyrrolidin-2-one oxime (L-54)

Step 1: To a solution of alcohol *D-33* (125 mg, 0.3 mmol) in DCM (5 mL) at 0 °C was added pyridine (0.06 mL, 0.75 mmol, 2.5 equiv.). The reaction mixture was stirred for 10 min prior to dropwise addition of triflic anhydride (0.06 mL, 0.38 mmol, 1.25 equiv.). The reaction

mixture was further stirred at 0 °C for 15 min. before being diluted with DCM (30 mL), washed with ice cold HCl (10 mL, 1 M), followed by sat. aq. NaHCO₃ (15 mL), dried over Na₂SO₄, and filtered. The residue (*R*_f = 0.71, Pet. ether/EtOAc 7:3) was concentrated under reduced pressure and used directly in the following step.

Step 2: Step 2: To a suspension of NH₂OH•HCl (112.5 mg, 1.62 mmol) in EtOH (2.0 mL) was added Et₃N (0.23 mL, 1.62 mmol) dropwise at 0 °C under argon. The resulting mixture was stirred for 30 min at rt before adding a solution of the residue from step 1 in EtOH (2.5 mL) at 0 °C under argon. The resulting reaction mixture was stirred for 17 h at rt. Volatiles were then removed under reduced pressure. The residue was subjected to flash column chromatography (CH₃Cl/MeOH, 99:1--> 96:4). Collection of the appropriate fractions (*R*_f = 0.34; CH₃Cl/MeOH, 9:1) provided compound L-54 (34mg, 26%) and compound L-59 (22 mg, 17%) as clear colorless oils.

Spectroscopic data for L-54:

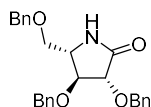
$$[\alpha]_D^{24.5\text{ }^\circ\text{C}} = +14 \text{ (} c \text{ 1.0 in CHCl}_3 \text{)}$$

¹H NMR (MeOD, 400 MHz): δ = 7.35-7.26 (m, 15H, ArH), 4.86 (d, *J*_{4,3} = 3.7 Hz, 1H, H-4), 4.69 (d, *J* = 11.4 Hz, 1H, CHPh), 4.61 (d, *J* = 11.4 Hz, 1H, CHPh), 4.56-4.49 (m, 4H, CHPh), 4.32 (t, *J* = 3.7 Hz, 1H, H-3), 4.01 (app. dd, *J* = 4.5 Hz, 8.3 Hz, 1H, H-2) 3.65 (dd, *J*_{2'a,2} = 4.5 Hz, *J*_{2'a,2'b} = 10.3 Hz, 1H, H-2'a), 3.58 (dd, *J*_{2'b,2} = 4.5 Hz, *J*_{2'b,2'a} = 10.3 Hz, 1H, H-2'b),

¹³C NMR (MeOD, 100 MHz): δ = 162.8 (N=C), 138.9 (Ar), 138.5 (Ar), 137.9 (Ar), 129.8-128.9 (Ar), 82.7 (C-4), 82.1 (C-3), 74.4 (CH₂), 74.2 (CH₂), 73.3 (CH₂), 69.6 (C-2'), 64.7 (C-2).

IR (ATR, cm⁻¹): 3029, 2928, 2883, 2799, 1702, 1496, 1453, 1396, 1364, 1285, 1239, 1209, 1090, 1027, 911, 819, 733.

HRMS (ESI): m/z $[M+Na]^+$ calcd. for $C_{26}H_{28}O_4N_2Na$: 455.1946, found: 455.1941.



(3R,4S,5S)-3,4-bis(benzyloxy)-5-((benzyloxy)methyl)pyrrolidin-2-one (L-59)

The spectroscopic data were in full accord with the previously reported data of the opposite enantiomer.¹³⁴

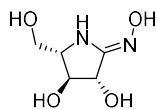
$[\alpha]_D^{24.6\text{ }^\circ\text{C}} = +2.2$ (c 0.9 in $CHCl_3$) (lit.¹³⁴ $[\alpha]_D = -3.9$ (c 0.77 in $CHCl_3$) opposite enantiomer)

1H NMR (MeOD, 400 MHz): $\delta = 7.42$ - 7.22 (m, 15H, Ar-H), 5.83 (br. s, 1H, NH), 5.12 (d, $J = 11.5$ Hz, 1H, CHPh), 4.80 (d, $J = 11.5$ Hz, 1H, CHPh), 4.61 (d, $J = 11.7$ Hz, 1H, CHPh), 4.51-4.49 (m, 3H, CHPh), 4.22 (d, $J = 5.8$ Hz, 1H, H-4), 3.89 (t, $J = 5.8$ Hz, 1H, H-3), 3.70-3.66 (m, 1H, H-2), 3.64-3.60 (m, 1H, H-6a), 3.34-3.29 (m, 1H, 6b).

^{13}C NMR (MeOD, 100 MHz): $\delta = 173.0$ (C=N), 137.7 (Ar), 137.51 (Ar), 137.50 (Ar), 128.7-128.5 (Ar), 128.1-127.9 (Ar), 81.3 (C-3), 80.9 (C-4), 73.6 (CH₂), 72.7 (CH₂), 72.4 (CH₂), 71.6 (C-6), 56.1 (C-2).

IR (ATR, cm^{-1}): 3213, 3062, 3030, 2920, 2559, 1707, 1496, 1453, 1356, 1310, 1280, 1206, 1092, 1026, 909, 819, 732.

HRMS (ESI): m/z $[M+Na]^+$ calcd. for $C_{26}H_{27}O_4NNa$: 440.1837, found: 440.1833.



(3S,4S,5S)-3,4-dihydroxy-5-(hydroxymethyl)pyrrolidin-2-one oxime (L-58)

A solution of L-54 (27 mg, 0.06 mmol) in DCM (6 mL) at -78 °C under argon was added BCl₃ (1 M in heptane, 0.36 mL, 2 equiv. pr benzyl). The reaction was stirred at -78 °C for 3h and then slowly allowed the reaction to reach 0 °C over 15 h. The reaction was then quenched with EtOH (1 mL) at 0 °C before volatiles were removed with reduced pressure. The residue was subjected to gravity column chromatography (MeCN/H₂O (0.05 M HCl) 97:3). Collection of appropriate fractions (*R_f* = 0.37, MeCN/H₂O 8:2) provided L-58 (5.0 mg, 50%) as a yellow wax; $[\alpha]_{\text{D}}^{23.9\text{ }^{\circ}\text{C}} = +26.4$ (*c* 0.53 in MeOH).

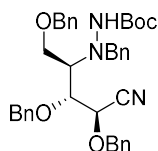
¹H NMR (D₂O, 400 MHz): δ = 4.93 (d, *J*_{4,3} = 7.4 Hz, 1H, H-4), 4.24 (t, *J* = 7.2 Hz, 1H, H-3), 3.91-3.87 (m, 1H, H-2'a), 3.77-3.73 (m, 2H, H-2+H-2'b).

¹³C NMR (D₂O, 100 MHz): δ = 162.7 (C=N), 75.2 (C-3), 74.9 (C-4), 62.4 (C-2), 59.0 (C-2').

IR (ATR, cm⁻¹): 3160, 1700, 1405, 1333, 1270, 1200, 1096, 1042, 990, 886.

HRMS (ESI): *m/z* [M+H]⁺ calcd. for C₅H₁₀O₄N₂: 163.0718; found 163.0712.

7.3 Synthesis Towards the Glucono-Hydrazide Imide



2,3,5-Tri-*O*-benzyl-4-(1-*N*-benzyl-(2-*tert*-butoxycarbonyl)hydrazinyl)-4-deoxy-*D*-arabinonitrile (D-67)

To a solution of compound D-44 (104 mg, 0.20 mmol) in DCE was added Na(OAc)₃BH (116 mg, 2.7 equiv.) followed by benzaldehyde (0.04 mL, 2.0 equiv.) and AcOH (0.07 mL, 6.2 equiv.). The reaction was stirred at room temp. for 18 h. The reaction mixture was then quenched with sat. aq. NaHCO₃ (5 mL) and EtOAc (10 mL) was added. The two phases were separated, and the aq. phase was extracted with EtOAc (2 x 10 mL). The combined organic fractions were evaporated to dryness under vacuo. Excess of benzaldehyde was removed under vacuum at 60 °C for 1 h. The residue was purified by flash column chromatography (Pet. ether/EtOAc 9:1). Collection of the appropriate fractions (*R*_f = 0.25, Pet. ether/EtOAc 9:1) provided compound D-67 (89 mg, 73%) as a light-yellow oil.

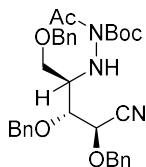
¹H NMR (CDCl₃, 400 MHz): δ = 7.41-6.96 (m, 20H, ArH), 6.28 and 5.84 (br.s, 1.4:1, 1H, NH), 5.52 and 5.22 (br.s, 1.5:1, 1H, H-2), 4.98 (d, *J* = 10.9 Hz, 1H, CHPh), 4.84 (d, *J* = 10.3 Hz, 1H, CHPh), 4.60 (d, *J* = 10.8 Hz, 1H, CHPh), 4.58 (d, *J* = 10.3 Hz, 1H, CHPh), 4.49 (d, *J* = 11.2 Hz, 2H, 2CHPh), 4.00-3.68 (m, 5H, 2CHPh, H-5a, H-5b, H-3), 3.34 (brs, 1H, H-4), 1.32-1.24 (m, 9H).

¹³C NMR (CDCl₃, 100 MHz): δ = 155.9 (C=O), 137.8-136.1 (Ar), 130.0-127.5 (Ar), 118.9-118.6 (CN), 80.8 and 80.0 (C), 78.4 (C-3), 75.2 and 74.9 (CH₂), 73.8 and 73.6 (CH₂), 73.2 and 72.8 (CH₂), 67.6 and 66.7 (C-

2), 67.0 (CH₂), 63.6 and 61.9 (C-5), 61.6 and 60.7 (C-4), 28.3 and 28.1 (CH₃).

IR (ATR, cm⁻¹): 3355, 3031, 2925, 2866, 1950, 1725, 1706, 1496, 1454, 1392, 1243, 1160, 1124, 1072, 1027, 913.

HRMS (ESI): *m/z* [M+Na]⁺ calcd. for C₃₈H₄₃O₅N₃Na: 644.3095; found: 644.3088.



2,3,5-Tri-*O*-benzyl-4-(2-*N*-acetyl-(2-*tert*-butoxycarbonyl)hydrazinyl)-4-deoxy-D-arabinonitrile (D-75)

To a solution of compound D-44 (21 mg, 0.04 mmol) in Ac₂O (0.4 mL) under argon at rt was added pyridine (0.05 mL). The reaction was stirred for 20 h before volatiles were removed under reduced pressure. The residue was subjected to flash column chromatography (Pet. ether/EtOAc 4:1). Collection of the appropriate fractions (*R_f* = 0.67, Pet. ether/EtOAc 3:1) provided compound D-75 (17 mg, 75%) as a clear colorless oil; $[\alpha]_D^{25.3} = -32$ (*c* 1.5 in CHCl₃).

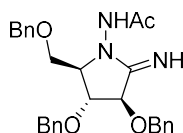
¹H NMR (CDCl₃, 400 MHz): δ = 7.34-7.36 (m, 15H, Ar-H), 5.66 (d, *J* = 7.5 Hz, 1H, NH), 4.89 (d, *J* = 11.1 Hz, 1H, CHPh), 4.83 (d, *J* = 11.3 Hz, 1H, CHPh), 4.72 (d, *J* = 11.1 Hz, 1H, CHPh), 4.71 (d, *J*_{4,3} = 6.3 Hz, 1H, H-4) 4.56 (d, *J* = 11.3 Hz, 1H, CHPh), 4.44 (br. s., 2H, CHPh), 3.99 (dd, *J*_{3,4} = 6.3 Hz, *J*_{3,2} = 4.1 Hz, 1H, H-3), 3.67 (dd, *J*_{1a,1b} = 9.7 Hz, *J*_{1a,2} = 6.5 Hz, 1H, H-1a), 3.57 (dd, *J*_{1b,1a} = 9.7 Hz, *J*_{1b,2} = 4.5 Hz, 1H, H-1b), 3.50-3.44 (m, 1H, H-2), 2.44 (s, 3H, Ac), 1.53 (s, 9H, Boc).

Experimental Methods

¹³C NMR (CDCl₃, 100 MHz): δ = 172.1 (CO, Ac), 152.3 (CO, Boc), 138.1 (Ar), 137.9 (Ar), 136.1 (Ar), 128.7-128.5 (Ar), 128.0-127.8 (Ar), 117.4 (CN), 84.6 (C), 79.4 (C-3), 75.3 (CH₂Ph), 73.5 (CH₂Ph), 73.0 (CH₂Ph), 70.1 (C-4), 67.3 (C-1), 59.9 (C-2), 28.1 (CH₃, Boc), 26.0 (CH₃, Ac).

IR (ATR, cm⁻¹): 3030, 2926, 2867, 1735, 1686, 1553, 1496, 1454, 1394, 1368, 1328, 1244, 1144, 1090, 1028, 982, 735.

HRMS (ESI): m/z [M+Na]⁺ calcd. for C₃₃H₃₉O₆N₃: 596.2736, found: 596.2731.



***N*-((2*R*,3*R*,4*R*)-3,4-bis(benzyloxy)-2-((benzyloxy)methyl)-5-iminopyrrolidin-1-yl)acetamide (D-76)**

A solution of compound D-75 (15 mg, 0.03 mmol) in DCM/TFA (9:1, 1 mL) was stirred at rt for 3 h before volatiles were removed under reduced pressure. The residue was subjected to flash column chromatography (CH₃Cl/MeOH (0.1 M HCl) 95:5). Collection of the appropriate fractions (R_f = 0.30, CH₃Cl/MeOH (0.1 M HCl) 9:1) provided compound D-76 (12 mg, 85%) as a clear colorless oil.

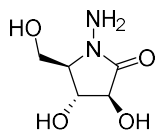
¹H NMR (MeOD, 400 MHz): δ = 7.39-7.24 (m, 15 H, Ar-H), 4.97 (d, $J_{4,3}$ = 4.5 Hz, 1H, H-4), 4.78 (d, J = 11.4 Hz, 1H CHPh), 4.68 (d, J = 11.4 Hz, 1H CHPh), 4.56 (d, J = 11.6 Hz, 1H, CHPh), 4.49 (br. s, 2H, CHPh), 4.42 (d, J = 11.6 Hz, 1H, CHPh), 4.34 (t, J = 4.5 Hz, 1H, H-3), 4.09 (m, 1H, H-2), 3.71 (dd, $J_{6a,4}$ = 3.4 Hz, $J_{6a,6b}$ = 11.1 Hz, 1H, H-6a), 3.59 dd, $J_{6b,4}$ = 3.8 Hz, $J_{6b,6a}$ = 11.1 Hz, 1H, H-6b), 2.04 (s, 3H).

Experimental Methods

¹³C NMR (MeOD, 100 MHz): δ = 171.0 (C=O), 168.1 (C=N), 138.8 (ArC), 138.4 (ArC), 137.9 (ArC), 129.6-128.8 (ArCH), 81.9 (C-4), 79.5 (C-3), 74.3 (2CH₂Ph), 73.5 (CH₂Ph), 69.4 (C-2), 66.7 (C-6), 20.6 (CH₃).

IR (ATR, cm⁻¹): 3061, 3031, 2925, 2868, 1728, 1696, 1497, 1454, 1366, 1250, 1207, 1101, 1028, 738.

HRMS (ESI): m/z [M+H]⁺ calcd. for C₂₈H₃₂O₄N₃: 474.2392, found: 474.2389.



(3*S*,4*R*,5*R*)-1-Amino-3,4-dihydroxy-5-(hydroxymethyl)-2-pyrrolidinone hydrochloride (D-80)

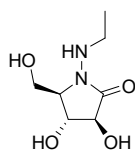
A solution of compound D-47 (8 mg, 0.04 mmol) in MeOH (0.05 M HCl, 1 mL) was subjected to microwave radiation (150 °C) for 90 min. The reaction mixture was then cooled to ambient temperature before volatiles were removed under reduced pressure. The residue was evaporated to dryness to afford the HCl salt. The salt residue was subjected to gravity column chromatography (MeCN/H₂O 98:2). Collection of the appropriate fractions (R_f = 0.41, MeCN/H₂O 85:15) provided compound D-80 (4.7 mg, 60%) as a white wax; $[\alpha]_D^{25.5\text{ }^\circ\text{C}}$ = - 5.1 (c 0.39 in MeOH).

¹H NMR (D₂O, 400 MHz): δ = 4.31 (d, $J_{3,4}$ = 7.1 Hz, 1H, H-3), 4.10 (t, J = 7.1 Hz, 1H, H-4), 4.05 (dd, $J_{5'a,5}$ = 2.7 Hz, $J_{5'a,5'b}$ = 12.9 Hz, 1H, 5'a), 3.79 (dd, $J_{5'b,5}$ = 2.5 Hz, $J_{5'b,5'a}$ = 12.9 Hz, 1H, 5'b), 3.47 (m, 1H, H-5).

¹³C NMR (D₂O, 100 MHz): δ = 172.5 (CO), 75.2 (C-3), 72.3 (C-4), 65.3 (C-5), 57.2 (C-5').

IR (ATR, cm^{-1}): 3295, 2926, 2855, 2358, 1699, 1455, 1349, 1261, 1200, 095, 909.

HRMS (ESI): m/z $[\text{M}+\text{H}]^+$ calcd. for $\text{C}_5\text{H}_{11}\text{O}_4\text{N}_2$, 163.0719; found, 163.0721.



(3*S*,4*R*,5*R*)-1-(ethylamino)-3,4-dihydroxy-5-(hydroxymethyl)-2-pyrrolidinone (D-81)

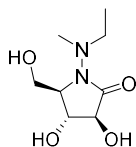
A solution of compound D-48 (3.79) (20 mg, 0.09 mmol) in MeOH (0.05 M HCl, 3 mL) was subjected to microwave radiation (150 °C) for 4 h. The reaction mixture was then cooled to ambient temperature before volatiles were removed under reduced pressure. The residue was evaporated to dryness to afford the HCl salt. The salt residue was subjected to gravity column chromatography (MeCN/H₂O 99:1 → 97:3). Collection of the appropriate fractions provided compound D-82 (R_f = 0.56, MeCN/H₂O 9:1) (4.8 mg, 23%) and compound D-81 (R_f = 0.41, MeCN/H₂O 9:1) (11.0 mg, 55%) as white waxes.

¹H NMR (D₂O, 400 MHz): δ = 4.26 (d, $J_{3,4}$ = 6.8 Hz, 1H, H-3), 4.07 (t, J = 6.7 Hz, 1H, H-4), 3.98 (dd, $J_{5'a,5}$ = 3.1, $J_{5'a,5'b}$ = 12.5 Hz, 1H, H-5'a), 3.87 (dd, $J_{5'b,5}$ = 3.7, $J_{5'b,5'a}$ = 12.5 Hz, 1H, H-5'b), 3.57-3.56 (m, 1H, H-5), 3.27-3.18 (m, 1H, CH₂a), 3.04-2.96 (m, 1H, CH₂b) 2.81 (s, 3H, NCH₃), 1.06 (t, J = 7.2 Hz, 3H, CCH₃).

¹³C NMR (D₂O, 100 MHz): δ = 173.0 (CO), 74.5 (C-3), 71.9 (C-4), 63.8 (C-5), 58.4 (C-5'), 49.8 (CH₂), 41.6 (NCH₃), 12.0 (CH₃).

IR (ATR, cm^{-1}): 3328, 2969, 2929, 2874, 1686, 1445, 1416, 1383, 1261, 1197, 1142, 1099, 1057, 1036, 963, 907, 869, 797.

HRMS (ESI): sample sent for analysis.



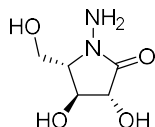
(3*S*,4*R*,5*R*)-1-(ethyl(methyl)amino)-3,4-dihydroxy-5-(hydroxymethyl)-2-pyrrolidinone (D-82):

¹H NMR (D₂O, 400 MHz): δ = 4.35 (d, $J_{3,4}$ = 7.1 Hz, 1H, H-3), 4.14 (t, J = 6.9 Hz, 1H, H-4), 4.02 (dd, $J_{5'a,5}$ = 2.8, $J_{5'a,5'b}$ = 12.8 Hz, 1H, H-5'a), 3.83 (dd, $J_{5'b,5}$ = 2.8, $J_{5'b,5'a}$ = 12.8 Hz, 1H, H-5'b), 3.64 (dt, $J_{5,5'}$ = 2.8 Hz, $J_{5,4}$ = 6.7 Hz, 1H, H-5), 3.04-2.95 (m, 1H, CH_{2a}), 2.92-2.84 (m, 1H, CH_{2b}), 1.08 (t, J = 7.3 Hz, 3H, CH₃).

¹³C NMR (D₂O, 100 MHz): δ = 172.2 (CO), 74.3 (C-3), 71.8 (C-4), 62.2 (C-5), 56.7 (C-5'), 43.2 (CH₂), 11.8 (CH₃).

IR (ATR, cm⁻¹): 3276, 2969, 2924, 1695, 1450, 1381, 1355, 1262, 1200, 1099, 1061, 965, 908, 796.

HRMS (ESI): m/z [M+Na]⁺ calcd. for C₈H₁₆N₂O₄, 227.1007; found, 227.1001.



(3R,4S,5S)-1-Amino-3,4-dihydroxy-5-(hydroxymethyl)-2-pyrrolidinone (L-80)

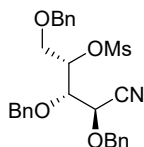
A solution of compound L-47 (13 mg, 0.07 mmol) in methanolic HCl (0.5 M, 1 mL) was subjected to microwave radiation (150 °C) for 1.5 h. Volatiles were removed under reduced pressure. The resulting black residue was subjected to gravity column chromatography (MeCN/ H₂O 97:3). Collection of the appropriate fractions ($R_f = 0.37$, MeCN/H₂O 8:2) provided compound L-80 (10 mg, 0.05 mmol, 72%) as a brown wax; $[\alpha]_D^{26.2^\circ\text{C}} = +5.1$ (c 0.39 in MeOH).

¹H NMR (D₂O, 400 MHz): $\delta = 4.31$ (d, $J_{4,3} = 7.1$ Hz, 1H, H-3), 4.10 (t, $J = 7.1$ Hz, 1H, H-4), 4.05 (dd, $J_{5'a,5} = 2.7$ Hz, $J_{5'a,5'b} = 12.9$ Hz, 1H, 5'a), 3.79 (dd, $J_{5'b,5} = 2.5$ Hz, $J_{5'b,5'a} = 12.9$ Hz, 1H, 5'b), 3.47 (m, 1H, H-5).

¹³C NMR (D₂O, 100 MHz): $\delta = 172.5$ (C=O), 75.2 (C-3), 72.3 (C-4), 65.3 (C-5), 57.2 (C-5').

IR (ATR, cm⁻¹): 3295, 2926, 2855, 2358, 1699, 1455, 1349, 1261, 1200, 1095, 909.

HRMS (ESI): m/z $[M+H]^+$ calcd. for C₅H₁₁O₄N₂, 163.0719; found, 163.0721.

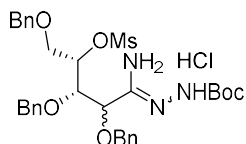


**(2*S*,3*S*,4*R*)-1,3,4-tris(benzyloxy)-4-cyanobutan-2-yl
methanesulfonate (L-87)²⁰⁴**

To a solution of alcohol L-33 (270 mg, 0.65 mmol) and 4 Å MS (5 mg) in DCM (3 mL) was added Et₃N (0.14 mL, 1.0 mmol) followed by MsCl (0.07 mL, 0.90 mmol) at 0 °C under argon. The reaction was stirred at 0 °C for 20 min before addition of sat. aq. NaHCO₃ (6 mL). The aqueous phase was extracted with DCM (10 mL x 2) and combined organic fractions were concentrated under reduced pressure. The residue was subjected to flash column chromatography (Pet. ether/EtOAc 3:1). Collection of the appropriate fractions (*R*_f = 0.40, Pet. ether/EtOAc 3:1) provided the mesylate L-87 (306 mg, 0.61 mmol, 95%) as a clear colorless oil; $[\alpha]_D^{25.2} = -40^\circ$ (*c* 0.7 in CHCl₃), (lit.²⁰⁴: $[\alpha]_D^{20} = -39^\circ$ (*c* 0.6 in CHCl₃)) The spectroscopic data were in full accord with the previously reported data.²⁰⁴

¹H NMR (CDCl₃, 400 MHz): δ = 7.38-7.24 (m, 15H, ArH), 4.93 (m, 1H, H-2), 4.84 (d, *J* = 11.6 Hz, 1H, CHPh), 4.79 (d, *J* = 11.2 Hz, 1H, CHPh), 4.68 (d, *J* = 11.2 Hz, 1H, CHPh), 4.45 (d, *J* = 11.6 Hz, 1H, CHPh), 4.44 (d, *J* = 11.8 Hz, 1H, CHPh), 4.37 (d, *J* = 11.8 Hz, 1H, CHPh), 4.26 (d, *J*_{4,3} = 4.5 Hz, 1H, H-4), 4.03 (dd, *J*_{3,4} = 4.6 Hz, *J*_{3,2} = 5.1 Hz, 1H, H-3), 3.73 (dd, *J*_{1a,2} = 4.5 Hz, *J*_{1a,1b} = 11.0 Hz, 1H, H-1a), 3.58 (dd, *J*_{1b,2} = 5.4 Hz, *J*_{1b,1a} = 11.0 Hz, 1H, H-1b), 2.96 (s, 3H, CH₃).

¹³C NMR (CDCl₃, 100 MHz): δ = 137.2 (ArC), 136.7 (ArC), 135.0 (ArC), 129.0-128.1 (ArCH), 116.3 (CN), 78.9 (C-3), 76.7 (CH₂Ph), 75.6 (CH₂Ph), 73.6 (CH₂Ph), 72.9 (C-1), 68.3 (C-2), 67.2 (C-4), 38.5 (CH₃).



***tert*-butyl-2-((3*S*,4*S*)-1-amino-2,3,5-tris(benzyloxy)-4-((methylsulfonyl)oxy)pentylidene)-1-carboxylate hydrochloride (L-90 + L-*lyxo*-90) hydrazine**

A solution of compound L-87 (100 mg, 0.2 mmol) in EtOH (3.5 mL) was added a solution of 0.43 M NaOEt in EtOH (0.5 mL, 1.08 equiv.) at 0 °C. The reaction was stirred for 19 h followed by addition of 0.1 M ethanolic HCl (1 mL) to form the corresponding Pinner salt. Volatiles were removed under reduced pressure. The residue was added 4 Å MS and a solution of *tert*-butyl carbazate (100mg, 0.76 mmol) in dry THF (4 mL). The reaction was stirred at rt under nitrogen for 45 min before volatiles were removed under reduced pressure. The residue was subjected to flash column chromatography (DCM/MeOH (0.1 M HCl), 95:5). Collection of the appropriate fractions ($R_f = 0.33$; DCM/MeOH, 97:3) provided compound L-90 + L-*lyxo*-90 (40 mg, 30%) as a clear, slightly yellow oil.

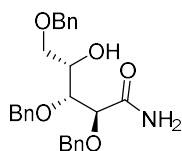
¹H NMR (CDCl₃, 400 MHz): $\delta = 7.47$ -7.26 (m, 30H), 5.18 (ddd, $J = 1.7, 5.9, 7.4$ Hz, 1H, H4, *lyxo*), 4.92 (dd, $J = 3.0, 6.7$ Hz, 1H, H4), 4.75 (d, $J = 11.5$ Hz, 1H), 4.67 (m, 2H), 4.63 (d, $J = 3.2$ Hz, 1H), 4.53 (d, $J = 5.2$ Hz, 1H), 4.50-4.49 (m, 1H), 4.49-4.45 (m, 2H, H2), 4.41 (d, $J = 7.3$ Hz, 1H), 4.36 (d, $J = 11.5$ Hz, 1H), 4.05 (dd, $J = 1.9, 9.2$ Hz, 1H, H3, *lyxo*), 3.99 (dd, $J = 2.9, 6.9$ Hz, 1H, H3), 3.79 (dd, $J = 7.3, 10.2$ Hz, 1H, H5a, *lyxo*), 3.67 (dd, $J = 5.8, 10.2$ Hz, 1H, H5b, *lyxo*), 3.60 (dd, $J = 2.8, 11.6$ Hz, 1H, H5a), 3.52 (dd, $J = 6.3, 11.6$ Hz, 1H, H5b), 3.12 (s, 3H, CH₃, OMs, *lyxo*), 2.99 (s, 3H, CH₃, OMs), 1.53 (br. s, 18H, Boc).

¹³C NMR (CDCl₃, 100 MHz): $\delta = 169.9$ (C=N), 168.7 (C=N, *lyxo*), 155.9 (C=O, Boc), 138.8 (ArC), 138.7 (ArC), 138.3 (ArC), 138.2 (ArC), 137.2 (ArC), 136.7 (ArC), 130.4-129.1 (ArCH), 83.7 (C, Boc), 83.6 (C,

Boc), 81.5 (C4), 79.5 (C3), 79.2 (C4, *lyxo*), 79.0 (C3, *lyxo*), 76.54 (C2), 76.50, 76.4, 75.7 (C2), 74.4, 74.33, 74.30, 74.1, 69.6 (C5), 69.4 (C5, *lyxo*), 39.0 (CH₃, OMs), 38.7 (CH₃, OMs, *lyxo*), 28.4 (CH₃, Boc).

IR (ATR, cm⁻¹): 2924, 1735, 1685, 1454, 1341, 1250, 1171, 1093, 1068, 1026, 969, 918.

HRMS (ESI): *m/z* [M+H]⁺ calcd. for C₃₂H₄₂O₈N₃S: 628.2693, found: 628.2688.



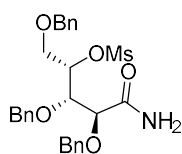
2,3,5-Tri-*O*-benzyl-L-xylo-2-amine (L-94)²⁰⁵

A solution of L-**36** (1.39 g, 3.31 mmol) and I₂ (1.22 g, 4.81 g) in 25% aq NH₃ (40 mL) and THF (10 mL) was stirred under argon at rt for 16 h. A solution of 5% aq. Na₂S₂O₃ was added to the reaction mixture until the brown color disappeared. The resulting mixture was extracted with EtOAc (150 mL x 3). The organic fractions were combined, dried over Na₂SO₄, filtered, and concentrated under reduced pressure. The residue was used directly in the next step without further purification; $[\alpha]_D^{26.2}$ °C = - 2.0 (*c* 1.0 in CHCl₃). The spectroscopic data were in full accord with the previously reported data.²⁰⁵

¹H NMR (CDCl₃, 400 MHz): δ = 7.35-7.25 (m, 15H, ArH), 6.65 (br.s, 1H, NH), 5.87 (br.s, 1H, NH), 4.72 (d, *J* = 11.2 Hz, 1H, CHPh), 4.60 (app. t, *J* = 10.8 Hz, 2H, CHPh), 4.47 (d, *J* = 11.4 Hz, 1H, CHPh), 4.46 (d, *J* = 11.9 Hz, 1H, CHPh), 4.43 (d, *J* = 11.9 Hz, 1H, CHPh), 4.09 (d, *J*_{2,3} = 4.3 Hz, 1H, H-2), 4.01 (ddd, *J*_{4,3} = 4.5 Hz, *J*_{4,5a} = 5.7 Hz, *J*_{4,5b} = 5.7 Hz, 1H, H-4) 3.92 (t, *J* = 4.4 Hz, 1H, H-3), 3.44 (dd, *J*_{5a,4} = 5.6 Hz,

$J_{5a,5b} = 9.6$ Hz, 1H, H-5a), 3.40 (dd, $J_{5b,4} = 5.8$ Hz, $J_{5b,5a} = 9.6$ Hz, 1H, H-5b).

^{13}C NMR (CDCl_3 , 100 MHz): $\delta = 173.9$ (CO), 138.04 (ArC), 137.99 (ArC), 136.7 (ArC), 128.8-127.9 (ArCH), 81.0 (C-2), 80.2 (C-3), 75.5 (PhCH₂), 73.9 (PhCH₂), 73.5 (PhCH₂), 70.7 (C-4), 70.6 (C-5).



(2*S*,3*S*,4*S*)-5-amino-1,3,4-tris(benzyloxy)-5-oxopentane-2-yl methanesulfonate (L-95)

A solution of compound L-94 (700 mg, 1.6 mmol), 4 Å MS (10 pcs), and Et₃N (0.34 mL, 2.44 mmol) in DCM (7 mL) was added MsCl (0.16 mL, 2.07 mmol) and stirred under argon at 0 °C for 20 min. The reaction mixture was then added sat. aq. NaHCO₃ (20 mL) and extracted with DCM (40 mL x 2). The combined organic fractions were concentrated under reduced pressure. The residue was subjected to flash column chromatography (PE/EtOAc, 3:2→2:3). Collection of the appropriate fractions ($R_f = 0.25$; Pet. ether/EtOAc, 1:1) provided compound L-95 (670 mg, 82%) as a white solid; mp = 104-105 °C; $[\alpha]_D^{26.7} = -0.9$ (c 8.5 in CHCl₃).

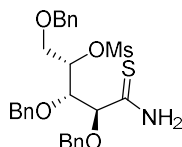
^1H NMR (CDCl_3 , 400 MHz): $\delta = 7.37$ -7.21 (m, 15H, ArH), 6.66 (br.s, 1H, NH), 5.98 (br.s, 1H, NH), 4.86 (ddd, $J_{2,1a} = 2.8$ Hz, $J_{2,1b} = 5.4$ Hz, $J_{2,3} = 7.7$ Hz, 1H, H-2), 4.65 (d, $J = 10.7$ Hz, 1H, CHPh), 4.60 (d, $J = 10.7$ Hz, 1H, CHPh), 4.59 (d, $J = 11.5$ Hz, 1H, CHPh), 4.45 (d, $J = 11.9$ Hz, 1H, CHPh), 4.33 (d, $J = 11.9$ Hz, 1H, CHPh), 4.27 (d, $J = 11.5$ Hz, 1H, CHPh), 4.18, (dd $J_{3,4} = 2.7$ Hz, $J_{3,2} = 7.7$ Hz, 1H, H-3), 3.97 (d, $J_{4,3} = 2.7$ Hz, 1H, H-4), 3.57 (dd, $J_{1a,2} = 2.8$ Hz, $J_{1a,1b} = 11.4$ Hz, 1H, H-1a), 3.34 (dd, $J_{1b,2} = 5.4$ Hz, $J_{1b,1a} = 11.4$ Hz, 1H, H-1b), 2.89 (s, 3H).

Experimental Methods

¹³C NMR (CDCl₃, 100 MHz): δ = 172.9 (CO), 137.4 (ArC), 137.3 (ArC), 136.2 (ArC), 128.9-128.1 (ArCH), 81.6 (), 78.8 (), 78.7 (), 76.0 (), 73.53 (), 73.48 (), 68.6 (), 38.4 (CH₃).

IR (ATR, cm⁻¹): 3384, 3183, 3064, 3032, 2919, 2869, 2809, 1639, 1496, 1454, 1412, 1365, 1347, 1263, 1214, 1164, 1123, 1067, 972, 926, 795, 743.

HRMS (ESI): m/z [M+Na]⁺ calcd. for C₂₇H₃₁O₇NS: 536.1718; found 536.1715.



(2*S*,3*S*,4*S*)-5-amino-1,3,4-tris(benzyloxy)-5-thioxopentan-2-yl methanesulfonate (L-93)

A solution of compound L-95 (410 mg, 0.80 mmol) in toluene (5 mL) was added Lawesson's reagent (325 mg, 0.80 mmol) and stirred under argon at 65 °C for 30 min. The mixture was then diluted with EtOAc (100 mL) and washed with sat. aq. NaHCO₃ (40 mL) followed by brine (40 mL). The organic fraction was dried over Na₂SO₄ and concentrated under reduced pressure. The residue was subjected to a short flash column chromatography (Pet. ether/EtOAc 3:1). Collection of the appropriate fractions (R_f = 0.66, Pet. ether/EtOAc 3:2) provided compound L-93 (355 mg, 84%) as a white foam; $[\alpha]_D^{27.0}$ = -40.0 (*c* 1.0 in CHCl₃).

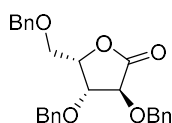
¹H NMR (CDCl₃, 400 MHz): δ = 7.99 (br. s, 1H, NH), 7.61 (br. s, 1H, NH), 7.39-7.19 (m, 15H, ArH), 4.85 (ddd, $J_{2,1a}$ = 2.5 Hz, $J_{2,1b}$ = 5.2 Hz, $J_{2,3}$ = 7.7 Hz, 1H, H-2), 4.73 (d, J = 10.6 Hz, 1H, CHPh), 4.60 (d, J = 10.6 Hz, 1H, CHPh), 4.49 (d, J = 11.5 Hz, 1H, CHPh), 4.48 (d, J = 11.9

Hz, 1H, CHPh), 4.39-4.36 (m, 2H, H-3 + H-4), 4.30 (d, $J = 11.9$ Hz, 1H, CHPh), 4.13 (d, $J = 11.5$ Hz, 1H, CHPh), 3.52 (dd, $J_{1a,2} = 2.5$ Hz, $J_{1a,1b} = 11.5$ Hz, 1H, H-1a), 3.26 (dd, $J_{1b,2} = 5.2$ Hz, $J_{1b,1a} = 11.5$ Hz, 1H, H-1b), 2.89 (s, 3H, CH₃).

¹³C NMR (CDCl₃, 100 MHz): $\delta = 204.0$ (C=S), 137.5 (ArC), 137.3 (ArC), 135.8 (ArC), 129.1-128.2 (ArCH), 84.6 (C-4), 82.2 (C-2), 80.1 (C-3), 77.0 (CHPh), 73.5 (CHPh), 72.8 (CHPh), 68.5 (C-1), 38.6 (CH₃).

IR (ATR, cm⁻¹): 3422, 3306, 3169, 3030, 2924, 2870, 1733, 1606, 1496, 1454, 1412, 1349, 1265, 1234, 1211, 1172, 1113, 1058, 1026, 1001, 970, 916, 882, 836, 805, 774, 734.

LRMS (ESI): m/z [M+H]⁺ calcd. for C₂₇H₃₂O₆NS₂: 530; found 530.

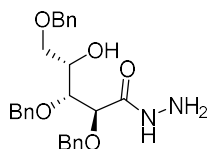


3,4,5-Tri-*O*-benzyl-L-xylonolactone (L-38)¹²⁸

A solution of compound L-36 (1.92 g, 4.57 mmol) in *tert*-butanol (15 mL) was added I₂ (2.32 g, 2 equiv.) and K₂CO₃ (1.26 g, 2 equiv.) at 70 °C. The purple reaction mixture was stirred at reflux for 2 h and then stirred at 35 °C for 19 h. The reaction was then added EtOAc (50 mL) and 5% aq. Na₂S₂O₃ (50 mL) and stirred at rt until colorless. The aq. phase was extracted with EtOAc (100 mL x2) and combined organic fractions were concentrated under reduced pressure. The residue was subjected to flash column chromatography (Pet. ether/EtOAc 5:1). Collection of the appropriate fractions ($R_f = 0.40$, Pet. ether/EtOAc 4:1) provided compound L-38 (1.66 g, 87%) as a clear light-yellow oil. The spectroscopic data for compound L-38 were in full accord with the previously reported data.¹²⁸

$^1\text{H NMR}$ (CDCl_3 , 400 MHz): $\delta = 7.36\text{-}7.25$ (m, 15 H), 5.05 (d, $J = 11.5$ Hz, 1 H), 4.60-4.50 (m, 5 H), 4.37 (t, $J = 7.1$ Hz, 1 H), 3.77 (dd, $J = 2.9$ Hz, $J = 10.8$ Hz, 1 H), 3.71 (dd, $J = 3.2$ Hz, $J = 10.8$ Hz, 1 H).

$^{13}\text{C NMR}$ (CDCl_3 , 100 MHz): $\delta = 173.5$ (CO), 137.8 (ArC), 137.4 (ArC), 137.2 (ArC), 128.7-127.7 (ArCH), 79.5, 77.4 (2CH₂), 73.8, 72.8, 72.7, 67.3.



**(2S,3R,4S)-2,3,5-tris(benzyloxy)-4-hydroxypentanehydrazide
(L-101)**

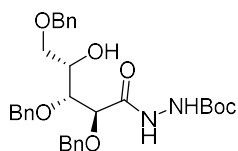
A solution of $\text{H}_2\text{NNH}_2\cdot\text{HCl}$ (1.23 g, 18 mmol) and Et_3N (1.67 mL, 12 mmol) in THF (5 mL) was stirred at rt for 5 h before a solution of L-38 (1.26 g, 3 mmol) in THF (3 mL) was added. The resulting reaction was stirred under nitrogen at rt for 45 h. Volatiles were then removed under reduced pressure. The residue was dissolved in DCM (20 mL), filtered to remove residual $\text{H}_2\text{NNH}_2\cdot\text{HCl}$, and the filtrate was concentrated under reduced pressure. The residue was subjected to flash column chromatography (PE/EtOAc 1:4 \rightarrow EtOAc/MeOH 95:5). Collection of the appropriate fractions ($R_f = 0.48$, EtOAc/MeOH 95:5) provided L-101 (799 mg, 59%) as a white solid; mp = 126.0-127.8 °C; $[\alpha]_D^{25.8} = -6.2$ (c 0.65 in CHCl_3).

$^1\text{H NMR}$ (CDCl_3 , 400 MHz): $\delta = 7.74$ (br. s, 1H, NH), 7.36-7.27 (m, 15H, ArCH), 4.64-4.58 (m, 3H, PhCH), 4.47-4.45 (m, 3H, PhCH), 4.18 (d, $J = 4.2$ Hz, 1H, H-2), 4.00 (app. dd, $J_{4,3} = 4.5$ Hz, $J_{4,5} = 5.7$ Hz, 1H, H-4), 3.92 (app. t, $J = 4.4$ Hz, 1H, H-3), 3.78 (br. s, 2H, NH₂), 3.45 (dd, $J_{5a,4} = 5.6$ Hz, $J_{5a,5b} = 9.6$ Hz, 1H, H-5a), 3.42 (dd, $J_{5b,4} = 5.8$ Hz, $J_{5b,5a} = 9.6$ Hz, 1H, H-5b), 2.88 (br. s, 1H, OH).

^{13}C NMR (CDCl_3 , 100 MHz): δ = 171.0 (C=O), 138.0 (ArC), 137.9 (ArC), 136.6 (ArC), 128.7-127.9 (ArCH), 80.4 (C-2), 80.0 (C-3), 75.4 (CHPh), 73.8 (CHPh), 73.4 (CHPh), 70.7 (C-5), 70.4 (C-4).

IR (ATR, cm^{-1}): 3294, 3170, 3060, 3028, 2917, 2875, 1655, 1625, 1523, 1495, 1453, 1408, 1365, 1321, 1302, 1118, 1054, 1026, 1001.

HRMS (ESI): m/z $[\text{M}+\text{Na}]^+$ calcd. for $\text{C}_{26}\text{H}_{30}\text{O}_5\text{N}_2$: 473.2052; found 473.2050.



tert-butyl-2-((2S,3R,4S)-2,3,5-tris(benzyloxy)-4-hydroxypentanoyl)hydrazine-1-carboxylate (L-102)

A heterogeneous white suspension of compound **L-101** (623 mg, 1.38 mmol) and Boc_2O (0.32 mL, 1 equiv.) in MeOH (10 mL) and aq. sat. NaHCO_3 (1 mL) was stirred at rt for 16 h. The resulting blank solution was concentrated under reduced pressure and dried from toluene. The residue was subjected to flash column chromatography (Pet. ether/EtOAc 3:2 \rightarrow 1:1). Collection of the appropriate fractions (R_f = 0.41; Pet. ether/EtOAc 3:2) provided compound **L-102** (690 mg, 91%) as a white foam.

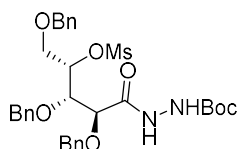
^1H NMR (CDCl_3 , 400 MHz): δ = 8.38 (br. s, 1H, (CO)NH), 7.36-7.31 (m, 15H, ArH), 6.74 (br. s, 1H, (Boc)NH), 4.79 (d, J = 11.3 Hz, 1H, CHPh), 4.78 (d, J = 11.3 Hz, 1H, CHPh), 4.63 (d, J = 11.3 Hz, 1H, CHPh), 4.53 (d, J = 11.3 Hz, 1H, CHPh), 4.47 (br. s, 2H, CH_2Ph), 4.28 (d, $J_{2,3}$ = 4.6 Hz, 1H, H2), 4.08 (ddd, J = 4.4, 5.8, 9.9 Hz, 1H, H4), 3.94 (t, J = 4.4 Hz, 1H, H3), 3.46 (d, J = 5.8 Hz, 2H, H5), 3.13 (br.s, 1H, OH), 1.52 (br.s, 9H, CH_3 , Boc).

Experimental Methods

^{13}C NMR (CDCl_3 , 100 MHz): δ = 170.5 (CO), 155.2 (CO, Boc), 138.0 (ArC), 137.9 (ArC), 136.7 (ArC), 128.6-127.6 (ArCH), 81.8 (C), 80.0 (C2), 79.7 (C3), 75.1 (CHPh), 73.5 (CHPh), 73.3 (CHPh), 70.6 (C5), 70.0 (C4), 28.2 (CH_3).

IR (ATR, cm^{-1}): 3336, 2922, 2853, 1786, 1701, 1496, 1453, 1366, 1241, 1157, 1098, 1056, 1026.

HRMS (ESI): m/z $[\text{M}+\text{Na}]^+$ calcd. for $\text{C}_{31}\text{H}_{38}\text{O}_7\text{N}_2$: 573.2576; found 573.2573.



***tert*-butyl-2-((2*S*,3*S*,4*S*)-2,3,5-tris(benzyloxy)-4-((methylsulfonyl)oxy)pentanoyl)hydrazine-1-carboxylate (L-98)**

A solution of compound L-102 (600 mg, 1.09 mmol) and Et_3N (0.18 mL, 1.18 equiv.) in DCM (6 mL) at 0 °C under nitrogen was added MsCl (0.09 mL, 1.06 equiv.) dropwise and stirred for 20 min. The reaction mixture was diluted with DCM (30 mL) and added sat. aq. NaHCO_3 (30 mL). The aqueous phase was extracted with DCM (50 mL) and combined organic fractions were washed with aq. 0.3 M HCl (30 mL), dried over NaSO_4 , and concentrated under reduced pressure. The residue was subjected to flash column chromatography (PE/EtOAc, 3:1 \rightarrow 1:1). Collection of the appropriate fractions provided compound L-103 (R_f = 0.58; Pet. ether/EtOAc, 3:2) (72 mg, 10%) as a white solid; mp = 56-58 °C and compound L-98 (R_f = 0.53; Pet. ether/EtOAc, 3:2) (252 mg, 37%) as a white solid; mp = 50-51 °C.

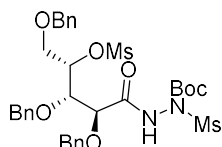
$[\alpha]_D^{26.9} = -40^\circ$ (c 0.5 in CHCl_3)

¹H NMR (CDCl₃, 400 MHz): δ = 8.12 (br. s, 1H, CH(CO)NH), 7.38-7.27 (m, 15H, ArCH), 6.24 (br. s, 1H, O(CO)NH), 4.88 (ddd, $J_{4,5a} = 2.9$ Hz, $J_{4,5b} = 5.7$ Hz, $J_{4,3} = 6.7$ Hz, 1H, H-4), 4.77 (d, $J = 11.3$ Hz, 1H, CHPh), 4.69 (d, $J = 11.2$ Hz, 1H, CHPh), 4.59 (d, $J = 11.2$ Hz, 1H, CHPh), 4.45 (d, $J = 11.8$ Hz, 1H, CHPh), 4.36 (d, $J = 11.3$ Hz, 1H, CHPh), 4.35 (d, $J = 11.8$ Hz, 1H, CHPh), 4.14-4.11 (m, 2H, H-2 + H-3), 3.58 (dd, $J_{5a,4} = 2.9$ Hz, $J_{5a,5b} = 11.4$ Hz, 1H, H-5a), 3.39 (dd, $J_{5b,4} = 5.7$ Hz, $J_{5b,5a} = 11.4$ Hz, 1H, H-5b), 2.93 (s, 3H, CH₃), 1.50 (s, 9H, CH₃).

¹³C NMR (CDCl₃, 100 MHz): δ = 169.0 (CH(CO)NH), 155.0 (O(CO)NH), 137.4 (ArC), 137.3 (ArC), 136.1 (ArC), 129.0-128.1 (ArCH), 82.0 (C), 81.3 (C-4), 78.6 (CH), 78.5 (CH), 75.9 (CHPh), 73.6 (CHPh), 73.5 (CHPh), 68.6 (C-5), 38.5 (CH₃), 28.3 (CH₃).

IR (ATR, cm⁻¹): 3356, 3029, 2976, 2930, 2870, 1701, 1496, 1454, 1351, 1238, 1170, 1069, 1026, 966.

HRMS (ESI): m/z [M+Na]⁺ calcd. for C₃₂H₄₀O₉N₂S: 651.2352, found: 651.2348.



***tert*-butyl-1-(methylsulfonyl)-2-((2*S*,3*S*,4*S*)-2,3,5-tris(benzyloxy)-4-((methylsulfonyl)oxy)pentanoyl)hydrazine-1-carboxylate (L-103)**

$[\alpha]_D^{26.5\text{ }^\circ\text{C}} = -32$ (c 0.5 in CHCl₃)

¹H NMR (CDCl₃, 400 MHz): δ = 8.68 (br.s, 1H, (CO)NH), 7.35-7.25 (m, 15H, ArH), 4.86 (d, $J = 11.0$ Hz, 1H, CHPh), 4.81 (td, $J = 3.5, 6.1$ Hz, 1H, H4), 4.74 (d, $J = 10.9$ Hz, 1H, CHPh), 4.54-4.49 (m, 1H), 4.44 (d, $J = 11.3$ Hz, 2H, CHPh), 4.37 (d, $J = 11.8$ Hz, 1H, CHPh), 4.23 (d,

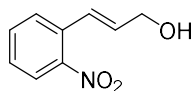
$J_{2,3} = 3.7$ Hz, 1H, H2), 4.15-4.10 (m, 1H, H3), 3.71 (dd, $J = 3.4, 11.3$ Hz, 1H, H5a), 3.52-3.52 (m, 1H, H5b), 3.48 (br.s, 3H, Ms), 2.91-2.88 (m, 3H, Ms), 1.54 (br.s, 9H, Boc).

^{13}C NMR (CDCl_3 , 100 MHz): $\delta = 169.8$ (CO), 137.6-135.9 (ArC), 128.9-128.0 (ArCH), 80.3 (C4), 78.6 (C2), 78.0 (C3), 75.7 (CHPh), 73.7 (CHPh), 73.4 (CHPh), 68.8 (C5), 42.5 (CH_3 , Ms), 38.4 (CH_3 , Ms), 28.1 (CH_3 , Boc).

IR (ATR, cm^{-1}): 3349, 3030, 2927, 2872, 1743, 1706, 1454, 1360, 1240, 1172, 965.

HRMS (ESI): m/z $[\text{M}+\text{Na}]^+$ calcd. for $\text{C}_{33}\text{H}_{42}\text{N}_2\text{O}_{11}\text{S}_2$: 729.2127, found: 729.2122.

7.4 Synthesis Towards the Martinella Alkaloids



(*E*)-3-(2-nitrophenyl)prop-2-en-1-ol (**198**)²⁰⁶

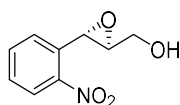
To a solution of cinnamic ester **200** (304 mg, 1.47 mmol) in DCM (16 mL) at -78 °C under nitrogen was added DIBAL (4.4 mL, 4.4 mmol, 3.0 equiv., 1 M in toluene) dropwise. The reaction was left stirring at -78 °C for 30 min, and then added EtOH (5 mL) dropwise. After addition, the reaction mixture was allowed to reach 0 °C before addition of sat. aq. NH_4Cl (10 mL). The resultant mixture was kept stirring at rt for 1 h. After this time, the mixture was filtered through a bed of Celite with the aid of EtOAc (50 mL). Filtrate phases were separated, and organic layer was washed with water and concentrated under reduced pressure. The resulting yellow oil was subjected to flash chromatography (Pet.

Experimental Methods

ether/EtOAc 1:1 → 2:3). Collection of the appropriate fractions ($R_f = 0.24$, Pet. ether/EtOAc 7:3) provided cinnamyl alcohol **198** (240 mg, 91 %) as a yellow solid; mp = 62.8-63.1 °C. The spectroscopic data were in full accord with the previously reported data.²⁰⁶

¹H NMR (400 MHz, CDCl₃) δ 7.90 (d, $J = 8.0$ Hz, ArH, 1H), 7.60-7.53 (m, ArH, 2H), 7.40-7.36 (m, ArH, 1H), 7.07 (1H, d, $J = 15.9$ Hz, -CH=CH-CH₂-OH), 6.35 and 6.31 (d, $J = 10.5, 15.6$ Hz, -CH=CH-CH₂-OH, 1H), 4.37 (dd, $J = 1.4, 5.2$ Hz, -CH=CH-CH₂-OH, 2H), 2.12 (1H, bs, OH).

¹³C NMR (100 MHz, CDCl₃) δ 148.0 (-CH=CH-CH₂-OH), 134.3 (Ar), 133.2 (Ar), 132.6 (Ar), 128.9 (Ar), 128.2 (Ar), 125.9 (-CH=CH-CH₂-OH), 124.6 (Ar), 63.4 (-CH=CH-CH₂-OH).



((2*S*,3*S*)-3-(2-nitrophenyl)oxiran-2-yl)methanol (199**)¹⁹⁸**

m-CPBA (mixture of epimers):

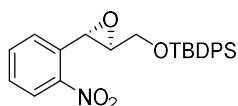
To a solution of compound **198** (130 mg, 0.73 mmol) in DCM (6 mL) at 0 °C was added *m*-CPBA (235 mg, 1.36 mmol, 1.87 equiv.). The reaction mixture was warmed to rt and stirred for 16 h before sat. aq. NaHCO₃ (10 mL) and Et₂O (10 mL) was added. The phases were separated, and organic phase was concentrated under reduced pressure. The residue was purified by flash column chromatography (Pet. ethe/EtOAc 7:3 → 1:1). Collection of the appropriate fractions ($R_f = 0.44$, Pet. ether/EtOAc 23:17) provided product **199** (130 mg, 92% yield) as a white crystalline solid.

Sharpless epoxidation:

To a suspension of activated 4 Å MS in DCM under a nitrogen atmosphere at -20 °C was added Ti(OiPr)₄ (33 μL, 20 mol%) and (+)-DET (29 μL, 30 mol%), and stirred for 30 min. A solution of compound **198** (100 mg, 0.56 mmol) in DCM (0.6 mL) was then added dropwise. The reaction was stirred for another 45 min and then added TBHP (225 μL, 2.5 equiv.). The resulting reaction was stirred for 6 days at -20 °C. After this time the mixture was allowed to reach 0 °C (ice bath) and added a solution of 2.5 M NaOH saturated with NaCl (1 mL). The heterogeneous mixture was stirred for 1 h and then filtered through Celite by the aid of DCM. The filtrate was concentrated under reduced pressure and subjected to flash column chromatography (Pet. ether/EtOAc 3:2→1:1). Collection of the appropriate fractions (*R_f* = 0.44, Pet. ether/EtOAc 23:17) provided compound (-)-**199** (17 mg, 16%) as a white crystalline solid; mp = 84.0-84.5 °C; $[\alpha]_D^{25.7} = -86.6$ (c 0.3 in CHCl₃) (lit.¹⁹⁸: ($[\alpha]_D = +122.64$ (c 1.0 in EtOAc) opposite enantiomer); The spectroscopic data were in full accord with the previously reported data.¹⁹⁸

¹H NMR (400 MHz, CDCl₃) δ 8.17 (dd, *J* = 1.1, 8.2 Hz, 1H), 7.70-7.63 (m, 2H), 7.51-7.47 (ddd, *J* = 1.9, 6.7, 7.0 Hz, 1H), 4.47 (d, *J* = 2.1 Hz, 1H), 4.09 (d, *J* = 12.7 Hz, 1H), 3.92 (m, 1H), 3.10 (dt, *J* = 2.6, 4.2 Hz, 1H), 1.91 (bs, 1H).

¹³C NMR (100 MHz, CDCl₃) δ 147.5 (Ar), 134.6 (Ar), 134.1 (Ar), 128.8 (Ar), 127.4 (Ar), 124.9 (Ar), 61.9 (CH₂CH), 61.8 (CHCH₂), 54.5 (ArCH).



***tert*-butyl((*rac*-(2*S*,3*S*)-3-(2-nitrophenyl)oxiran-2-yl)methoxy)diphenylsilane (209)**

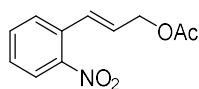
To a solution of compound **198** (110 mg, 0.56 mmol) and imidazole (116 mg, 3.0 equiv.) in DMF (5 mL) was added TBDPS-Cl (0.20 mL, 1.4 equiv.) at 0 °C under a nitrogen atmosphere. The reaction was stirred at rt for 2 h. The mixture was then added brine (60 mL) and extracted with EtOAc (30 mL x 3). Combined organic fractions were concentrated under reduced pressure. The residue was subjected to flash column chromatography (Pet. ether/EtOAc 4:1 → 1:1). Collection of the appropriate fractions ($R_f = 0.36$, Pet. ether/EtOAc 4:1) provided compound **209** (230 mg, 95 %) as a white oil.

^1H NMR (400 MHz, CDCl_3) δ 8.16 (d, $J = 8.2$ Hz, 1H), 7.76-7.72 (m, 4H), 7.67-7.65 (m, 2H), 7.49-7.39 (m, 7H), 4.53 (d, $J = 2.2$ Hz, 1H), 4.15 (dd, $J = 12.2, 2.2$ Hz, 1H), 3.89 (dd, $J = 12.2, 4.5$ Hz, 1H), 3.08 (quint. $J = 2.2$ Hz, 1H), 1.08 (s, 9H).

^{13}C NMR (100 MHz, CDCl_3) δ 147.7 (Ar), 135.8 (Ar), 135.4 (Ar), 135.0 (Ar), 134.6 (Ar), 134.4 (Ar), 133.3 (Ar), 129.9 (Ar), 129.8 (Ar), 128.6 (Ar), 127.94 (Ar), 127.86 (Ar), 127.4 (Ar), 124.8 (Ar), 63.2 (CH_2), 62.4 (CH), 53.8 (CH), 26.9 (CH_3), 26.7 (CH_3), 19.4 (C), 19.2 (C).

IR (ATR, cm^{-1}): 3047, 2931, 2900, 2856, 1528, 1471, 1447, 1427, 1342, 1133, 1099, 966, 899, 848.

HRMS (ESI): m/z $[\text{M}+\text{Na}]^+$ calcd. for $\text{C}_{25}\text{H}_{27}\text{O}_4\text{NSiNa}$: 456.1607; found 456.1609



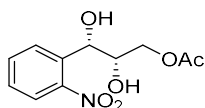
(E)-3-(2-nitrophenyl)allyl acetate (210)²⁰⁷

Following the literature procedure,²⁰⁸ a solution of cinnamyl alcohol **198** (190 mg, 1.06 mmol) and DMAP (7 mg, 5 mol%) in pyridine at 0 °C under nitrogen was added Ac_2O . The resulting mixture was stirred at rt

for 16 h. After this time the reaction solution was poured into water (15 mL), and the aq. phase was extracted with EtO₂ (3 x 15 mL). The combined organic layers were washed with 1 M HCl (15 mL), water (10 mL), dried over MgSO₄, and concentrated under reduced pressure. The residue was subjected to flash chromatography (Pet. ether/EtOAc 3:1). Collection of the appropriate fractions ($R_f = 0.47$, Pet. ether/EtOAc 3:1) provided compound **210** (235 mg, 99%) as a yellow oil. The spectroscopic data were in full accord with the previously reported data.²⁰⁷

¹H NMR (400 MHz, CDCl₃) δ 7.94 (d, 1H, $J=8.2$ Hz), 7.61-7.55 (m, 2H), 7.44-7.40 (m, 1H), 7.13 (d, 1H, $J=15.7$ Hz), 6.26 (dt, 1H, $J=15.7, 6.0$ Hz), 4.77 (dd, 2H, $J=5.8, 1.0$ Hz), 2.12 (s, 3H).

¹³C NMR (100 MHz, CDCl₃) δ 170.8 (Ar), 148.0 (C=O), 133.3 (Ar), 132.2 (Ar), 128.9 (Ar), 128.9 (Ar-CH=CH-CH₂), 128.8 (Ar-CH=CH-CH₂), 128.7 (Ar), 124.7 (Ar), 64.5 (CH₂), 21.0 (CH₃).



(2S,3S)-2,3-dihydroxy-3-(2-nitrophenyl)propyl acetate (211)

To a solution of compound **210** (25 mg, 0.11 mmol) in acetone (3 mL) and water (1.2 mL) was added NMO (20 mg, 0.17 mmol) and OsO₄ (0.07 mL, 5 mol%). The reaction was stirred at rt for 5 h and then quenched with 0.5 M NaS₂O₃ (1 mL). After quenching, the reaction mixture was kept stirring for 30 min. Aqueous phase was the extracted with EtOAc (10 mL x 3). Organic fractions were collected and washed with water (10 mL), dried over MgSO₄, and concentrated under reduced pressure. The residue was subjected to flash column chromatography (Pet. ether/EtOAc 7:3 \rightarrow 1:1). Collection of the appropriate fractions ($R_f =$

0.27, Pet. ether/EtOAc 1:1) provided compound **211** (27 mg, 96 %) as a yellow syrup.

Asymmetric:

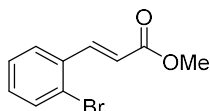
To a *t*-BuOH/H₂O (16 mL, 1:1) solution was added AD-mix α (729 mg, 1.56 mmol), (DHQ)₂PHAL (36 mg, 0.05 mmol, 0.09 equiv.), K₂O₅O₂(OH)₄ (1.5 mg, 0.004 mmol, 0.008 equiv.), and MeSO₂NH₂ (148 mg, 1.56 mmol). The heterogeneous mixture was stirred for 1 hour. The resulting clear yellow solution was cooled to 0 °C and was added cinnamyl acetate **210** (116 mg, 0.52 mmol). The reaction was left stirring for 18 h at 0 °C. After this time, the reaction was quenched with Na₂S₂O₃•3H₂O (1.01 g, 4.07 mmol) and left stirring for 30 min. The resulting mixture was then diluted with H₂O (10 mL), extracted with EtOAc (3 x 15 mL), dried over MgSO₄, and concentrated under reduced pressure. The residue was subjected to flash column chromatography (Pet. ether/EtOAc 7:3 → 1:1). Collection of the appropriate fractions (*R*_f = 0.27, Pet. ether/EtOAc 1:1) provided compound (+)-**211** (80 mg, 60%) as a yellow syrup; $[\alpha]_D^{25.3} = +12$ (c 0.5 in CHCl₃).

¹H NMR (400 MHz, CDCl₃) δ 7.99 (dd, *J* = 8.1, 1.3 Hz, ArH, 1H), 7.82 (dd, *J* = 7.9, 1.1 Hz, ArH, 1H), 7.67 (td, *J* = 7.7, 1.1 Hz, ArH, 1H), 7.47 (td, *J* = 7.7, 1.3 Hz, ArH, 1H), 5.38 (dd, *J* = 5.0, 3.0 Hz, 1H), 4.27 (dd, *J* = 11.5, 5.5 Hz, 1H) 4.22 (dd, *J* = 11.6, 6.1 Hz, 1H), 4.06 (ddd, *J* = 9.1, 6.2, 3.0 Hz, 1H), 3.35 (d, *J* = 5.5 Hz, OH, 1H), 2.86 (d, *J* = 6.3 Hz, OH, 1H), 2.11 (s, 3H).

¹³C NMR (100 MHz, CDCl₃) δ 171.8 (C=O), 147.8 (Ar), 136.8 (Ar), 133.6 (Ar), 129.2 (Ar), 128.8 (Ar), 124.8 (Ar), 72.5 (CH₂), 68.4 (CH₂), 65.7 (CH₂), 21.0 (CH₃).

IR (NaCl) 3363, 3106, 2933, 1723, 1646, 1563, 1525, 1430, 1398, 1346, 1267, 1112, 1045, 981, 857, 788, 714.

HRMS (ESI): m/z $[M+Na]^+$ calcd. for $C_{11}H_{13}O_6NNa$: 278.0641; found 278.0642.

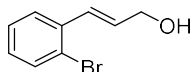


Methyl (*E*)-3-(2-bromophenyl)acrylate (222)²⁰⁹

To a solution of carboxylic acid **215** (200 mg, 0.89 mmol) in DMF (stored over 4Å mol. sieves) (3 mL) at rt was added K_2CO_3 (123 mg, 0.89 mmol) and iodomethane (0.07 mL, 1.12 mmol, 1.26 equiv.). The reaction mixture was kept stirring for 3 h. After this time, the “foggy” reaction mixture was poured into water (10 mL) and extracted with Et_2O (3 x 10 mL). The combined organic fractions were washed with brine (2 x 10 mL) and water (10 mL), dried over $MgSO_4$, filtered, and concentrated under reduced pressure. The residue was subjected to flash chromatography (Pet. ether/ $EtOAc$ 4:1). Collection of the appropriate fractions ($R_f = 0.46$, Pet. ether/ $EtOAc$ 4:1) provided methyl ester **222** (190 mg, 88%) as a clear, colorless oil. The spectroscopic data were in full accord with the previously reported data.²⁰⁹

1H NMR (400 MHz, $CDCl_3$) δ 8.04 (d, 1H, $J = 15.9$), 7.62-7.57 (m, 2H), 7.35-7.29 (m, 1H), 7.25-7.19 (m, 1H), 6.38 (d, 1H, $J = 16.0$), 3.82 (s, 3H).

^{13}C NMR (100 MHz, $CDCl_3$) δ 166.8(Ar-Br), 143.2 (Ar- $\underline{C}H=CH$), 134.5 (C=O), 133.5 (ArCH), 131.2 (ArCH), 127.8 (ArCH), 127.7 (ArCH), 125.3 (ArC), 120.7 (Ar- $\underline{C}H=CH$), 51.9 (CH_3).

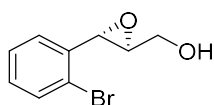


(*E*)-3-(2-bromophenyl)prop-2-en-1-ol (216)²¹⁰

To a solution of methyl ester **222** (4.10 g, 17.0 mmol) in DCM at -78 °C under nitrogen was added DIBAL (34 mL, 34 mmol, 1 M in toluene) dropwise. After addition the solution was kept stirring for 30 min and then added EtOH (25 mL). The solution was heated to 0 °C and then added sat. aq. NH₄Cl (20 mL). The resulting heterogeneous mixture was stirred for 1 h and then filtered through Celite. The organic fraction was concentrated under reduced pressure. The residue was subjected to flash chromatography (Pet. ether/EtOAc 4:1). Collection of the appropriate fractions ($R_f = 0.19$; Pet. ether/EtOAc 4:1) provided cinnamyl alcohol **216** (3.20 g, 89%) as a clear, colorless oil. The spectroscopic data were in full accord with the previously reported data.²¹⁰

¹H NMR (400 MHz, CDCl₃) δ 7.55 (dd, $J = 1.0, 8.0$ Hz, 1H), 7.52 (dd, $J = 1.5, 7.9$ Hz, 1H), 7.27 (t, 1H, $J = 7.3$ Hz), 7.11 (td, 1H, $J = 1.5, 7.7$ Hz), 6.96 (d, 1H, $J = 15.8$ Hz), 6.31 (dt, 1H, $J = 6.6, 15.8$ Hz), 4.37 (d, 2H, $J = 4.9$ Hz), 1.56 (bs, 1H).

¹³C NMR (100 MHz, CDCl₃) δ 136.7 (Ar), 133.1 (Ar), 131.8 (Ar-CH=CH), 129.9 (Ar-CH=CH), 129.1 (Ar), 127.7(Ar), 127.3(Ar), 123.8 (Ar), 63.7 (CH₂).



((2S,3S)-3-(2-bromophenyl)oxiran-2-yl)methanol (217)²¹¹

A solution of cinnamyl alcohol **216** (3.17 g, 13.72 mmol) in DCM (100 mL) at 0 °C was added *m*-CPBA (3.75 g, 16.7 mmol) and the reaction was stirred at rt for 6 h. The reaction was then quenched with sat. aq. NaHCO₃ (60 mL) and added Et₂O (70 mL). The organic phase was washed with water (30 mL), dried over MgSO₄, filtered, and concentrated under reduced pressure. The residue was subjected to flash column chromatography (Pet. ether/EtOAc 4:1). Collection of the

appropriate fractions ($R_f = 0.18$, Pet. ether/EtOAc 4:1) provided epoxide **217** (3.06 g, 97%) as a white crystalline solid; mp: 73.0-74.5 °C. The spectroscopic data were in full accord with the previously reported data.²¹¹

¹H NMR (400 MHz, CDCl₃) δ 7.54 (dd, $J = 8.0, 1.0$ Hz, 1H), 7.33-7.25 (m, 2H), 7.19-7.15 (m, 1H), 4.19 (d, $J = 2.2$ Hz, 1H), 4.09 (ddd, $J = 12.8, 5.1, 2.5$ Hz, 1H), 3.86 (ddd, $J = 12.8, 7.4, 4.2$ Hz, 1H), 3.08 (dt, $J = 4.1, 2.4$ Hz, 1H), 2.06 (bs, 1H).

¹³C NMR (100 MHz, CDCl₃) δ 136.5 (Ar), 132.4 (Ar), 129.5 (Ar), 127.8 (Ar), 126.5 (Ar), 122.5 (Ar), 62.1 (CH), 61.6 (CH), 55.7 (CH₂).

Asymmetric:

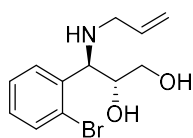
To a suspension of activated powdered molecular sieves (3Å, 48 mg) in DCM (6 mL) under nitrogen at -25 °C was added (+)-DET (120 μ L, 0.70 mmol) and Ti(O*i*Pr)₄ (140 μ L, 0.47 mmol) dropwise. The mixture was kept stirring for 1 h and then added cinnamyl alcohol **216** (500 mg, 2.35 mmol, dissolved in 4 mL DCM with powdered molecular sieves (3 Å, 30 mg)) dropwise. The reaction mixture was kept stirring for 1.5 h and then added *tert*-butyl hydroperoxide (1.07 mL, 5.88 mmol, 2.5 equiv.) dropwise over 10 min. The reaction was kept stirring at -25 °C for 13 h. After this time the reaction was allowed to reach 0 °C and added 2.5 M NaOH saturated with NaCl (1 mL) and left stirring at rt for 1 h. The heterogeneous mixture was filtered through Celite and the organic fraction was concentrated under reduced pressure. The residue was subjected to flash column chromatography (Pet. ether/EtOAc 3:2). Collection of the appropriate fractions ($R_f = 0.56$, Pet. ether/EtOAc 3:2) provided epoxide (+)-**217** (496 mg, 92%) as a white crystalline solid; mp: 73.6-74.2 °C; $[\alpha]_D^{25.7} = +17.3$ ($c = 1.5$ in CHCl₃).

¹H NMR (400 MHz, CDCl₃) δ 7.54 (dd, *J* = 8.0, 1.0 Hz, 1H), 7.33-7.25 (m, 2H), 7.19-7.15 (m, 1H), 4.19 (d, *J* = 2.2 Hz, 1H), 4.09 (ddd, *J* = 12.8, 5.1, 2.5 Hz, 1H), 3.86 (ddd, *J* = 12.8, 7.4, 4.2 Hz, 1H), 3.08 (dt, *J* = 4.1, 2.4 Hz, 1H), 2.06 (bs, 1H).

¹³C NMR (100 MHz, CDCl₃) δ 136.5 (Ar), 132.4 (Ar), 129.5 (Ar), 127.8 (Ar), 126.5 (Ar), 122.5 (Ar), 62.1 (CH), 61.6 (CH), 55.7 (CH₂).

IR (ATR, cm⁻¹): 3361, 3061, 2989, 2922, 2863, 1590, 1567, 1474, 1437, 1068, 1022, 965, 898, 861, 837, 745, 700.

HRMS (ESI): *m/z* [M+Na]⁺ calcd. for C₉H₉O₂BrNa: 250.9684 and 252.9663; found 250.9686 and 252.9669.



Rac-(2*R*,3*R*)-3-(allylamino)-3-(2-bromophenyl)propane-1,2-diol (218)

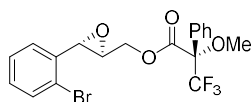
A solution of epoxide **217** (50 mg, 0.22 mmol) in DCM (1 mL) at rt under nitrogen was added Ti(O*i*Pr)₄ (0.25 mL, 1.32 mmol, 4 equiv.). After stirring for 30 min the reaction mixture was added allylamine (0.045 mL, 0.67 mmol, 3 equiv.), heated to 55 °C, and kept stirring for 17 h. After this time the reaction mixture was added 2.5 M NaOH saturated with NaCl (0.5 mL) and the milky white solution was left stirring for 8 h. The heterogeneous mixture was filtered through Celite by the aid of DCM and the organic fraction was concentrated under reduced pressure. The residue was subjected to flash column chromatography (DCM/MeOH/Et₃N 9:1:0.1). Collection of the appropriate fractions (*R_f* = 0.33, DCM/MeOH/Et₃N 9:1:0.1) provided amine **218** (61 mg, 97%) as a white solid; mp: 76.2 – 76.9 °C.

¹H NMR (400 MHz, CDCl₃) δ 7.56 (dd, *J* = 8.0, 1.2 Hz, 1H), 7.47 (dd, *J* = 7.7, 1.6 Hz, 1H), 7.35 (td, *J* = 7.6, 1.1 Hz, 1H), 7.15 (td, *J* = 7.7, 1.7 Hz, 1H), 5.85 (dddd, *J* = 17.0, 10.3, 6.4, 5.6 Hz, 1H), 5.12 (ddd, *J* = 17.1, 3.2, 1.6 Hz, 1H), 5.10 (ddd, *J* = 10.3, 2.8, 1.6 Hz, 1H), 4.45 (d, *J* = 5.3 Hz, 1H), 4.00 (ddd, *J* = 5.2, 5.2, 4.0 Hz, 1H), 3.61 (dd, *J* = 11.6, 3.9 Hz, 1H), 3.53 (dd, *J* = 11.6, 5.1 Hz, 1H), 3.17 (ddt, *J* = 14.0, 5.6, 1.4 Hz, 1H), 3.08 (bs, 3H), 3.00 (ddt, *J* = 14.0, 6.4, 1.3 Hz, 1H).

¹³C NMR (100 MHz, CDCl₃) δ 138.1 (Ar), 135.8 (CH), 133.4 (Ar), 129.2 (Ar), 128.8 (Ar), 128.0 (Ar), 124.9 (Ar), 117.0 (CH₂), 71.9 (CH-OH), 64.34 (CH-NH), 64.27 (CH₂-OH), 49.9 (CH₂).

IR (NaCl) 3323, 3077, 2930, 1647, 1560, 1437, 1400, 1269, 1095, 1046, 923, 879, 756.

HRMS (ESI): *m/z* [M+H]⁺ calcd. for C₁₂H₁₆O₂NBrNa: 286.0443 and 288.0422; found 286.0446 and 288.0423.



((2*S*,3*S*)-3-(2-bromophenyl)oxiran-2-yl)methyl-(*S*)-3,3,3-trifluoro-2-methoxy-2-phenylpropanoate (+)-223

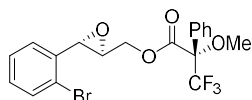
A solution of epoxide (+)-**217** (3.5 mg, 0.015 mmol) and pyridine (7 μL, 6 equiv.) in CDCl₃ (300 μL) was added (*S*)-(+)-MTPA-Cl (10 μL, 3.5 equiv.) and stirred for 3 h at rt before volatiles were removed by reduced pressure. The residue was subjected to flash column chromatography (in a glass pipette) (Pet. ether/EtOAc 6:1). Collection of the appropriate fractions (*R*_f = 0.72, Pet. ether/EtOAc 4:1) provided compound (+)-**223** (6.0 mg, 87%) as a clear colorless oil; [α]_D^{27.6} = + 47.3 (*c* = 0.55 in CDCl₃).

¹H NMR (400 MHz, CDCl₃) δ 7.57-7.52 (m, 3H, ArH), 7.42-7.39 (m, 3H, ArH), 7.31-7.28 (m, 1H, ArH), 7.23-7.17 (m, 2H, ArH), 4.76 (dd, *J* = 3.1, 12.4 Hz, 1H), 4.43 (dd, *J* = 5.8, 12.4 Hz, 1H), 4.08 (d, *J* = 2.0 Hz, 1H), 3.61-3.60 (m, 3H), 3.18-3.13 (m, 1H).

¹³C NMR (100 MHz, CDCl₃) δ 166.5 (CO), 135.7, 132.5, 132.2, 129.9, 129.8, 128.7, 127.9, 127.5, 126.4, 124.8, 122.5, 121.9, 85.0 (C), 65.5 (CH₂), 58.3 (CH), 56.2 (CH), 55.8 (CH₃).

IR (ATR, cm⁻¹): 3065, 2949, 2848, 1751, 1449, 1269, 1238, 1167, 1120, 1021, 753.

HRMS (ESI): *m/z* [M+H]⁺ calcd. for C₁₉H₁₇BrF₃O₄: 445.0262, sample sent for analysis.



(*Rac*-(2*S*,3*S*)-3-(2-bromophenyl)oxiran-2-yl)methyl-(*S*)-3,3,3-trifluoro-2-methoxy-2-phenylpropanoate (223)

A solution of epoxide **217** (3.5 mg, 0.015 mmol) and pyridine (7 μL, 6 equiv.) in CDCl₃ (300 μL) was added (*S*)-(+)-MTPA-Cl (10 μL, 3.5 equiv.) and stirred for 3 h at rt before volatiles were removed by reduced pressure. The residue was subjected to flash column chromatography (in a glass pipette) (Pet. ether/EtOAc 6:1). Collection of the appropriate fractions (*R_f* = 0.72, Pet. ether/EtOAc 4:1) provided compound **223** (6.2 mg, 90%) as a clear colorless oil.

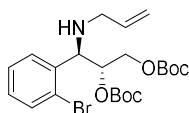
¹H NMR (400 MHz, CDCl₃) δ 7.57-7.52 (m, 3H, ArH), 7.42-7.39 (m, 3H, ArH), 7.31-7.28 (m, 1H, ArH), 7.23-7.17 (m, 2H, ArH), 4.08 (dd, *J* = 3.0, 12.4 Hz, 1H, *R*), 4.76 (dd, *J* = 3.1, 12.4 Hz, 1H, *S*), 4.43 (dd, *J* = 5.8, 12.4 Hz, 1H, *S*), 4.41 (dd, *J* = 5.4, 12.5 Hz, 1H, *R*), 4.10 (d, *J* = 2.0

Hz, 1H, *R*), 4.08 (d, $J = 2.0$ Hz, 1H, *S*), 3.61-3.60 (m, 3H), 3.18-3.13 (m, 1H).

^{13}C NMR (100 MHz, CDCl_3) δ 166.5 (CO), 135.7, 132.5, 132.2, 129.9, 129.8, 128.7, 127.9, 127.5, 126.4, 124.8, 122.5, 121.9, 85.0 (C), 65.5 (CH₂), 58.3 (CH), 56.2 (CH), 55.8 (CH₃).

IR (ATR, cm^{-1}): 3065, 2950, 2849, 1751, 1449, 1269, 1238, 1167, 1120, 1021, 753.

HRMS (ESI): m/z $[\text{M}+\text{H}]^+$ calcd. for $\text{C}_{19}\text{H}_{17}\text{BrF}_3\text{O}_4$: 445.0262, sample sent for analysis.



***Rac*-(2*R*,3*R*)-3-(allylamino)-3-(2-bromophenyl)propane-1,2-diyl di-tert-butyl bis(carbonate) (225)**

To a solution of compound **218** (130 mg, 0.45 mmol) in DCM (1.5 mL) was added DMAP (2 mg, 0.016 mmol) and Boc_2O (0.21 mL, 2.03 equiv.). The reaction was stirred at rt under nitrogen for 2 h and then concentrated under reduced pressure. The residue was subjected to flash column chromatography (Pet. ether/EtOAc 9:1→85:15). Collection of the appropriate fractions ($R_f = 0.36$, Pet. ether/EtOAc 18:2) provided compound **225** (166 mg, 76%) as a clear colorless oil.

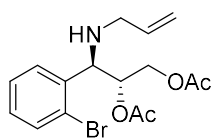
^1H NMR (400 MHz, CDCl_3) δ 7.54 (dd, $J = 8.0, 1.3$ Hz, 1H), 7.53 (dd, $J = 7.8, 1.4$ Hz, 1H), 7.31 (td, $J = 7.5, 1.3$ Hz, 1H), 7.13 (td, $J = 7.6, 1.7$ Hz, 1H), 5.82 (dddd, $J = 17.0, 10.3, 6.4, 5.3$ Hz, 1H), 5.29 (ddd, $J = 8.4, 5.7, 3.0$ Hz, 1H), 5.12 (ddd, $J = 17.3, 3.4, 1.7$ Hz, 1H), 5.06 (ddd, $J = 10.2, 3.0, 1.4$ Hz, 1H), 4.47 (d, $J = 5.5$ Hz, 1H), 4.30 (dd, $J = 11.9, 2.9$ Hz, 1H), 4.17 (dd, $J = 11.9, 8.2$ Hz, 1H), 3.09 (ddt, $J = 14.2, 5.3, 1.6$ Hz,

1H), 2.99 (ddt, $J = 14.2, 6.4, 1.3$ Hz, 1H), 1.73 (br. s, 1H), 1.44 (br. s, 9H), 1.42 (br. s, 9H).

^{13}C NMR (100 MHz, CDCl_3) δ 153.3(CO), 152.8 (CO), 137.6 (Ar), 136.4 ($\text{CH}=\text{CH}_2$), 133.3 (Ar), 129.9 (Ar), 129.3 (Ar), 127.8 (Ar), 124.9 (Ar), 116.3 ($\text{CH}=\text{CH}_2$), 82.5 (C), 82.2 (C), 75.2 (CH), 65.6 (CH_2), 61.3 (CH) 49.7 (CH_2), 27.9 (CH_3), 27.8 (CH_3).

IR (ATR, cm^{-1}): 2980, 2933, 1740, 1369, 1269, 1247, 1154, 1090, 1043, 1022, 933, 916, 858, 845, 788, 733.

HRMS (ESI): m/z $[\text{M}+\text{H}]^+$ calcd. for $\text{C}_{22}\text{H}_{33}\text{O}_6\text{NBr}$: 486.1491 and 488.1471; found 486.1495 and 488.1484.



Rac-(2R,3R)-3-(allylamino)-3-(2-bromophenyl)propane-1,2-diyl diacetate

To a solution of compound **218** (100 mg, 0.35 mmol) in DCM (0.8 mL) under nitrogen at rt, was added pyridine (0.4 mL, 4.95 mmol), a solution of DMAP (2 mg, 0.016 mmol) in DCM (0.2 mL), followed by acetic anhydride (0.08 mL, 2.4 equiv.). The reaction was stirred at rt for 1 h. After this time the reaction mixture was diluted with DCM (10 mL), washed with water (10 mL), dried over MgSO_4 , filtered and concentrated under reduced pressure. The residue was subjected to flash column chromatography (Pet. ether/EtOAc 7:3 \rightarrow 3:2). Collection of the appropriate fractions ($R_f = 0.27$, Pet. ether/EtOAc 3:1) provided compound **226** (111 mg, 86%) as a clear colorless oil.

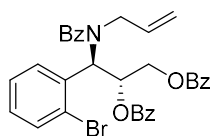
^1H NMR (400 MHz, CDCl_3) δ 7.54 (dd, $J = 8.0, 1.2$ Hz, 1H), 7.46 (dd, $J = 7.8, 1.6$ Hz, 1H), 7.31 (td, $J = 7.6, 1.2$ Hz, 1H), 7.13 (td, $J = 7.7, 1.8$

Hz, 1H), 5.82 (dddd, $J = 16.9, 10.2, 6.3, 5.5$ Hz, 1H), 5.40 (td, $J = 7.0, 3.0$ Hz, 1H), 5.13 (ddd, $J = 17.2, 3.3, 1.7$ Hz, 1H), 5.08 (ddd, $J = 10.2, 2.9, 1.4$ Hz, 1H), 4.46 (d, $J = 6.5$ Hz, 1H), 4.38 (dd, $J = 12.0, 3.0$ Hz, 1H), 4.20 (dd, $J = 12.0, 7.3$ Hz, 1H), 3.11 (ddt, $J = 14.2, 5.4, 1.6$ Hz, 1H), 3.09 (ddt, $J = 14.2, 6.4, 1.3$ Hz, 1H), 2.01 (s, 3H), 1.95 (s, 3H), 1.66 (br. s, 1H).

^{13}C NMR (100 MHz, CDCl_3) δ 170.9 (CO), 170.0 (CO), 138.2 (Ar), 136.4 (CH), 133.2 (Ar), 129.3 (Ar), 127.8 (Ar), 125.2 (Ar), 116.4 (CH_2), 72.9 (CH), 63.3 (CH_2), 61.0 (CH), 49.8 (CH_2), 20.9 (CH_3).

IR (ATR, cm^{-1}): 2979, 2934, 1751, 1458, 1368, 1247, 1154, 1090, 1022, 915, 886, 788, 753.

HRMS (ESI): m/z $[\text{M}+\text{H}]^+$ calcd. for $\text{C}_{22}\text{H}_{33}\text{O}_6\text{NBr}$: 370.0654 and 372.0634; found 370.0659 and 372.0638.



***Rac*-(2*R*,3*R*)-3-(*N*-allylbenzamido)-3-(2-bromophenyl)propane-1,2-diyl dibenzoate (227)**

To a solution of compound **218** (163 mg, 0.57 mmol) in DCM was added DMAP (3 mg, 0.025 mmol) and Et_3N (0.79 mL, 5.7 mmol) followed by dropwise addition of benzyl chloride (0.40 mL, 6.05 equiv.) at 0 °C under nitrogen. The reaction was stirred at rt for 48 h. After this time the reaction mixture was added water (15 mL) and extracted with EtOAc (15 mL x 3). Organic fractions were collected and concentrated under reduced pressure. The residue was subjected to flash column chromatography (Pet. ether/EtOAc 4:1). Collection of the appropriate

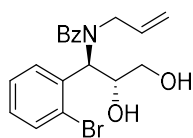
fractions ($R_f = 0.56$, Pet. ether/EtOAc 4:1) provided compound **227** (227 mg, 67%) as a white foam.

$^1\text{H NMR}$ (400 MHz, CDCl_3) δ 8.11-7.92 (m, 5H), 7.59-7.36 (m, 12 H), 7.30 (td, $J = 7.7, 1.4$ Hz, 1H), 7.14 (td, $J = 7.5, 1.7$ Hz, 1H), 6.72-6.69 (m, 1H), 6.20 (d, $J = 10.2$ Hz, 1H), 5.57 (ddt, $J = 16.9, 12.5, 6.3$ Hz, 1H), 4.94-4.91 (m, 1H), 4.87 (ddd, $J = 10.2, 2.7, 1.3$ Hz, 1H), 4.81 (ddd, $J = 16.9, 2.7, 1.4$ Hz, 1H), 4.79-4.74 (m, 1H), 3.79-3.63 (m, 1H).

$^{13}\text{C NMR}$ (100 MHz, CDCl_3) δ 172.9 (CO), 166.4 (CO), 165.7 (CO), 136.7 (Ar), 136.1 (Ar), 133.7 (CH), 133.5 (Ar), 133.3 (Ar), 133.2 (Ar), 130.7 (Ar), 130.3 (Ar), 130.1 (Ar), 130.0-129.9 (Ar), 129.7 (Ar), 128.6-128.5 (Ar), 128.0 (Ar), 126.5 (Ar), 126.4 (Ar), 118.8 (CH_2), 71.6 (CH), 64.6 (CH_2), 58.4 (CH), 51.0 (CH_2).

IR (ATR, cm^{-1}): 3048, 2963, 2930, 2898, 2857, 1611, 1527, 1470, 1426, 1342, 1132, 1100, 1001, 967, 898, 848, 824, 790, 738.

HRMS (ESI): m/z $[\text{M}+\text{H}]^+$ calcd. for $\text{C}_{33}\text{H}_{29}\text{O}_5\text{NBr}$: 598.1229 and 600.1209; found 598.1228 and 600.1212.



***N*-allyl-*N*-(*rac*-(1*R*,2*R*)-1-(2-bromophenyl)-2,3-dihydroxypropyl)benzamide (**228**)**

A solution of compound **227** (280 mg, 0.47 mmol) in MeOH (2.6 mL) was added a solution of 0.13 M NaOH in MeOH (1.9 mL) and stirred for 3 h. The reaction mixture was then diluted with DCM (20 mL), added water (15 mL) and neutralized by dropwise addition of 1 M aq. HCl. The aqueous phase was extracte3d with DCM (30 mL). Combined organic fractions were concentrated under reduced pressure and the residue was

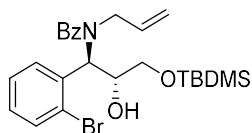
subjected to flash column chromatography (Pet. ether/EtOAc 7:13→3:7). Collection of the appropriate fractions ($R_f = 0.30$, Pet. ether/EtOAc 7:13) provided compound **228** (140 mg, 76%) as a white solid; mp = 111-112 °C.

$^1\text{H NMR}$ (400 MHz, CDCl_3) δ 7.68-7.65 (m, 2H), 7.44-7.387 (m, 6H), 7.26-7.22 (m, 1H), 5.77 (d, $J = 10.1$ Hz, 1H), 5.37 (dddd, $J = 17.3, 10.1, 7.6, 5.3$ Hz, 1H), 4.93 (d, $J = 10.2$ Hz, 1H), 4.70 (d, $J = 17.1$ Hz, 1H), 4.35 (t, $J = 7.7$ Hz, 1H), 4.25-4.22 (m, 1H, OH), 3.90-3.74 (m, 3H), 3.28 (dd, $J = 16.3, 7.6$ Hz, 1H), 3.02 (d, $J = 8.8$ Hz, 1H, OH).

$^{13}\text{C NMR}$ (100 MHz, CDCl_3) δ 174.0 (CO), 135.9 (ArC), 135.5 (ArC), 133.78 ($\text{CH}=\text{CH}_2$), 133.76 (ArCH), 131.2 (ArCH), 130.0 (ArCH), 129.9 (ArCH), 128.7 (2ArCH), 127.4 (ArCH), 127.2 (ArC-Br), 126.5 (2ArCH), 118.7 ($\text{CH}_2=\text{CH}$), 69.2 (CH), 62.2 (CH_2), 59.2 (CH), 49.7 (CH_2).

IR (ATR, cm^{-1}): 3310, 3155, 2816, 1668, 1629, 1389, 1345, 1045, 1000.

HRMS (ESI): m/z $[\text{M}+\text{H}]^+$ calcd. for $\text{C}_{19}\text{H}_{21}\text{O}_3\text{NBr}$: 390.0705 and 392.0695; found 390.0708 and 392.0691.



***N*-allyl-*N*-(*rac*-(**1R,2R**)-1-(2-bromophenyl)-3-((tert-butylidimethylsilyl)oxy)-2-hydroxypropyl) benzamide (**229**)**

A solution of compound **228** (100 mg, 0.26 mmol) in DMF (1.6 mL) was added a solution of imidazole (138 mg, 1.5 mmol), DMAP (5.5 mg, 0.037 mmol), TBDMS-Cl (60 mg, 1.5 equiv.) in DMF (0.6 mL) dropwise. The resulting reaction was stirred at rt for 20 h before adding sat. aq. NaHCO_3 (5 mL) and DCM (10 mL). The aq. phase was extracted

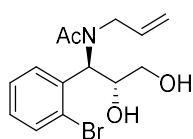
with DCM (20 mL x 2) and combined organic fractions were concentrated under reduced pressure. The residue was subjected to flash column chromatography (Pet. ether/EtOAc 4:1). Collection of the appropriate fractions ($R_f = 0.43$, Pet. ether/EtOAc 4:1) provided compound **229** (94 mg, 73%) as a clear colorless oil.

^1H NMR (400 MHz, CDCl_3) δ 8.00 (d, $J = 7.8$ Hz, 1H), 7.58 (d, $J = 7.9$ Hz, 1H), 7.38-7.33 (m, 6H), 7.20-7.16 (m, 1H), 5.62 (app. ddd, $J = 16.2$, 10.8, 5.7 Hz, 1H), 5.54 (d, $J = 5.3$ Hz, 1H), 5.07 (d, $J = 10.3$ Hz, 1H), 5.01 (d, $J = 17.2$ Hz, 1H), 4.61-4.59 (m, 1H), 4.21 (br. s, 1H), 3.82-3.66 (m, 4H), 0.94 (s, 9H), 0.12 (s, 3H), 0.10 (s, 3H).

^{13}C NMR (100 MHz, CDCl_3) δ 173.3 (CO), 137.3 (ArC), 137.1 (ArC), 133.6 ($\underline{\text{C}}\text{H}=\text{CH}_2$), 133.0 (ArCH), 132.2 (ArCH), 129.7 (ArCH), 129.6 (ArCH), 128.6 (2ArCH), 127.6 (ArCH), 126.3 (2ArCH), 118.2 ($\underline{\text{C}}\text{H}_2=\text{CH}$), 72.9 (CH), 64.1 (CH_2), 61.8 (CH), 52.5 (CH_2), 26.0 (CH_3), 18.3 (C), -5.2 (CH_3).

IR (ATR, cm^{-1}): 3325, 3200, 2970, 2926, 1655, 1621, 1415, 1389, 1340, 1264, 1201, 1120, 1020.

HRMS (ESI): m/z $[\text{M}+\text{H}]^+$ calcd. for $\text{C}_{25}\text{H}_{35}\text{O}_3\text{NBr}$: 504.1564 and 506.1550; found 504.1565 and 506.1553.



***N*-allyl-*N*-(*rac*-(1*R*,2*R*)-1-(2-bromophenyl)-2,3-dihydroxypropyl)acetamide (**232**)**

To a solution of amine **218** (2.70 g, 9.4 mmol) in Ac_2O (12 mL) at rt was added *p*-TsOH (2.20 g, 11.6 mmol). The reaction was kept stirring for 5 h until TLC analysis indicated full conversion of starting material.

Experimental Methods

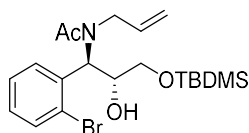
Excess Ac₂O was removed under reduced pressure and the triacetylated product was dissolved in MeOH (30 mL) followed by addition of 25% aq. NH₃ (10 mL). After addition the reaction was kept stirred at rt for 5 h before a second addition of 25% aq. NH₃ (10 mL). After stirring for another 5 h, volatiles were removed under reduced pressure. The residue was subjected to flash chromatography (DCM/MeOH 9:1) to afford, after concentration of the appropriate fractions (*R_f* = 0.33, DCM/MeOH, 9:1) acetamine **232** (2.33 g, 76%) as a white solid; mp = 93.7-94 °C.

¹H NMR (400 MHz, CDCl₃) δ 7.60 (m, 2H), 7.36 (td, 1H, *J* = 7.7, 1.2 Hz), 7.19 (td, 1H, *J* = 7.7, 1.5 Hz), 5.68 (d, 1H, *J* = 10.2 Hz), 5.35-5.25 (dddd, *J* = 17.0, 10.3, 6.3, 5.4 Hz, 1H), 5.00 (ddd, *J* = 10.3, 2.6, 1.4 Hz, 1H), 4.93 (ddd, *J* = 17.1, 2.7, 1.5 Hz, 1H), 4.15-4.11 (m, 1H), 4.07-4.03 (m, 1H), 3.76-3.61 (m, 3H), 3.52 (ddt, *J* = 17.1, 6.4, 1.5 Hz, 1H), 2.81-2.79 (m, 1H), 2.18 (s, 3H).

¹³C NMR (100 MHz, CDCl₃) δ 173.3 (CO), 135.6 (Ar), 133.7 (Ar), 133.2 (Ar), 131.0 (CH=CH₂), 129.8 (Ar), 127.44 (Ar), 127.39 (Ar), 118.1 (CH₂=CH), 69.1 (CH), 62.2 (CH₂), 58.5 (CH), 48.4 (CH₂), 22.2 (CH₃).

IR (ATR, cm⁻¹): 3300, 3150, 2816, 1671, 1629, 1389, 1354, 1147, 1045, 1005, 872, 797.

HRMS (ESI): *m/z* [M+Na]⁺ calcd. for C₁₄H₁₈O₃NBr: 350.0367 and 352.0347; found 350.0360 and 352.0334.



***N*-allyl-*N*-(*rac*-(1*R*,2*R*)-1-(2-bromophenyl)-3-((*tert*-butyldimethylsilyloxy)-2-hydroxypropyl) acetamide (233)**

Experimental Methods

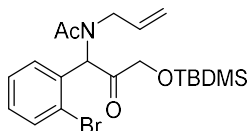
To a solution of diol **232** (2.10 g, 6.4 mmol) in DMF (15 mL) at 0 °C under nitrogen was added imidazole (1.36 g, 20.0 mmol), and DMAP (10 mg, 1.3 mol%) followed by TBDMS-Cl (1.27 g, 8.43 mmol). The reaction was heated to rt and stirred for 1 h. After this time the reaction was quenched with sat. aq. NaHCO₃ (20 mL). The reaction mixture was extracted with EtOAc (50 mL x 3). Combined organic fractions were concentrated under reduced pressure and the residue was subjected to flash chromatography (Pet. ether/EtOAc 7:3→3:2). Concentration of appropriate fractions (*R_f* = 0.24, Pet. ether/EtOAc 3:1) provided silyl protected product **233** (2.41 g, 85 %) as a white foam.

¹H NMR (400 MHz, CDCl₃) δ 7.86 (d, *J* = 7.9 Hz, 1H), 7.55 (d, *J* = 7.9 Hz, 1H), 7.30 (t, *J* = 7.6 Hz, 1H), 7.14 (t, *J* = 7.7 Hz, 1H), 5.59-5.50 (m, 2H), 5.08 (d, *J* = 10.0 Hz, 1H), 5.05-5.04 (m, 1H), 4.39-4.34 (m, 1H), 3.93 (d, *J* = 3.1 Hz, 1H), 3.87-3.74 (m, 2H), 3.66 (dd, *J* = 10.1, 6.4 Hz, 1H), 3.56 (dd, *J* = 10.1, 5.8 Hz, 1H), 2.12 (br.s, 3H), 0.90 (br.s, 9H), 0.07 (s, 3H), 0.06 (s, 3H).

¹³C NMR (100 MHz, CDCl₃) δ 172.1 (CO), 137.0, (Ar), 133.3 (CH), 133.0 (Ar), 132.3 (Ar), 129.5 (Ar), 127.4 (Ar), 126.3 (Ar), 117.2 (CH₂), 72.9 (CH), 64.2 (CH₂), 61.2 (CH), 51.1 (CH₂), 26.0 (CH₃), 22.8 (CH₃), 18.3 (C), -5.2 (CH₃), -5.3 (CH₃).

IR (ATR, cm⁻¹): 3331, 3205, 2971, 2926, 1663, 1611, 1464, 1412, 1387, 1340, 1264, 1189, 1123, 1020, 922, 827, 731.

HRMS (ESI): *m/z* [M+Na]⁺ calcd. for C₂₀H₃₂O₃NSiBrNa: 464.1233 and 466.1212; found 464.1237 and 466.1224.



***N*-allyl-*N*-(1-(2-bromophenyl)-3-((tert-butyldimethylsilyloxy)-2-oxopropyl)acetamide (**234**)**

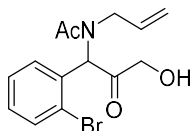
To a solution of compound **233** (940 mg, 2.12 mmol) in DCM (10 mL) at 0 °C under nitrogen was added Dess Martin Periodinane (1.09 g, 2.58 mmol, 1.2 equiv.). The reaction was stirred at rt for 1 h before volatiles were removed under reduced pressure. The residue was subjected to flash column chromatography (Pet. ether/EtOAc 9:1→8:2). Collection of the appropriate fractions ($R_f = 0.41$, Pet. ether/EtOAc 8:2) provided compound **234** (735 mg, 80%) as a clear colorless oil.

¹H NMR (400 MHz, CDCl₃) δ 7.61 (d, $J = 7.9$ Hz, 1H), 7.30-7.26 (m, 1H), 7.23-7.19 (m, 1H), 7.16-7.14 (m, 1H), 6.58 (s, 1H, H-7), 5.49-5.40 (m, 1H, H-15), 4.97-4.89 (m, 2H, H-16), 4.30 (d, $J = 5.3$ Hz, 2H, H-9), 3.87 (dd, $J = 5.6, 17.7$ Hz, 1H, H-14a), 3.75 (dd, $J = 5.7, 17.7$ Hz, 1H, H-14b), 2.16 (s, 3H, COCH₃), 0.78 (s, 9H), -0.01 (s, 3H), -0.07 (s, 3H).

¹³C NMR (100 MHz, CDCl₃) δ 206.9 (C=OCH₂), 171.6 (C=OCH₃), 133.8 (Ar), 133.7 (Ar), 133.68 (CHCH₂), 130.9 (Ar), 130.4 (Ar), 127.7 (Ar), 127.0 (Ar), 116.7 (CHCH₂), 68.8 (COCH₂), 64.3 (NCH), 49.3 (NCH₂), 25.8 (COCH₃), 21.9(CCH₃), 18.4 (CCH₃), -5.6 (CH₃).

IR (ATR, cm⁻¹): 2926, 2855, 1732, 1630, 1470, 1445, 1400, 1344, 1321, 1258, 1216, 1151, 1101, 1027, 929, 837, 790, 751, 730.

HRMS (ESI): m/z [M+H]⁺ calcd. for C₂₀H₃₁O₃NSiBr: 440.1257 and 442.1236; found 440.1259 and 442.1246.



***N*-allyl-*N*-(1-(2-bromophenyl)-3-hydroxy-2-oxopropyl)acetamide
(238)**

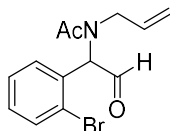
To a solution of compound **234** (160 mg, 0.36 mmol) in MeCN was added KF (58 mg, 1.0 mmol) followed by TMS-Cl (0.1 mL, 2.2 equiv.) at rt. The reaction was stirred at rt for 20 h. Volatiles were then removed under reduced pressure and the residue was subjected to flash column chromatography (DCM/MeOH 1:0→95:5). Collection of the appropriate fractions ($R_f = 0.21$; DCM/MeOH 95:5) provided compound **238** (100 mg, 85%) as a clear light-yellow oil.

^1H NMR (400 MHz, CDCl_3) δ 7.55 (dd, $J = 7.8, 1.2$ Hz, 1H), 7.28-7.16 (m, 3H), 5.88 (s, 1H), 5.57-5.47 (m, 1H), 5.07 (dd, $J = 17.2, 1.1$ Hz, 1H), 5.01 (dd, $J = 10.3, 1.1$ Hz, 1H), 4.19 (s, 2H), 3.87 (ddt, $J = 17.5, 5.0, 1.7$ Hz, 1H), 3.67 (ddt, $J = 17.5, 5.8, 1.5$ Hz, 1H), 3.15 (br.s, 1H), 2.11 (s, 3H).

^{13}C NMR (100 MHz, CDCl_3) δ 205.1 (COCH₂), 171.8 (COCH₃), 133.6 (Ar), 132.8 (Ar), 132.6 (CH), 130.8 (Ar), 130.7 (Ar), 128.1 (Ar), 126.3 (Ar), 117.8 (CH₂), 67.4 (CH₂), 64.9 (CH), 50.1 (CH₂), 21.6 (CH₃).

IR (ATR, cm^{-1}): 3368, 3070, 2921, 1726, 1624, 1468, 1405, 1255, 1207, 1120, 1042, 1024, 985, 929, 826, 753, 731.

HRMS (ESI): m/z $[\text{M}+\text{Na}]^+$ calcd. for $\text{C}_{14}\text{H}_{16}\text{O}_3\text{NBrNa}$: 348.0211 and 350.0191; found 348.0214 and 350.0192.



***N*-allyl-*N*-(1-(2-bromophenyl)-2-oxoethyl)acetamide (**232**)**

To a solution of diol **232** (105 mg, 0.33 mmol) in DCM (2 mL) at 0 °C was added NaIO₄ (210 mg, 0.98 mmol, 2.97 equiv.) followed by dropwise addition of sat. aq. NaHCO₃. The reaction was kept stirring at rt for 20 h before volatiles were removed under reduced pressure. The residue was subjected to flash column chromatography (Pet. ether/EtOAc 1:1). Collection of the appropriate fractions (*R*_f = 0.40, Pet. ether/EtOAc 1:1) provided aldehyde **240** (74 mg, 78%) as a clear colorless oil.

¹H NMR (400 MHz, CDCl₃) δ 9.61 (s, 1H), 7.62-7.60 (m, 1H), 7.36-7.31 (m, 2H), 7.25-7.21 (m, 1H), 5.78-5.69 (m, 1H), 5.33-5.21 (4m, 2H), 5.30 (s, 1H), 4.12-4.06 (2m, 1H), 3.79-3.73 (2m, 1H), 2.21 (s, 3H).

¹³C NMR (100 MHz, CDCl₃) δ 193.1 (CHO), 171.5 (CO), 133.6 (ArC), 133.3 (ArC), 132.1 (CH=CH₂), 130.5 (ArC), 130.4 (ArC), 128.2 (ArC), 125.4 (ArC), 118.3 (CH₂=CH), 68.5 (CH-CHO), 51.4 (CH₂-N), 21.2 (CH₃).

IR (NaCl) 3067, 2926, 2851, 1731, 1643, 1470, 1428, 1322, 1250, 1197, 1025, 931, 750.

HRMS (ESI): sample sent for analysis.

References

1. Cahn, R. S.; Ingold, C.; Prelog, V., Specification of molecular chirality. *Angew. Chem. Int. Ed.* **1966**, *5*, 385-415.
2. Bonner, W. A., Chirality and life. *Orig. Life Evol. Biosph.* **1995**, *25*, 175-190.
3. Easson, L. H.; Stedman, E., Studies on the relationship between chemical constitution and physiological action: Molecular dissymmetry and physiological activity. *Biochem. J.* **1933**, *27*, 1257-1266.
4. McConathy, J.; Owens, M. J., Stereochemistry in drug action. *Prim. Care Companion J. Clin. Psychiatry* **2003**, *5*, 70.
5. Mayer, J.; Testa, B., Pharmacodynamics, pharmacokinetics and toxicity of ibuprofen enantiomers. *Drugs Future* **1997**, *22*, 1347-1366.
6. Food; Administration, D., FDA's policy statement for the development of new stereoisomeric drugs. *57 Fed. Reg.* **1992**, *22*, 249.
7. De Camp, W. H., The FDA perspective on the development of stereoisomers. *Chirality* **1989**, *1*, 2-6.
8. Calcaterra, A.; D'Acquarica, I., The market of chiral drugs: Chiral switches versus de novo enantiomerically pure compounds. *J. Pharm. Biomed. Anal.* **2018**, *147*, 323-340.
9. De Camp, W. H., Chiral drugs: the FDA perspective on manufacturing and control. *J. Pharm. Biomed. Anal.* **1993**, *11*, 1167-1172.
10. Caner, H.; Groner, E.; Levy, L.; Agranat, I., Trends in the development of chiral drugs. *Drug Discov. Today* **2004**, *9*, 105-110.
11. Murakami, H., From racemates to single enantiomers—chiral synthetic drugs over the last 20 years. In *Novel optical resolution technologies*, Sakai, K.; Hirayama, N.; Tamura, R., Eds. Springer: Berlin, Heidelberg, **2006**; pp 273-299.
12. Helmchen, G., The 50th Anniversary of the Cahn–Ingold–Prelog Specification of Molecular Chirality. *Angew. Chem. Int. Ed.* **2016**, *24*, 6798-6799.
13. Moss, G. P., Basic terminology of stereochemistry (IUPAC Recommendations 1996). *Pure Appl. Chem.* **1996**, *68*, 2193-2222.
14. Rosanoff, M. A., On Fischer's Classification of Stereo-Isomers. *J. Am. Chem. Soc.* **1906**, *28*, 114-121.
15. Webb, E. C., Enzyme nomenclature 1992. *Recommendations of the Nomenclature Committee of the International Union of Biochemistry*

and Molecular Biology on the Nomenclature and Classification of Enzymes. Academic Press: **1992**.

16. Henrissat, B., A classification of glycosyl hydrolases based on amino acid sequence similarities. *Biochem. J.* **1991**, *280*, 309-316.

17. Sinnott, M. L., Catalytic mechanism of enzymic glycosyl transfer. *Chem. Rev.* **1990**, *90*, 1171-1202.

18. Vasella, A.; Davies, G. J.; Böhm, M., Glycosidase mechanisms. *Curr. Opin. Chem. Biol.* **2002**, *6*, 619-629.

19. Sinnott, M. L.; Souchard, I. J., The mechanism of action of β -galactosidase. Effect of aglycone nature and α -deuterium substitution on the hydrolysis of aryl galactosides. *Biochem. J.* **1973**, *133*, 89-98.

20. Vocadlo, D. J.; Davies, G. J.; Laine, R.; Withers, S. G., Catalysis by hen egg-white lysozyme proceeds via a covalent intermediate. *Nature* **2001**, *412*, 835-838.

21. Gloster, T. M.; Davies, G. J., Glycosidase inhibition: assessing mimicry of the transition state. *Org. Biomol. Chem.* **2010**, *8*, 305-320.

22. Vocadlo, D. J.; Davies, G. J., Mechanistic insights into glycosidase chemistry. *Curr. Opin. Chem. Biol.* **2008**, *12*, 539-555.

23. Gloster, T. M.; Meloncelli, P.; Stick, R. V.; Zechel, D.; Vasella, A.; Davies, G. J., Glycosidase inhibition: an assessment of the binding of 18 putative transition-state mimics. *J. Am. Chem. Soc.* **2007**, *129*, 2345-2354.

24. Ganem, B.; Papandreou, G., Mimicking the glucosidase transition state: shape/charge considerations. *J. Am. Chem. Soc.* **1991**, *113*, 8984-8985.

25. Zechel, D. L.; Boraston, A. B.; Gloster, T.; Boraston, C. M.; Macdonald, J. M.; Tilbrook, D. M. G.; Stick, R. V.; Davies, G. J., Iminosugar glycosidase inhibitors: structural and thermodynamic dissection of the binding of isofagomine and 1-deoxynojirimycin to β -glucosidases. *J. Am. Chem. Soc.* **2003**, *125*, 14313-14323.

26. Taylor, E. J.; Goyal, A.; Guerreiro, C. I.; Prates, J. A.; Money, V. A.; Ferry, N.; Morland, C.; Planas, A.; Macdonald, J. A.; Stick, R. V., How family 26 glycoside hydrolases orchestrate catalysis on different polysaccharides: structure and activity of a *Clostridium thermocellum* lichenase, CtLic26A. *J. Biol. Chem.* **2005**, *280*, 32761-32767.

27. Gloster, T. M.; Vocadlo, D. J., Developing inhibitors of glycan processing enzymes as tools for enabling glycobiology. *Nat. Chem. Biol.* **2012**, *8*, 683-694.

28. Brás, N. F.; Cerqueira, N. M.; Ramos, M. J.; Fernandes, P. A., Glycosidase inhibitors: a patent review (2008–2013). *Expert Opin. Ther. Pat.* **2014**, *24*, 857-874.
29. Roth, J., Protein N-glycosylation along the secretory pathway: relationship to organelle topography and function, protein quality control, and cell interactions. *Chem. Rev.* **2002**, *102*, 285-304.
30. Hart, G. W.; Slawson, C.; Ramirez-Correa, G.; Lagerlof, O., Cross talk between O-GlcNAcylation and phosphorylation: roles in signaling, transcription, and chronic disease. *Annu. Rev. Biochem.* **2011**, *80*, 825-858.
31. Lanctot, P. M.; Gage, F. H.; Varki, A. P., The glycans of stem cells. *Curr. Opin. Chem. Biol.* **2007**, *11*, 373-380.
32. Imberty, A.; Varrot, A., Microbial recognition of human cell surface glycoconjugates. *Curr. Opin. Struct. Biol.* **2008**, *18*, 567-576.
33. Brockhausen, I., Mucin-type O-glycans in human colon and breast cancer: glycodynamics and functions. *EMBO reports* **2006**, *7*, 599-604.
34. Wolfert, M. A.; Boons, G.-J., Adaptive immune activation: glycosylation does matter. *Nat. Chem. Biol.* **2013**, *9*, 776-784.
35. Ohtsubo, K.; Marth, J. D., Glycosylation in cellular mechanisms of health and disease. *Cell* **2006**, *126*, 855-867.
36. Freeze, H. H., Congenital disorders of glycosylation: CDG-I, CDG-II, and beyond. *Curr. Mol. Med.* **2007**, *7*, 389-396.
37. Lebrilla, C. B.; An, H. J., The prospects of glycan biomarkers for the diagnosis of diseases. *Mol. Biosyst.* **2009**, *5*, 17-20.
38. Asano, N., Glycosidase inhibitors: update and perspectives on practical use. *Glycobiology* **2003**, *13*, 93R-104R.
39. Salsali, A.; Nathan, M., A review of types 1 and 2 diabetes mellitus and their treatment with insulin. *Am. J. Ther.* **2006**, *13*, 349-361.
40. Perfetti, R.; Barnett, P. S.; Mathur, R.; Egan, J. M., Novel therapeutic strategies for the treatment of type 2 diabetes. *Diabetes Metab. Rev.* **1998**, *14*, 207-225.
41. van de Laar, F. A., Alpha-glucosidase inhibitors in the early treatment of type 2 diabetes. *Vasc. Health Risk Manage.* **2008**, *4*, 1189.
42. Varki, A., Biological roles of oligosaccharides: all of the theories are correct. *Glycobiology* **1993**, *3*, 97-130.
43. Varki, A., *Essentials of Glycobiology*, Cold Spring Harbor Laboratory Press, Cold Spring Harbor, NY, USA, **1999**.

References

44. Stanley, P., Golgi glycosylation. *Cold Spring Harb. Perspect. Biol.* **2011**, *3*, a005199.
45. Hossain, F.; Andreana, P. R., Developments in carbohydrate-based cancer therapeutics. *Pharmaceuticals* **2019**, *12*, 84.
46. Vigerust, D. J.; Shepherd, V. L., Virus glycosylation: role in virulence and immune interactions. *Trends Microbiol.* **2007**, *15*, 211-218.
47. Williams, S. J.; Goddard-Borger, E. D., α -glucosidase inhibitors as host-directed antiviral agents with potential for the treatment of COVID-19. *Biochem. Soc. Trans.* **2020**.
48. Chang, J.; Block, T. M.; Guo, J.-T., Antiviral therapies targeting host ER alpha-glucosidases: Current status and future directions. *Antiviral Res.* **2013**, *99*, 251-260.
49. Sadat, M. A.; Moir, S.; Chun, T.-W.; Lusso, P.; Kaplan, G.; Wolfe, L.; Memoli, M. J.; He, M.; Vega, H.; Kim, L. J., Glycosylation, hypogammaglobulinemia, and resistance to viral infections. *New Engl. J. Med.* **2014**, *370*, 1615-1625.
50. Navarrete-Martínez, J. I.; Limón-Rojas, A. E.; de Jesús Gaytán-García, M.; Reyna-Figueroa, J.; Wakida-Kusunoki, G.; del Rocío Delgado-Calvillo, M.; Cantú-Reyna, C.; Cruz-Camino, H.; Cervantes-Barragán, D. E., Newborn screening for six lysosomal storage disorders in a cohort of Mexican patients: three-year findings from a screening program in a closed Mexican health system. *Mol. Genet. Metab.* **2017**, *121*, 16-21.
51. Meikle, P. J.; Fietz, M. J.; Hopwood, J. J., Diagnosis of lysosomal storage disorders: current techniques and future directions. *Expert Rev. Mol. Diagn.* **2004**, *4*, 677-691.
52. Wennekkes, T.; van den Berg, R. J.; Boot, R. G.; van der Marel, G. A.; Overkleeft, H. S.; Aerts, J. M., Glycosphingolipids—nature, function, and pharmacological modulation. *Angew. Chem. Int. Ed.* **2009**, *48*, 8848-8869.
53. Parenti, G.; Andria, G.; Valenzano, K. J., Pharmacological chaperone therapy: preclinical development, clinical translation, and prospects for the treatment of lysosomal storage disorders. *Mol. Ther.* **2015**, *23*, 1138-1148.
54. Benito, J. M.; Garcia Fernandez, J. M.; Mellet, C. O., Pharmacological chaperone therapy for Gaucher disease: a patent review. *Expert Opin. Ther. Pat.* **2011**, *21*, 885-903.

55. Ishii, S., Pharmacological chaperone therapy for Fabry disease. *Proc. Japan Acad., Ser. B* **2012**, *88*, 18-30.
56. Lukas, J.; Cimmaruta, C.; Liguori, L.; Pantoom, S.; Iwanov, K.; Petters, J.; Hund, C.; Bunschowski, M.; Hermann, A.; Cubellis, M. V., Assessment of gene variant amenability for pharmacological chaperone therapy with 1-deoxygalactonojirimycin in Fabry disease. *Int. J. Mol. Sci.* **2020**, *21*, 956.
57. Compain, P.; Martin, O. R., *Iminosugars: From synthesis to therapeutic applications*. John Wiley & Sons: 2007.
58. Mellor, H. R.; Neville, D. C.; Harvey, D. J.; Platt, F. M.; Dwek, R. A.; Butters, T. D., Cellular effects of deoxynojirimycin analogues: uptake, retention and inhibition of glycosphingolipid biosynthesis. *Biochem. J.* **2004**, *381*, 861-866.
59. Nash, R. J.; Kato, A.; Yu, C.-Y.; Fleet, G. W., Iminosugars as therapeutic agents: recent advances and promising trends. *Future Med. Chem.* **2011**, *3*, 1513-1521.
60. Asano, N., Sugar-mimicking glycosidase inhibitors: bioactivity and application. *Cell. Mol. Life Sci.* **2009**, *66*, 1479-1492.
61. Winchester, B. G., Iminosugars: from botanical curiosities to licensed drugs. *Tetrahedron: Asymmetry* **2009**, *20*, 645-651.
62. Dutcher, J. D., Chemistry of the amino sugars derived from antibiotic substances. *Adv. Carbohydr. Chem.* **1963**, *18*, 259-308.
63. Hanessian, S.; Haskell, T. H., Synthesis of 5-Acetamido-5-deoxypentoses. Sugar Derivatives Containing Nitrogen in the Ring1. *J. Org. Chem.* **1963**, *28*, 2604-2610.
64. Paulsen, H., Carbohydrates containing nitrogen or sulfur in the "hemiacetal" ring. *Angew. Chem. Int. Ed.* **1966**, *5*, 495-510.
65. Paulsen, H.; Sangster, I.; Heyns, K., Monosaccharide mit stickstoffhaltigem Ring, XIII. Synthese und Reaktionen von Keto-piperidinosen. *Chem. Ber.* **1967**, *100*, 802-815.
66. Inouye, S.; Tsuruoka, T.; Nida, T., The structure of nojirimycin, a piperidinose sugar antibiotic. *J. Antibiot.* **1966**, *19*, 288-292.
67. Inouye, S.; Tsuruoka, T.; Ito, T.; Niida, T., Structure and synthesis of nojirimycin. *Tetrahedron* **1968**, *24*, 2125-2144.
68. Niwa, T.; Inouye, S.; Tsuruoka, T.; Koaze, Y.; Niida, T., "Nojirimycin" as a potent inhibitor of glucosidase. *Agric. Biol. Chem.* **1970**, *34*, 966-968.

References

69. Yagi, M.; Kouno, T.; Aoyagi, Y.; Murai, H., The structure of moranoline, a piperidine alkaloid from *Morus* species. *J. Agric. Chem. Soc. Japan* **1976**, *50*, 571-572.
70. Asano, N.; Oseki, K.; Tomioka, E.; Kizu, H.; Matsui, K., N-containing sugars from *Morus alba* and their glycosidase inhibitory activities. *Carbohydr. Res.* **1994**, *259*, 243-255.
71. Asano, N.; Tomioka, E.; Kizu, H.; Matsui, K., Sugars with nitrogen in the ring isolated from the leaves of *Morus bombycis*. *Carbohydr. Res.* **1994**, *253*, 235-245.
72. Asano, N.; Oseki, K.; Kizu, H.; Matsui, K., Nitrogen-in-the-ring pyranoses and furanoses: structural basis of inhibition of mammalian glycosidases. *J. Med. Chem.* **1994**, *37*, 3701-3706.
73. Hettkamp, H.; Legler, G.; Bause, E., Purification by affinity chromatography of glucosidase I, an endoplasmic reticulum hydrolase involved in the processing of asparagine-linked oligosaccharides. *Eur. J. Biochem.* **1984**, *142*, 85-90.
74. Schweden, J.; Borgmann, C.; Legler, G.; Bause, E., Characterization of calf liver glucosidase I and its inhibition by basic sugar analogs. *Arch. Biochem. Biophys.* **1986**, *248*, 335-340.
75. Nash, R. J.; Bell, E. A.; Williams, J. M., 2-Hydroxymethyl-3,4-dihydroxypyrrolidine in fruits of *Angylocalyx boutiqueanus*. *Phytochemistry* **1985**, *24*, 1620-1622.
76. Welter, A.; Jadot, J.; Dardenne, G.; Marlier, M.; Casimir, J., 2,5-Dihydroxymethyl 3,4-dihydroxypyrrolidine dans les feuilles de *Derris elliptica*. *Phytochemistry* **1976**, *15*, 747-749.
77. Watanabe, S.; Kato, H.; Nagayama, K.; Abe, H., Isolation of 2R,5R-Dihydroxymethyl-3R,4R-dihydroxypyrrolidine (DMDP) from the Fermentation Broth of *Streptomyces* sp. KSC-5791. *Biosci., Biotechnol., Biochem.* **1995**, *59*, 936-937.
78. Hohenschutz, L. D.; Bell, E. A.; Jewess, P. J.; Leworthy, D. P.; Pryce, R. J.; Arnold, E.; Clardy, J., Castanospermine, a 1,6,7,8-tetrahydroxyoctahydroindolizine alkaloid, from seeds of *Castanospermum australe*. *Phytochemistry* **1981**, *20*, 811-814.
79. Molyneux, R. J.; Roitman, J. N.; Dunnheim, G.; Szumilo, T.; Elbein, A. D., 6-Epicastanospermine, a novel indolizidine alkaloid that inhibits α -glucosidase. *Arch. Biochem. Biophys.* **1986**, *251*, 450-457.

References

80. Saul, R.; Ghidoni, J. J.; Molyneux, R. J.; Elbein, A. D., Castanospermine inhibits alpha-glucosidase activities and alters glycogen distribution in animals. *Proc. Natl. Acad. Sci.* **1985**, *82*, 93-97.
81. Molyneux, R. J.; Benson, M.; Wong, R. Y.; Tropea, J. E.; Elbein, A. D., Australine, a novel pyrrolizidine alkaloid glucosidase inhibitor from *Castanospermum australe*. *J. Nat. Prod.* **1988**, *51*, 1198-1206.
82. Asano, N.; Nash, R. J.; Molyneux, R. J.; Fleet, G. W., Sugar-mimic glycosidase inhibitors: natural occurrence, biological activity and prospects for therapeutic application. *Tetrahedron: Asymmetry* **2000**, *11*, 1645-1680.
83. Kato, A.; Kato, N.; Miyauchi, S.; Minoshima, Y.; Adachi, I.; Ikeda, K.; Asano, N.; Watson, A. A.; Nash, R. J., Iminosugars from *Baphia nitida* Lodd. *Phytochemistry* **2008**, *69*, 1261-1265.
84. Pauling, L., Nature of Forces between Large Molecules of Biological Interest*. *Nature* **1948**, *161*, 707-709.
85. Kato, A.; Kato, N.; Kano, E.; Adachi, I.; Ikeda, K.; Yu, L.; Okamoto, T.; Banba, Y.; Ouchi, H.; Takahata, H., Biological properties of D- and L-1-deoxyazasugars. *J. Med. Chem.* **2005**, *48*, 2036-2044.
86. Dong, W.; Jespersen, T.; Bols, M.; Skrydstrup, T.; Sierks, M. R., Evaluation of isofagomine and its derivatives as potent glycosidase inhibitors. *Biochemistry* **1996**, *35*, 2788-2795.
87. Ernholz, B. V.; Thomsen, I. B.; Lohse, A.; Plesner, I. W.; Jensen, K. B.; Hazell, R. G.; Liang, X.; Jakobsen, A.; Bols, M., Enantiospecific Synthesis of 1-Azafagomine. *Chem. - Eur. J* **2000**, *6*, 278-287.
88. Papandreou, G.; Tong, M. K.; Ganem, B., Amidine, amidrazone, and amidoxime derivatives of monosaccharide aldonolactams: synthesis and evaluation as glycosidase inhibitors. *J. Am. Chem. Soc.* **1993**, *115*, 11682-11690.
89. Jensen, H. H.; Lyngbye, L.; Jensen, A.; Bols, M., Stereoelectronic substituent effects in polyhydroxylated piperidines and hexahydropyridazines. *Chem. - Eur. J* **2002**, *8*, 1218-1226.
90. Varrot, A.; Tarling, C. A.; Macdonald, J. M.; Stick, R. V.; Zechel, D. L.; Withers, S. G.; Davies, G. J., Direct observation of the protonation state of an imino sugar glycosidase inhibitor upon binding. *J. Am. Chem. Soc.* **2003**, *125*, 7496-7497.
91. Jespersen, T. M.; Dong, W.; Sierks, M. R.; Skrydstrup, T.; Lundt, I.; Bols, M., Isofagomine, a potent, new glycosidase inhibitor. *Angew. Chem. Int. Ed.* **1994**, *33*, 1778-1779.

References

92. Bols, M.; Hazell, R. G.; Thomsen, I. B., 1-Azafagomine: A Hydroxyhexahydropyridazine That Potently Inhibits Enzymatic Glycoside Cleavage. *Chem. - Eur. J* **1997**, *3*, 940-947.
93. Tong, M. K.; Papandreou, G.; Ganem, B., Potent, broad-spectrum inhibition of glycosidases by an amidine derivative of D-glucose. *J. Am. Chem. Soc.* **1990**, *112*, 6137-6139.
94. Lindback, E.; Lopez, O.; Tobiesen, A.; Fernandez-Bolanos, J. G.; Sydnés, M. O., Sugar hydrazide imides: a new family of glycosidase inhibitors. *Org. Biomol. Chem.* **2017**, *15*, 8709-8712.
95. Lindbäck, E.; López, O. s.; Fernandez-Bolanos, J. G.; Sauer, S. P.; Bols, M., An isofagomine analogue with an amidine at the pseudoanomeric position. *Org. Lett.* **2011**, *13*, 2908-2911.
96. Elbein, A. D.; Tropea, J. E.; Mitchell, M.; Kaushal, G. P., Kifunensine, a potent inhibitor of the glycoprotein processing mannosidase I. *J. Biol. Chem.* **1990**, *265*, 15599-605.
97. Riccio, E.; Zanfardino, M.; Ferreri, L.; Santoro, C.; Cocozza, S.; Capuano, I.; Imbriaco, M.; Feriozzi, S.; Pisani, A., Switch from enzyme replacement therapy to oral chaperone migalastat for treating fabry disease: real-life data. *Eur. J. Hum. Genet.* **2020**, *28*, 1662-1668.
98. Bischoff, J.; Kornfeld, R., The effect of 1-deoxymannojirimycin on rat liver α -mannosidases. *Biochem. Biophys. Res. Commun.* **1984**, *125*, 324-331.
99. Ayers, B. J.; Ngo, N.; Jenkinson, S. F.; Martínez, R. F.; Shimada, Y.; Adachi, I.; Weymouth-Wilson, A. C.; Kato, A.; Fleet, G. W. J., Glycosidase Inhibition by All 10 Stereoisomeric 2,5-Dideoxy-2,5-iminoheptitols Prepared from the Enantiomers of Glucuronolactone. *J. Org. Chem.* **2012**, *77*, 7777-7792.
100. Liu, K. K.; Kajimoto, T.; Chen, L.; Zhong, Z.; Ichikawa, Y.; Wong, C. H., Use of dihydroxyacetone phosphate-dependent aldolases in the synthesis of deoxy aza sugars. *J. Org. Chem.* **1991**, *56*, 6280-6289.
101. Kato, A.; Kato, N.; Kano, E.; Adachi, I.; Ikeda, K.; Yu, L.; Okamoto, T.; Banba, Y.; Ouchi, H.; Takahata, H.; Asano, N., Biological Properties of d- and l-1-Deoxyazasugars. *J. Med. Chem.* **2005**, *48*, 2036-2044.
102. Asano, N.; Ikeda, K.; Yu, L.; Kato, A.; Takebayashi, K.; Adachi, I.; Kato, I.; Ouchi, H.; Takahata, H.; Fleet, G. W., The L-enantiomers of D-sugar-mimicking iminosugars are noncompetitive inhibitors of D-glycohydrolase? *Tetrahedron: Asymmetry* **2005**, *16*, 223-229.

103. Fleet, G.; Nicholas, S.; Smith, P.; Evans, S. V.; Fellows, L.; Nash, R., Potent competitive inhibition of α -galactosidase and α -glucosidase activity by 1, 4-dideoxy-1, 4-iminopentitols: syntheses of 1, 4-dideoxy-1, 4-imino-d-lyxitol and of both enantiomers of 1, 4-dideoxy-1, 4-iminoarabinitol. *Tetrahedron Lett.* **1985**, *26*, 3127-3130.
104. Scofield, A.; Fellows, L.; Nash, R.; Fleet, G., Inhibition of mammalian digestive disaccharidases by polyhydroxy alkaloids. *Life Sci.* **1986**, *39*, 645-650.
105. Yu, C.-Y.; Asano, N.; Ikeda, K.; Wang, M.-X.; Butters, T. D.; Wormald, M. R.; Dwek, R. A.; Winters, A. L.; Nash, R. J.; Fleet, G. W. J., Looking glass inhibitors: l-DMDP, a more potent and specific inhibitor of α -glucosidases than the enantiomeric natural product DMDP. *Chem. Commun.* **2004**, 1936-1937.
106. D'Alonzo, D.; De Fenza, M.; Porto, C.; Iacono, R.; Huebecker, M.; Cobucci-Ponzano, B.; Priestman, D. A.; Platt, F.; Parenti, G.; Moracci, M., N-Butyl-1-deoxynojirimycin (l-NBDNJ): Synthesis of an allosteric enhancer of α -glucosidase activity for the treatment of pompe disease. *J. Med. Chem.* **2017**, *60*, 9462-9469.
107. Mena-Barragán, T.; García-Moreno, M. I.; Nanba, E.; Higaki, K.; Concia, A. L.; Clapés, P.; Fernández, J. M. G.; Mellet, C. O., Inhibitor versus chaperone behaviour of d-fagomine, DAB and LAB sp2-iminosugar conjugates against glycosidases: A structure–activity relationship study in Gaucher fibroblasts. *Eur. J. Med. Chem.* **2016**, *121*, 880-891.
108. Best, D.; Jenkinson, S. F.; Saville, A. W.; Alonzi, D. S.; Wormald, M. R.; Butters, T. D.; Norez, C.; Becq, F.; Blériot, Y.; Adachi, I., Cystic fibrosis and diabetes: isoLAB and isoDAB, enantiomeric carbon-branched pyrrolidine iminosugars. *Tetrahedron Lett.* **2010**, *51*, 4170-4174.
109. Horne, G., Iminosugars: therapeutic applications and synthetic considerations. In *Carbohydrates as drugs*, Springer: 2014; pp 23-51.
110. Fleet, G. W.; Karpas, A.; Dwek, R. A.; Fellows, L. E.; Tyms, A.; Petursson, S.; Namgoong, S. K.; Ramsden, N. G.; Smith, P. W.; Son, J. C., Inhibition of HIV replication by amino-sugar derivatives. *FEBS Lett.* **1988**, *237*, 128-132.
111. Durantel, D., Celgosivir, an α -glucosidase I inhibitor for the potential treatment of hepatitis C virus infection. *Curr. Opin. Invest. Drugs* **2009**, *10*, 860-870.

References

112. Whitby, K.; Taylor, D.; Patel, D.; Ahmed, P.; Tyms, A. S., Action of celgosivir (6 O-butanoyl castanospermine) against the pestivirus BVDV: implications for the treatment of hepatitis C. *Antiviral Chem. Chemother.* **2004**, *15*, 141-151.
113. Simone, M. I.; Soengas, R. G.; Jenkinson, S. F.; Evinson, E. L.; Nash, R. J.; Fleet, G. W., Synthesis of three branched iminosugars [(3R,4R,5S)-3-(hydroxymethyl) piperidine-3,4,5-triol, (3R,4R,5R)-3-(hydroxymethyl) piperidine-3,4,5-triol and (3S,4R,5R)-3-(hydroxymethyl) piperidine-3,4,5-triol] and a branched trihydroxynipepic acid [(3R,4R,5R)-3,4,5-trihydroxypiperidine-3-carboxylic acid] from sugar lactones with a carbon substituent at C-2. *Tetrahedron: Asymmetry* **2012**, *23*, 401-408.
114. Soengas, R. G.; Simone, M. I.; Hunter, S.; Nash, R. J.; Evinson, E. L.; Fleet, G. W., Hydroxymethyl-Branched Piperidines from Hydroxymethyl-Branched Lactones: Synthesis and Biological Evaluation of 1, 5-Dideoxy-2-C-hydroxymethyl-1, 5-imino-D-mannitol, 1, 5-Dideoxy-2-C-hydroxymethyl-1, 5-imino-L-gulitol and 1, 5-Dideoxy-2-C-hydroxymethyl-1, 5-imino-D-talitol. *Eur. J. Org. Chem.* **2012**, *2012*, 2394-2402.
115. al Daher, S.; Fleet, G.; Namgoong, S. K.; Winchester, B., Change in specificity of glycosidase inhibition by N-alkylation of amino sugars. *Biochem. J.* **1989**, *258*, 613-615.
116. Kumar, Y.; Goyal, R.; Thakur, A., Pharmacotherapeutics of miglitol: an α -glucosidase inhibitor. *J Anal Pharm Res* **2018**, *7*, 617-619.
117. Hollak, C. E.; Hughes, D.; Van Schaik, I. N.; Schwierin, B.; Bembi, B., Miglustat (Zavesca®) in type 1 Gaucher disease: 5-year results of a post-authorisation safety surveillance programme. *Pharmacoepidemiol. Drug Saf.* **2009**, *18*, 770-777.
118. Kato, A.; Hayashi, E.; Miyauchi, S.; Adachi, I.; Imahori, T.; Natori, Y.; Yoshimura, Y.; Nash, R. J.; Shimaoka, H.; Nakagome, I.; Koseki, J.; Hirono, S.; Takahata, H., α -1-C-Butyl-1,4-dideoxy-1,4-imino-l-arabinitol as a Second-Generation Iminosugar-Based Oral α -Glucosidase Inhibitor for Improving Postprandial Hyperglycemia. *J. Med. Chem.* **2012**, *55*, 10347-10362.
119. De Fenza, M.; D'Alonzo, D.; Esposito, A.; Munari, S.; Loberto, N.; Santangelo, A.; Lampronti, I.; Tamanini, A.; Rossi, A.; Ranucci, S., Exploring the effect of chirality on the therapeutic potential of N-alkyl-deoxyiminosugars: anti-inflammatory response to *Pseudomonas*

References

- aeruginosa infections for application in CF lung disease. *Eur. J. Med. Chem.* **2019**, *175*, 63-71.
120. Horne, G.; Wilson, F. X., Therapeutic applications of iminosugars: current perspectives and future opportunities. *Prog. Med. Chem.* **2011**, *50*, 135-176.
121. D'Alonzo, D.; Guaragna, A.; Palumbo, G., Glycomimetics at the mirror: medicinal chemistry of L-iminosugars. *Curr. Med. Chem.* **2009**, *16*, 473-505.
122. Castellan, T.; Garcia, V.; Rodriguez, F.; Fabing, I.; Shchukin, Y.; Tran, M. L.; Ballereau, S.; Levade, T.; Génisson, Y.; Dehoux, C., Concise asymmetric synthesis of new enantiomeric C-alkyl pyrrolidines acting as pharmacological chaperones against Gaucher disease. *Org. Biomol. Chem.* **2020**, *18*, 7852-7861.
123. Tschamber, T.; Siendt, H.; Tarnus, C.; Deredas, D.; Frankowski, A.; Kohler, S.; Streith, J., Stereomeric Pyrrolidinopentoses Bearing an Imidazole Ring– Synthesis, Chiroptical Properties, and Evaluation as Potential Sugar-Mimic Glycosidase Inhibitors. *Eur. J. Org. Chem.* **2002**, *2002*, 702-712.
124. Tschamber, T.; Gessier, F.; Dubost, E.; Newsome, J.; Tarnus, C.; Kohler, J.; Neuburger, M.; Streith, J., Carbohydrate transition state mimics: synthesis of imidazolo-pyrrolidinoses as potential nectrisine surrogates. *Biorg. Med. Chem.* **2003**, *11*, 3559-3568.
125. Arora, I.; Kashyap, V. K.; Singh, A. K.; Dasgupta, A.; Kumar, B.; Shaw, A. K., Design, Synthesis and Biological evaluation of Bicyclic Iminosugar Hybrids: Conformational constraint as an effective tool for tailoring the selectivity of α -glucosidase inhibitors. *Org. Biomol. Chem.* **2014**, *12*, 6855-6868.
126. Evangelista, T. C. S.; Lopez, O.; Sydnes, M. O.; Fernandez-Bolanos, J. G.; Ferreira, S. B.; Lindbäck, E., Bicyclic 1-azafagomine derivatives: synthesis and glycosidase inhibitory testing. *Synthesis* **2019**, *51*, 4066-4077.
127. Ermert, P.; Vasella, A., Synthesis of a Glucose-Derived Tetrazole as a New β -Glucosidase Inhibitor. A New Synthesis of 1-Deoxynojirimycin. *Helv. Chim. Acta* **1991**, *74*, 2043-2053.
128. Meng, Q.; Hesse, M., A New Synthesis of (2S,3R,4R)-2-(Hydroxymethyl) pyrrolidine-3,4-diol. *Helv. Chim. Acta* **1991**, *74*, 445-450.

129. Bailey, P. D.; Beard, M. A.; Dang, H. P.; Phillips, T. R.; Price, R. A.; Whittaker, J. H., Debenzylation using catalytic hydrogenolysis in trifluoroethanol, and the total synthesis of (-)-raumacline. *Tetrahedron Lett.* **2008**, *49*, 2150-2153.
130. Rasmussen, T. S.; Koldsø, H.; Nakagawa, S.; Kato, A.; Schiøtt, B.; Jensen, H. H., Synthesis of uronic-Noeurostegine—a potent bacterial β -glucuronidase inhibitor. *Org. Biomol. Chem.* **2011**, *9*, 7807-7813.
131. Sydnes, M. O.; Isobe, M., One-pot reductive monoalkylation of nitro aryls with hydrogen over Pd/C. *Tetrahedron Lett.* **2008**, *49*, 1199-1202.
132. Esaki, H.; Ohtaki, R.; Maegawa, T.; Monguchi, Y.; Sajiki, H., Novel Pd/C-catalyzed redox reactions between aliphatic secondary alcohols and ketones under hydrogenation conditions: application to H–D exchange reaction and the mechanistic study. *J. Org. Chem.* **2007**, *72*, 2143-2150.
133. Boutellier, M.; Horenstein, B. A.; Semenyaka, A.; Schramm, V. L.; Ganem, B., Amidrazone analogs of D-ribofuranose as transition-state inhibitors of nucleoside hydrolase. *Biochemistry* **1994**, *33*, 3994-4000.
134. Overkleeft, H. S.; van Wiltenburg, J.; Pandit, U. K., A facile transformation of sugar lactones to azasugars. *Tetrahedron* **1994**, *50*, 4215-4224.
135. Stephenson, L.; Warburton, W.; Wilson, M., Reaction of some aromatic nitriles with hydroxylamine to give amides, and an alternative preparation of amidoximes. *J. Chem. Soc. C.* **1969**, 861-864.
136. Vörös, A.; Mucsi, Z.; Baán, Z.; Timári, G.; Hermeicz, I.; Mizsey, P.; Finta, Z., An experimental and theoretical study of reaction mechanisms between nitriles and hydroxylamine. *Org. Biomol. Chem.* **2014**, *12*, 8036-8047.
137. Haarr, M. B.; Lopéz, O. s.; Pejov, L.; Fernández-Bolaños, J. G.; Lindbäck, E.; Sydnes, M. O., 1,4-dideoxy-1,4-imino-D-arabinitol (DAB) analogues possessing a hydrazide imide moiety as potent and selective α -mannosidase inhibitors. *ACS omega* **2020**, *5*, 18507-18514.
138. Venkata Ramana, C.; Vasella, A., Sugar-Derived Di- and Tetrahydropyridazinones: Synthesis of New Glycosidase Inhibitors. *Helv. Chim. Acta* **2000**, *83*, 1599-1610.
139. Neilson, D. G.; Roger, R.; Heatlie, J.; Newlands, L., Chemistry of amidrazones. *Chem. Rev.* **1970**, *70*, 151-170.

References

140. Wang, L.; Liang, T.; Fang, Z., Chemical synthesis and preliminary biological evaluation of C-6-O-methyl-1-deoxynojirimycin as a potent α -glucosidase inhibitor. *J. Carbohydr. Chem.* **2020**, *39*, 36-49.
141. Mori, N.; Togo, H., Facile oxidative conversion of alcohols to esters using molecular iodine. *Tetrahedron* **2005**, *61*, 5915-5925.
142. Howard, S.; Braun, C.; McCarter, J.; Moremen, K. W.; Liao, Y.-F.; Withers, S. G., Human lysosomal and jack bean α -mannosidases are retaining glycosidases. *Biochem. Biophys. Res. Commun.* **1997**, *238*, 896-898.
143. Goss, P. E.; Baker, M. A.; Carver, J. P.; Dennis, J. W., Inhibitors of carbohydrate processing: A new class of anticancer agents. *Clin. Cancer. Res.* **1995**, *1*, 935-944.
144. Yang, Q.; Hughes, T. A.; Kelkar, A.; Yu, X.; Cheng, K.; Park, S.; Huang, W.-C.; Lovell, J. F.; Neelamegham, S., Inhibition of SARS-CoV-2 viral entry upon blocking N-and O-glycan elaboration. *Elife* **2020**, *9*, e61552.
145. Witherup, K. M.; Ransom, R. W.; Graham, A. C.; Bernard, A. M.; Salvatore, M. J.; Lumma, W. C.; Anderson, P. S.; Pitzenberger, S. M.; Varga, S. L., Martinelline and martinellie acid, novel G-protein linked receptor antagonists from the tropical plant *Martinella iquitosensis* (Bignoniaceae). *J. Am. Chem. Soc.* **1995**, *117*, 6682-6685.
146. Elvis-Offiah, U. B.; Bafor, E. E.; Eze, G. I.; Igbinumwen, O.; Viegelmann, C.; Edrada-Ebel, R., In vivo investigation of female reproductive functions and parameters in nonpregnant mice models and mass spectrometric analysis of the methanol leaf extract of *Emilia Coccinea* (Sims) G Dons. *Physiol. Rep.* **2016**, *4*, e13047.
147. Zulfiker, A. H. M.; Sohrabi, M.; Qi, J.; Matthews, B.; Wei, M. Q.; Grice, I. D., Multi-constituent identification in Australian cane toad skin extracts using high-performance liquid chromatography high-resolution tandem mass spectrometry. *J. Pharm. Biomed. Anal.* **2016**, *129*, 260-272.
148. Abhimannue, A. P.; Mohan, M. C.; B, P. K., Inhibition of Tumor Necrosis Factor- α and Interleukin-1 β Production in Lipopolysaccharide-Stimulated Monocytes by Methanolic Extract of *Elephantopus scaber* Linn and Identification of Bioactive Components. *Appl. Biochem. Biotechnol.* **2016**, *179*, 427-443.
149. Gentry, A. H.; Cook, K., *Martinella* (Bignoniaceae): a widely used eye medicine of South America. *J. Ethnopharmacol.* **1984**, *11*, 337-343.

References

150. Ogunlesi, M.; Okiei, W.; Ademoye, M., Medicinal Plants Used in Treating Eye Infections in Nigeria. In *A Textbook of Medicinal Plants from Nigeria*, Odugbemi, T., Ed. University of Lagos Press: Nigeria, 2008; p 305.
151. Ikeda, S.; Shibuya, M.; Iwabuchi, Y., Asymmetric total synthesis of martinelline and martinellie acid. *Chem. Commun.* **2007**, 504-506.
152. Nyerges, M., Construction of pyrrolo [3,2-c] quinolines: Recent advances in the synthesis of the martinelline alkaloids. *Heterocycles* **2004**, *63*, 1685-1712.
153. Lovely, C. J.; Bararinarayana, V., Synthetic studies toward the Martinella alkaloids. *Curr. Org. Chem.* **2008**, *12*, 1431-1453.
154. Haarr, M. B.; Sydnes, M. O., Synthesis of the Hexahydropyrrolo-[3,2-c]-quinoline Core Structure and Strategies for Further Elaboration to Martinelline, Martinellie Acid, Incargranine B, and Seneciobipyrrolidine. *Molecules* **2021**, *26*, 341.
155. Reuter, G., Arginin als Vorstufe von Galegin in Galega officinalis L. Zur Biochemie und Physiologie von Galegin in Galega officinalis L., III. Mitt. *Arch. Pharm.* **1963**, *296*, 516-522.
156. Eichholzer, J. V.; Lewis, I. A.; Macleod, J. K.; Oelrichs, P. B.; Vallely, P. J., Galegine and a new dihydroxyalkylacetamide from *Verbesina enceloiodes*. *Phytochemistry* **1982**, *21*, 97-99.
157. Regasini, L. O.; Castro-Gamboa, I.; Silva, D. H. S.; Furlan, M.; Barreiro, E. J.; Ferreira, P. M. P.; Pessoa, C.; Lotufo, L. c. V. C.; de Moraes, M. O.; Young, M. C. M., Cytotoxic guanidine alkaloids from *Pterogyne nitens*. *J. Nat. Prod.* **2009**, *72*, 473-476.
158. Ma, D.; Xia, C.; Jiang, J.; Zhang, J., First total synthesis of martinellie acid, a naturally occurring bradykinin receptor antagonist. *Org. Lett.* **2001**, *3*, 2189-2191.
159. Davies, S. G.; Fletcher, A. M.; Lee, J. A.; Lorkin, T. J.; Roberts, P. M.; Thomson, J. E., A diastereodivergent strategy for the asymmetric syntheses of (-)-martinellie acid and (-)-4-epi-martinellie acid. *Tetrahedron* **2013**, *69*, 9779-9803.
160. Davies, S. G.; Fletcher, A. M.; Lee, J. A.; Lorkin, T. J.; Roberts, P. M.; Thomson, J. E., Asymmetric synthesis of (-)-martinellie acid. *Org. Lett.* **2013**, *15*, 2050-2053.
161. Rong, Z.; Li, Q.; Lin, W.; Jia, Y., Reagent-free synthesis of 2,3,4-polysubstituted tetrahydroquinolines: application to the formal synthesis

References

- of (\pm)-martinellic acid and martinelline. *Tetrahedron Lett.* **2013**, *54*, 4432-4434.
162. Yoshitomi, Y.; Arai, H.; Makino, K.; Hamada, Y., Enantioselective synthesis of martinelline chiral core and its diastereomer using asymmetric tandem Michael–aldol reaction. *Tetrahedron* **2008**, *64*, 11568-11579.
163. He, Y.; Mahmud, H.; Moningka, R.; Lovely, C. J.; Dias, H. R., Cyclization reactions of N-acryloyl-2-aminobenzaldehyde derivatives: formal total synthesis of martinelline. *Tetrahedron* **2006**, *62*, 8755-8769.
164. Hadden, M.; Nieuwenhuyzen, M.; Osborne, D.; Stevenson, P. J.; Thompson, N.; Walker, A. D., Synthesis of the heterocyclic core of martinelline and martinelline. *Tetrahedron* **2006**, *62*, 3977-3984.
165. Powell, D. A.; Batey, R. A., Total synthesis of the alkaloids martinelline and martinelline via a hetero Diels–Alder multicomponent coupling reaction. *Org. Lett.* **2002**, *4*, 2913-2916.
166. Snider, B. B.; Ahn, Y.; O'Hare, S. M., Total synthesis of (\pm)-martinellic acid. *Org. Lett.* **2001**, *3*, 4217-4220.
167. Hadden, M.; Nieuwenhuyzen, M.; Osborne, D.; Stevenson, P. J.; Thompson, N., Synthesis of the heterocyclic core of the alkaloids martinelline and martinelline. *Tetrahedron Lett.* **2001**, *42*, 6417-6419.
168. Xia, C.; Heng, L.; Ma, D., Total synthesis of (\pm)-martinelline. *Tetrahedron Lett.* **2002**, *43*, 9405-9409.
169. Batey, R. A.; Powell, D. A., Multi-component coupling reactions: synthesis of a guanidine containing analog of the hexahydropyrrolo [3, 2-c] quinoline alkaloid martinelline. *Chem. Commun.* **2001**, 2362-2363.
170. Jones, J. H., The terminology of guanidine formation. Wiley Online Library: 2002.
171. Ma, D.; Xia, C.; Jiang, J.; Zhang, J.; Tang, W., Aromatic nucleophilic substitution or CuI-catalyzed coupling route to martinelline. *J. Org. Chem.* **2003**, *68*, 442-451.
172. Snider, B. B.; O'Hare, S. M., Synthesis of the hindered N,N,N'-trisubstituted guanidine moiety of martinelline and martinelline. *Tetrahedron Lett.* **2001**, *42*, 2455-2458.
173. Rasmussen, S. C., The nomenclature of fused-ring arenes and heterocycles: a guide to an increasingly important dialect of organic chemistry. *ChemTexts* **2016**, *2*, 1-13.

References

174. Batey, R.; Simoncic, P.; Smyj, R.; Lough, A., A three-component coupling protocol for the synthesis of substituted hexahydropyrrolo [3, 2-c] quinolines. *Chem. Commun.* **1999**, 651-652.
175. Hadden, M.; Stevenson, P. J., Regioselective synthesis of pyrroloquinolines—Approaches to Martinelline. *Tetrahedron Lett.* **1999**, *40*, 1215-1218.
176. He, L.; Liu, H.-B.; Zhao, L.; Wang, D.-X.; Wang, M.-X., Lewis acid-catalyzed reaction between tertiary enamides and imines of salicylaldehydes: expedient synthesis of novel 4-chromanamine derivatives. *Tetrahedron* **2015**, *71*, 523-531.
177. Yu, J.; Jiang, H.-J.; Zhou, Y.; Luo, S.-W.; Gong, L.-Z., Sodium Salts of Anionic Chiral Cobalt(III) Complexes as Catalysts of the Enantioselective Povarov Reaction. *Angew. Chem. Int. Ed.* **2015**, *54*, 11209-11213.
178. Liu, X.; Toy, P. H., Halogen Bond-Catalyzed Povarov Reactions. *Adv. Synth. Catal.* **2020**, *362*, 3437-3441.
179. Reyes-Gutiérrez, P. E.; Amatov, T. T.; Švec, P.; Císařová, I.; Šaman, D.; Pohl, R.; Teplý, F.; Pospíšil, L., Helquats as Promoters of the Povarov Reaction: Synthesis of 1,2,3,4-Tetrahydroquinoline Scaffolds Catalyzed by Helicene-Viologen Hybrids. *ChemPlusChem* **2020**, *85*, 2212-2218.
180. Škopić, M. K.; Götte, K.; Gramse, C.; Dieter, M.; Pospich, S.; Raunser, S.; Weberskirch, R.; Brunschweiler, A., Micellar Brønsted Acid Mediated Synthesis of DNA-Tagged Heterocycles. *J. Am. Chem. Soc.* **2019**, *141*, 10546-10555.
181. Xu, H.; Zuend, S. J.; Woll, M. G.; Tao, Y.; Jacobsen, E. N., Asymmetric Cooperative Catalysis of Strong Brønsted Acid-Promoted Reactions Using Chiral Ureas. *Science* **2010**, *327*, 986-990.
182. Gerard, B.; O'Shea, M. W.; Donckele, E.; Kesavan, S.; Akella, L. B.; Xu, H.; Jacobsen, E. N.; Marcaurelle, L. A., Application of a catalytic asymmetric Povarov reaction using chiral ureas to the synthesis of a tetrahydroquinoline library. *ACS Comb. Sci.* **2012**, *14*, 621-630.
183. Danishefsky, S.; Singh, R., Spiroactivated vinylcyclopropane. *J. Org. Chem.* **1975**, *40*, 3807-3808.
184. Badarinarayana, V.; Lovely, C. J., Total synthesis of (-)-martinellic acid. *Tetrahedron Lett.* **2007**, *48*, 2607-2610.
185. Shirai, A.; Miyata, O.; Tohnai, N.; Miyata, M.; Procter, D. J.; Sucunza, D.; Naito, T., Total Synthesis of (-)-Martinelllic Acid via

- Radical Addition– Cyclization– Elimination Reaction. *J. Org. Chem.* **2008**, *73*, 4464-4475.
186. Miyata, O.; Shirai, A.; Yoshino, S.; Takeda, Y.; Sugiura, M.; Naito, T., An Improved Synthesis of (-)-Martinelllic Acid via Radical Addition-Cyclization-Elimination Reaction of Chiral Oxime Ether. *Synlett* **2006**, *2006*, 893-896.
187. Davies, S. G.; Ichihara, O.; Walters, I., Asymmetric-synthesis of syn- α -alkyl- β -amino acids. *J. Chem. Soc., Perkin Trans. 1* **1994**, *9*, 1141-1147.
188. Pappoppula, M.; Aponick, A., Enantioselective Total Synthesis of (-)-Martinelllic Acid. *Angew. Chem. Int. Ed.* **2015**, *54*, 15827-15830.
189. Lindbäck, E.; Sydnes, M. O., Catalytic Enantioselective Synthesis of the Partially Reduced Tricyclic Pyrrolo [3,2-c] quinoline Core Structure of the Martinella Alkaloids. *ChemistrySelect* **2016**, *1*, 1837-1840.
190. Duvall, J. R.; Bedard, L.; Naylor-Olsen, A. M.; Manson, A. L.; Bittker, J. A.; Sun, W.; Fitzgerald, M. E.; He, Z.; Lee IV, M. D.; Marie, J.-C.; Muncipinto, G.; Rush, D.; Xu, D.; Xu, H.; Zhang, M.; Earl, A. M.; Palmer, M. A.; Foley, M. A.; Vacca, J. P.; Scherer, C. A., Identification of highly specific diversity-oriented synthesis-derived inhibitors of *Clostridium difficile*. *ACS Infect. Dis.* **2017**, *3*, 349-359.
191. Park, S. W.; Casalena, D. E.; Wilson, D. J.; Dai, R.; Nag, P. P.; Liu, F.; Boyce, J. P.; Bittker, J. A.; Schreiber, S. L.; Finzel, B. C., Target-based identification of whole-cell active inhibitors of biotin biosynthesis in *Mycobacterium tuberculosis*. *Chem. Biol.* **2015**, *22*, 76-86.
192. Katsuki, T.; Sharpless, K. B., The first practical method for asymmetric epoxidation. *J. Am. Chem. Soc.* **1980**, *102*, 5974-5976.
193. Medina, E.; Vidal-Ferran, A.; Moyano, A.; Pericàs, M. A.; Riera, A., Enantioselective synthesis of N-Boc-1-naphthylglycine. *Tetrahedron: Asymmetry* **1997**, *8*, 1581-1586.
194. Gao, S.; Wang, Q.; Huang, L. J.-S.; Lum, L.; Chen, C., Chemical and biological studies of nakiterpiosin and nakiterpiosinone. *J. Am. Chem. Soc.* **2010**, *132*, 371-383.
195. Schwab, P.; France, M. B.; Ziller, J. W.; Grubbs, R. H., A Series of Well-Defined Metathesis Catalysts–Synthesis of $[\text{RuCl}_2(\text{CHR}')(\text{PR}_3)_2]$ and Its Reactions. *Angew. Chem. Int. Ed.* **1995**, *34*, 2039-2041.

References

196. Schwab, P.; Grubbs, R. H.; Ziller, J. W., Synthesis and applications of $\text{RuCl}_2(\text{CHR}')(\text{PR}_3)_2$: the influence of the alkylidene moiety on metathesis activity. *J. Am. Chem. Soc.* **1996**, *118*, 100-110.
197. Ng, P. Y.; Masse, C. E.; Shaw, J. T., Cycloaddition reactions of imines with 3-thiosuccinic anhydrides: Synthesis of the tricyclic core of martinellie acid. *Org. Lett.* **2006**, *8*, 3999-4002.
198. Deobald, A. M.; Corrêa, A. G.; Rivera, D. G.; Paixão, M. W., Organocatalytic asymmetric epoxidation and tandem epoxidation/Passerini reaction under eco-friendly reaction conditions. *Org. Biomol. Chem.* **2012**, *10*, 7681-7684.
199. Dale, J. A.; Mosher, H. S., Nuclear magnetic resonance enantiomer reagents. Configurational correlations via nuclear magnetic resonance chemical shifts of diastereomeric mandelate, O-methylmandelate, and α -methoxy- α -trifluoromethylphenylacetate (MTPA) esters. *J. Am. Chem. Soc.* **1973**, *95*, 512-519.
200. Hoye, T. R.; Jeffrey, C. S.; Shao, F., Mosher ester analysis for the determination of absolute configuration of stereogenic (chiral) carbinol carbons. *Nat. Protoc.* **2007**, *2*, 2451-2458.
201. Lombardo, L., Methylenation of carbonyl compounds with $\text{Zn CH}_2\text{Br}_2 \text{ TiCl}_4$. Application to gibberellins. *Tetrahedron Lett.* **1982**, *23*, 4293-4296.
202. Peng, Y.; Li, W.-D. Z., A mild and efficient desilylation of O-tert-butyltrimethylsilyl ethers mediated by chlorotrimethylsilane and potassium fluoride dihydrate in acetonitrile. *Synlett* **2006**, *2006*, 1165-1168.
203. Nicolaou, K.; Snyder, S. A.; Longbottom, D. A.; Nalbandian, A. Z.; Huang, X., New uses for the Burgess reagent in chemical synthesis: Methods for the facile and stereoselective formation of sulfamidates, glycosylamines, and sulfamides. *Chem. - Eur. J* **2004**, *10*, 5581-5606.
204. Laroche, C.; Behr, J.-B.; Szymoniak, J.; Bertus, P.; Schütz, C.; Vogel, P.; Plantier-Royon, R., Spirocyclopropyl pyrrolidines as a new series of α -L-fucosidase inhibitors. *Biorg. Med. Chem.* **2006**, *14*, 4047-4054.
205. Sivertsen, A. C.; Gasior, M.; Bjerring, M.; Hansen, S. U.; Lopez Lopez, O.; Nielsen, N. C.; Bols, M., Active Site Protonation of 1-Azafagomine in Glucosidases Studied by Solid-State NMR Spectroscopy. Wiley Online Library: 2007.

References

206. Morrill, C.; Grubbs, R. H., Highly selective 1,3-isomerization of allylic alcohols via rhenium oxo catalysis. *J. Am. Chem. Soc.* **2005**, *127*, 2842-2843.
207. Serra-Muns, A.; Guérinot, A.; Reymond, S.; Cossy, J., Silica gel-mediated rearrangement of allylic acetates. Application to the synthesis of 1, 3-enynes. *Chem. Commun.* **2010**, *46*, 4178-4180.
208. Okuro, K.; Gurnham, J.; Alper, H., Ionic diamine rhodium complex catalyzed reductive N-heterocyclization of 2-nitrovinylarenes. *J. Org. Chem.* **2011**, *76*, 4715-4720.
209. Felpin, F. X.; Fouquet, E.; Zakri, C., Heck Cross-Coupling of Aryldiazonium Tetrafluoroborate with Acrylates Catalyzed by Palladium on Charcoal. *Adv. Synth. Catal.* **2008**, *350*, 2559-2565.
210. West, T. H.; Daniels, D. S.; Slawin, A. M.; Smith, A. D., An isothiurea-catalyzed asymmetric [2,3]-rearrangement of allylic ammonium ylides. *J. Am. Chem. Soc.* **2014**, *136*, 4476-4479.
211. Liu, Y.; Li, X.; Lin, G.; Xiang, Z.; Xiang, J.; Zhao, M.; Chen, J.; Yang, Z., Synthesis of catechins via thiourea/AuCl₃-catalyzed cycloalkylation of aryl epoxides. *J. Org. Chem.* **2008**, *73*, 4625-4629.

Paper I

1,4-Dideoxy-1,4-imino-D-arabinitol (DAB) Analogues Possessing a Hydrazone Imide Moiety as Potent and Selective α -Mannosidase Inhibitors

*Marianne B. Haarr, Óscar Lopéz, Ljupcho Pejov, José G. Fernández-
Bolanõs, Emil Lindbäck, and Magne O. Sydnes*

ACS Omega **2020**, *5*, 18507.

DOI: 10.1021/acsomega.0c02466

1,4-Dideoxy-1,4-imino-D-arabinitol (DAB) Analogues Possessing a Hydrazide Imide Moiety as Potent and Selective α -Mannosidase Inhibitors

Marianne B. Haarr, Óscar Lopéz, Ljupcho Pejov, José G. Fernández-Bolaños, Emil Lindbäck,* and Magne O. Sydnes*



Cite This: *ACS Omega* 2020, 5, 18507–18514



Read Online

ACCESS |



Metrics & More



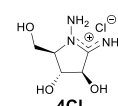
Article Recommendations



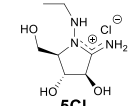
Supporting Information

ABSTRACT: The synthesis of two polyhydroxylated pyrrolidines as 1,4-dideoxy-1,4-imino-D-arabinitol (DAB) analogues bearing a hydrazide moiety is described. The DAB analogues act as selective and potent inhibitors of α -mannosidase in the submicromolar concentration ranges (K_i values ranging from 0.23 to 1.4 μM).

Selective and potent inhibitors of α -mannosidase



$K_i = 0.23 \pm 0.07 \mu\text{M}$



$K_i = 1.4 \pm 0.4 \mu\text{M}$

INTRODUCTION

Glycosidases represent a group of enzymes that is abundant in essentially all living organisms, in which they catalyze the hydrolysis of glycosidic bonds.¹ Such hydrolases are, for instance, involved in the intestinal digestion of starch, the biosynthesis of oligosaccharide chains, and the hydrolysis of glycoconjugates in the lysosomes. Thus, the diverse biological roles of glycosidases have labeled glycosidase inhibitors as attractive pharmaceutical targets.²

The most common type of glycosidase inhibitor is azasugars (such as isofagomine (1) (Figure 1)) and iminosugars, in

diabetes, cancer, viral infections, and lysosomal storage disorders.⁷ However, in many cases, a limitation of iminosugars as drug candidates is that they display low glycosidase inhibition selectivity and thus they interact with glycosidases that are not involved in the disease that they are targeted to tackle;⁸ as a result, severe side effects can be triggered when this lack of selectivity is present.

Aza- and iminosugars are believed to act as glycosidase inhibitors due to their ability to be protonated at physiological pH and thus resemble the charge in the transition state of glycosidase-catalyzed cleavage of glycosidic bonds.⁹ Aza- and iminosugars have therefore been used as tools to explore the mechanism of glycosidases.¹⁰ Thus, many aza- and iminosugars have been designed and synthesized to resemble the charge and/or shape of the transition state of catalyzed cleavage of glycosidic bonds.^{10,11} One such example is isofagomine (1), which was found to be a very potent inhibitor of β -glucosidase (K_i , 0.11 μM).¹² Interestingly, X-ray analysis of a cellobio-derived isofagomine in complex with Cel5A confirmed that the isofagomine derivative is bound to the enzyme in its protonated form and as such establishes an ion–ion interaction with the catalytic nucleophile.¹³ The importance of ion–ion interactions between the enzyme and the inhibitor and Ganem et al.'s hypothesis that sugar amidines behave as broad spectrum glycosidase inhibitors because they resemble the shape of the transition state of enzymatic cleavage of glycosides,¹⁴ even though the full understanding of the features of the transition state of such enzymes is missing,¹⁵ led to the

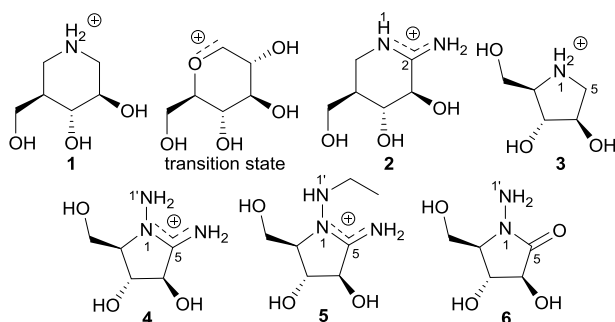


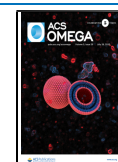
Figure 1. Compounds 1–3 and the target compounds 4–6 in this project.

which a carbon atom or the endocyclic oxygen atom in a saccharide has been replaced by a nitrogen atom, respectively.³ Currently, three iminosugars, namely, Glyset (*N*-(2-hydroxyethyl)-1-deoxynojirimycin),⁴ Zavesca (*N*-butyl-1-deoxynojirimycin),⁵ and Galafold (1-deoxygalactonojirimycin),⁶ are marketed for the treatment of type 2 diabetes, Gaucher disease, and Fabry disease, respectively. In addition, due to their glycosidase inhibitory properties, aza- and iminosugars serve as lead compounds for the treatment of diseases such as

Received: May 26, 2020

Accepted: June 30, 2020

Published: July 15, 2020



synthesis of an amidine analogue of isofagomine, namely, isofagomidine (**2**).¹⁶ This compound was found to display a very narrow glycosidase inhibitory spectrum along with a very different glycosidase inhibition profile compared to isofagomine (**1**). Indeed, **2** was found to be a selective inhibitor (K_i , 0.75 μM) of jack-bean α -mannosidase, which is a member of the retaining glycosidase hydrolase family 38 that includes α -mannosidases with medicinal relevance.¹⁷ The difference in the glycosidase inhibition profile between **1** and **2** was supported by DFT calculations and was attributed to a very different charge distribution within the two compounds in their protonated forms.¹⁶

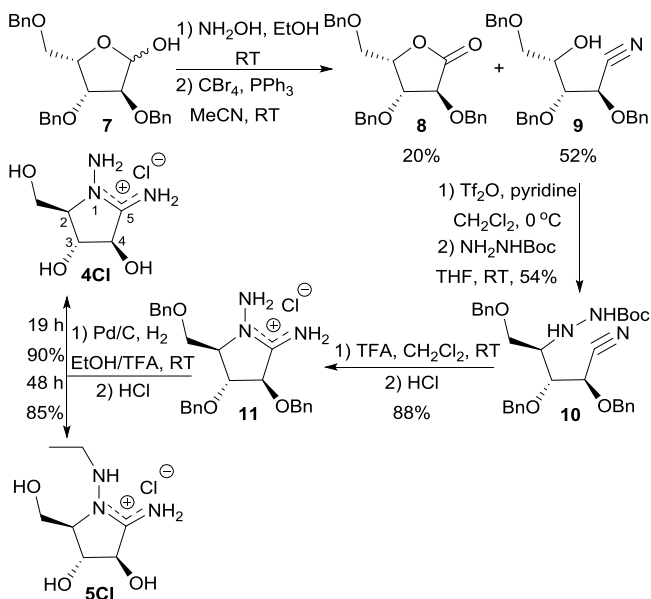
Many polyhydroxylated pyrrolidines such as 1,4-dideoxy-1,4-imino-D-arabinitol (DAB, **3**) (Figure 1) have been found to be potent glycosidase inhibitors.^{7,18} In addition, many of them inhibit a rather broad spectra of glycosidases, which has been attributed to the flexibility of the five-membered ring system¹⁹ including, in some cases, their ability to form a half chairlike conformation.²⁰

DAB (**3**) has been found to display inhibition of various types of α -glucosidases.²¹ However, it has been shown that selectivity for other glycosidases can be achieved upon chemical modifications.²² Thus, as part of our ongoing research on sugar hydrazide imides,²³ we wanted to investigate whether the insertion of a hydrazide imide moiety into DAB to obtain arabinohydrazide imides **4** and **5** would have any impact on the inhibition profile as was the case when isofagomine (**1**) was converted into its corresponding amidine **2**. In this paper, we present the synthesis of **4**, **5**, and **6** and DFT calculations shedding light on their charge distribution, in addition to their glycosidase inhibitory activity.

RESULTS AND DISCUSSION

The synthesis of hydrazide imides **4Cl** and **5Cl** commenced from 2,3,5-tri-*O*-benzyl-L-xylofuranose (**7**) (Scheme 1), which in turn was obtained from L-xylose in three steps by following reported procedures.²⁴ Thus, by following a protocol reported by Ermert and Vasella for the synthesis of 2,3,4,6-tetra-

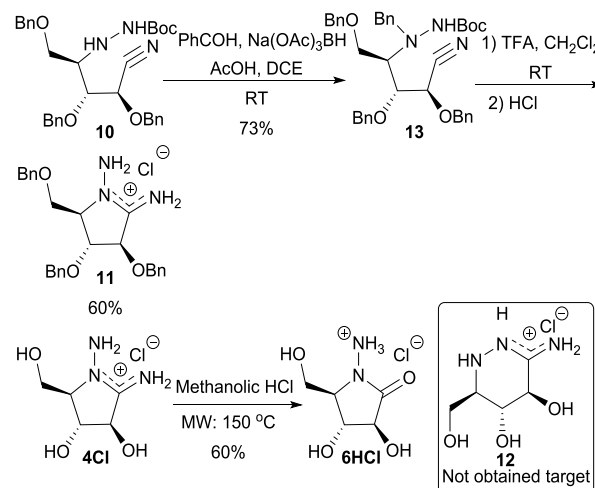
Scheme 1. Synthesis of D-Arabinohydrazide Imides 4Cl and 5Cl



benzyl-D-glucononitrile,²⁵ condensation of **7** with hydroxyl amine to provide an aldoxime intermediate followed by dehydration under Appel conditions provided nitrile **9** in 52% yield along with known L-xylofuranose **8**.²⁶ In the subsequent step, compound **9** underwent stereospecific hydrazidation into hydrazide **10** in 54% yield involving triflation of the free hydroxyl group on C4 followed by treatment with Boc-hydrazide. TFA-promoted removal of the Boc-protective group activated the cyclization into hydrazide imide **11** after treatment with HCl. The benzyl protective groups were removed by palladium-catalyzed hydrogenation in EtOH/TFA to provide hydrazide imide **4Cl** after counterion exchange with HCl. In order to exclude any unexpected epimerization in the synthesis of **4Cl**, a NOESY experiment was conducted, which showed interaction between the protons in the 2- and 4-position as expected. Interestingly, when the hydrogenation time was extended from 19 to 48 h, the *N*-ethyl hydrazide imide **5Cl** was obtained in 85% yield. Similar *N*-ethylation observations have been made both by Jensen and co-workers²⁷ and Sydnes and Isobe²⁸ when ethanol was employed as a solvent for palladium-catalyzed hydrogenation to remove benzyl groups from iminosugars and to reduce nitrobenzenes, respectively. In the latter case, it was proposed that acetaldehyde was the alkylating agent formed through a β -hydride elimination mechanism, first proposed by Sajiki and co-workers.²⁹

We also attempted to obtain sugar hydrazide imide **12** (Scheme 2), with a six-membered ring system. Thus, the

Scheme 2. Synthesis of Hydrazide 6HCl and Attempted Synthesis of Hydrazide Imide 12



amino group of hydrazide **10** was benzyl-protected into compound **13** upon reductive amination with benzaldehyde and sodium triacetoxyborohydride. Unfortunately, TFA-promoted removal of the Boc-protective group triggered the cyclization into the five-membered ring system **11** and not the six-membered ring as anticipated. We also envisaged that **4Cl** should rearrange into **12** via an imidate intermediate upon treatment with HCl in methanol. However, when **4Cl** was treated with methanolic HCl at elevated temperature, we did not observe any reaction. When we attempted the same reaction in the microwave at 150 $^{\circ}\text{C}$, we realized that **4Cl** underwent hydrolysis into the corresponding hydrazide **6HCl** in 60% yield.

Compounds **4Cl**, **5Cl**, and **6HCl**, in addition to positive reference compounds isofagomine (**1**) and 1-deoxynojirimycin (DNJ), underwent screening as glycosidase inhibitors on a panel of commercial glycosidases including α -glucosidase (*Saccharomyces cerevisiae*), β -glucosidase (almonds), α -galactosidase (green coffee beans), β -galactosidase (*Aspergillus oryzae*), β -galactosidase (*Escherichia coli*), α -mannosidase (jack beans), and β -mannosidase (*Helix pomatia*) (Table 1). The inhibition data demonstrate clearly that the inhibition profile for hydrazone imides **4Cl** and **5Cl** and compound **6HCl** is very different from that of DAB (**3**) with respect to β -glucosidase activity. In contrast to **3**, which behaves as a micromolar inhibitor for β -glucosidase,²² **4Cl**, **5Cl**, and **6HCl** display no or very low inhibition of that enzyme. Comparison of the inhibition profiles for **4Cl** and **5Cl** with isofagomidine (**2**) demonstrates that they are very similar and display competitive inhibition of α -mannosidase down to the submicromolar concentration range ($K_i = 0.23 \mu\text{M}$ for **4Cl**), indicating the profit of a hydrazone imide or amidine moiety for the binding to the enzyme. The only difference in the inhibition profile between hydrazone imides **4Cl** and **5Cl** differing in only one *N*-ethyl group is that the former behaves as a competitive inhibitor for α -glucosidase in the micromolar concentration range. Moreover, alkylation of the exocyclic nitrogen atom furnishes a roughly 6-fold impairment in the activity against α -mannosidase. These data mean that a high degree of selectivity was achieved in both DAB analogues, with a selectivity index ranging from 22 to >400; accordingly, severe side effects derived from the unselective inhibitory profile of many other iminosugars can be avoided. The selectivity toward α -mannosidase inhibition by **4Cl** and **5Cl** is interesting from a medicinal perspective, given that α -mannosidase is a relevant target against tumorigenic processes.³⁰

In order to gain more insight into the different inhibition profile for hydrazone imides **4Cl** and **5Cl** compared to **6HCl**, the charge distribution within the systems **3–6** was calculated employing the Mulliken partitioning scheme as well as by fitting atom-centered point charges to reproduce the molecular electrostatic potential with different schemes (Table 2). Due to the electronic similarities between sugar amidrazones with a pK_a of 8.7 and our hydrazone imides **4** and **5**,³¹ we assumed that they exist in their acidic forms in the calculations since the glycosidase inhibitory testing was performed at $6.8 \geq \text{pH}$ (6.8 for glucosidases and galactosidases and 5.6 for mannosidases). For compounds **4–6**, the atomic charge for N1 varied from essentially zero up to positive values. The functional group charges for $\text{NH}_2\text{1}'$ in **4** and **6** and $\text{NH1}'$ in **5** were less consequent as they varied from negative up to positive values. The most striking difference between hydrazone amides **4** and **5** compared to hydrazone **6** is that **4** and **5** host a positively charged $\text{NH}_2\text{5}$ group in the position in which **6** contains an oxygen (O5) with a negative atomic charge. Thus, the difference in charge distribution between **4** and **5** compared to **6** might be the reason for their different inhibition profiles. In addition, because **4** and **5** possess very similar charge distributions, we propose that the *N*-ethyl group of **5** disrupts its binding to α -glucosidase as **4** binds to the same enzyme in the micromolar concentration range. Another interesting observation was made when **4** and **5** was compared with isofagomidine (**2**),¹⁶ another α -mannosidase selective inhibitor; it was observed that this compound in line with **4** and **5** also possesses an exocyclic NH_2 group ($\text{NH}_2\text{2}$), which hosts a positive functional group charge. Note that the atomic charges

Table 1. Screening of Compounds **4Cl**, **5Cl**, and **6HCl** as Glycosidase Inhibitors

enzyme	compounds						
	4Cl	5Cl	6HCl	3	1	2	DNJ
α -glucosidase (<i>S. cerevisiae</i>)	$\text{IC}_{50} = 6.6 \pm 1.2 \mu\text{M}$ $K_i = 5.0 \pm 1.0 \mu\text{M}$	$\text{IC}_{50} > 100 \mu\text{M}^a$	$\text{IC}_{50} > 100 \mu\text{M}^a$	$\text{IC}_{50} > 100 \mu\text{M}^a$	$\text{IC}_{50} = 32 \pm 8 \mu\text{M}$		$\text{IC}_{50} = 34 \pm 1 \mu\text{M}$
β -glucosidase (almonds)	$\text{IC}_{50} > 100 \mu\text{M}^a$	N.I. ^b	N.I. ^b	$K_i = 35 \pm 42 \mu\text{M}^c$	$\text{IC}_{50} = 0.48 \pm 0.01 \mu\text{M}$	$K_i > 210 \mu\text{M}^d$	$\text{IC}_{50} = 78 \pm 2 \mu\text{M}$
α -galactosidase (green coffee beans)	N.I. ^b	N.I. ^b	N.I. ^b		N.I. ^b	N.I. ^d	N.T. ^e
β -galactosidase (<i>A. oryzae</i>)	N.I. ^b	N.I. ^b	N.I. ^b		N.I. ^b	$K_i = 210 \mu\text{M}^d$	N.I. ^b
β -galactosidase (<i>E. coli</i>)	N.I. ^b	N.I. ^b	N.I. ^b		N.I. ^b	N.I. ^d	N.I. ^b
α -mannosidase (jack beans)	$K_i = 0.23 \pm 0.07 \mu\text{M}$	$K_i = 1.4 \pm 0.4 \mu\text{M}$	N.I. ^b		N.T. ^e	$K_i = 210 \mu\text{M}^d$	N.T. ^e
β -mannosidase (<i>H. pomatia</i>)	N.I. ^b	N.I. ^b	N.I. ^b		N.T. ^e	$K_i = 210 \mu\text{M}^d$	N.T. ^e

^aMaximum inhibitor concentration tested. ^bAt $100 \mu\text{M}$ inhibitor concentration. ^cRef 22. ^dRef 16. ^eNot tested.

Table 2. Calculation of Charge Distribution within 2–6

comp.	N1 ^a /NH ₂ 1 ^b	NH ₂ 1 ^c /NH1 ^d	C5	NH ₂ 5 ^e /O5 ^f
4	+0.16 ^g	−0.01	+0.54	+0.16
	+0.18 ^h	0.00	+0.22	+0.17
	+0.08 ^j	+0.18	+0.27	+0.37
5	+0.07	−0.31	+0.54	+0.10
	−0.05	−0.27	+0.53	+0.10
	+0.23	+0.14	+0.46	+0.36
6	+0.29	−0.12	+0.50	−0.55
	+0.08	−0.08	+0.51	−0.56
	−0.09	+0.29	+0.28	−0.33
3	+0.21		−0.04	
	+0.20		0.09	
	+0.61		−0.40	
2 ^j	−0.1 ⁱ (NH1)		0.5 (C2)	0.1 (NH ₂)

^a4–6. ^b3. ^c4 and 6. ^d5. ^e4 and 5. ^f6. ^gHLY. ^hCHelpG. ⁱMulliken. ^jRef 16. All calculations have been done at the B3LYP/6-311++G(d,p) level of theory (for the geometries optimized at the same level, see the Experimental Section for further technical details).

reported for 2¹⁶ have been computed with the same DFT method but using a smaller basis set for orbital expansion (6-31G) so that a direct comparison with the data from our current study is somewhat hampered.

Based on the calculated charge distributions and the coupling constants between the ring protons in the ¹H NMR spectra, we expect compounds 4Cl and 5Cl to anticipate a ³E conformation (Figure 2). However, the coupling constants

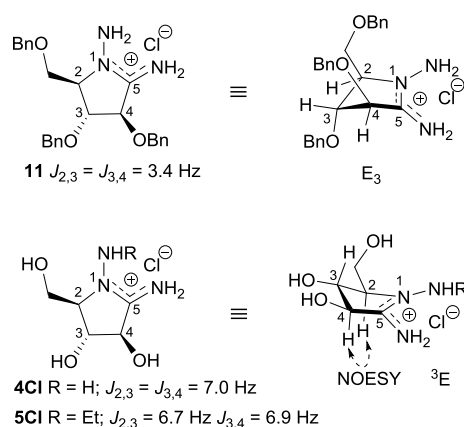


Figure 2. Suggested envelope conformations of compounds 4Cl, 5Cl, and 11.

between the ring protons in the benzyl-protected counterpart 11 are significantly smaller, which could signify an E₃ conformation. A more in-depth study of conformational dependence on charge distribution and spin–spin coupling constants in the present molecular systems is in progress.

CONCLUSIONS

In the work presented herein, we obtained two 1,4-dideoxy-1,4-imino-D-arabinitol (DAB) analogues 4Cl and 5Cl possessing a hydrazide imide. These two compounds behave as selective α -mannosidase inhibitors down to $K_i = 230$ nM. When comparing 4Cl and 5Cl, two observations were made: the *N*-ethyl group of 5Cl slightly impaired the inhibition of α -mannosidase and the same group had a positive influence for the selectivity toward α -mannosidase.

EXPERIMENTAL SECTION

General Information. All chemicals were obtained from Sigma Aldrich/Merck or VWR and used as supplied. When specified, solvents were dried by storing over 4 Å molecular sieves. For petroleum ether (PE), the 40–65 °C fraction was used. All reactions were carried out under a nitrogen or argon atmosphere, unless otherwise specified. TLC analyses were performed on Merck silica gel 60 F254 plates using UV light, KMnO₄, or heat for detection. Silica gel NORMASIL 60 40–63 μ m was used for flash column chromatography. Nuclear magnetic resonance (NMR) spectra were recorded on a Bruker AscendTM 400 series, operating at 400.13 MHz for ¹H and 100.61 MHz for ¹³C in CDCl₃, CD₃OD, D₂O, or DMSO-*d*₆. The assignment of signals in all NMR spectra was assisted by conducting ¹H–¹H correlation spectroscopy, ¹H–¹³C/¹H–¹⁵N heteronuclear single-quantum correlation spectroscopy, and/or ¹H–¹³C/¹H–¹⁵N heteronuclear multiple bond correlation spectroscopy. Chemical shifts (δ) are reported in ppm relative to an internal standard of residual chloroform ($\delta = 7.26$ ppm for ¹H NMR; $\delta = 77.16$ ppm for ¹³C NMR), residual methanol ($\delta = 3.31$ ppm for ¹H NMR; $\delta = 49.00$ ppm for ¹³C NMR), residual dimethyl sulfoxide ($\delta = 2.50$ ppm for ¹H NMR; $\delta = 39.52$ ppm for ¹³C NMR), or residual water ($\delta = 4.79$ ppm for ¹H NMR). Infrared spectroscopy (IR) was performed on a Cary 360 FTIR spectrophotometer. High-resolution mass spectra (HRMS) were recorded from MeOH solutions on a JMS-T100LC AccuTOFTM in positive electrospray ionization (ESI) mode. The microwave-assisted experiments were performed in a CEM Focused Microwave Synthesis System, model type Discover, operating at 0–300 W at a temperature of 118 °C and a pressure range of 0–290 psi, with reactor vial volumes of 10 mL.

2,3,5-Tri-*O*-benzyl-L-xylofuranose (7). Step 1: To a solution of AcCl (0.29 mL, 4 mmol) in MeOH (40 mL) was added L-xylose (3 g, 20 mmol) at rt. The reaction mixture was kept stirring at rt for 5.5 h. The reaction mixture was then cooled to 0 °C, and pH was adjusted to ca. 9 with NaOH (1 M). The solvent was then removed under reduced pressure, and the resulting residue was suspended in toluene (6 \times 10 mL) and concd to dryness. Step 2: The residue from step 1 was dissolved in dry DMF (64 mL), and NaH (4.24 g, 5.3 equiv) was added at rt. The reaction mixture was then cooled to 0 °C prior to addition of BnBr (11.9 mL, 5 equiv). The reaction mixture was stirred at rt for 23 h before being extracted with EtOAc (2 \times 75 mL). The combined extracts were dried over MgSO₄ and concd in vacuo. Step 3: The residue from step 2 was dissolved in dioxane (60 mL) and HCl (60 mL, 4 M) and stirred at 65 °C for 4 days. The reaction mixture was then extracted with EtOAc (2 \times 75 mL), and the combined organic fractions were concentrated and subjected to flash column chromatography (PE/EtOAc, 17:3 \rightarrow 3:1). Collection of the appropriate fractions ($R_f = 0.25$; PE/EtOAc, 3:1) provided compound 7 (4.97 g, 59%) as a clear light-yellow oil. The spectroscopic data were in full accord with the previously reported data.²³

2,3,5-Tri-*O*-benzyl-L-xylonitrile (9). Step 1: To a solution of Na (315 mg, 13.7 mmol) dissolved in absolute EtOH (60 mL) was added NH₂OH·HCl (1.77 g, 27.5 mmol). The reaction mixture was stirred at rt for 5 min before a solution of furanose 7 (1.44 g, 3.42 mmol) in absolute EtOH (11 mL) was added. The resulting reaction mixture was stirred at rt for 1 h before volatiles were removed by reduced pressure. To the

residue were then added water (50 mL) and EtOAc (50 mL). The two phases were separated, and the aq phase was extracted with EtOAc (2 × 50 mL). The combined organic fractions were dried with MgSO₄, filtered, and concentrated in vacuo. The residue ($R_f = 0.4$; PE/EtOAc, 3:2) was dissolved in toluene, concentrated, and used directly in the following step. Step 2: To a solution of PPh₃ (1.89 g, 6.84 mmol, 2 equiv) in MeCN (27 mL) at rt was added the residue from step 1. The reaction mixture was stirred at rt for 20 min before a solution of CBr₄ (2.84 g, 8.55 mmol, 2.5 equiv) in MeCN (11 mL) was added. The reaction mixture was then stirred at rt for 20 min before adding a solution of PPh₃ (472 mg, 1.71 mmol, 0.5 equiv) in a 1:5.5 mixture of MeCN/MeOH (45 mL). The reaction mixture was then stirred for an additional 15 min before the solvent was removed under reduced pressure. The residue was subjected to flash chromatography (silica; PE/EtOAc, 1:0 → 9:1). Collection of the first fraction ($R_f = 0.6$; PE/EtOAc, 3:1) provided lactone **8** (286 mg, 20%) as a clear colorless oil. Collection of the appropriate fractions ($R_f = 0.4$; PE/EtOAc, 3:1) provided nitrile **9** (741 mg, 52%) as a clear colorless oil. $[\alpha]_D^{26.6 \text{ } ^\circ\text{C}} -29$ (c 0.5 in CHCl₃); ¹H NMR (CDCl₃, 400 MHz): $\delta = 7.37\text{--}7.24$ (m, 15 H, Ar-H), 4.88 (d, $J = 11.5$ Hz, 1H, CHPh), 4.82 (d, $J = 11.2$ Hz, 1H, CHPh), 4.60 (d, $J = 11.2$ Hz, 1H, CHPh), 4.55 (d, $J = 11.5$ Hz, 1H, CHPh), 4.45 (d, $J = 1.5$ Hz, 2H, CHPh), 4.43 (d, $J = 6.6$ Hz, 1H, H-2), 4.11 (m, 1H, H-4), 3.88 (dd, $J_{3,4} = 2.9$ Hz, $J_{3,2} = 6.6$ Hz, 1H, H-3), 3.45 (ddd in 1:2:2:1 ratio, $J_{5a,4} = 6.0$ Hz, $J = 9.5$ Hz, $J_{5b,4} = 16.3$ Hz, 2H, H-5), 2.29 (d, $J = 7.2$ Hz, 1H, OH); ¹³C NMR (CDCl₃, 100 MHz): $\delta = 137.7$ (Ar), 137.3 (Ar), 135.7 (Ar), 128.8–128.0 (Ar), 116.8 (CN), 78.1 (C-3), 75.2 (CH₂), 73.4 (CH₂), 73.0 (CH₂), 70.4 (C-5), 69.6 (C-4), 69.3 (C-2). IR (ATR, cm⁻¹): 3470, 3065, 3032, 2920, 2870, 1955, 1882, 1812, 1554, 1497, 1455, 1398, 1353, 1250, 1210, 1096, 1028, 1002, 913, 821, 738; HRMS (ESI): m/z [M + Na]⁺ calcd for C₂₆H₂₇O₄NNa, 440.1832; found, 440.1827. Data for **8**: ¹H NMR (CDCl₃, 400 MHz): $\delta = 7.36\text{--}7.25$ (m, 15H), 5.05 (d, $J = 11.5$ Hz, 1H), 4.60–4.50 (m, 5H), 4.37 (t, $J = 7.1$ Hz, 1H), 3.77 (dd, $J = 2.9$ Hz, $J = 10.8$ Hz, 1H), 3.71 (dd, $J = 3.2$ Hz, $J = 10.8$ Hz, 1H). ¹³C NMR (CDCl₃, 100 MHz): $\delta = 173.5$, 137.8, 137.4, 137.2, 128.7–127.7, 79.5, 77.4 (2 × C), 73.8, 72.8, 72.7, 67.3. The spectroscopic data for compound **8** were in full accord with the previously reported data.²⁶

2,3,5-Tri-O-benzyl-4-(2-tert-butoxycarbonyl)hydrazinyl-4-deoxy-D-arabinonitrile (10). Step 1: To a solution of alcohol **9** (200 mg, 0.48 mmol) in DCM (4 mL) at 0 °C was added pyridine (0.1 mL, 1.24 mmol, 2.6 equiv). The mixture was stirred for 10 min prior to dropwise addition of triflic anhydride (0.1 mL, 0.60 mmol, 1.25 equiv). The reaction mixture was further stirred at 0 °C for 15 min before being diluted with DCM (20 mL), washed with cold HCl (10 mL, 1 M) and saturated aq NaHCO₃ (12 mL), dried over MgSO₄, and filtered. The residue ($R_f = 0.71$; PE/EtOAc, 7:3) was concentrated under reduced pressure and used directly in the following step. Step 2: To a solution of the triflate from step 1 in THF (1.5 mL) at 0 °C was added *tert*-butylcarbazate (320 mg, 2.42 mmol, 5 equiv). The reaction mixture was stirred at rt for 44 h before volatiles were removed under reduced pressure. The residue was subjected to flash column chromatography (PE/EtOAc, 95:5 → 9:1). Collection of the appropriate fractions ($R_f = 0.28$; PE/EtOAc, 9:1) provided hydrazide **10** (138 mg, 54%) as a clear white oil. ¹H NMR (CDCl₃, 400 MHz): $\delta = 7.36\text{--}7.28$ (m, 15H), 5.77 (brs, 1H, NH), 4.88 (d, $J = 11.5$ Hz, 1H, CHPh), 4.84 (d, $J = 11.1$ Hz, 1H, CHPh),

4.73 (d, $J_{2,3} = 3.7$ Hz, 1H, H-2), 4.64 (d, $J = 11.1$ Hz, 1H, CHPh), 4.57 (d, $J = 11.5$ Hz, 1H, CHPh), 4.52 (d, $J = 11.8$ Hz, 1H, CHPh), 4.45 (d, $J = 11.8$ Hz, 1H, CHPh), 3.82 (dd, $J_{2,3} = 3.7$ Hz, $J_{3,4} = 7.0$ Hz, 1H, H-3), 3.71 (dd, $J_{5a,4} = 4.4$ Hz, $J_{5a,5b} = 9.7$ Hz, 1H, H-5a), 3.60 (dd, $J_{5b,4} = 5.7$ Hz, $J_{5b,5a} = 9.7$ Hz, 1H, H-5b), 3.27 (ddd, $J_{4,5a} = 4.4$ Hz, $J_{4,5b} = 5.7$ Hz, $J_{4,3} = 7.0$ Hz, 1H, H-4), 1.44 (s, 9H); ¹³C NMR (CDCl₃, 100 MHz): $\delta = 156.7$ (C=O), 137.9 (Ar), 137.5 (Ar), 136.0 (Ar), 128.8–128.0 (Ar), 117.8 (CN), 80.6 (C(CH₃)₃), 78.1 (C-3), 74.9 (CH₂), 73.5 (CH₂), 72.9 (CH₂), 68.3 (C-2), 67.8 (C-5), 60.5 (C-4), 28.4 (CH₃); IR (ATR, cm⁻¹): 3339, 3014, 2979, 2929, 2870, 1718, 1497, 1454, 1393, 1367, 1249, 1216, 1157, 1088, 1073, 1028; HRMS (ESI): m/z [M + H]⁺ calcd for C₃₁H₃₈O₅N₃, 532.2806; found, 532.2802.

(2R,3R,4R)-1-Amino-3,4-bis(benzyloxy)-2-((benzyloxy)methyl)-5-iminopyrrolidin Hydrochloride (11). To a solution of nitrile **10** (140 mg, 0.26 mmol) in DCM (10 mL) at rt was added TFA (2 mL) dropwise. The reaction mixture was stirred at rt for 3 h before toluene was added, and the volatiles were removed in vacuo. The residue was then purified by flash column chromatography (DCM/MeOH (0.1 M HCl), 94:6). Collection of the appropriate fractions ($R_f = 0.35$; DCM/MeOH (0.1 M HCl), 9:1) provided the title compound (98.3 mg, 88%) as a clear colorless oil. $[\alpha]_D^{27.2 \text{ } ^\circ\text{C}} -11$ (c 0.20 in MeOH); ¹H NMR (MeOD, 400 MHz): $\delta = 7.34\text{--}7.25$ (m, 15H, ArH), 4.82 (d, $J_{4,3} = 3.9$ Hz, 1H, H-4), 4.73 (d, $J = 11.5$ Hz, 1H, CHPh), 4.63 (d, $J = 11.5$ Hz, 1H, CHPh), 5.59 (d, $J = 11.8$ Hz, 1H, CHPh), 4.48 (bs, 2H, CHPh), 4.47 (d, $J = 11.8$ Hz, 1H, CHPh), 4.25 (t, $J = 3.9$ Hz, 1H, H-3), 3.96 (m, 1H, H-2), 3.89 (dd, $J_{\text{CHaOH},2} = 3.4$ Hz, $J_{\text{CHaOH},\text{CHbOH}} = 10.9$ Hz, 1H, CHaOH), 3.63 (dd, $J_{\text{CHbOH},2} = 3.2$ Hz, $J_{\text{CHbOH},\text{CHaOH}} = 10.9$ Hz, 1H, CHbOH); ¹³C NMR (MeOD, 100 MHz): $\delta = 166.7$ (C=N), 138.9 (Ar), 138.4 (Ar), 138.1 (Ar), 129.6–129.1 (Ar), 82.3 (C-4), 79.6 (C-3), 74.2 (CH₂), 74.0 (CH₂), 73.3 (CH₂), 71.0 (C-2), 66.3 (CH₂OH); IR (ATR, cm⁻¹): 3029, 2929, 2110, 1953, 1882, 1811, 1702, 1624, 1495, 1453, 1362, 1261, 1209, 1121, 1099, 1063, 1028, 971, 915; HRMS (ESI): m/z [M + H]⁺ calcd for C₂₆H₃₀O₃N₃, 432.2282; found, 432.2276.

(2R,3R,4R)-1-Amino-3,4-dihydroxy-2-(hydroxymethyl)-5-iminopyrrolidine Hydrochloride (4C1). A degassed suspension of per-*O*-benzylated hydrazide imide **11** (98 mg, 0.23 mmol) and Pd/C (280 mg) in EtOH/TFA (10 mL, 9:1) was hydrogenated at 1 atm at rt for 19 h. The reaction mixture was then filtered through Celite and washed with EtOH before the filtrate was concentrated in vacuo. The residue was dissolved in methanolic HCl (0.5 M) and evaporated to dryness to afford the HCl salt. The salt residue was purified by flash column chromatography (MeCN/H₂O, 92:8). Collection of the appropriate fractions ($R_f = 0.42$; MeCN/H₂O (0.1 M HCl), 85:15) provided pyrrolidine **4C1** (40 mg, 90%) as a yellow solid; mp 156.0–156.2 °C (decomposes); $[\alpha]_D^{27.2 \text{ } ^\circ\text{C}} -5.7$ (c 0.35 in MeOH); ¹H NMR (D₂O, 400 MHz): $\delta = 4.83$ (d, $J_{4,3} = 7.0$ Hz, 1H, H-4), 4.27 (t, $J = 7.0$ Hz, 1H, H-3), 4.13 (dd, $J_{\text{CHaOH},2} = 2.6$ Hz, $J_{\text{CHaOH},\text{CHbOH}} = 13.3$ Hz, 1H, CHaOH), 3.87 (dd, $J_{\text{CHbOH},2} = 2.5$ Hz, $J_{\text{CHbOH},\text{CHaOH}} = 13.3$ Hz, 1H, H-6b), 3.72 (app. dt, $J_{2,\text{CHOH}} = 2.5$ Hz, $J_{2,3} = 7.0$ Hz, 1H, H-2); ¹³C NMR (D₂O, 100 MHz): $\delta = 167.4$ (C=N), 74.1 (C-4), 72.7 (C-3), 68.7 (C-2), 55.5 (CH₂OH). IR (ATR, cm⁻¹): 3369, 2125, 1724, 1624, 1205, 1109, 1063 cm⁻¹; HRMS (ESI): m/z [M + H]⁺ calcd for C₅H₁₂O₃N₃, 162.0873; found, 162.0871.

(2R,3R,4R)-1-(Ethylamino)-3,4-dihydroxy-2-(hydroxymethyl)-5-iminopyrrolidine Hydrochloride (5C1). A degassed

suspension of pyrrolidine **11** (95 mg, 0.20 mmol) and Pd/C (235 mg) in EtOH/TFA (2 mL, 9:1) was hydrogenated at 1 atm at rt for 48 h. The reaction mixture was then filtered through Celite and washed with EtOH before the filtrate was concentrated in vacuo. The residue was dissolved in methanolic HCl (0.5 M) and evaporated to dryness to afford the HCl salt. The salt residue was purified by flash column chromatography (MeCN/H₂O, 88:12). Collection of the appropriate fractions ($R_f = 0.44$; MeCN/H₂O, 9:1) provided the title compound (39 mg, 85%) as a yellow solid; mp 130.2–130.4 °C (decomposes); $[\alpha]_D^{25.2}$ °C + 12.0 (c 0.17 in MeOH) ¹H NMR (D₂O, 400 MHz): $\delta = 4.90$ (d, $J_{4,3} = 6.9$ Hz, 1H, H-4), 4.31 (app. t, $J = 6.8$ Hz, 1H, H-3), 4.07 (dd, $J_{\text{CHaOH},6b} = 13.0$ Hz, $J_{\text{CHbOH},2} = 2.6$ Hz, 1H, CHaOH), 4.03 (dt, $J_{2,3} = 6.7$ Hz, $J_{2,\text{CHbOH}} = 2.7$ Hz, $J_{2,\text{CHaOH}} = 2.6$ Hz, 1H, H-2), 3.90 (dd, $J_{\text{CHbOH},\text{CHaOH}} = 13.0$ Hz, $J_{\text{CHbOH},2} = 2.7$ Hz, 1H, CHbOH), 3.04 (dq, $J_{1'a,1'b} = 11.7$ Hz, $J_{1'a,2'} = 7.3$ Hz, 1H, H-1'a), 2.91 (dq, $J_{1'b,1'a} = 11.7$ Hz, $J_{1'b,2'} = 7.1$ Hz, 1H, H-1'b), 1.09 (app. t, $J = 7.2$ Hz, 3H, H-2'); ¹³C NMR (D₂O, 100 MHz): $\delta = 167.9$ (C=N), 73.9 (C-4), 73.0 (C-3), 64.8 (C-2), 56.0 (CH₂OH), 42.0 (C-7), 11.8 (C-8); IR (ATR, cm⁻¹): 3215, 2977, 2934, 2878, 2110, 1702, 1637, 1454, 1383, 1332, 1276, 1201, 1103, 1063, 905; HRMS (ESI): m/z [M + H]⁺ calcd for C₇H₁₆O₃N₃, 190.1186; found, 190.1184.

(3S,4R,5R)-1-Amino-3,4-dihydroxy-5-(hydroxymethyl)-2-pyrrolidinone Hydrochloride (6HCl). A solution of pyrrolidine **4Cl** (8 mg, 0.04 mmol) in MeOH (0.05 M HCl, 1 mL) was subjected to microwave radiation (150 °C) for 90 min. The reaction mixture was then cooled to ambient temperature before volatiles were removed by reduced pressure. The residue was evaporated to dryness to afford the HCl salt. The salt residue was subjected to gravity column chromatography (MeCN/H₂O, 98:2). Collection of the appropriate fractions ($R_f = 0.41$; MeCN/H₂O, 85:15) provided hydrazide amide **6HCl** (4.7 mg, 60%) as a white wax. $[\alpha]_D^{25.5}$ °C - 5.1 (c 0.39 in MeOH); ¹H NMR (D₂O, 400 MHz): $\delta = 4.31$ (d, $J_{4,3} = 7.1$ Hz, 1H, H-3), 4.10 (t, $J = 7.1$ Hz, 1H, H-4), 4.05 (dd, $J_{\text{CHaOH},2} = 2.7$ Hz, $J_{\text{CHaOH},\text{CHbOH}} = 12.9$ Hz, 1H, CHaOH), 3.79 (dd, $J_{\text{CHbOH},2} = 2.5$ Hz, $J_{\text{CHbOH},\text{CHaOH}} = 12.9$ Hz, 1H, CHbOH), 3.47 (m, 1H, H-5); ¹³C NMR (D₂O, 100 MHz): $\delta = 172.5$ (C=O), 75.2 (C-3), 72.3 (C-4), 65.3 (C-5), 57.2 (CH₂OH); IR (ATR, cm⁻¹): 3295, 2926, 2855, 2358, 1699, 1455, 1349, 1261, 1200, 1095, 909. LRMS (ESI): m/z [M + H]⁺ calcd for C₅H₁₁O₄N₂, 163.0719; found, 163.0721.

2,3,5-Tri-O-benzyl-4-(1-N-benzyl-(2-tert-butoxycarbonyl)-hydrazinyl)-4-deoxy-D-arabinonitrile (13). To a solution of compound **10** (104 mg, 0.20 mmol) in DCE was added Na(OAc)₃BH (116 mg, 2.7 equiv) followed by benzaldehyde (0.04 mL, 2.0 equiv) and AcOH (0.07 mL, 6.2 equiv). The reaction mixture was stirred at rt for 18 h. The reaction mixture was then quenched with saturated aq NaHCO₃ (5 mL), and EtOAc (10 mL) was added. The two phases were separated, and the aq phase was extracted with EtOAc (2 × 10 mL). The combined organic fractions were evaporated to dryness in vacuo. Excess of benzaldehyde was removed under vacuum at 60 °C for 1 h. The residue was purified by flash column chromatography (PE/EtOAc, 9:1). Collection of the appropriate fractions ($R_f = 0.25$; PE/EtOAc, 9:1) provided compound **13** (89 mg, 73%) as a light-yellow oil. ¹H NMR (CDCl₃, 400 MHz): $\delta = 7.41$ –6.96 (m, 20H, ArH), 6.28 and 5.84 (br.s, 1.4:1, 1H, NH), 5.52 and 5.22 (br.s, 1.5:1, 1H, H-2), 4.98 (d, $J = 10.9$ Hz, 1H, CHPh), 4.84 (d, $J = 10.3$ Hz, 1H, CHPh), 4.60 (d, $J = 10.8$ Hz, 1H, CHPh), 4.58 (d, $J = 10.3$ Hz,

1H, CHPh), 4.49 (d, $J = 11.2$ Hz, 2H, 2CHPh), 4.00–3.68 (m, 5H, 2CHPh, H-5a, H-5b, H-3), 3.34 (brs, 1H, H-4), 1.32–1.24 (m, 9H); ¹³C NMR (CDCl₃, 100 MHz): $\delta = 155.9$ (C=O), 137.8–136.1 (Ar), 130.0–127.5 (Ar), 118.9–118.6 (CN), 80.8 and 80.0 (C), 78.4 (C-3), 75.2 and 74.9 (CH₂), 73.8 and 73.6 (CH₂), 73.2 and 72.8 (CH₂), 67.6 and 66.7 (C-2), 67.0 (CH₂), 63.6 and 61.9 (C-5), 61.6 and 60.7 (C-4), 28.3 and 28.1 (CH₃); IR (ATR, cm⁻¹): 3355, 3031, 2925, 2866, 1950, 1725, 1706, 1496, 1454, 1392, 1243, 1160, 1124, 1072, 1027, 913; HRMS (ESI): m/z [M + Na]⁺ calcd for C₃₈H₄₃O₅N₃Na, 644.3095; found, 644.3088.

Glycosidase Inhibition Assays. Inhibition assays for glycosidases were accomplished using the methodology reported by Bols and co-workers.³² The percentage of inhibition was measured by preparing two 1.2 mL samples in PS cuvettes containing 0.1 M phosphate buffer (pH 6.8 or 5.6 for mannosidases) and the corresponding *o*- or *p*-nitrophenyl-glycopyranoside at a concentration equal to the expected value of K_M : [S] = 0.25 mM for α -glucosidase, 4.0 mM for β -glucosidase; 0.60 mM for α -galactosidase, 0.51 mM for β -galactosidase (*E. coli*), 1.5 mM for β -galactosidase (*A. oryzae*), 0.90 mM for α -mannosidase, and 0.58 mM for β -mannosidase. DMSO (control) or inhibitor solution (DMSO) plus water was added up to a constant volume of 1.14 mL. Screenings were conducted using a 100 μ M final inhibitor concentration.

Reactions were started by adding 60 μ L of properly diluted enzyme solution at 25 \pm 0.1 °C or 35 \pm 0.1 °C (for mannosidases), and the formation of the corresponding *o*- or *p*-nitrophenolate was monitored for 125 s by measuring the increase in absorbance at 400 nm (glucosidases and α -galactosidase) or 420 nm (β -galactosidases) for 125 s. For α - and β -mannosidases, an aliquot (200 μ L) was taken every 60 s and added to a 1 M Na₂CO₃ solution (1.8 mL), and the absorbance was measured at 400 nm over a period of 4 min.

Initial rates (slopes of the plots Abs vs t) were used for calculating %I, according to the following expression:

$$\% \text{ inhibition} = \frac{v_0 - v}{v_0} \times 100$$

where v_0 is the reaction rate for the enzyme solution and v is the reaction rate for the reactions incorporating an inhibitor.

DMSO concentration was maintained at 5% (v/v) of the total assay mixture for glycosidases.

The inhibitory constants (K_i) were determined using five different substrate concentrations, ranging from 0.25 to 4.0 K_M at a fixed inhibitor concentration (two to three different inhibitor concentrations). The mode of inhibition was determined using the Cornish-Bowden method,³³ which involves the use of two different plots: $1/v$ vs $[I]$ (Dixon plot) and $[S]/v$ vs $[I]$. For the calculation of kinetic parameters (K_M , V_{max}), a nonlinear regression analysis (least-squares fit) was used.

Compounds **4Cl** and **5Cl** turned out to be competitive inhibitors (binding only to the free enzyme), and the corresponding inhibition constants (K_i) were calculated using the following equation:

$$K_{ia} = \frac{[I]}{\frac{K_{Mapp}}{K_M} - 1}$$

Computational Details. Geometries of the investigated molecular systems were optimized with Schlegel's gradient optimization algorithm.³⁴ Subsequent to geometry optimiza-

tion, the second derivative Hessian matrices were evaluated analytically for the located stationary points on the explored potential energy surfaces (PESs). The absence of negative eigenvalues of the Hessians (and consequently, imaginary harmonic vibrational frequencies) indicated that true minima have been located.

Throughout the study, the hybrid HF-DFT approach was implemented, using the combination of three-parameter adiabatic connection exchange functional constructed by Becke (B3)³⁵ with the Lee–Yang–Parr correlation functional (LYP;³⁶ B3-LYP). The Pople-style triple-zeta quality 6-311++G(*d,p*) basis set was used for orbital expansion. Numerical integration was performed using a pruned “ultrafine” (99,590) grid, constituted by 99 radial shells and 590 angular points per shell.

Charge distribution for the structure corresponding to the located minima on the studied PESs was investigated employing a variety of methods for computation/assignment of atomic charges. Aside from the widely used Mulliken partitioning scheme and the Weinhold’s natural population analysis,³⁷ also several electrostatic potential-based (ESP) schemes were employed.^{38–41} The ESP schemes are based on computation of molecular ESP from the DFT density (which is an exact procedure) followed by assignment of charges to atomic centers within the molecule, such as reproducing the exactly computed ESP at series of chosen points. The second segment of the overall task is a fitting procedure. As the ESP fit does not lead to a unique solution of the problem (neither does any of the algorithms for charge assignments), we have used many different algorithms for choosing the set of points for fitting the charges (MK, CHelp, CHelpG, etc.; see the results in Table 2 within the main text). This was done in order to get a wider overview of the performances of different methods. We have also focused on trends throughout the series of investigated compounds instead of the absolute values of the charges.

■ ASSOCIATED CONTENT

Supporting Information

The Supporting Information is available free of charge at <https://pubs.acs.org/doi/10.1021/acsomega.0c02466>.

¹H NMR, ¹³C NMR, and IR spectra of synthesized compounds (PDF)

■ AUTHOR INFORMATION

Corresponding Authors

Emil Lindbäck – Department of Chemistry, Bioscience and Environmental Engineering, Faculty of Science and Technology, University of Stavanger, 4036 Stavanger, Norway;
Email: emil.lindback@uis.no

Magne O. Sydnes – Department of Chemistry, Bioscience and Environmental Engineering, Faculty of Science and Technology, University of Stavanger, 4036 Stavanger, Norway;
orcid.org/0000-0001-9413-6969;
Email: magne.o.sydnes@uis.no

Authors

Marianne B. Haarr – Department of Chemistry, Bioscience and Environmental Engineering, Faculty of Science and Technology, University of Stavanger, 4036 Stavanger, Norway
Óscar López – Departamento de Química Orgánica, Facultad De Química, Universidad de Sevilla, 41012 Sevilla, Spain

Ljupcho Pejov – Department of Chemistry, Bioscience and Environmental Engineering, Faculty of Science and Technology, University of Stavanger, 4036 Stavanger, Norway

José G. Fernández-Bolaños – Departamento de Química Orgánica, Facultad De Química, Universidad de Sevilla, 41012 Sevilla, Spain; orcid.org/0000-0003-1499-0650

Complete contact information is available at:
<https://pubs.acs.org/doi/10.1021/acsomega.0c02466>

Notes

The authors declare no competing financial interest.

■ ACKNOWLEDGMENTS

We thank the ToppForsk program at the University of Stavanger, Dirección General de Investigación of Spain (CTQ2016-78703-P), Junta de Andalucía (FQM134), and FEDER (501100008530) for financial support. COST Action Multi-target paradigm for innovative ligand identification in the drug discovery process (MuTaLig) (CA15135) is also acknowledged (Ó.L. and M.O.S.).

■ REFERENCES

- (1) Gloster, T. M.; Davies, G. J. Glycosidase inhibition: assessing mimicry of the transition state. *Org. Biomol. Chem.* **2010**, *8*, 305–320.
- (2) Asano, N. Glycosidase inhibitors: update and perspectives on practical use. *Glycobiology* **2003**, *13*, 93R–104R.
- (3) Stütz, A. E.; Wrodnigg, T. M. Imino sugars and glycosyl hydrolases. *Adv. Carbohydr. Chem. Biochem.* **2011**, *66*, 187–298.
- (4) Sugimoto, S.; Nakajima, H.; Kosaka, K.; Hosoi, H. Review: Miglitol has potential as a therapeutic drug against obesity. *Nutr. Metab.* **2015**, *12*, 51.
- (5) Stirnemann, J.; Belmatoug, N.; Camou, F.; Serratrice, C.; Froissart, R.; Caillaud, C.; Levade, T.; Astudillo, L.; Serratrice, J.; Brassier, A.; Rose, C.; Billette de Villemeur, T.; Berger, M. A review of Gaucher disease pathophysiology, clinical presentation and treatments. *Int. J. Mol. Sci.* **2017**, *18*, E441.
- (6) Sunder-Plassmann, G.; Schiffmann, R.; Nicholls, K. Migalstat for the treatment of Fabry disease. *Expert Opin. Orphan Drugs* **2018**, *6*, 301–309.
- (7) Asano, N.; Nash, R. J.; Molyneux, R. J.; Fleet, G. W. J. Sugar-mimic glycosidase inhibitors: natural occurrence, biological activity and prospects for therapeutic application. *Tetrahedron: Asymmetry* **2000**, *11*, 1645–1680.
- (8) Kiappes, J. L.; Hill, M. L.; Alonzi, D. S.; Miller, J. L.; Iwaki, R.; Sayce, A. C.; Caputo, A. T.; Kato, A.; Zitzmann, N. ToP-DNJ, a selective inhibitor of endoplasmic reticulum α -glucosidase II exhibiting antiviral activity. *ACS Chem. Biol.* **2017**, *13*, 60–65.
- (9) (a) Asano, N. Naturally occurring iminosugars and related compounds: structure, distribution, and biological activity. *Curr. Top. Med. Chem.* **2003**, *3*, 471–484. (b) Dehoux-Baudoin, C.; Génisson, Y. C-Branched Imino sugars: Synthesis and biological relevance. *Eur. J. Org. Chem.* **2019**, 4765–4777.
- (10) Heightman, T. D.; Vasella, A. T. Recent insights into inhibition, structure, and mechanism of configuration-retaining glycosidases. *Angew. Chem. Int. Ed.* **1999**, *38*, 750–770.
- (11) (a) Lillelund, V. H.; Jensen, H. H.; Liang, X.; Bols, M. Recent developments of transition-state analogue glycosidase inhibitors of non-natural product origin. *Chem. Rev.* **2002**, *102*, 515–554. (b) Stütz, A. E.; Wrodnigg, T. M. Positive attitude, shape, flexibility, added-value accessories or “just being different”: how to attract a glycosidase. *Carbohydr. Chem.* **2013**, *39*, 120–149.
- (12) Jespersen, T. M.; Dong, W.; Sierks, M. R.; Skrydstrup, T.; Lundt, I.; Bols, M. Isofagomine, a potent, new glycosidase inhibitor. *Angew. Chem., Int. Ed. Engl.* **1994**, *33*, 1778–1779.
- (13) Varrot, A.; Tarling, C. A.; Macdonald, J. M.; Stick, R. V.; Zechel, D. L.; Withers, S. G.; Davies, G. J. Direct observation of the

protonation state of an imino sugar glycosidase inhibitor upon binding. *J. Am. Chem. Soc.* **2003**, *125*, 7496–7497.

(14) Tong, M. K.; Papandreou, G.; Ganem, B. Potent, broad-spectrum inhibition of glycosidases by an amidine derivative of D-glucose. *J. Am. Chem. Soc.* **1990**, *112*, 6137–6139.

(15) Whitworth, G. E.; Macauley, M. S.; Stubbs, K. A.; Dennis, R. J.; Taylor, E. J.; Davies, G. J.; Greig, I. R.; Vocadlo, D. J. Analysis of PUGNAc and NAG-thiazoline as Transition State Analogues for Human O-GlcNAcase: Mechanistic and Structural Insights into Inhibitor Selectivity and Transition State Poise. *J. Am. Chem. Soc.* **2007**, *129*, 635–644.

(16) Lindbäck, E.; López, Ó.; Fernández-Bolaños, J. G.; Sauer, S. P. A.; Bols, M. An isofagomine analogue with an amidine at the pseudoanomeric position. *Org. Lett.* **2011**, *13*, 2908–2911.

(17) Gnanesh Kumar, B. S.; Pohlentz, G.; Schulte, M.; Mormann, M.; Siva Kumar, N. Jack bean α -mannosidase: Amino acid sequencing and N-glycosylation analysis of a valuable glycomics tool. *Glycobiology* **2014**, *24*, 252–261.

(18) (a) Bols, M.; López, Ó.; Ortega-Caballero, F. Glycosidase inhibitors: structure, activity, synthesis, and medical relevance. in *Comprehensive Glycoscience-From Chemistry to Systems Biology*; Kamerling, J. P. (Ed), Elsevier: 2007, pp. 815–884. (b) López, O.; Merino-Montiel, P.; Martos, S.; González-Benjumea, A. Glycosidase inhibitors: versatile tools in glycobiology. in *Carbohydrate Chemistry-Chemical and Biological Approaches*; Rauter, A. P.; Lindhorst, T. K. (Eds), RSC: 2012, Vol. 38, pp. 215–262.

(19) Suzuki, K.; Nakahara, T.; Kanie, O. 3,4-Dihydropyridine as glycosidase inhibitor. *Curr. Top. Med. Chem.* **2009**, *9*, 34–57.

(20) (a) Liu, K. K.-C.; Kajimoto, T.; Chen, L.; Zhong, Z.; Ichikawa, Y.; Wong, C.-H. Use of dihydroxyacetone phosphate-dependent aldolases in the synthesis of deoxy aza sugars. *J. Org. Chem.* **1991**, *56*, 6280–6289. (b) Wong, C.-H.; Provencher, L.; Porco, J. A.; Jung, S.-H.; Wang, Y.-F.; Chen, L.; Wang, R.; Steensma, D. H. Synthesis and evaluation of homoaza sugars as glycosidase inhibitors. *J. Org. Chem.* **1995**, *60*, 1492–1501.

(21) Garrabou, X.; Gómez, L.; Joglar, J.; Gil, S.; Parella, T.; Bujons, J.; Clapés, P. Structure-Guided Minimalist Redesign of the L-fuculose-1-phosphate aldolase active site: Expedient synthesis of novel polyhydroxylated pyrrolizidines and their inhibitory properties against glycosidases and intestinal disaccharidases. *Chem. – Eur. J.* **2010**, *16*, 10691–10706.

(22) Mena-Barragán, T.; García-Moreno, M. I.; Nanba, E.; Higaki, K.; Concia, A. L.; Clapés, P.; García Fernández, J. M.; Ortiz Mellet, C. Inhibitor versus chaperone behaviour of d-fagomine, DAB and LAB sp2-iminosugar conjugates against glycosidases: A structure–activity relationship study in Gaucher fibroblasts. *Eur. J. Med. Chem.* **2016**, *121*, 880–891.

(23) Lindbäck, E.; López, Ó.; Tobiesen, Å.; Fernández-Bolaños, J. G.; Sydnes, M. O. Sugar hydrazide imides: a new family of glycosidase inhibitors. *Org. Biomol. Chem.* **2017**, *15*, 8709–8712.

(24) Santos Evangelista, T. C.; López, Ó.; Sydnes, M. O.; Fernández-Bolaños, J. G.; Baptista Ferreira, S.; Lindbäck, E. Bicyclic 1-azafagomine derivatives: synthesis and glycosidase inhibitory testing. *Synthesis* **2019**, *51*, 4066–4077.

(25) Ermert, P.; Vasella, A. Synthesis of a glucose-derived tetrazole as a new β -glucosidase inhibitor: A new synthesis of 1-deoxyojirmycin. *Helv. Chim. Acta* **1991**, *74*, 2043–2053.

(26) Meng, Q.; Hesse, M. A new synthesis of (2S,3R,4R)-2-(hydroxymethyl)pyrrolidine-3,4-diol. *Helv. Chim. Acta* **1991**, *74*, 445–450.

(27) Rasmussen, T. S.; Koldsø, H.; Nakagawa, S.; Kato, A.; Schiøtt, B.; Jensen, H. H. Synthesis of uronic-noeurostegine -a potent bacterial β -glucuronidase inhibitor. *Org. Biomol. Chem.* **2011**, *9*, 7807–7813.

(28) Sydnes, M. O.; Isobe, M. One-pot reductive monoalkylation of nitro aryls with hydrogen over Pd/C. *Tetrahedron Lett.* **2008**, *49*, 1199–1202.

(29) Esaki, H.; Ohtaki, R.; Maegawa, T.; Monguchi, Y.; Sajiki, H. Novel Pd/C-catalyzed redox reactions between aliphatic secondary alcohols and ketones under hydrogenation conditions: application to

H-D exchange reaction and the mechanistic study. *J. Org. Chem.* **2007**, *72*, 2143–2150.

(30) Franconetti, A.; López, Ó.; Fernandez-Bolanos, J. G. Carbohydrates: potential sweet tools against cancer. *Curr. Med. Chem.* **2020**, *27*, 1206–1242.

(31) Ganem, B.; Papandreou, G. Mimicking the glucosidase transition state: shape/charge considerations. *J. Am. Chem. Soc.* **1991**, *113*, 8984–8985.

(32) Bols, M.; Hazell, R. G.; Thomsen, I. B. 1-Azafagomine: A hydroxyhexahydropyridazine that potently inhibits enzymatic glycoside cleavage. *Chem. – Eur. J.* **1997**, *3*, 940–947.

(33) Cornish-Bowden, A. A simple graphical method for determining the inhibition constants of mixed, uncompetitive and non-competitive inhibitors. *Biochem. J.* **1974**, *137*, 143.

(34) Bernhard Schegel, H. Optimization of equilibrium geometries and transition structures. *J. Comput. Chem.* **1982**, *3*, 214–218.

(35) Becke, A. D. Becke's three parameter hybrid method using the LYP correlation functional. *J. Chem. Phys.* **1993**, *98*, 5648–5652.

(36) Lee, C.; Yang, W.; Parr, R. G. Development of the Colle-Salvetti correlation-energy formula into a functional of the electron density. *Phys. Rev. B* **1988**, *37*, 785–789.

(37) Foster, J. P.; Weinhold, F. Natural hybrid orbitals. *J. Am. Chem. Soc.* **1980**, *102*, 7211–7218.

(38) Singh, U. C.; Kollman, P. A. An approach to computing electrostatic charges for molecules. *J. Comput. Chem.* **1984**, *5*, 129–145.

(39) Chirlian, L. E.; Francl, M. M. Atomic charges derived from electrostatic potentials: A detailed study. *J. Comput. Chem.* **1987**, *8*, 894–905.

(40) Breneman, C. M.; Wiberg, K. B. Determining atom-centered monopoles from molecular electrostatic potentials. The need for high sampling density in formamide conformational analysis. *J. Comput. Chem.* **1990**, *11*, 361–373.

(41) Hu, H.; Lu, Z.; Yang, W. Fitting molecular electrostatic potentials from quantum mechanical calculations. *J. Chem. Theory Comput* **2007**, *3*, 1004–1013.

Paper II

Synthesis of the Hexahydropyrrolo-[3,2-c]-quinoline Core Structure and Strategies for Further Elaboration to Martinelline, Martinellic Acid, Incargranine B, and Seneciobipyrrolidine



Marianne B. Haarr and Magne O. Sydnes

Molecules **2021**, *26*, 341.

DOI: 10.3390/ molecules26020341

Review

Synthesis of the Hexahydropyrrolo-[3,2-c]-quinoline Core Structure and Strategies for Further Elaboration to Martinelline, Martinellic Acid, Incargranine B, and Seneciobipyrrolidine

Marianne B. Haarr  and Magne O. Sydnes * 

Department of Chemistry, Bioscience and Environmental Engineering, Faculty of Science and Technology, University of Stavanger, NO-4036 Stavanger, Norway; marianne.b.haarr@uis.no

* Correspondence: magne.o.sydnes@uis.no

Abstract: Natural products are rich sources of interesting scaffolds possessing a plethora of biological activity. With the isolation of the martinella alkaloids in 1995, namely martinelline and martinellic acid, the pyrrolo[3,2-c]quinoline scaffold was discovered. Since then, this scaffold has been found in two additional natural products, viz. incargranine B and seneciobipyrrolidine. These natural products have attracted attention from synthetic chemists both due to the interesting scaffold they contain, but also due to the biological activity they possess. This review highlights the synthetic efforts made for the preparation of these alkaloids and formation of analogues with interesting biological activity.

Keywords: natural product synthesis; hexahydropyrrolo-[3,2-c]-quinoline; scaffold; martinelline; martinellic acid; incargranine B; seneciobipyrrolidine



Citation: Haarr, M.B.; Sydnes, M.O. Synthesis of the Hexahydropyrrolo-[3,2-c]-quinoline Core Structure and Strategies for Further Elaboration to Martinelline, Martinellic Acid, Incargranine B, and Seneciobipyrrolidine. *Molecules* **2021**, *26*, 341. <https://doi.org/10.3390/molecules26020341>

Academic Editor: David Barker
Received: 23 December 2020
Accepted: 7 January 2021
Published: 11 January 2021

Publisher's Note: MDPI stays neutral with regard to jurisdictional claims in published maps and institutional affiliations.



Copyright: © 2021 by the authors. Licensee MDPI, Basel, Switzerland. This article is an open access article distributed under the terms and conditions of the Creative Commons Attribution (CC BY) license (<https://creativecommons.org/licenses/by/4.0/>).

1. Introduction

Natural products have been and continue to be an immense source of inspiration for organic chemists looking for challenging synthetic targets to test new synthetic strategies and methodologies [1–9]. In addition, natural products are good sources for discovery of novel scaffolds, which is important inspiration for new structural motifs in medicinal chemistry and eventually for drug discovery [10–12]. As of today, approximately 50% of all drugs approved by the US Food and Drug Administration (FDA) are based on natural products or derived from a natural product scaffold [13–16]. Many natural products are rich in stereocenters and possess a high degree of unsaturated carbon bonds. These properties are highly desirable in the development of pharmaceutically active compounds, since the clinical success of drug candidates directly correlates to their three-dimensional structure [17,18].

One such scaffold comprised of three stereocenters is the hexahydropyrrolo[3,2-c]quinoline scaffold, which was first discovered in the martinella alkaloids in 1995 (Figure 1) by Witherup and co-workers at the Merck laboratories [19]. They isolated martinelline (1) and martinellic acid (2) from the roots of the tropical plants *Martinella iquitosensis* and *Martinella obovata*. In 2016, martinelline (1) was also isolated from the leaves of *Emilia coccinea* (Sims) G Dons originating from Southern Nigeria [20]. The same year, martinellic acid (2) was identified in the Australian cane toad skin *Bufo marinus* [21], as well as in the flowering plant *Elephantopus scaber* [22]. The biological properties displayed by the martinella alkaloids included high binding affinity to bradykinin-, α_1 -adrenergic-, and muscarinic receptors, as well as antimicrobial activity [19]. In fact, the juice from the martinella and emilia plants have been used by South American natives and Nigerians, respectively, to treat eye infections [23,24]. The emilia leaves have also traditionally been used in Southern Nigeria for birth control [20].

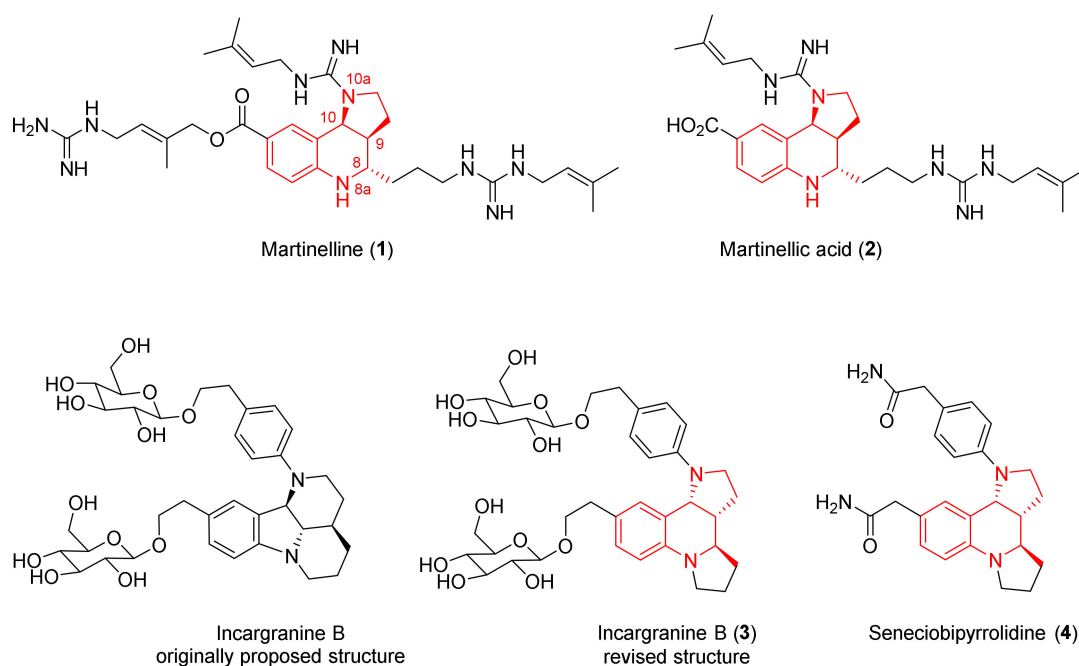


Figure 1. The structure of martinelline (1), martinellic acid (2), incargranine B (3) (originally proposed structure and revised structure), and seneciobipyrrolidine (4). The pyrrolo[3,2-*c*] scaffold is highlighted in red with atom numbering.

Since the discovery of the martinella alkaloids, the partially reduced pyrrolo[3,2-*c*]quinoline scaffold has been found in two additional natural products, namely incargranine B (3) and seneciobipyrrolidine (4) (Figure 1). Incargranine B (3) was isolated from *Incarvillea mairei* var. *grandiflora* by the Zhang group in 2010. They incorrectly identified the alkaloid as comprising an indolo-[1,7]-naphthyridine core structure [25]. The Lawrence group suggested that incargranine B (3) contained a dipyrroloquinoline scaffold after structural revision of the alkaloid [26]. A second dipyrroloquinoline alkaloid was isolated in 2013 from *Senecio scandens* and termed seneciobipyrrolidine (4) [27]. Despite the fact that *Senecio scandens* is a common Chinese herbal medicine used for treatment of a variety of ailments [28], neither of the dipyrroloquinolines have been assessed for biological activity.

All four natural products (1–4) have been isolated with an *exo*-stereochemistry, i.e., a trans-relationship between protons H-8 and H-9 and a cis-relationship between protons H-9 and H-10 (see martinelline (1) in Figure 1). Witherup and co-workers reported optical rotation values of $\alpha = +9.4$ ($c = 0.02$, MeOH) and $\alpha = -8.5$ ($c = 0.01$, MeOH) for martinelline (1) and martinellic acid (2), respectively. From synthetic preparation of the enantiopure alkaloids accompanied by reports of their optical rotation values (Table 1), one may conclude that the isolated compounds consisted of epimeric mixtures [29–32]. After synthetic preparation of incargranine B ((±)3), the Lawrence group also concluded that the aglycon of the isolated alkaloid 3 was a mixture of epimers [26]. No values for optical rotation have been reported for synthetically prepared seneciobipyrrolidine (4). However, the α -value for the isolated seneciobipyrrolidine (4) reported by the Tan group ($\alpha = -72.9$ ($c = 0.10$, MeOH)) may suggest that this alkaloid was of higher enantiopurity than the three other isolated natural products (1–3).

This review will highlight the synthetic efforts made for the preparation of these alkaloids, with particular focus on the assembly of the partially reduced pyrroloquinoline core structure, and formation of analogues with interesting biological activity. The review does not include synthetic approaches towards the structurally related hexahydroindolo-[3,2-*c*]quinoline or the hexahydropyrrolo-[3,4-*c*]pyrrole structures. Synthetic routes towards the martinella alkaloids have been reviewed in 2004 by Nyerges and in 2008 by Lovely and Bararinarayana [33,34]. Since 2008, new approaches towards the alkaloids have emerged,

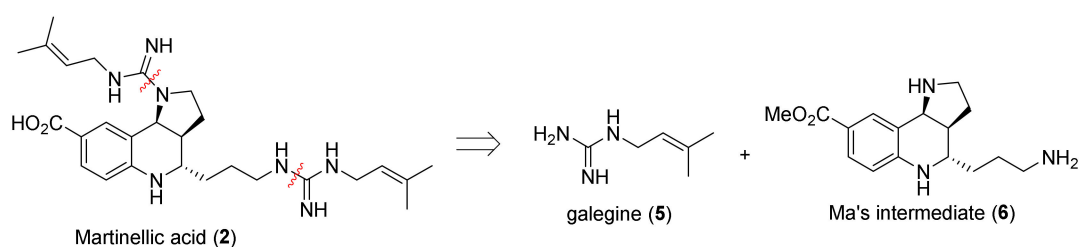
and medicinal applications of this core structure have been developed. Apart from specific prerequisite information, this review will not cover literature prior to the review in 2008.

Table 1. Reported optical rotation for the isolated and synthetically prepared natural products martinelline (1), martinelic acid (2), incargranine B (3), and seneciobipyrrolidine (4).

Compound	Optical Rotation [α_D]	Concentration (mg/ 10 cm ³)	Reference
1 (isolated)	+9.4	0.02	[19]
(-)-1	-108.0	0.09	[30]
(+)-1	+98.6	0.02	[30]
2 (isolated)	-8.5	0.01	[19]
(-)-2	-122.7	0.37	[29]
(-)-2	-118	0.3	[32]
(-)-2	-164.3	0.14	[30]
(+)-2	+165.5	0.11	[30]
(-)-2	-164.8	0.33	[31]
3 (isolated)	-12	0.275	[25]
(±)-3	-16.7	0.275	[26]
4 (isolated)	-72.9	0.10	[27]

2. Total and Formal Synthesis of Martinelic Acid (2)

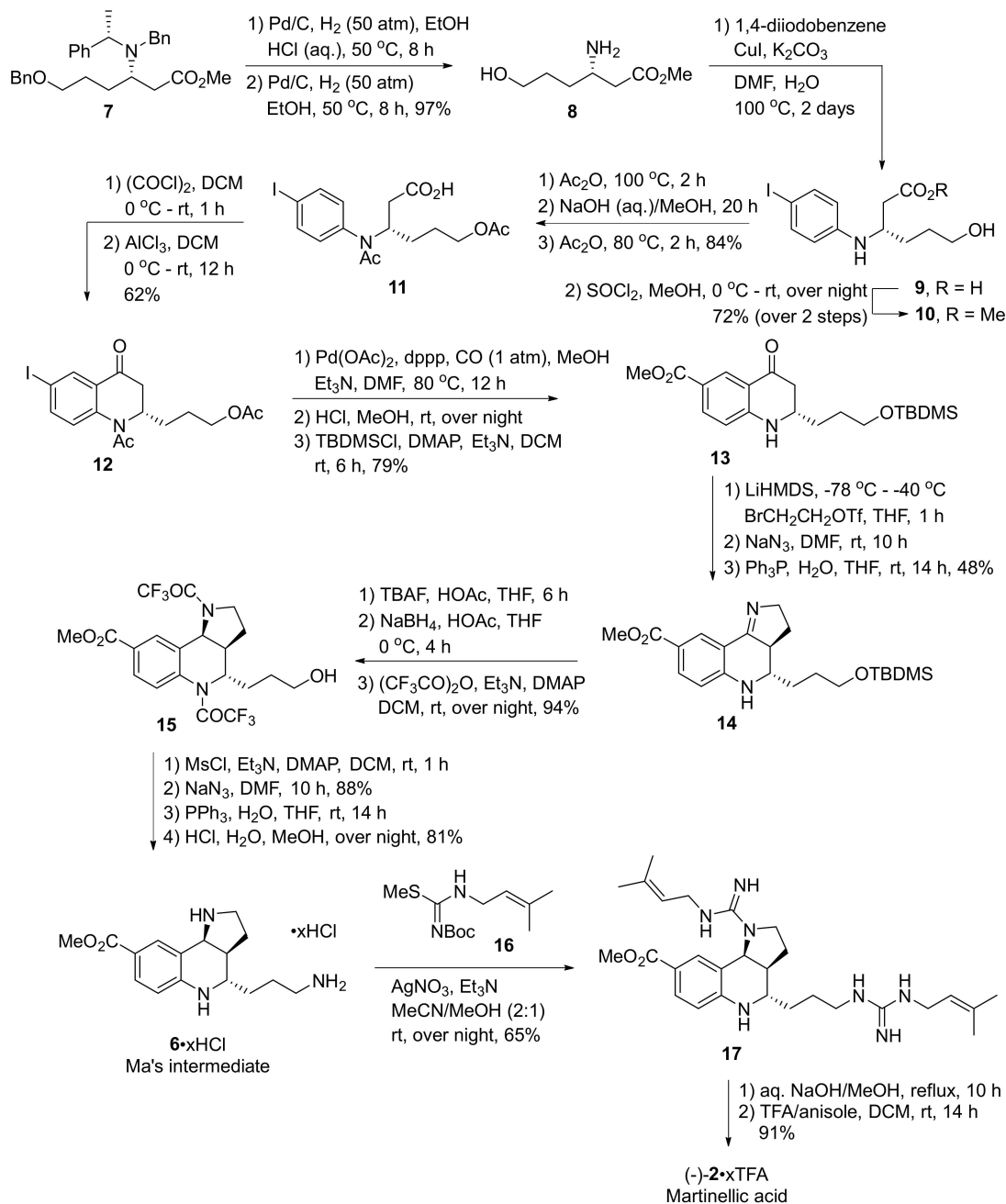
Synthesis of martinelic acid (2) has consistently been divided into two parts, namely assembly of the tricyclic scaffold and attachment of the galegine (5) side chains (Scheme 1). These guanidine-containing side chains were first isolated from *Verbesina encelioides* (Asteraceae) [35], and later identified as a toxic and antidiabetic component from *Galega officinalis* (Goat's Rue) [36]. Guanylation of the martinella scaffold has been conducted under different reaction conditions [30,37–39], one of which is presented below in Ma and coworkers' asymmetric synthesis of (-)-martinelic acid ((-)-2) from 2001 (Scheme 2) [29,37]. The precursor for the guanylation reaction in Ma and coworkers' protocol, namely triamine 6, has since 2001 been referred to as Ma's intermediate (6) and has been a key target compound in a handful of total and formal total syntheses of the martinella alkaloids [30,32,38–47]. We have therefore included a description of Ma and coworkers' asymmetric synthesis of (-)-martinelic acid ((-)-2) in this review.



Scheme 1. Retrosynthesis of the final assembly of Ma's intermediate (6) and the galegine (5) side chains to form martinelic acid (2).

In their 2001 publication, Ma and co-workers reported the first total synthesis of martinelic acid (2) [37]. The report was followed up in a full account in 2003 (Scheme 2) [29]. The synthesis was initiated from chiral β -amino ester 7, which was obtained from 1,4-butandiol using a chiral auxiliary, following a procedure developed by Davies and co-workers [48]. Copper catalyzed coupling of 1,4-diiodobenzene with β -amino ester 8 provided acid 9. In the following *N*-, *O*-acylation step, predominance of *O*-acylation over *N*-acylation of amino acid 9 was observed. It was thus found that the acid first had to be converted to the corresponding methyl ester 10 before treatment with acetic anhydride at elevated temperature facilitated acylation of both the amino- and hydroxy functionalities. The resulting *N*-, *O*-acylated methyl ester was then hydrolyzed to the corresponding acid followed by a re-acylation of the free hydroxyl group. This provided acid 11 in 84% yield

from methyl ester **10**. Formation of the acyl chloride upon treatment with oxalyl chloride followed by an aluminum chloride (AlCl_3) mediated intramolecular acylation provided ketone **12** in 62% yield.



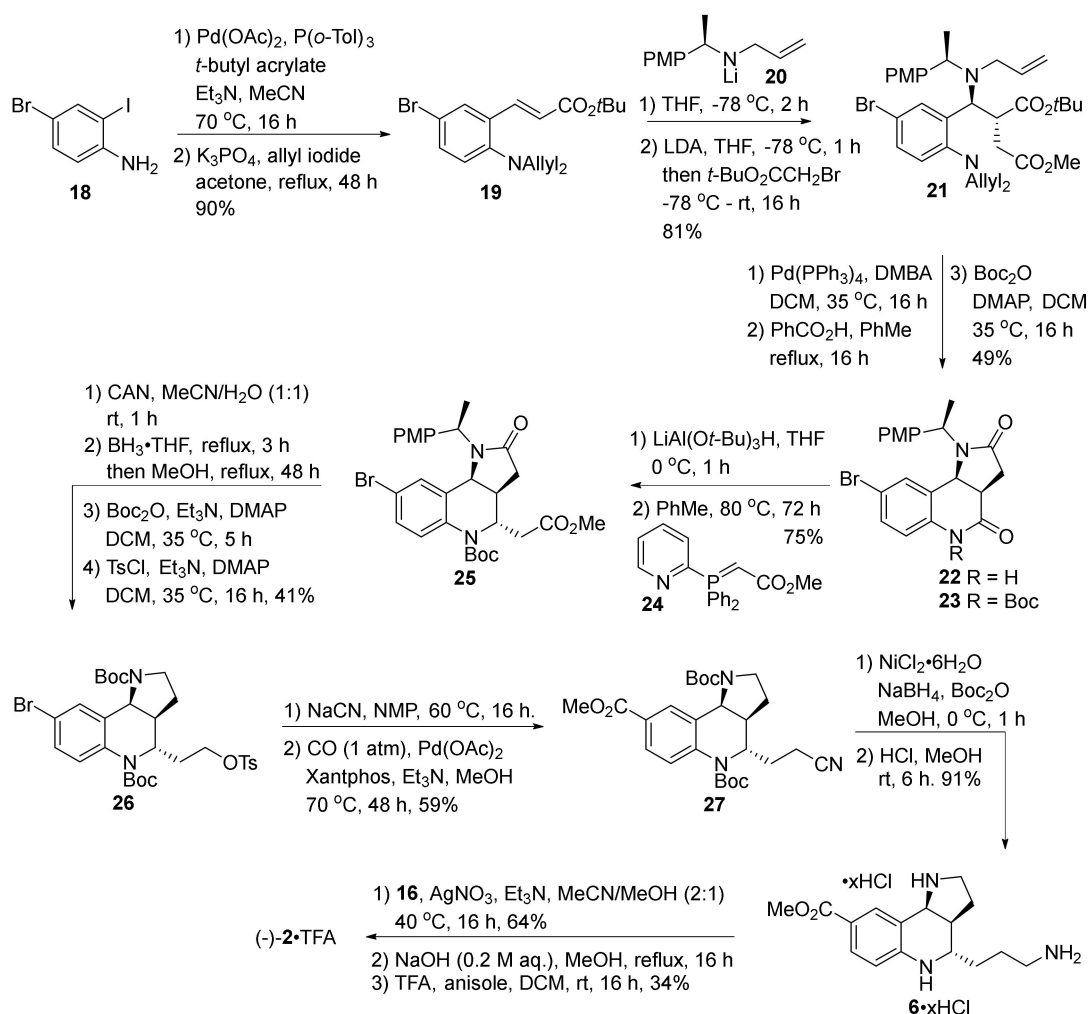
Scheme 2. Ma and co-workers' synthesis of Ma's intermediate and the endgame to martinelliac acid ((-)-2).

Palladium-catalyzed carbonylation of the iodide moiety within compound **12** followed by deacetylation and silyl protection of the hydroxyl group provided ketone **13**. Alkylation of ketone **13** was conducted by enolization with lithium bis(trimethylsilyl)amide (LiHMDS) followed by addition of 2-bromoethyl triflate as the alkylating agent. Ma and co-workers found that the resulting ethyl bromide product was unstable and therefore converted the bromide directly to the corresponding azide with sodium azide. Reduction of the azide with triphenyl phosphine and water provided imine **14** in 48% yield from ketone **13**. Reduction of imine **14** was found to work selectively with sodium borohydride only after deprotection of the *O*-silyl group. Protection of the resulting diamine with trifluoroacetic

anhydride provided compound **15** in 94% yield from imine **14**. A reaction sequence including mesylation, azidation, azide reduction, and *N*-deprotection gave triamine **6** (Ma's intermediate) as the HCl salt.

To further convert the triamine **6** to martinellinic acid, the primary amine and the hindered secondary amine functionality in the pyrrolidine ring was guanylated. Through experimentation, the Ma group found that the most efficient guanylation agent was *N*-Boc-protected methylisothiourea **16**. Since elevated temperatures led to decomposition of the triamine **6**, silver nitrate was used to promote the substitution of methanethiol in the guanylation reaction. By changing the solvent from acetonitrile to a mixture of acetonitrile and methanol (2:1), the yield for the reaction could be improved from 20% to 65%. This effect was most likely due to the poor solubility of triamine **6** in acetonitrile. The methyl ester **17** was finally converted to martinellinic acid ((-)-**2**), as the TFA salt in 91% yield through base catalyzed hydrolysis of the ester and subsequent treatment with TFA.

In 2013, Davies and co-workers published their own synthesis of (-)-martinellic acid ((-)-**2**) and (-)-*epi*-martinellic acid ((-)-*epi*-**2**) (Scheme 3) [32,40]. The synthesis began with a Heck cross-coupling between 2-iodo-4-bromoaniline **18** and *tert*-butyl acrylate, followed by bis-*N*-allyl protection, which provided ester **19** in 90% yield. Conjugate addition of (*R*)-lithium amide **20** to α,β -unsaturated ester **19** by means of a diastereoselective *aza*-Michael reaction was used to install the C-10 stereogenic center. Subsequent alkylation with methyl bromoacetate gave compound **21** as a single diastereomer.



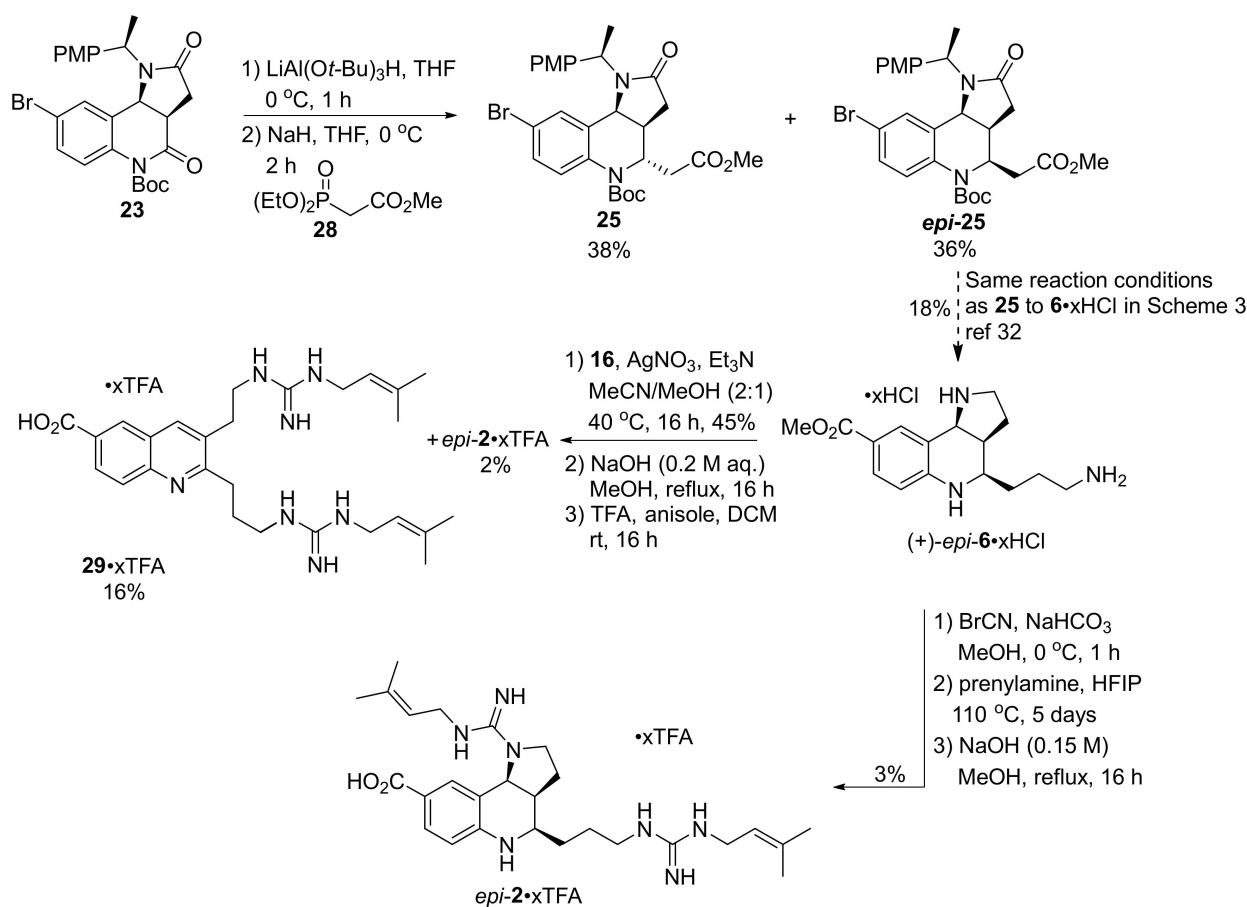
Scheme 3. The Davies group's synthesis of (-)-martinellic acid (**2**).

In preliminary studies, the Davies group attempted to form the pyrrolidine ring through a free amine (N-10a) by conducting a hydrogenolysis of all *N*-protecting groups. Neither acid promoted reaction of the free amine with *tert*-butyl ester nor did the methyl ester provide the desired five-membered cyclized product. However, upon removal of only the *N*-allyl groups with Pd(PPh₃)₄ and *N,N*-dimethylbarbituric acid (DMBA), followed by benzoic acid promoted cyclization of both rings, simultaneously, pyrroloquinolinone **22** was obtained. In order to further regioselectively reduce the six-membered lactam over the five membered lactam moiety in compound **22**, the electron withdrawing Boc-protecting group was introduced onto the N-8a nitrogen. The activated carbonyl group in compound **23** was then reduced with lithium tri-*t*-butoxyaluminum hydride LiAl(O*t*-Bu)₃H to form the hemiaminal. Treating the hemiaminal with phosphorane **24** allowed for olefination and an intramolecular *aza*-Michael addition to give compound **25** in 75% yield as a single diastereomer. Phosphorane **24** was used in the olefination reaction instead of the corresponding Wittig reagent due to issues with separating the reaction product from triphenylphosphine ylide residues.

The *p*-methoxyphenyl (PMP)-protection group within compound **25** could be removed upon treatment with ceric ammonium nitrate (CAN). The resulting substrate was then treated with borane (BH₃) to reduce the amide and ester functionalities to the corresponding amine and alcohol moieties, respectively. The amine was Boc-protected, and the alcohol was tosylated, which provided pyrroloquinoline **26** in 41% yield over four steps. Treatment of compound **26** with sodium azide in *N*-methyl-2-pyrrolidinone (NMP) followed by methoxycarbonylation provided methyl ester **27**. The nitrile group in compound **27** was then reduced to the corresponding amine upon treatment with sodium borohydride, and the resulting product was immediately Boc-protected in order to avoid formation of a tetracycle. Deprotection of the three *N*-Boc groups with methanolic HCl provided Ma's intermediate (6•*x*HCl) in 91% yield. (–)-Martinelllic acid ((–)-2•TFA) was finally obtained from the salt 6•*x*HCl in 49% yield using Ma's guanylation procedure [37].

Initial studies by Davies and co-workers showed that a strong base, such as NaH, led to equilibration between diastereomers **25** and epi-**25** (Scheme 4). Since this would provide access to the C(4)-epimer of martinelllic acid 2•*x*HCl, the Davies group also synthesized compound (+)-epi-6•*x*HCl by an analogous series of steps to the ones used for the synthesis of Ma's intermediate (–)-6•*x*HCl from pyrroloquinoline **25**, in 18% overall yield (Scheme 3). The corresponding guanylated product was provided in 45% yield by following Ma's protocol [37]. However, hydrolysis of the methoxy ester gave (–)-4-epi-Martinelllic acid epi-2•*x*TFA in only 2% yield, accompanied by quinoline 29•*x*TFA in 16% yield. By using the procedure reported by Snider et al., epi-martinelllic acid (epi-2•*x*TFA) was isolated in 3% yield over the three steps, and no formation of the quinoline 29•*x*TFA was observed [45].

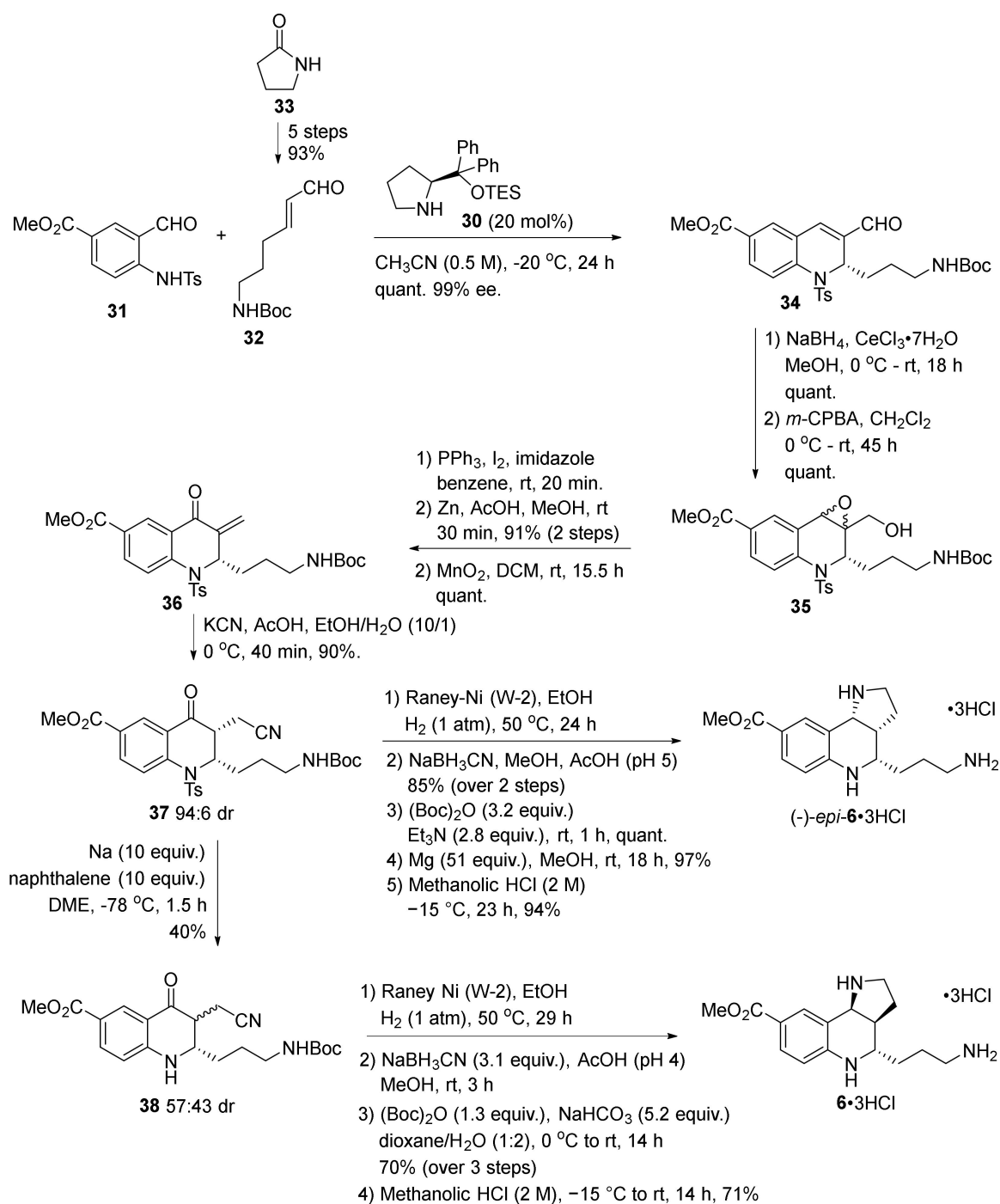
The Hamada group employed a previously reported asymmetric tandem Michael–aldol reaction using (*S*)-diphenylprolinol triethyl silyl ether **30** as an organocatalyst in the presence of sodium acetate (NaOAc) and four Å molecular sieves (4 Å MS) as starting point for their synthesis [42,49]. During optimization studies for the reaction between substrates **31** and **32** (obtained in 5 steps from pyrrole **33**), the group found that when performed in acetonitrile at –20 °C, the reaction proceeded smoothly without NaOAc and 4 Å MS (Scheme 5). By using two equivalents of the alkene **32**, due to slow reaction rate, together with 20 mol% of organocatalyst **30**, quinoline **34** was obtained in quantitative yield from compound **31** and high enantiomeric excess. The aldehyde moiety in compound **34** was further reduced to the allyl alcohol with sodium borohydride and cerium chloride.



Scheme 4. The Davies group's synthesis of *epi*(−)-martinellic acid (*epi*(−)-2).

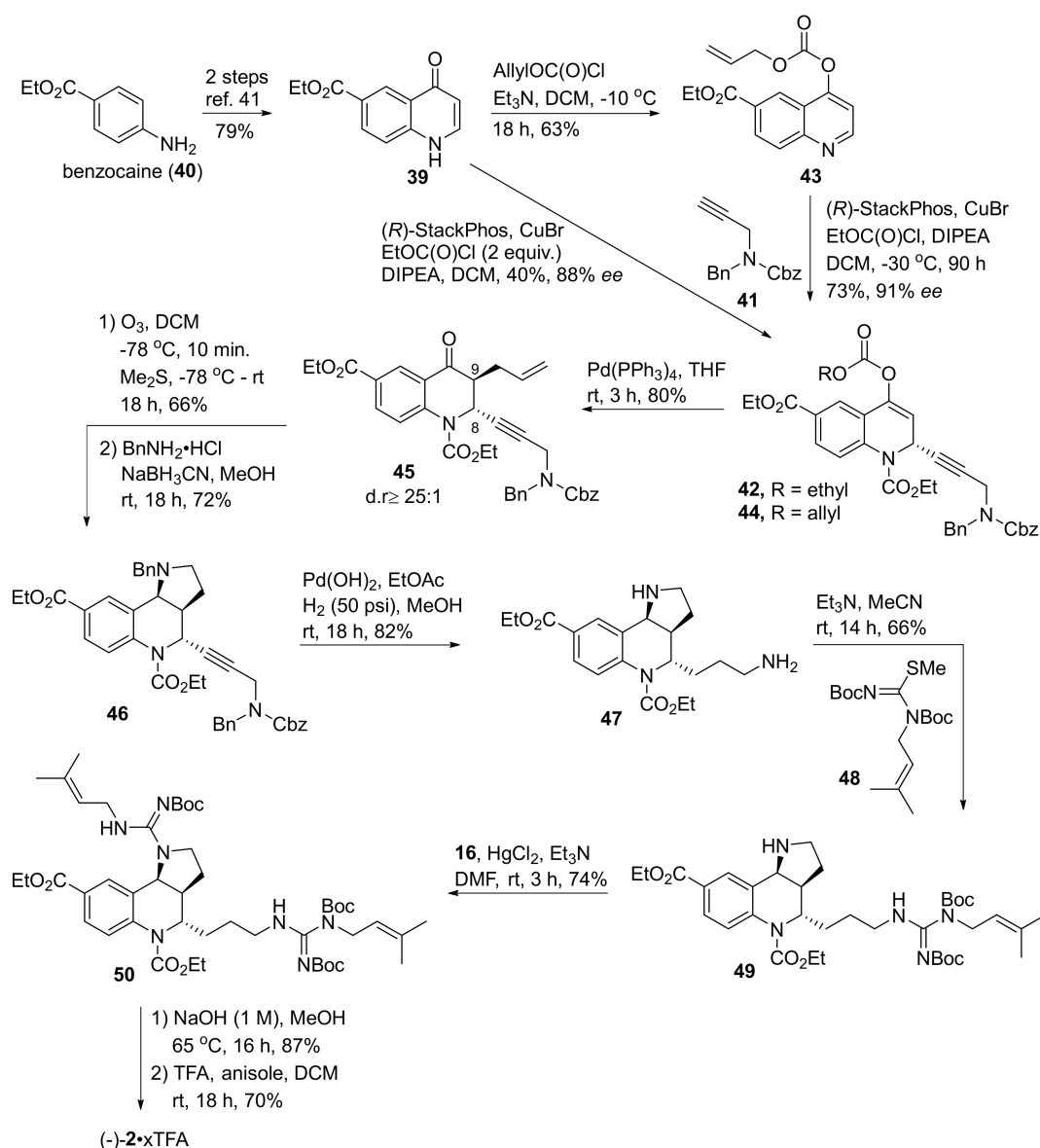
After several failed attempts to introduce the N-8a nitrogen to the allylic alcohol, Hamada employed a route to Ma's intermediate (6) previously reported in their group [50]. The allylic alcohol was treated with *m*-chloroperbenzoic acid (*m*-CPBA) to form epoxide 35. Iodination of compound 35 and subsequent treatment with zinc and acetic acid to cleave the epoxide ring gave an allylic alcohol that was further oxidized to ketone 36 with activated manganese dioxide. The α,β -unsaturated ketone 36 was subjected to hydrocyanation to provide quinolone 37 in 90% yield and 94:6 dr. Only after formation of (−)-*epi*-Ma's intermediate ((−)-*epi*-6) through a series of reduction and *N*-deprotection reactions could Hamada and co-workers conclude that cyano-quinolone diastereomer 37 exhibited *cis*-configuration. In their 2004 publication the Hamada group reported that the "2,3-*trans* arrangement was ambiguously confirmed by NMR" [50].

Base-promoted racemization of the cyano-sidechain with sodium naphthalenide and simultaneous *N*-tosyl-deprotection produced compound 38 as a diastereomeric mixture. The mixture was subjected to hydrogenation and reductive amination of the resulting imine followed by *N*-Boc protection. A final deprotection with methanolic HCl formed (−)-Ma's intermediate as its HCl salt ((−)-6•3HCl). Hamada and co-workers hypothesized that the *N*-protecting group (Ts) controls the *cis/trans* isomer formation during cyanation, through a pseudo-1,3-diaxial interaction between the *N*-toluenesulfonyl group and 3-cyanomethylone. Without the tosyl group, they imagined that the isomerization of the 3-cyanomethyl group takes place during the hydrogenation reaction, and that the *trans*-product 6 is more stable due to torsional strain between the 2-(3-*tert*-butoxycarbonylamino)propyl group and the pyrrolidine ring in a *cis*-product.



Scheme 5. Hamada and coworkers' synthesis of Ma's intermediate (6).

Another approach towards martinelliacid was presented by Pappoppula and Aponick in 2015 [51]. Their synthesis commenced from quinoline 39, which was synthesized in two steps from benzocaine (40) in 79% yield following a literature procedure (Scheme 6) [52]. The key step in this synthesis was a copper-catalyzed alkynylation reaction with alkyne 41, developed in the group, using (*R*)-StackPhos to set the C-8 stereochemistry. Their further strategy was to use an α -allylation reaction to diastereoselectively install the allyl group at C-9 [53]. To facilitate that chemistry, they therefore needed to convert ketone 39 to an aromatic enol.

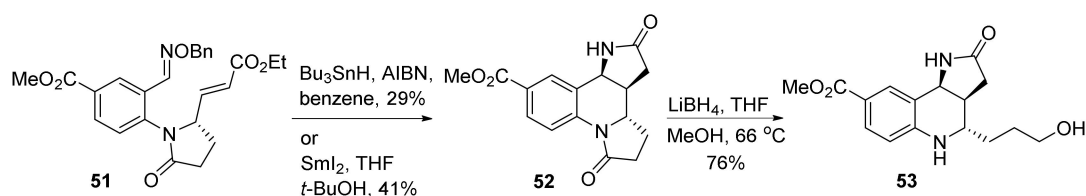


Scheme 6. Synthesis of (–)-martinellic acid ((–)-**2**•xTFA) by Pappoppula and Aponick.

In preliminary studies conducted by Pappoppula and Aponick, they wanted to see if it was possible to obtain alkyne **42** directly from quinoline **39**, by forming the corresponding carbonate in situ. This route gave the alkynylated product **42** in 40% yield and 88% ee. Attempts to increase the yield were, however, unsuccessful, because once the carbamate was formed, the quinolone did not undergo further alkynylation, resulting in the formation of an unreactive biproduct, viz. *N*-protected quinoline. Instead, the group prepared allylcarbonate **43** by treating quinolone **39** with alloc chloride. Stereoselective alkynylation of carbonate **43** at 0 °C for 15 h using (*R*)-StackPhos provided alkyne **44** in 95% yield and 86% ee. By running the reaction at –25 °C for 48 h and increasing the reaction concentration from 0.1 to 0.4 M, the title compound **44** was obtained in 90% ee, however at a lower conversion (70% yield). When scaling up the reaction, the copper bromide catalyst loading could be reduced from 5 to 2 mol% without affecting the yield and stereoselectivity, providing alkyne **44** in 73% yield and 91% ee. Diastereoselective decarboxylative α -allylation of allyl carbonate **44** further provided ketone **45** in 80% yield with a >25:1 diastereomeric ratio. Allyl **45** was then treated with ozone followed by a double reductive amination of the resulting 1,4-diacarbonyl using benzyl amine and sodium cyanoborohydride to provide the tricycle **46**. Reduction of the alkyne functionality upon treatment with

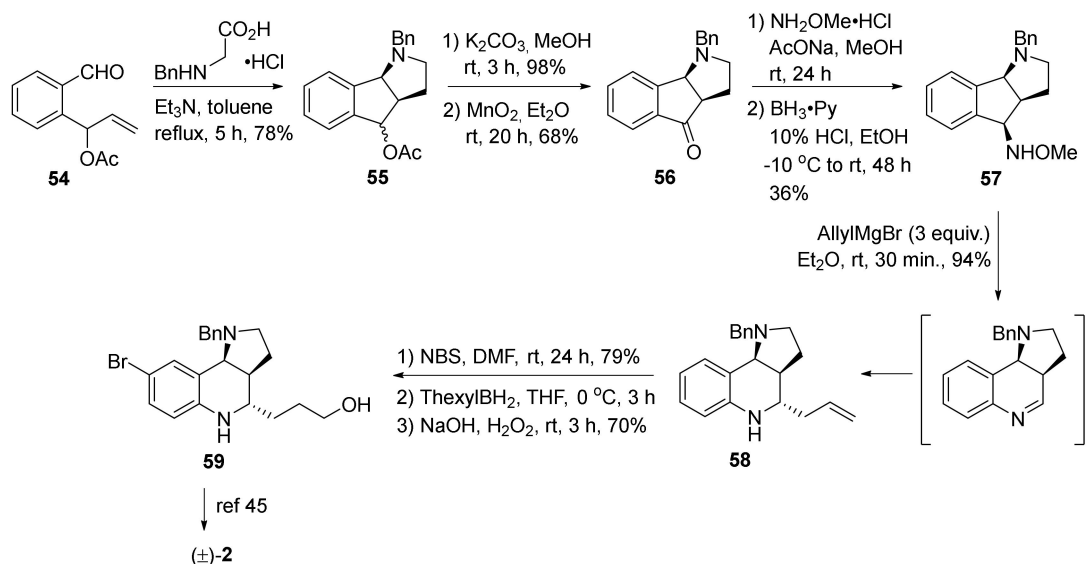
$\text{Pd}(\text{OH})_2$ and hydrogen (50 psi) while simultaneously removing three *N*-protecting groups resulted in the formation of amine **47** in 82% yield. Treating amine **47** with the di-Boc protected reagent **48** resulted in guanidinylation of the primary amine and formation of compound **49**. The sterically hindered secondary amine was then guanidinylated with the more reactive guanidine **16** to provide compound **50** in 74% yield. Finally, the TFA salt of martinellitic acid ((-)-**2**•*x*TFA) was obtained upon base catalyzed ethyl ester hydrolysis followed by deprotection of the *N*-Boc groups with TFA.

In 2008, Naito and co-workers presented the synthesis of (-)-martinellitic acid ((-)-**2**), where the key reaction was a radical addition–cyclization–elimination (RACE) reaction with a chiral oxime ether **51** forming lactam **52**. Lithium borohydride reduction of lactam **52** afforded pyrroloquinoline **53** (Scheme 7), which was brought forward to (-)-martinellitic acid ((-)-**2**) over seven steps [31]. A full report of this method has been covered in the review by Lovely and Bararinarayana [34]. The approach unfortunately experienced some unsatisfactory yields and stereoselectivity, which prompted a second approach to martinellitic acid.



Scheme 7. The key step in the Naito group's first approach to (-)-martinellitic acid ((-)-**2**), namely the radical addition–cyclization–elimination (RACE) reaction.

A formal synthesis of (±)-martinellitic acid was further reported by the Naito group together with Miyata in 2010 using a new approach based on ring expansion of an oxime ether through a domino reaction, including elimination of an alcohol, rearrangement of a metal aryl methylamide, and addition of an organomagnesium reagent (Scheme 8) [54].

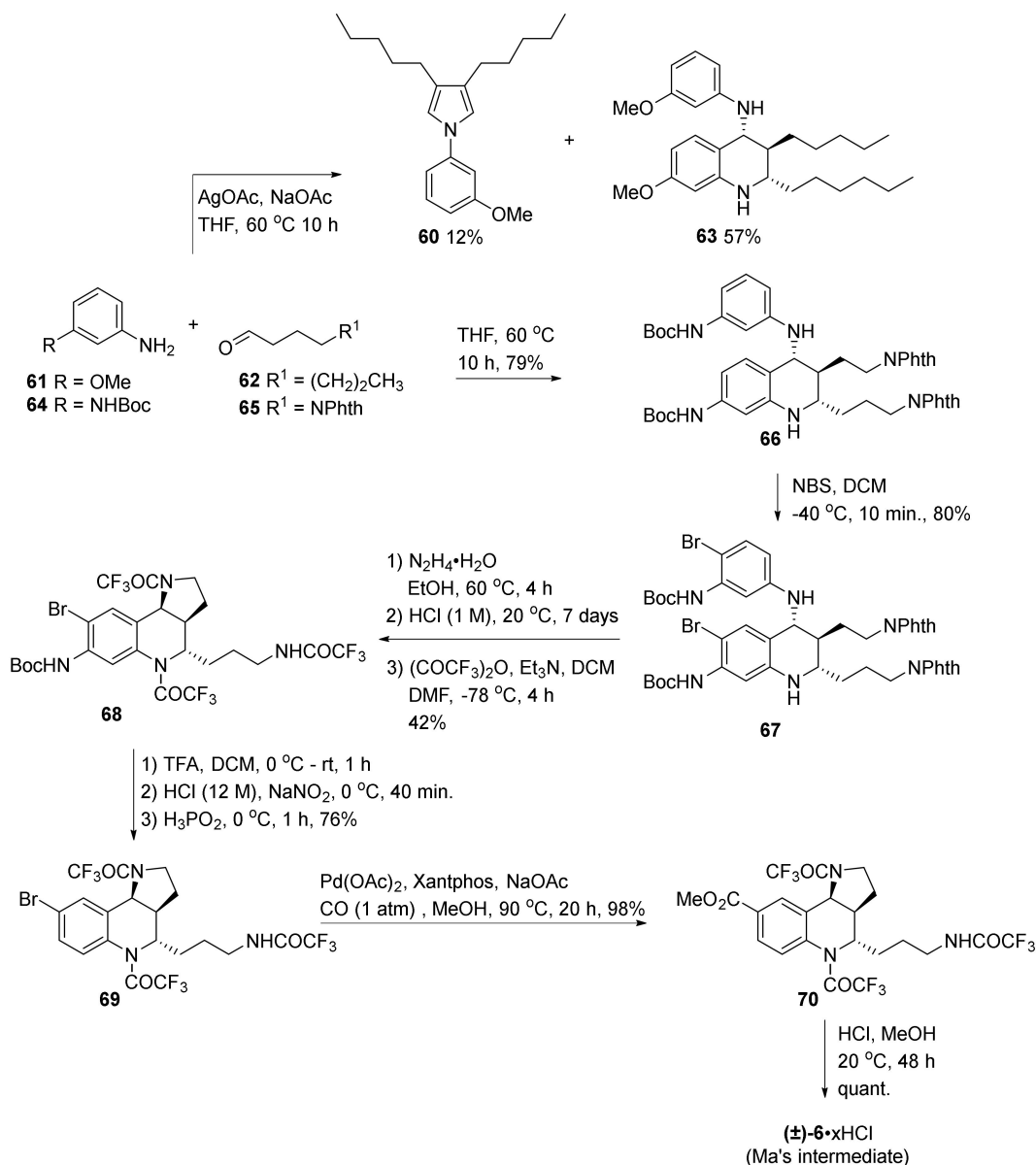


Scheme 8. The Naito group's second approach to martinellitic acid in collaboration with Miyata.

The work commenced by the condensation of aldehyde **54** with *N*-benzyloxycarbonyl-L-glycine hydrochloride followed by a spontaneous [3+2] cycloaddition of the resulting azomethine ylide gave indeno[1,2-*b*]pyrrolidine **55** in 78% yield [54]. Acetate hydrolysis and manganese dioxide (MnO_2) oxidation of the resulting alcohol provided ketone **56**. Condensation with *O*-methylhydroxylamine hydrochloride followed by borane reduction gave oxime ether **57**

in 36% yield. A domino reaction with allylmagnesium bromide proceeded stereoselectively from oxime ether **57** to afford amine **58** in 94% yield. Bromination was followed by hydroboration-oxidation of the alkene. The resulting pyrroloquinoline **59** is an intermediate in the synthesis of (\pm)-martinellic acid reported by Snider et al. [45], in which compound **59** was converted to (\pm)-martinellic acid over six steps.

During their synthetic studies of poly-substituted pyrroles such as pyrrole **60** from amine **61** and aldehyde **62** using silver acetate (AgOAc) as oxidant, Jia and co-workers unexpectedly observed formation of quinoline **63** (Scheme 9) [41]. They proposed that formation of the quinoline **63** occurred in a Povarov reaction.



Scheme 9. Jia and coworkers' approach to (\pm)-Ma's intermediate ((\pm)-**6**·xHCl).

On further inspection the Jia group found that the reaction proceeded in THF at elevated temperature without any additional reagents, in high yield and high stereoselectivity with various R groups. To utilize this reaction in the synthesis of Ma's intermediate (**6**), *N*-Boc protected amine **64** was reacted with *N*-phthaloyl protected aldehyde **65** to give quinoline **66** in 79% yield. In order to attach a handle for installing the methyl ester in Ma's

intermediate (**6**), the quinoline **66** was treated with *N*-bromosuccinimide (NBS) for 10 min to form bromide **67** in 80% yield.

N-phthaloyl groups were removed from bromide **67** upon treatment with hydrazine hydrate followed by treatment with HCl to facilitate ring closure of the five-membered ring. The resulting pyrroloquinoline was *N*-protected with trifluoroacetic anhydride to provide compound **68**. The bromo quinoline **69** was obtained by *N*-Boc deprotection followed by reductive removal of the resulting amine. Carbonylation of the bromo quinoline **69** to form the corresponding methyl ester **70**, followed by *N*-COCF₃ deprotection with HCl, afforded (±)-Ma's intermediate ((±)-**6**•*x*HCl).

3. Tricyclic Core Scaffold Synthesis

In addition to synthetic preparation of the martinella alkaloids the synthesis of the tricyclic core of the natural products has also attracted significant attention. To this day, no studies of how the hexahydropyrrolo[3,2-*c*]quinoline structure has arisen biosynthetically in nature have been published. However, in their synthesis of the martinella alkaloids, Batey and Powell put together the tricyclic core structure **71** in an acid catalyzed two-component Povarov reaction between aniline **72** and enamide **73a** (Scheme 10) and suggested that the martinella alkaloids may be naturally assembled in a related biosynthetic process [38,55]. The Povarov reaction (also known as the aza-Diels Alder reaction) has been a prevalent method for synthesizing *N*-heterocycles [56], including the pyrroloquinoline core structure [57]. Particularly, the assembly of the scaffold **74** from the aromatic imine **75** and the enamide **73** has been a well-studied reaction (Scheme 11) and will be firstly discussed in this section. However, other strategies have also been developed for the construction of the pyrroloquinoline scaffold, and these syntheses will further be presented in chronological order.



Scheme 10. Scaffold assembly by Batey and Powell.

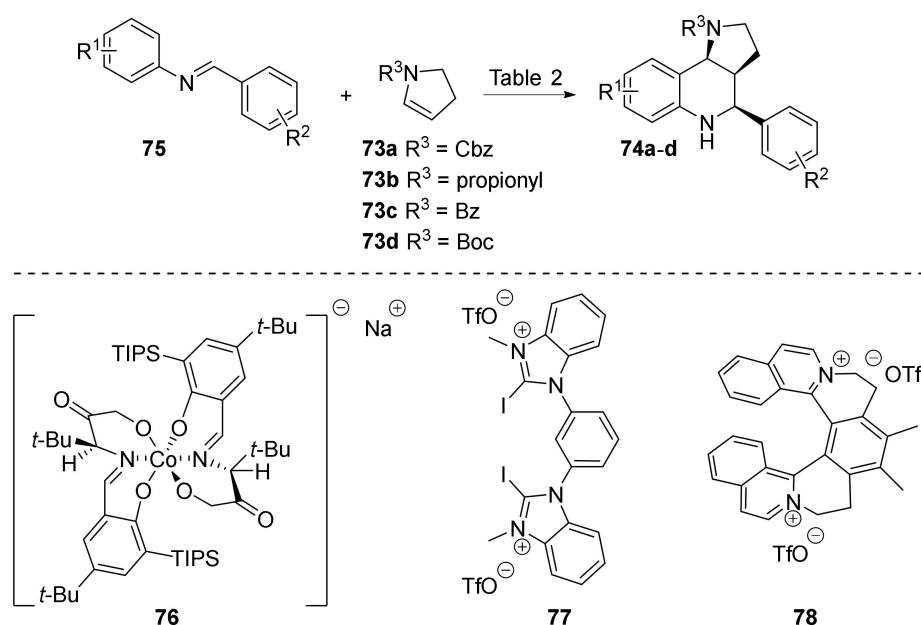
Table 2. Reaction conditions and outcome from the Povarov reaction between the aromatic imine **75** and enamide **73a–d** (Scheme 11).

Entry	Reaction Conditions	R ¹	R ²	Enamide	Yield	Endo:Exo	Reference
1	InCl ₃ (2 equiv.), MeCN, rt, 30 min	H	H	73b	41%	1:1	[58]
2		H	2-NO ₂	73b	50%	2:1	[58]
3	Zn(OTf) ₂ (10 mol%), DCM, rt	H	2-OH	73c	42%	>20:1	[59]
4	76 (10 mol%), 5 Å MS, <i>n</i> -hexane −40 °C, 72 h	H	H	73a	94%	>20:1	[60]
5	77 (10 mol%), MeCN, rt, 0.5–1 h	H	H	73a	95%	43:57	[61]
6	78 (10 mol%), MeCN, rt, 27 h	4-OMe	H	73d	86%	53:47	[62]
7	Micellar-SO ₃ H, H ₂ O, 25 °C, 18 h	H	4-O-DNA	73d	>90%	NR	[63]

NR = Not reported.

The formation of the 8-phenyl-pyrroloquinoline **74** from the Povarov reaction between aromatic imine **75** and *N*-protected enamide **73** has been a popular reaction for constructing the pyrroloquinoline scaffold (Scheme 11, Table 2). The reaction was first reported by Hadden and Stevenson in 1999 [58]. They enabled the reaction with indium chloride to obtain the pyrroloquinoline **74** in a 1:1 mixture of endo/exo isomers (Table 2, Entry 1). The use of a 2-nitro phenyl aromatic imine **75** in the reaction favored formation of the endo-product **74b** (Table 2, Entry 2). The endo-compound **74c** was also obtained from the zinc triflate catalyzed Povarov reaction conducted by Wang and co-workers (Table 2,

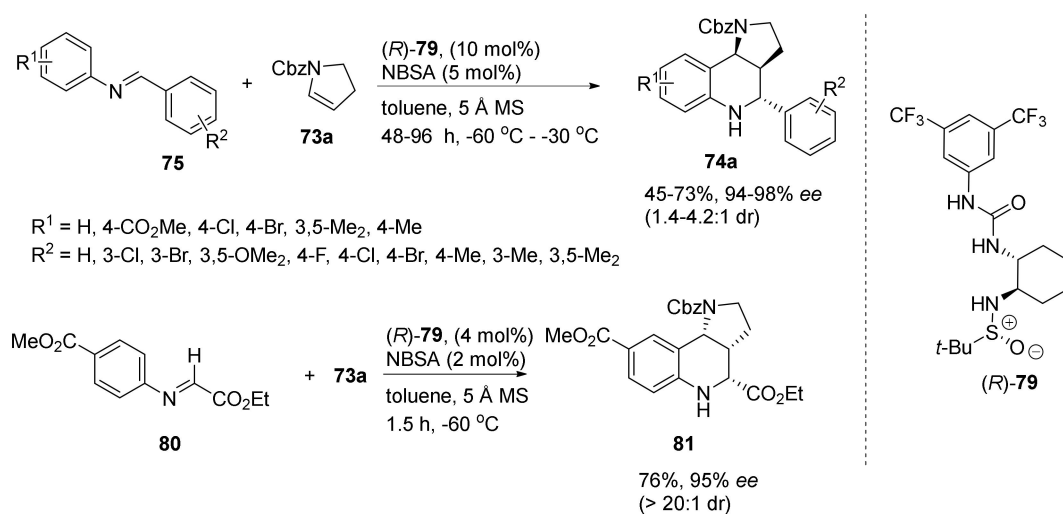
Entry 3) [59], as well as from the cobalt catalyzed reaction employing catalyst **76**, presented by Gong and co-workers (Table 2, Entry 4) [60]. Other catalysts that have been explored for this reaction are the iodo catalyst **77** (Table 2, Entry 5) and helquat catalyst **78** (Table 2, Entry 6), both of which facilitated formation of approximately 1:1 mixtures of endo/exo isomers [61,62]. Synthesis of a DNA-barcoded library that included the pyrroloquinoline scaffold has also utilized the Povarov reaction to assemble the scaffold **74d**, using a micellar sulfonic acid to catalyze the reaction [63].



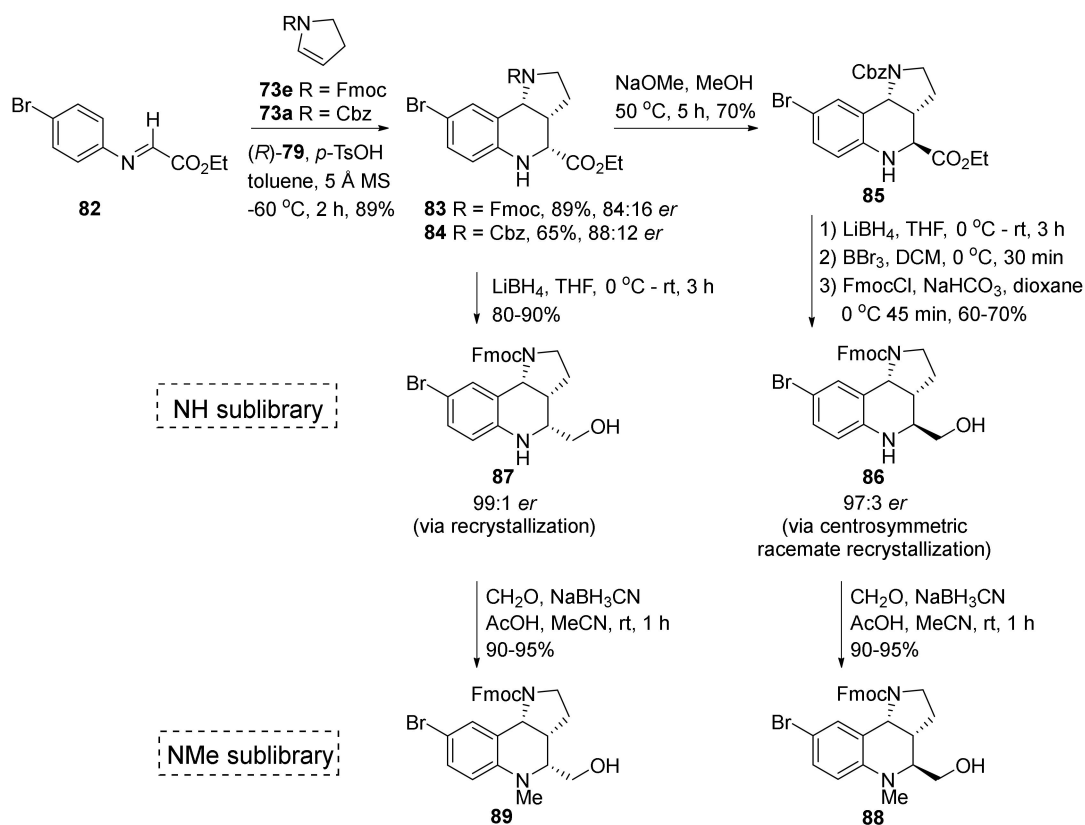
Scheme 11. Formation of 8-phenyl pyrroloquinoline **74a–d** in the Povarov reaction between the aromatic imine **75** and enamide **73a–d**. For more information, see Table 2.

The Jacobsen group produced the martinella scaffold in their experimental and computational study of Brønsted-acid promoted asymmetric Povarov reactions between *N*-aryl imines and electron rich alkenes [64]. They explored an anion-pathway for catalysts, such as urea (*R*)-**79**, in which the catalyst binds to the positively charged substrate through its counterion. They further showed that both the urea and sulfonyl functionalities were required for the catalyst **79** to facilitate the Povarov reaction. The exo-8-phenyl pyrroloquinoline **74a** was obtained as the major stereoisomer (94–98% ee) in the reaction between *N*-aryl imines **75** and enamide **73a** in the presence of urea (*R*)-**79** and ortho-nitrobenzene sulfonic acid (NBSA) (Scheme 12). Stereoselectivity was flipped when reacting glyoxylate imine **80** with the enamide **73a** in analogous conditions. In this case, the endo-isomer **81** was obtained as the major product in 95% enantiomeric excess.

The synthetic method developed in the Jacobsen laboratory (Scheme 12) was further utilized together with Marcaurelle and co-workers to set up a 2328-membered library consisting of four pyrroloquinoline stereoisomers flanked with a variety of side chains and functional groups for a Stereo/Structure–Activity–Relationship (SSAR) study [65]. The library was assembled in two consecutive parts, namely, asymmetric synthesis of the four possible pyrroloquinoline stereoisomers (Scheme 13) followed by a solid phase synthesis for further diversification of the pyrroloquinoline scaffold (Scheme 14).

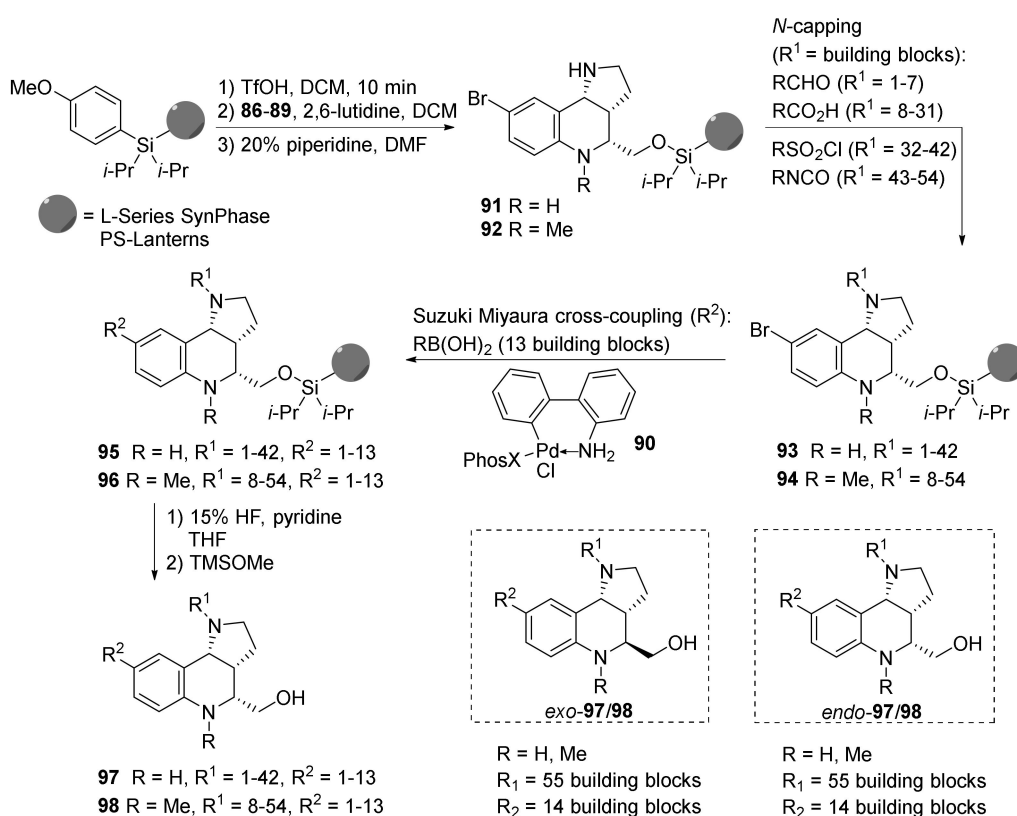


Scheme 12. Organocatalytic scaffold synthesis developed in the Jacobsen group.



Scheme 13. Large scale scaffold synthesis by Marcaurelle and co-workers.

The pyrroloquinoline scaffold was synthesized via the urea **79** catalyzed Povarov reaction between aromatic imine **82** and dihydropyrrolidine **73a** or **73e** (Scheme 13). Fmoc- and Cbz-protected pyrroloquinolines **83** and **84** were obtained in high yield and enantiomeric ratio. The imine **82** tended to hydrolyze when the reaction was run at larger scale. To solve this hydrolysis issue, the Brønsted acid NBSA initially used in the Jacobsen group was replaced by anhydrous *p*-toluene sulfonic acid (*p*-TsOH) when the reaction was conducted on gram scale.



Scheme 14. Solid support scaffold diversification by Marcaurelle and co-workers.

The tricycle mirror images ent-**83** and ent-**84** were obtained in the presence of urea catalyst (*S*)-**79**. To include all possible stereoisomers in the study, the group conducted an epimerization of the *N*-Cbz protected endo-isomers **84** and ent-**84**, employing sodium methoxide in methanol to afford the more thermodynamically stable exo-products **85** and ent-**85**. Reduction of the ester group in compound **85** with lithium borohydride followed by protecting group exchange from Cbz to the base labile Fmoc, a protecting group that was compatible with the following solid phase library synthesis, resulted in the formation of alcohol **86**. The endo-pyrroloquinoline **83** was reduced with lithium borohydride to afford the corresponding alcohol **87**. The *N*-Fmoc protected pyrroloquinolines **86** and **87** could be recrystallized to afford the enantiopure compounds in up to 97:3 and 99:1 *er*, respectively.

The quinoline amine in compounds **86** and **87** was the first site for the planned diversification of the scaffold. Marcaurelle and co-workers found that this secondary amine could be alkylated with only a limited number of aldehydes. The four enantiomers **86**/ent-**86** and **87**/ent-**87** were therefore *N*-alkylated prior to the solid phase diversification (Scheme 14), in a reductive amination reaction with formaldehyde, to afford *N*-methyl pyrroloquinolines **88**/ent-**88** and **89**/ent-**89**. This first step of diversification afforded two groups of compounds that consisted of amines **86**/ent-**86** and **87**/ent-**87** and methylamines **88**/ent-**88** and **89**/ent-**89**, which were referred to as the NH and NMe sublibraries, respectively.

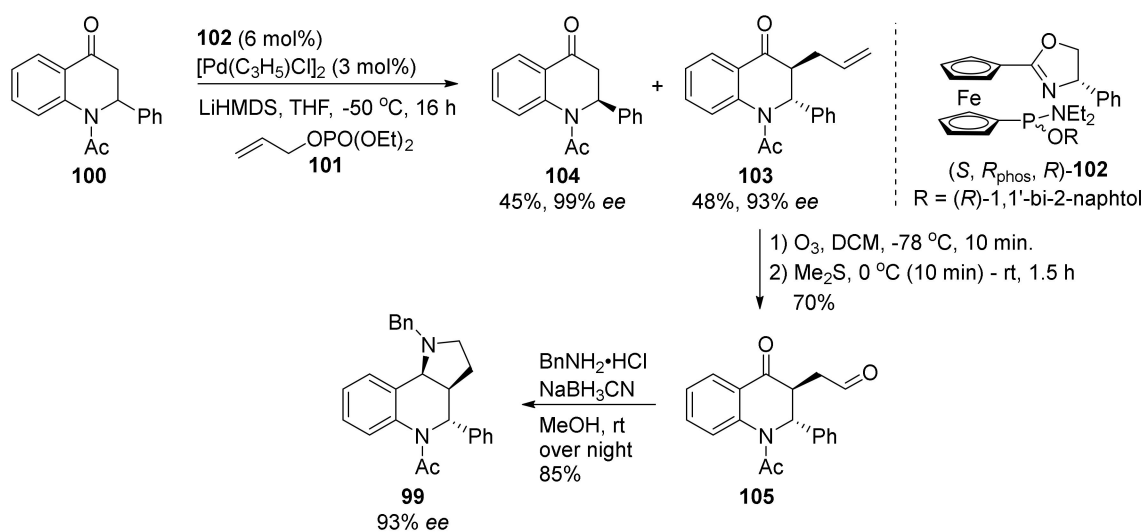
All four stereoisomers of the NH and NMe sublibraries were further diversified by amine capping of the secondary pyrrolidine amine and cross-coupling of the aryl bromide moiety with selected building blocks (Scheme 14). To find appropriate building blocks for the amine capping, Marcaurelle and co-workers firstly conducted a feasibility study with 54 pre-selected substituents, including sulfonyl chlorides, isocyanates, carboxylic acids, and aldehydes. They then observed bis-capping of the NH sublibrary in the presence of isocyanates, and decomposition in the NMe sublibrary during reductive amination with aldehydes. Therefore, isocyanates (building blocks 43–54) were removed from the NH sublibrary design and aldehydes (building blocks 1–7) were removed from the design of the NMe sublibrary. This was followed by a feasibility study of palladium cross-coupling

reactions. Since the Sonogashira cross-coupling conditions led to poor conversion, Suzuki–Miyaura cross-coupling conditions were further explored. A variety of ligands ($(P(t\text{-Bu})_3)$, PEPPSI, and *S*-Phos), palladium-catalysts ($\text{PdCl}_2(\text{PPh}_3)_2$ and $\text{Pd}(\text{dba})_2$), bases (TEA, K_3PO_4 , and CsCO_3), and solvents (EtOH, PhMe, 1,4-dioxane, and THF) were tested in order to minimize byproduct formation in the Suzuki–Miyaura cross-coupling reaction. Finally, appreciable conversion to the coupling products was achieved by using the Buchwald precatalyst **90** [66].

Based on the feasibility study, a virtual library including all possible combinations of a master list of building blocks was constructed, generating approximately 2400 compounds for each stereoisomer. A filter that excluded building block combinations with undesirable physicochemical properties (desirable properties: $\text{MW} \leq 500$, $\text{ALogP} -1$ to 5, H-bond acceptors + donors ≤ 10 , rotatable bonds ≤ 10 and $\text{TPSA} \leq 140$) was then applied to the dataset. This finally brought together a library of 274 compounds for each of the NH scaffolds and 310 compounds for each of the NMe scaffolds.

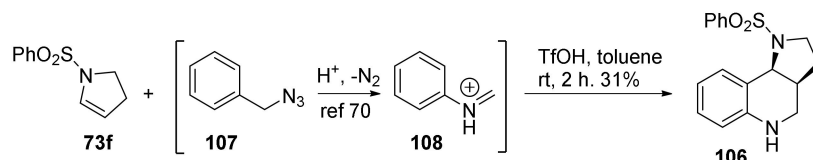
The 2328-membered library was finalized in a solid support synthesis (Scheme 14). The SynPhase Lanterns were activated by triflic acid (TfOH), and alcohols 86–89 were then loaded onto the solid support in the presence of 2,6-lutidine. Removal of the *N*-Fmoc group with piperidine in DMF afforded amines **91** and **92**, which were subjected to *N*-capping with the 54 pre-selected building blocks. Suzuki–Miyaura cross-coupling of the resulting bromoanilines **93** and **94** with 14 different boronic acid building blocks in the presence of the Buchwald catalyst **90** afforded coupling products **95** and **96** [66]. The diversified products **95** and **96** were subsequently liberated from the solid support upon treatment with HF and pyridine to afford compounds **97** and **98**. Analysis of the finalized library confirmed that the compounds exhibited suitable physicochemical properties for further biological testing. For this purpose, Marcaurelle and co-workers submitted the diversified pyrroloquinoline library to the NIH molecular library small molecule repository (NIH MLSMR).

Hou and co-workers obtained the *exo*-diastereomer of phenyl-pyrroloquinoline **99** in 93% ee by kinetic resolution (Scheme 15) [67]. Quinoline **100** was subjected to a palladium catalyzed asymmetric allylic alkylation reaction with 50 mol% of allyl reagent **101** and 6 mol% of catalyst **102** in the presence of lithium bis(trimethylsilyl)amide (LiHMDS). These conditions favored formation of the *trans*-enantiomer **103**, which at the same time enabled recovery of the close-to enantiopure hydroquinolone **104**. Alkene **103** was further converted to the pyrroloquinoline **99** by first performing an ozonolysis to afford aldehyde **105**, which was followed by a double reductive amination reaction with benzylamine and sodium cyanoborohydride as reducing agent to provide the tricyclic scaffold **99** in 85% yield.



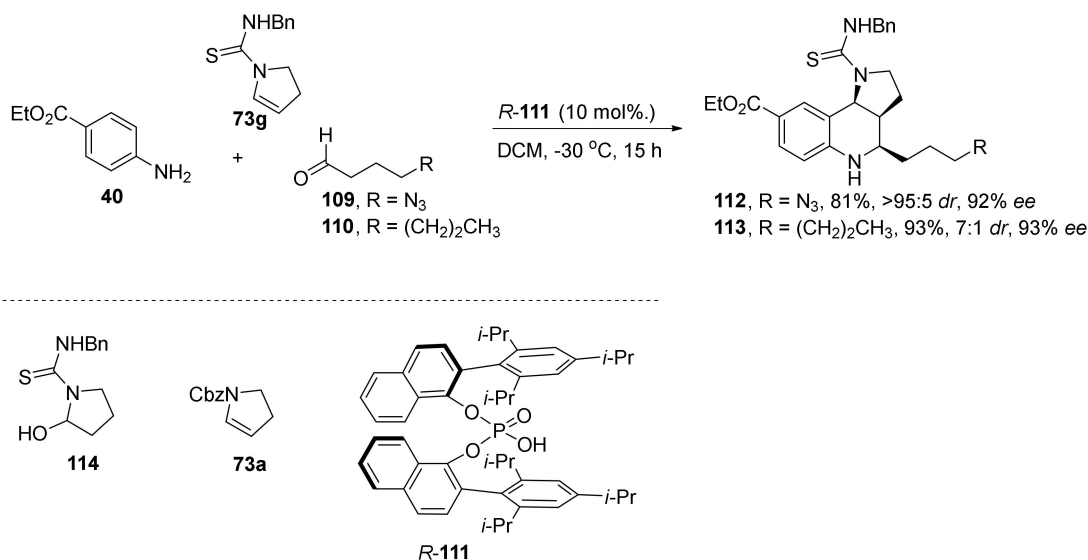
Scheme 15. Scaffold synthesis by Hou and co-workers.

Gilliaizeau and Gigant synthesized a variety of nitrogen-fused tetrahydroquinolines, such as pyrroloquinoline **106** (Scheme 16), from benzyl azide **107** and cyclic non-aromatic enamides **73f** [68]. A similar assemble of the corresponding indoloquinoline had previously been reported by the Zhai group [69]. The pyrroloquinoline **106** was obtained with a *cis* relationship between the two chiral centers, by reacting benzyl azide **107** with pyrrole **73f** in the presence of triflic acid in toluene. This synthesis, based on Aubè and co-workers' discovery of acid, promoted benzyl azide to imine rearrangement [70], included two sequential Pictet–Spengler reactions upon in situ formation of an iminium intermediate **108** from benzyl azide **107**.



Scheme 16. Scaffold synthesis by Gilliaizeau and Gigant.

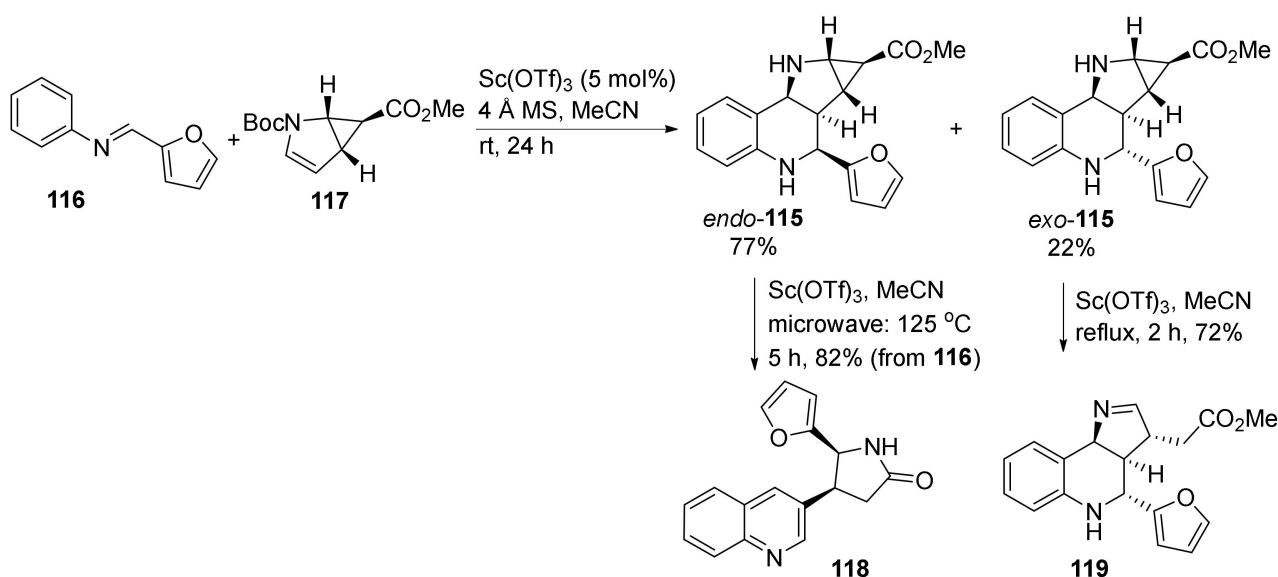
Masson and co-workers synthesized the endo-martinella scaffold in a chiral phosphoric acid-catalyzed enantioselective three-component Povarov reaction (Scheme 17) [71]. Aniline **40**, enamine **73g**, and aldehyde **109** or **110** were stirred together in the presence of phosphoric acid catalyst (*R*)-**111** to provide endo-martinella scaffolds **112** and **113** in high enantiomeric excess. A similar multicomponent reaction between aniline, benzaldehyde, and pyrrolidine **114**, catalyzed by lanthanide triflate to assemble the martinella scaffold was reported by Batey and Powell in 2001 [47]. Batey and Powell's incentive for using the thiourea-protected pyrrolidine **114** was to provide the martinella scaffold with the guanidine precursor moiety pre-installed on the sterically hindered pyrrolidine nitrogen. In addition to this, Batey and Powell found that using thiourea **114** as the dienophile, instead of *N*-Cbz enamide **73a**, favored formation of the *exo*-pyrroloquinoline scaffold.



Scheme 17. Scaffold synthesis by Masson and co-workers.

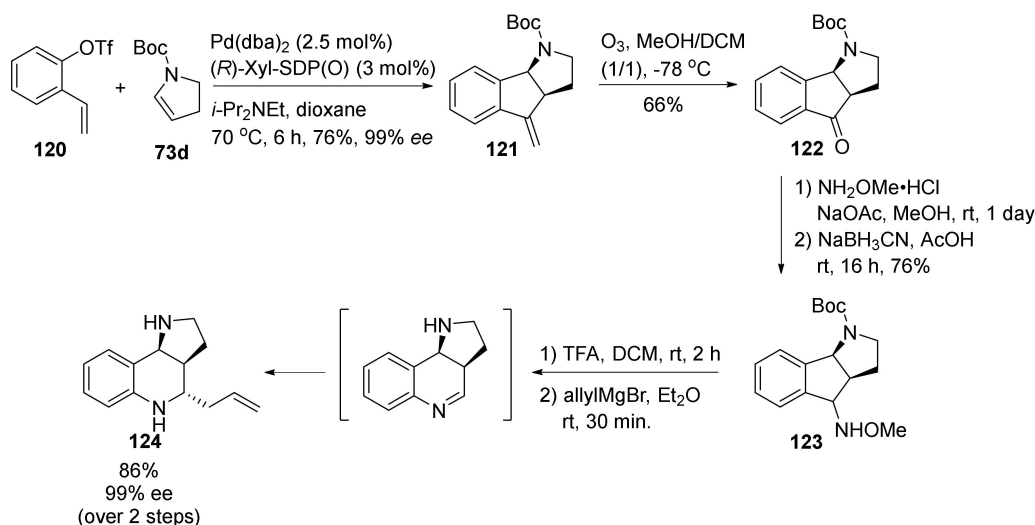
In the phosphoric acid (*R*)-**111** catalyzed reaction, Masson and co-workers hypothesized that the benzyl-NH function of thiourea **73g** participated together with the in situ formed imine in hydrogen bonding interactions with the phosphoric acid (*R*)-**111**. This dual activation thereby enhanced enantioselectivity of this reaction to provide endo-stereoisomers **112** and **113** in high ee.

Roy and Reiser assembled the pyrroloquinoline scaffold **115** in a scandium triflate catalyzed Povarov reaction between aldimine **116** and enamide **117** at ambient temperature (Scheme 18) [72]. Upon applying heat to the reaction, they obtained 4,5-*cis*-disubstituted pyrrolidinone **118**, a lead structure for pharmaceutical compounds that target diseases such as osteoporosis [73], in 82% yield. They further proposed a reaction mechanism for the formation of the pyrrolidinone **118** that included assembly of the tetracycle **115** in a Povarov reaction, which, upon ring opening of the cyclopropane, provided an iminium compound (such as imine **119**). Further migration of the furan group, followed by aromatization of the quinoline structure and lactamization of the pyrrolidine moiety upon Boc-deprotection, could then provide pyrrolidinone **118**. In the proposed mechanism, the *cis*-relationship between substituents on the pyrrolidinone **118** arose from the Povarov product *endo*-**115**. This proposal was confirmed when heating of tetracycle *exo*-**115** in the presence of scandium triflate provided pyrroloquinoline **119**, and not the pyrrolidinone **118**.



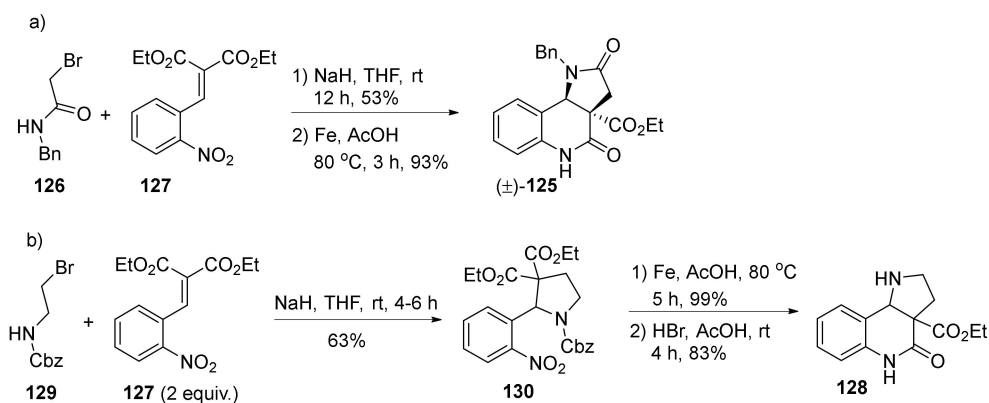
Scheme 18. Assembly of the pyrroloquinoline scaffold by Roy and Reiser.

Another asymmetric approach towards the pyrroloquinolines was presented by Zhou and co-workers in 2013 [74]. The stereochemistry was installed in a palladium catalyzed asymmetric intermolecular cyclization reaction between triflate **120** and Boc-protected pyrrolidine **73d** to obtain the tricyclic alkene **121** in 76% yield and excellent ee (Scheme 19). The following treatment with ozone afforded ketone **122**. Condensation of *O*-methyl hydroxylamine with the carbonyl moiety in ketone **122** followed by reduction of the resulting *O*-methyl oxime with sodium cyanoborohydride afforded amine **123**. With compound **123** in hand, the further plan was to use Miyata and co-workers' strategy (Scheme 8) for ring expansion to finalize the tricyclic scaffold **124** [54]. However, only upon *N*-Boc deprotection did ring expansion occur under Miyata and co-workers' reaction conditions. Thus, after removing the Boc group by treatment with trifluoroacetic acid (TFA), pyrroloquinoline **124** was obtained in 86% yield with retained enantioselectivity.



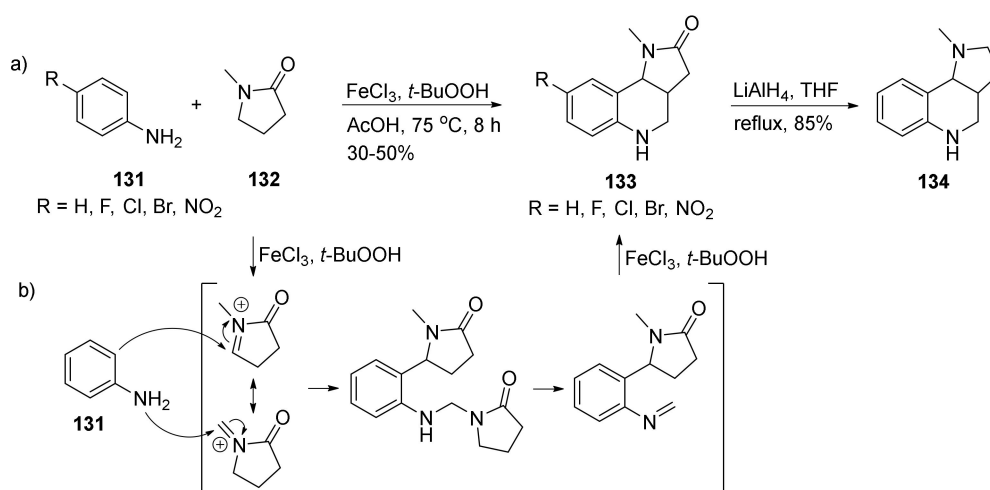
Scheme 19. Scaffold synthesis by Zhou and co-workers.

In a previously reported strategy, included in the 2008 review by Lovely and Barari-narayana [34], Daïch and co-workers reported the synthesis of the pyrroloquinoline scaffold **125** from α -bromoacetamide **126** and Michael acceptor **127** (Scheme 20a) [75]. In 2013, Daïch and co-workers reported an extension of this method in the synthesis of pyrroloquinoline **128** from bromoethyl carbamate **129** and diethyl malonate **127** (Scheme 20b) [76]. The reaction between carbamate **129** and Michael acceptor **127** in the presence of sodium hydride provided pyrrolidine **130** through an aza-Michael/intramolecular substitution reaction tandem sequence. The group experienced that all attempts to hydrogenate pyrrolidine **130** failed. They thus obtained the martinella scaffold **128** by iron-catalyzed reduction of nitrobenzyl-pyrrolidine **130** followed by acidic deprotection of the *N*-Cbz group.



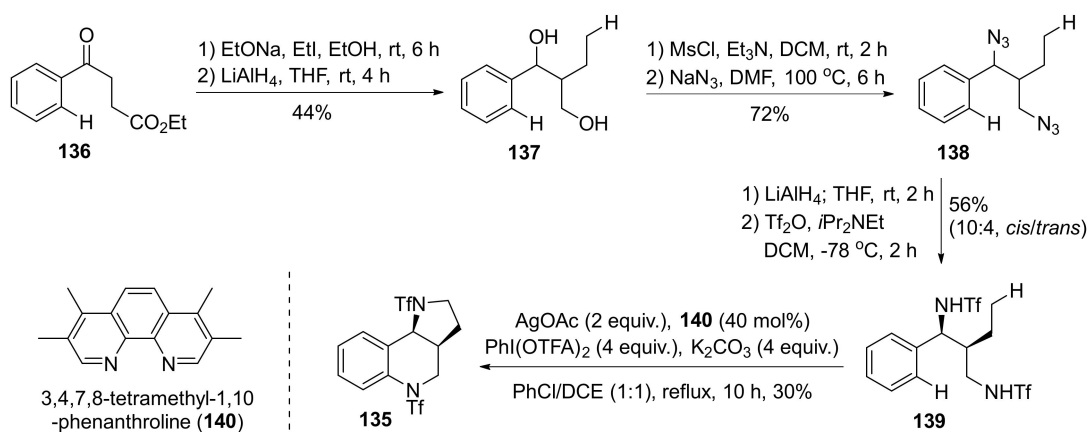
Scheme 20. Scaffold synthesis by Daïch and co-workers: (a) 2008 approach; (b) 2013 approach.

Bao and co-workers applied oxidative conditions to aniline and electron deficient anilines **131** dissolved in lactam **132** to form the tricyclic scaffold **133** (Scheme 21a) [77]. By using iron trichloride (FeCl_3) as catalyst and tert-butylperoxide (*t*-BuOOH) as oxidant in the presence of acetic acid (AcOH), the pyrroloquinoline **133** was formed in 30–50% yield. Bao and co-workers further presented a plausible mechanism for the formation of the tricyclic scaffold **133** (Scheme 21b). The mechanism commenced with a single electron transfer (SET) oxidation of lactam **132** to the corresponding iminium ions. One C–C and one C–N bond was further formed upon addition of aniline **131**. Elimination of a 2-pyrrolidone followed by an SET oxidation provided the pyrroloquinoline **133**. Further reduction of the lactam moiety, using lithium aluminum hydride, afforded the hexahydropyrroloquinoline structure **134** in 85% yield.



Scheme 21. (a) Reaction conditions and (b) the proposed mechanism for scaffold assembly by Bao and co-workers.

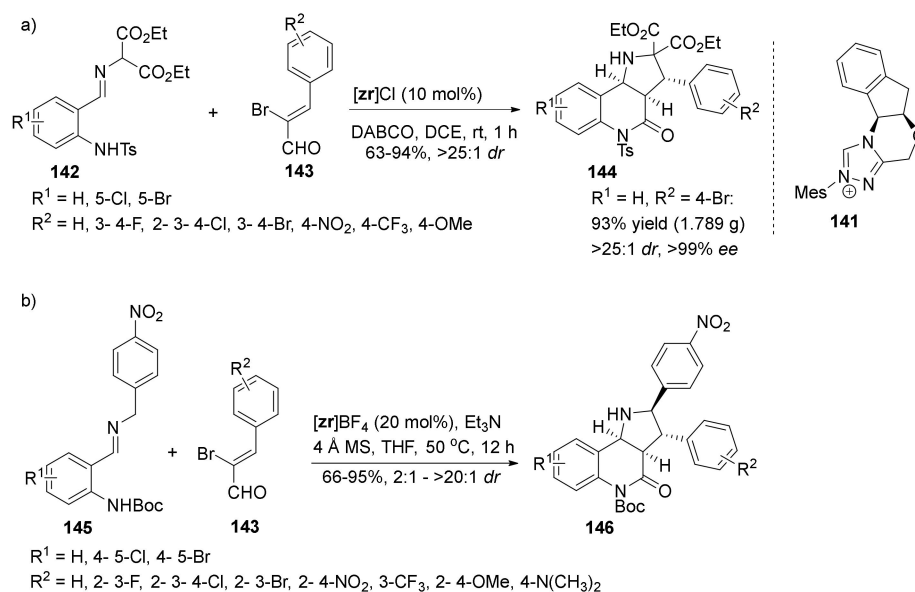
Shi and co-workers obtained the tricyclic scaffold **135** from silver catalyzed amination of inert CH-bonds (Scheme 22) [78]. The synthesis commenced from ketone **136**, which was alkylated with ethyl iodide, followed by a lithium aluminum hydride (LiAlH_4) reduction of the ketone and ester moieties. The resulting diol **137** was converted to the corresponding azide **138** via mesylation with mesyl chloride followed by treatment with sodium azide. Reduction of the diazide **138** with LiAlH_4 followed by *N*-triflation with triflic anhydride (Tf_2O) afforded diamine **139** with a 10:4 *cis/trans* relationship between the benzylic amine and the adjacent ethyl chain. The purity of the *cis*-isomer *cis*-**139** was further enhanced to approximately 90% by crystallizing out its isomer *trans*-**139**. Pyrroloquinoline **135** was finally obtained from diamine **139** by a silver catalyzed amination reaction employing silver acetate (AgOAc) as the silver source, phenanthroline **140** as the ligand, $\text{PhI}(\text{OTFA})_2$ as the oxidant, and potassium carbonate as the base in a 1:1 solvent mixture of chlorobenzene (PhCl) and dichloroethane (DCE). The reaction was run at reflux for 10 h to afford the tricyclic scaffold **135** in 30% yield.



Scheme 22. Scaffold synthesis by Zhang and co-workers.

In 2014, Hui and co-workers employed a stereoselective *N*-heterocyclic carbene **141** catalyzed cascade reaction between ortho-aromatic aldimines (such as **142**) and 2-bromoenals (such as **143**) to form the martinella scaffold in high yield and excellent enantioselectivity (Scheme 23a) [79]. They hypothesized that this one-pot cascade reaction includes a Michael addition followed by a Mannich reaction and a lactamization to produce the pyrroloquinoline scaffold with the formation of three stereocenters in the sequence. In their optimization studies, the group found that superior stereoselectivity of the reaction was observed when

using DABCO as the base rather than 1,8-diazabicyclo[5.4.0]undec-7-ene (DBU), triethylamine, or cesium carbonate. They also experienced that the choice of solvent was crucial for the stereoselective outcome of the reaction, with 1,2-dichloroethane (DCE) favoring the reaction with highest diastereoselectivity. A scope study revealed the generality of the reaction. The applicability of the reaction was finally demonstrated with a gram scale synthesis of the bromo-phenyl pyrroloquinoline **144** in 93% yield and >25:1 *dr*. The carbene catalyzed reaction was also explored by Jin, Chi, and co-workers in 2018 (Scheme 23b) [80]. Instead of the diester imine **142** employed by Hui and co-workers, the *p*-nitro benzyl imine **145** was reacted with bromoal **143** to form the pyrroloquinoline scaffold **146** in moderate to high yield and diastereomeric ratio.

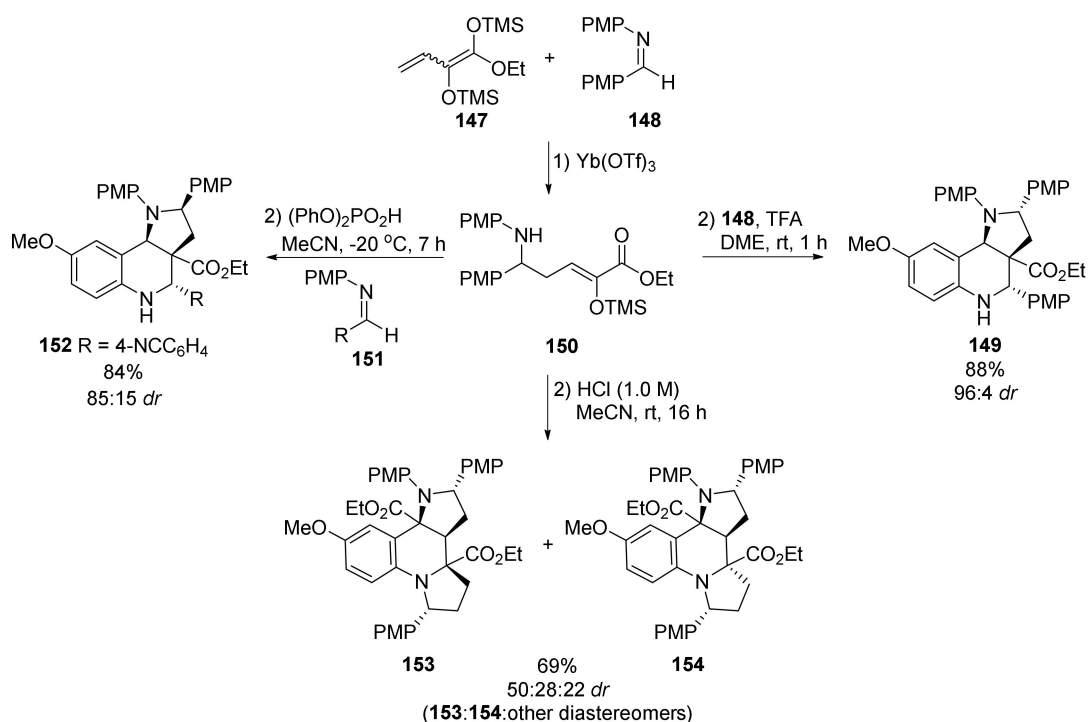


Scheme 23. Scaffold synthesis by (a) Hui and co-workers and (b) Jin, Chi, and co-workers.

Schneider and co-workers assembled the martinella scaffold in a sequential vinylogous Mannich–Mannich–Pictet–Spengler reaction [81]. Addition of bis-silyl dienediolate **147** to imine **148** in a vinylogous Mannich reaction followed by a second addition of imine **148** provided pyrroloquinoline **149** in high yield and high diastereoselectivity (Scheme 24). In their proposed mechanism, the imine was added to silyl enol **150** in a Mannich reaction to form a diamino- α -keto ester. This reactive intermediate could then spontaneously cyclize to an imine followed by a Pictet–Spengler reaction with the neighbouring anisidine to form pyrroloquinoline **149**.

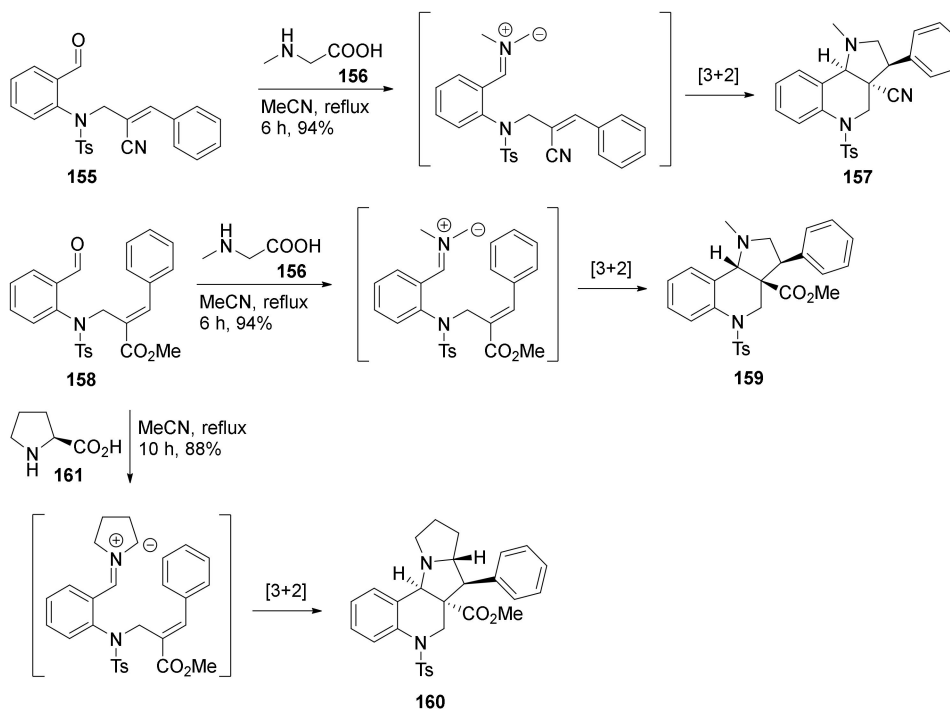
In a scope study, they observed that low diastereoselectivity was induced in the reactions between intermediate **150** and the electron poor imines, such as imine **151**. Through further work, they found that the diastereomeric outcome of the reaction could be flipped by altering reaction conditions. When acetonitrile was used as solvent, instead of 1,2-dimethoxyethane, and by altering the Brønsted acid from trifluoroacetic acid (TFA) to diphenyl phosphate, in addition to running the reaction at low temperature (−20 °C), they obtained diastereomer **152** with 85:15 *dr* in 84% yield.

The Schneider group reported a follow-up of this synthesis in 2018 [82]. When intermediate **150** was subjected to a Brønsted acid, such as HCl, dipyrroloquinolines **153** and **154** were formed in a combined yield of 69% and a ratio of 50:28:22 (**153**:**154**:other diastereomers) (Scheme 24). The group proposed that the cyclic imine formed from intermediate **150** in an acid catalyzed reaction reacted with its enamine tautomer in a Mannich reaction to form a dimer. This was then followed by a Pictet–Spengler cyclization to form the dipyrroloquinoline scaffold **153** and **154**, with the major diastereomer **153** in endo-configuration.



Scheme 24. Synthesis of the pyrroloquinoline and the dipyrroloquinoline scaffolds by Schneider and co-workers.

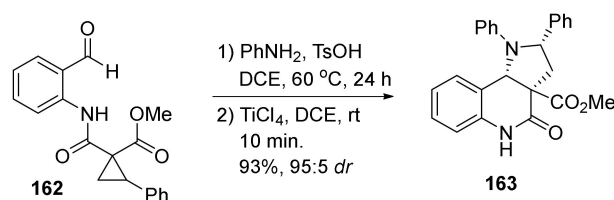
Bakthadoss and co-workers obtained the martinella scaffold from Bayliss Hillman derivatives via a 1,3-dipolar cycloaddition [83]. *N*-tosyl-*N*-allyl-2-aminobenzaldehyde (**155**) was treated with *N*-methyl glycine (**156**) to form pyrroloquinoline **157** in 94% yield through imine formation and decarboxylation followed by a 1,3-dipolar cyclization reaction (Scheme 25).



Scheme 25. Scaffold synthesis by Bakthadoss and co-workers.

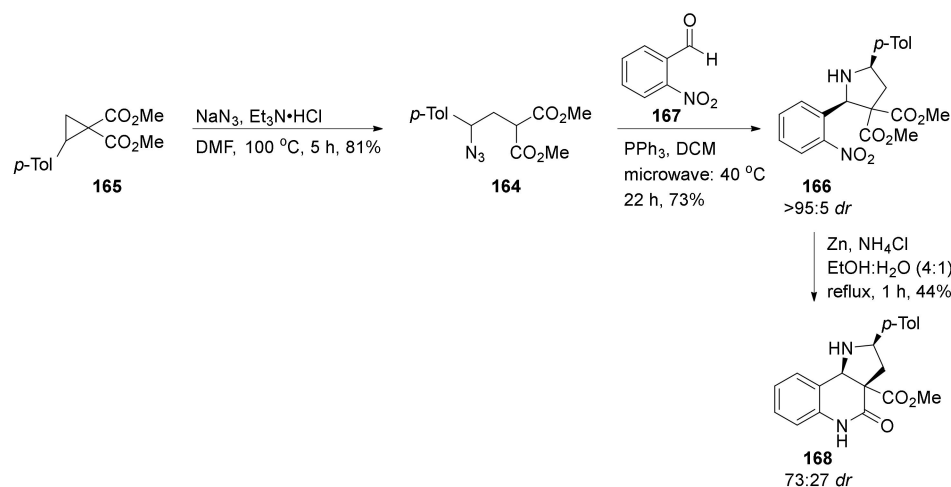
Pyrroloquinoline **157** comprised a *trans*-relationship between the nitrile and benzyl functionality. The reaction between *N*-allylated aldehyde **158** and glycine **156** provided pyrroloquinoline **159** with the benzyl moiety in *cis*-configuration to the methyl ester. The authors remark that the stereoselective outcomes coincide with the nature of the 1,3-dipolar addition reaction, with the *cis*- and *trans*-products **157** and **159** originating from *cis*-alkene **155** and *trans*-alkene **158**, respectively. The group further produced tetracyclic pyrrolizinoquinoline **160** by treating aldehyde **158** with L-proline (**161**), using the same conditions as previously described.

Xiang and co-workers produced the martinella scaffold in an intramolecular [3+2] annulation of an acceptor-donor cyclopropane and an imine formed in situ [84]. Amide functionalized cyclopropane **162** was treated with aniline, initially at room temperature for 48 h, followed by addition of titanium tetrachloride (TiCl₄) to provide pyrroloquinoline **163** in 40% yield and 8:2 dr (Scheme 26). The product **163** was obtained in 93% yield and 95:5 dr, and reaction time was decreased to 24 h when the reaction temperature was increased to 60 °C and using toluene sulfonic acid (TsOH) as an additive in the first reaction in the sequence.



Scheme 26. Scaffold synthesis by Xiang and co-workers.

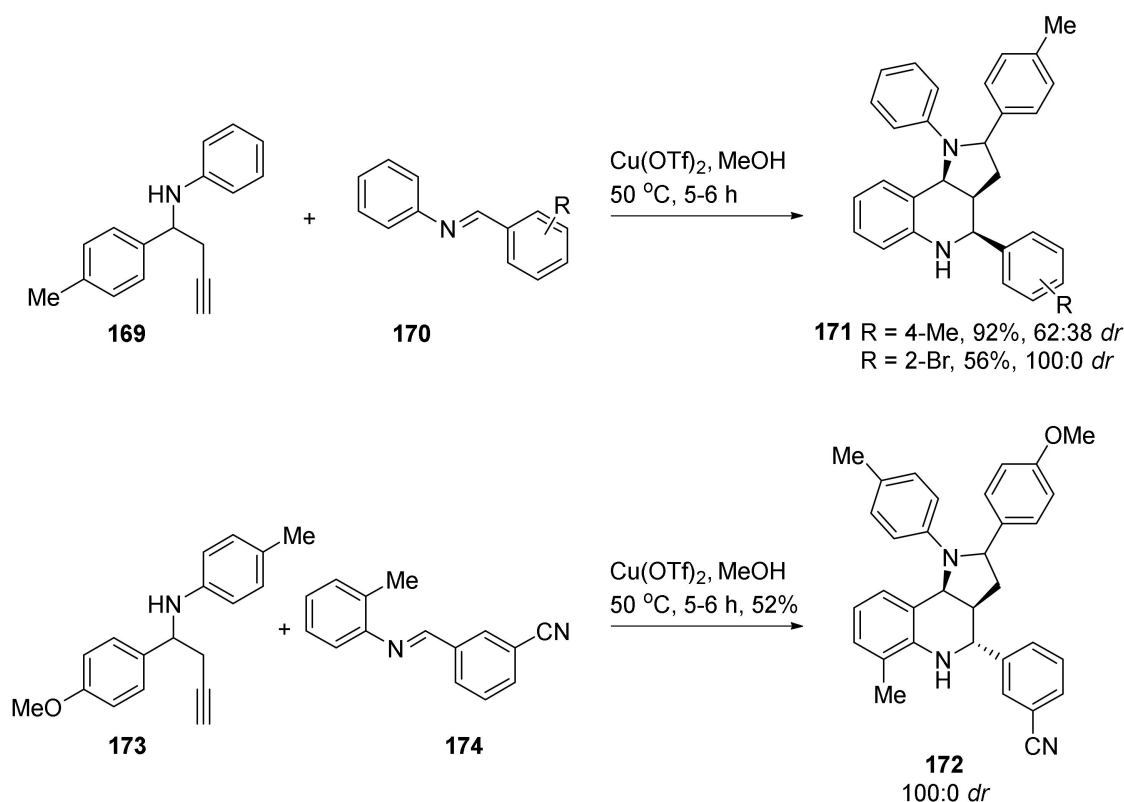
A similar version of the pyrroloquinoline scaffold **163** presented by Xiang and co-workers was also formed by Trushkov and co-workers as part of their combinatorial synthesis of di- and tetrahydropyrrole scaffolds (Scheme 27) [85]. The formation of the pyrroloquinoline scaffold commenced from azide **164**, a building block formed from cyclopropane **165** by a ring opening procedure developed in the Trushkov group [86]. The pyrroline **166** was further formed from azide **164** in a domino reaction including a Staudinger reduction of the azide functionality in compound **164**, followed by condensation with *p*-nitro benzaldehyde **167** and finally a reduction of the resulting iminium intermediate to the corresponding amine. Zinc mediated nitro reduction of the domino reaction product **166** facilitated the amidative ring closure and thus the formation of pyrroloquinoline **168**.



Scheme 27. Scaffold synthesis by Trushkov and co-workers.

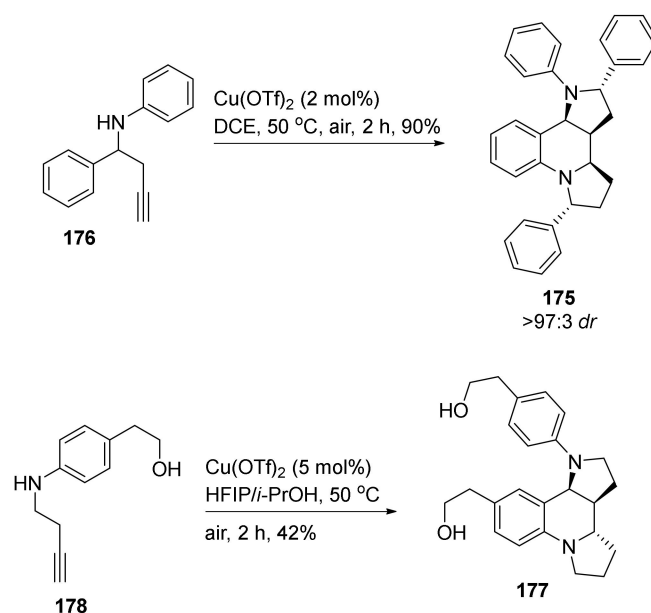
As part of a study on β -amino alkyne reactivity, Li and co-workers produced the martinella scaffold in a copper catalyzed cascade reaction including hydroamination of

a β -amino alkyne followed by a Povarov reaction (Scheme 28) [87]. The β -amino alkyne **169** was activated with copper triflate to form the corresponding cyclic enamine, which in a Povarov reaction with the aromatic imine **170**, formed pyrroloquinoline **171**, with the major diastereomer in endo-configuration. The group further examined the reaction outcome from replacing copper triflate with other catalysts. Comparable results were obtained with copper chloride and iron triflate ($\text{Fe}(\text{OTf})_3$); however, using zinc triflate or mercury triflate did not provide the desired product. The protic catalysts triflic acid and benzoic acid had no effect on the reaction. In work aimed at broadening the scope of the reaction the group observed that different R-groups on the aromatic rings facilitated variations in the endo/exo preference of the reaction products, exemplified here with the two diastereoselective reactions that generated the endo-**171** and exo-**172** products, respectively.



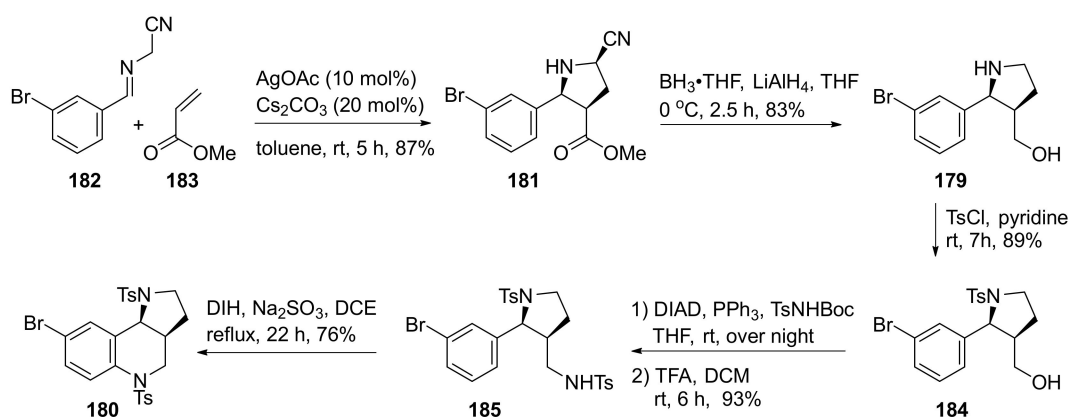
Scheme 28. Pyrroloquinoline scaffold synthesis by Li and co-workers.

Li and co-workers further extended the utility of the copper catalyzed reaction to include synthesis of dipyrroloquinolines (such as **175**) from aminoalkynes (such as **176**) (Scheme 29) [88]. Instead of using an aromatic imine **170** in a Povarov reaction, the dipyrroloquinoline **175** was formed as a dimer. The proposed mechanism for this dimerization was a formal [4+2]-cycloaddition of the enamine formed in situ from the copper catalyzed hydroamination of aminoalkyne **176**, to its imine tautomer. The group also showed that this method could be used to synthesize the aglycon moiety of Incargranine B (**177**) from aminoalkyne **178**.



Scheme 29. Dipyrroloquinoline scaffold synthesis by Li and co-workers.

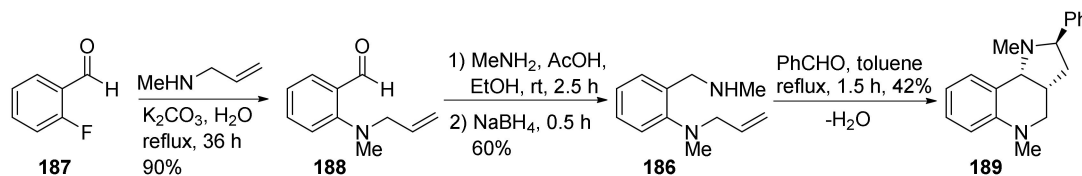
In a scope study of their synthetic route to multisubstituted β -prolinols such as **179**, the Zhang group put together the tricyclic scaffold **180** (Scheme 30) [89]. A [3+2] cycloaddition mediated by silver acetate provided cyanoester **181** from imine **182** and Michael acceptor **183**. Cyanoester **181** was then converted to prolinol **179** via ester reduction and concomitant reductive decyanation. For the reduction reaction, Zhang and co-workers explored a variety of reducing agents, including lithium aluminum hydride (LiAlH_4), diisobutylaluminum hydride (DIBAL-H), borohydride (BH_3), sodium borohydride (NaBH_4), and combinations of these. A combination of lithium aluminum hydride and borane provided prolinol **179** in highest yield. The *N*-tosylated prolinol **184** was obtained upon treatment with tosyl chloride, and further converted to the *N*-tosylated diamine **185** in a substitution reaction with *N*-Boc-toluenesulfonamide. A final aromatic C–H amination facilitated by 1,3-diiodo-5,5-dimethylhydantoin (DIH) furnished pyrroloquinoline **180** in 76% yield.



Scheme 30. Scaffold synthesis by Zhang and co-workers.

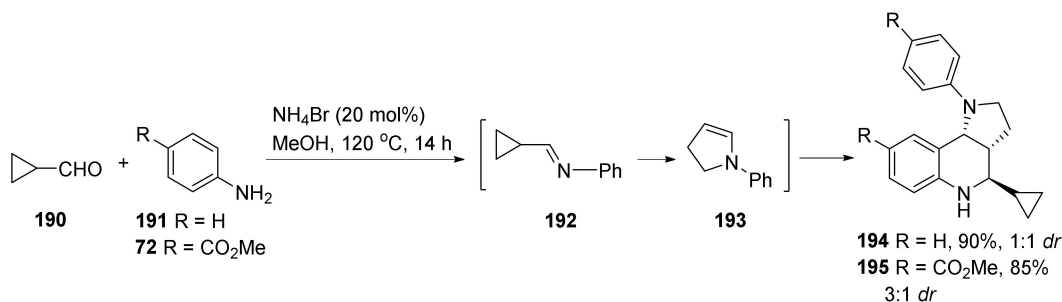
Xiang and co-workers formed the tricyclic scaffold from azomethine ylides (Scheme 31) [90]. Ylide **186** was prepared by coupling of 2-fluorobenzaldehyde **187** with *N*-methyl allylamine followed by condensation of the resulting aldehyde **188** with methylamine. The pyrroloquinoline **189** was formed as a mixture of enantiomers in moderate yield in a 1,3-dipolar cycloaddition between azomethine ylide **186** and benzaldehyde, while removing water by azeotropic distillation. Xiang and co-workers further observed that the

yield from the cycloaddition reaction was somewhat enhanced (53–56%) when the aromatic ring in aniline **186** contained electron withdrawing substituents, such as a chloro or nitro group. Conversely, they observed a decreased reaction yield (19%) when applying said reaction conditions to the *m*-methoxy derivative of aniline **186**.



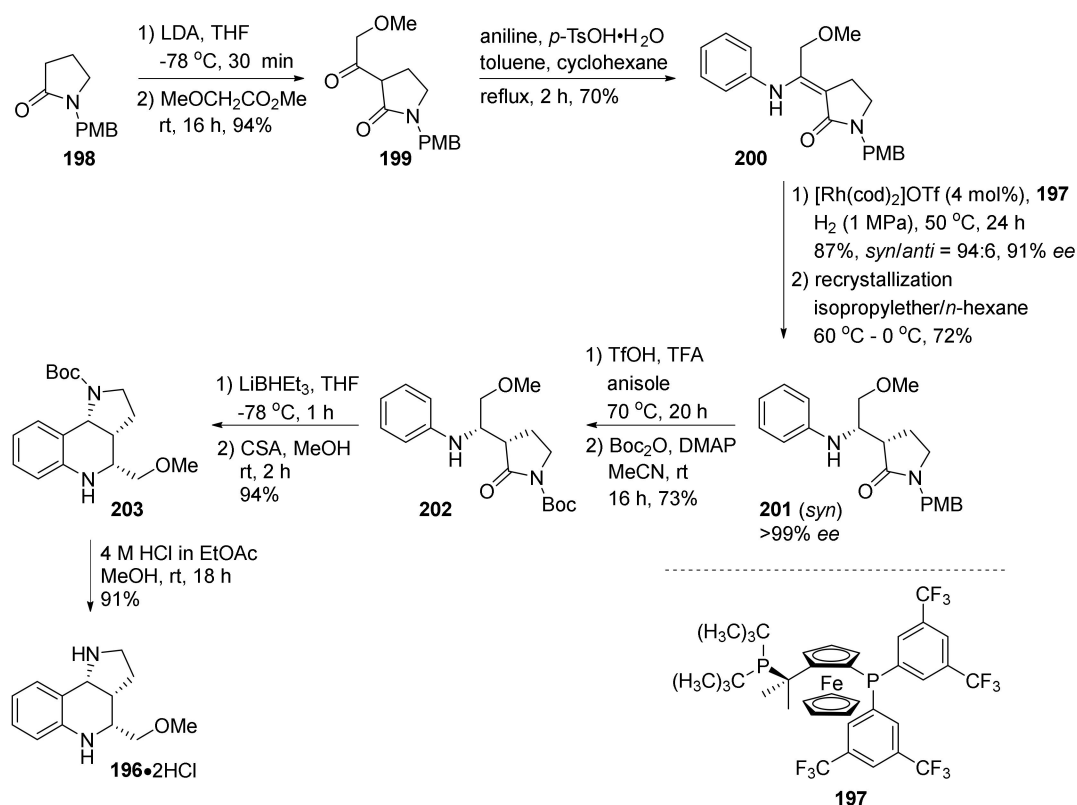
Scheme 31. Scaffold synthesis by Xiang and co-workers.

Another method for preparation of the tricyclic scaffold was presented by Huang and co-workers [91]. They treated cyclopropyl amine **190** and aniline **191** with ammonium bromide to promote formation of imine **192** in a condensation reaction (Scheme 32). Further catalytic isomerization of the cyclopropylimine **192** to dihydropyrrolidine **193** followed by a Povarov reaction between the imine **192** and the enamine **193** afforded pyrroloquinoline **194**. When conducting the reaction with halide-substituted anilines, the group found that the *p*-anilines provided the pyrroloquinolines in highest yield. Nearly all reactions provided the product in approximately 1:1 diastereomeric mixtures, except in the case of *p*-CO₂Me-aniline **72**, which afforded the product **195** with the major stereoisomer in *exo*-configuration.



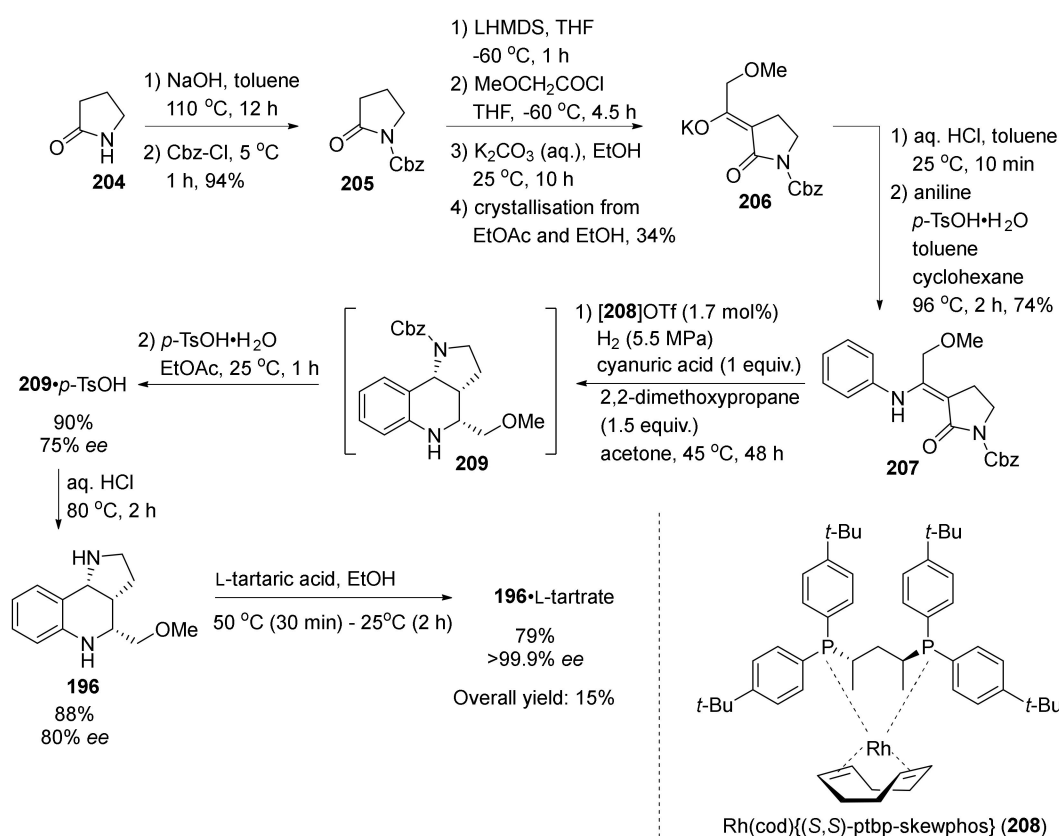
Scheme 32. Scaffold synthesis by Huang and co-workers.

Tatsuta and co-workers at Waseda University together with Kondo at Takeda Pharmaceutical company developed a method for the synthesis of pyrroloquinoline **196** via an asymmetric hydrogenation reaction using a rhodium catalyst together with the ferrophosphine ligand **197** (Scheme 33) [92,93]. The synthesis commenced from PMB-protected pyrrolidone **198**, which was alkylated with methyl methoxyacetate to form methoxy ketone **199**. Enamine **200** was obtained from the acid catalyzed condensation of ketone **199** with aniline. Rhodium-catalyzed asymmetric reduction of the enamine **200** followed by recrystallization in isopropylether and *n*-hexane afforded the enantiopure amine **201**. The *N*-protecting group was then converted from *p*-methoxybenzyl (PMB) to *t*-butyloxycarbonyl (Boc) to form compound **202**, which was compatible with the following amide reduction by lithium triethyl borohydride (LiBHET₃). Acid catalyzed intramolecular cyclization of the reduced product afforded pyrroloquinoline **203** in 94% yield over two steps. The final enantiopure product **196** was obtained in 21% overall yield as the HCl-salt upon acidic Boc-deprotection of carbamate **203**.



Scheme 33. First generation rhodium catalyzed asymmetric synthesis of the pyrroloquinoline scaffold by Tatsuta and co-workers at Waseda University together with Kondo at Takeda Pharmaceutical company.

A second generation asymmetric synthesis of the pyrroloquinoline methyl ether **196** (Scheme 33) was reported by Yamada and co-workers at Takeda Pharmaceutical company (Scheme 34) [94]. To avoid the need for changing the protecting group during the synthetic pathway, pyrrolidone **204** was protected with a benzyloxy carbonyl (Cbz) group. The resulting *N*-protected pyrrolidone **205** was acylated with methoxyacetyl chloride and converted to the more stable potassium salt **206** by treatment with potassium carbonate in ethanol followed by a recrystallization step. The salt **206** was liberated to the corresponding ketone by treatment with hydrochloric acid and then condensed with aniline to afford enamine **207** in 74% yield. Asymmetric hydrogenation of enamine **207** with rhodium catalyst **208** in the presence of cyanuric acid and 2,2-dimethoxypropane provided pyrroloquinoline **209**, which was converted into **209** \cdot *p*-TsOH by treatment with *p*-toluenesulfonic acid. The direct conversion of enamine **207** to the cyclized product **209** under said reduction conditions was a fortunate surprise for Yamada and co-workers. They hypothesized that the cyclization process proceeded in a four-step domino cascade. In their proposed mechanism, asymmetric hydrogenation of enamine **207** followed by a carbonyl reduction of the pyrrolidone formed the corresponding *N,O*-acetal, which was dehydrated and sulfonated with triflate present in the mixture. Finally, the triflate participated in a *cis*-selective intramolecular cyclization reaction with the aniline moiety to assemble the pyrroloquinoline scaffold **209**. Amine **196** was obtained in 88% yield and 80% ee upon removal of the *N*-Cbz protecting group. Further chiral resolution with *L*-tartaric acid afforded the enantiopure tartrate salt **196** \cdot *L*-tartrate. The reaction which was conducted in large scale gave 62 kg of the final product **196** \cdot *L*-tartrate.

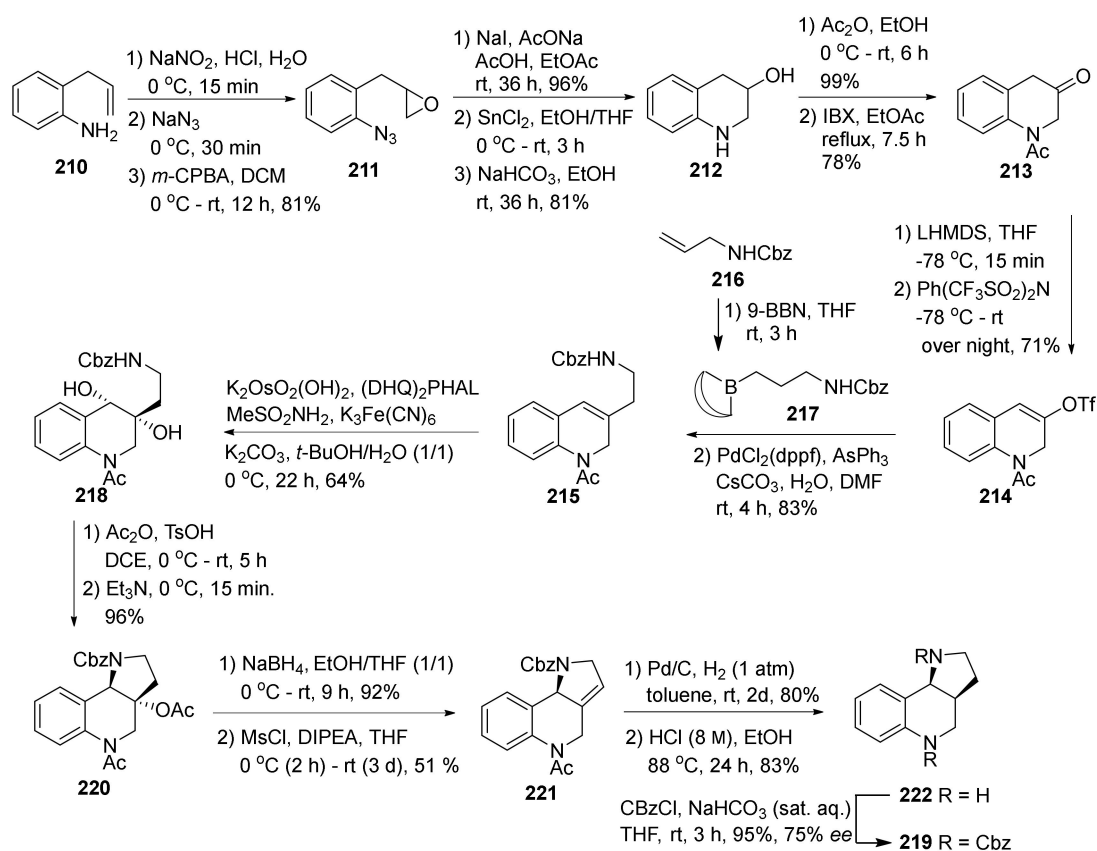


Scheme 34. Second generation rhodium catalyzed asymmetric synthesis of the pyrroloquinoline scaffold by Yamada and co-workers at Takeda Pharmaceutical company.

In our group, we investigated the applicability of Sharpless' asymmetric strategies to obtain the tricyclic scaffold stereoselectively without the use of chiral building blocks or chiral auxiliary (Scheme 35) [95]. Allylamine **210** was converted to cyano-epoxide **211** by treatment with sodium azide followed by *m*-chloroperbenzoic acid (*m*-CPBA) epoxidation. Ring-opening of the epoxide **211** with sodium iodide followed by azide reduction and resulting quinoline cyclization afforded quinoline-3-ol **212**. The quinoline amine **212** was then acetylated and the alcohol functionality was oxidized with 2-iodoxybenzoic acid. By treating the resulting ketone **213** with triflating agent *N*-phenyl-bis(trifluoromethanesulfonylimide), using lithium bis(trimethylsilyl)amide as the base, gave triflate **214** in 71% yield. The Sharpless dihydroxylation substrate, namely alkene **215**, was obtained from a sequential reaction entailing the hydroboration of *N*-Cbz-protected allylamine **216** followed by a Suzuki–Miyaura cross-coupling of the resulting boron **217** with triflate **214**. The alkene **215** was further subjected to Sharpless asymmetric dihydroxylation (AD) conditions, using (DHQ)₂PHAL as the chiral ligand, to enantioselectively afford diol **218** in 64% yield.

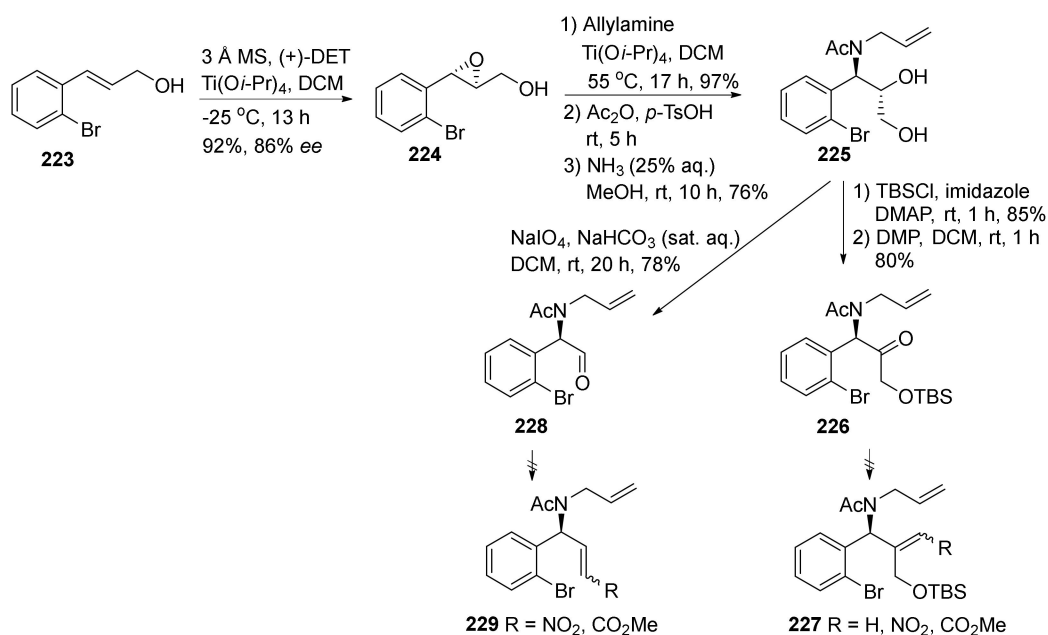
The stereochemistry of the diol **218** was assigned by using Sharpless mnemonic device, which is a tool that can rationalize face selectivity of the AD reaction [96]. The stereochemical outcome from the AD reaction was later confirmed by HPLC analysis of *N*-Cbz protected pyrroloquinoline **219** on a chiral column. Acid catalyzed acetylation of diol **218** facilitated formation of the tricyclic structure **220** via an intramolecular substitution reaction. Based on the mechanism proposed by Jagadeesh and Rao [97], we hypothesized that the diacetate first underwent an intramolecular S_N1 reaction, forming an acetoxonium ion intermediate. The cyclized cis-product **220** was subsequently generated from a nucleophilic attack on the acetoxonium ion by the Cbz-protected amine. Ester **220** was reduced with sodium borohydride to the corresponding alcohol and then dehydrated to alkene **221** by treatment with MsCl and Hunig's base (DIPEA). Hydrogenation of the

alkene **221** followed by acid promoted removal of the *N*-protecting groups, afforded the final product **222**.



Scheme 35. Scaffold synthesis by Lindbäck and Sydnes.

After the first generation of scaffold synthesis, an alternative synthetic strategy to enhance enantioselectivity of the pyrroloquinoline scaffold and at the same time install handles on the scaffold for further elaboration to martinellidic acid was initiated by Haarr and Sydnes (Scheme 36) [98]. Cinnamyl alcohol **223** was subjected to the Sharpless epoxidation reaction to afford bromo-epoxide **224** in 86% ee. Epoxide **224** was then regioselectively ring opened with allylamine in the presence of titanium(IV)isopropoxide to afford the corresponding amino-diol, which was subjected to a protection–deprotection sequence to afford the *N*-acetylated diol **225**. In our synthetic design, we envisioned using the two alcohol moieties to first perform ring closing of the pyrrolidine ring followed by ring closing of the hetero-quinoline ring. Attempts to selectively oxidize the primary or the secondary alcohol moieties was unsuccessful. Selective silyl protection of the primary alcohol was thus conducted, followed by oxidation of the secondary alcohol using Dess Martin Periodinane (DMP) to form ketone **226**. In order to accomplish cyclization of the pyrrolidine ring via a ring closing metathesis with the *N*-allyl functionality, we attempted to convert ketone **226** to alkene **227**. No reaction took place under Wittig or Lombardo reaction conditions. Attempts to form the corresponding nitroalkene by reacting ketone **226** with nitromethane followed by a mesylation–elimination sequence was also unsuccessful. We speculated that there could be steric issues that caused the failure to install the alkene. Diol **225** was thus subjected to sodium periodate mediated oxidative cleavage to obtain aldehyde **228**. Attempts of alkene formation were again unsuccessful and no conversion of aldehyde **228** to its corresponding alkene **229** was observed. Other efforts to work around the encountered synthetic challenges were conducted; however, those efforts were in vain.



Scheme 36. Synthetic approach towards the pyrroloquinoline scaffold by Haarr and Sydnes.

4. Synthesis of Dipyrroloquinolines Towards Natural Products Seneciobipyrrolidine (3) and Incargranine B (4)

As mentioned in the introduction, the Zhang group isolated incargranine B (3) in 2010 from *Incarvillea mairei* var. *grandiflora* [25]. Based on the spectroscopical data, they proposed an indolo-[1,7]naphthyridine core structure for the alkaloid (Figure 2a). When Lawrence and co-workers later studied the most likely biogenesis route to incargranine B (3) from the main sources of alkaloid building blocks, they firstly recognized that incargranine B appeared to be a dimer biosynthesized from the glycosylated tyrosine precursor, salidroside (Figure 2, red part) [26]. However, they struggled to propose a plausible mechanism for the synthesis of the heterocyclic part (Figure 2a, blue part) of incargranine B. This led them to hypothesize that the originally proposed structure was wrongly assigned and that incargranine B in fact was a dipyrroloquinoline (Figure 2b) [26].

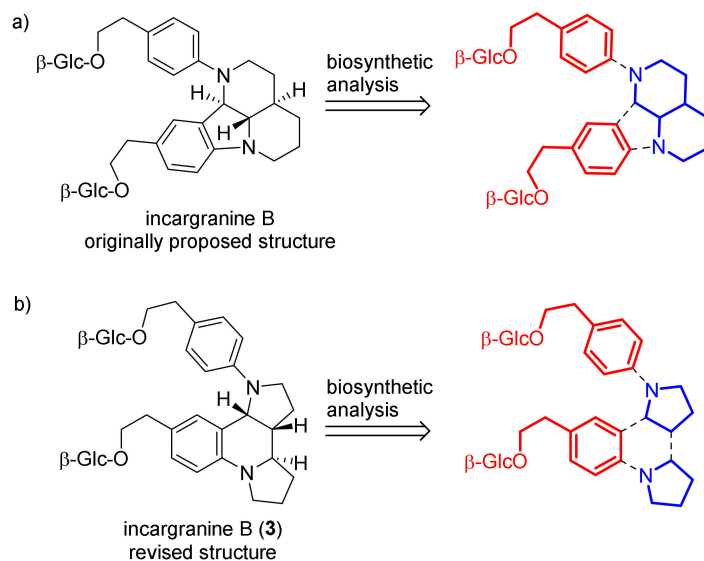
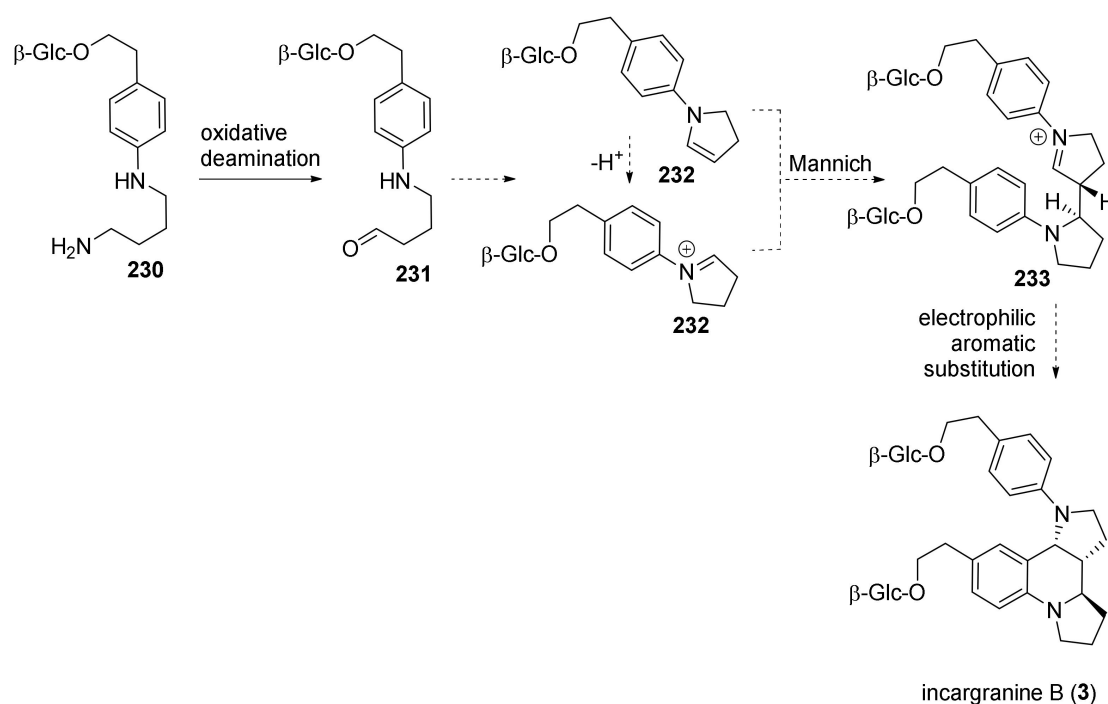


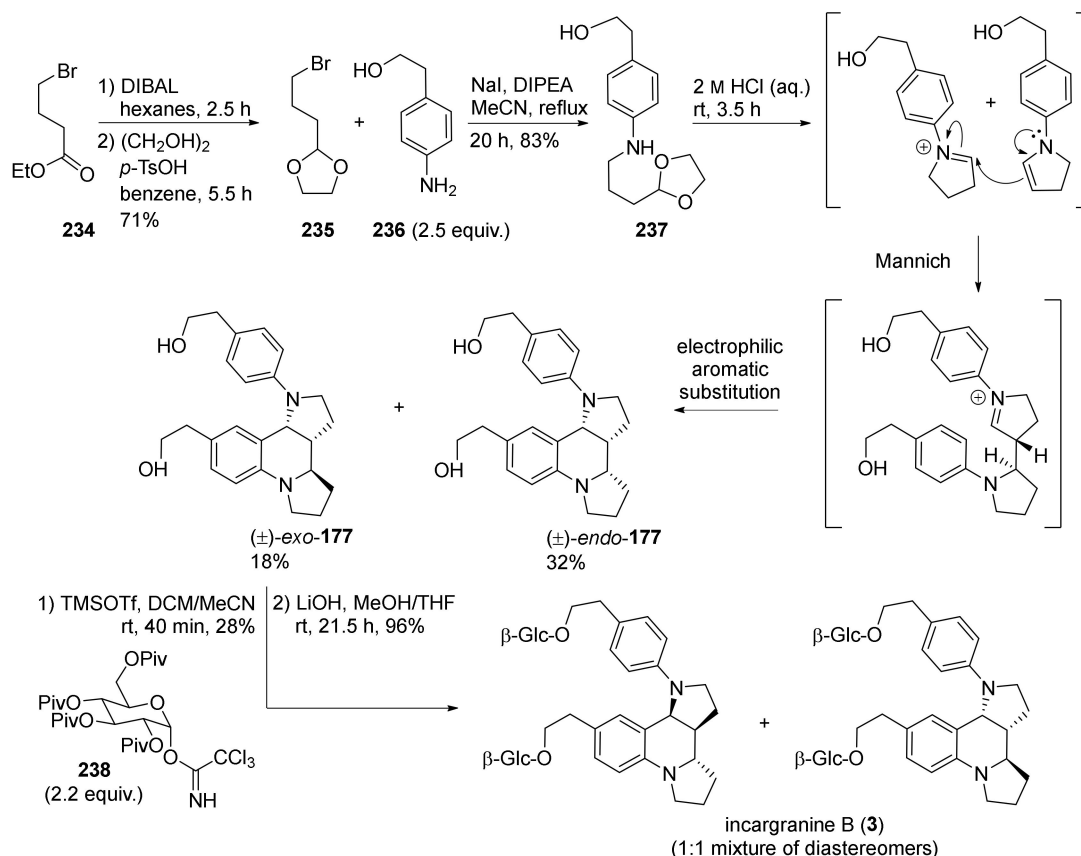
Figure 2. Biosynthetic analysis of incargranine B. (a) Originally proposed structure. (b) Revised structure.

With this hypothesis in mind, Lawrence and co-workers suggested a biosynthetic route towards incargranine B (**3**), where phenylethanoid-diamine **230** was a reasonable precursor (Scheme 37). Diamine **230** could undergo oxidative deamination to form an amino aldehyde **231** that would undergo an intramolecular condensation to give imine/enamine **232**. Dimerization of the imine/enamine **232** through a Mannich reaction to form an imine intermediate **233** that could be trapped in an electrophilic aromatic substitution reaction would provide incargranine B (**3**).



Scheme 37. Lawrence and co-workers' proposed biosynthetic pathway to incargranine B (**3**).

To confirm their structural revision work and suggested biosynthetic pathway, Lawrence and co-workers completed a biomimetic total synthesis of the revised structure for incargranine B (**3**) (Scheme 38). Reduction of ester **234** with DIBAL followed by acetal protection of the resulting aldehyde provided acetal **235** in 71% yield. Alkylation of aniline **236** with acetal **235** gave the dimerization precursor, acetal **237**. Acidic hydrolysis of the acetal to form the corresponding aldehyde facilitated condensation with the amine to form the enamine in equilibrium with the iminium ion. Further dimerization in a Mannich reaction followed by electrophilic aromatic substitution provided dipyrroloquinoline **177** as a close to racemic mixture (scalemic mixture). The isolated diastereomer (\pm)-*exo*-**177** was further glycosylated with *O*-pivaloyl-protected glucoside **238**. After basic deprotection of pivaloyl-groups with lithium hydroxide, incargranine B (**3**) was obtained as a mixture of diastereomers. The spectroscopic data of the synthesized incargranine B (**3**) were in full accord with the data reported by Zhang for the isolated natural product.



Scheme 38. Synthesis of Incargranine B completed in the Lawrence group.

The optical rotation of the diastereomeric mixture **3** ($\alpha = -16.7$ ($c = 0.275$, MeOH)) was close to the reported optical rotation of the isolated natural product ($\alpha = -12$ ($c = 0.275$, MeOH)). Lawrence and co-workers therefore suggested that the isolated natural product **3** also consists of a mixture of diastereomers. They further drew a parallel to the biosynthetically related diglycosidic alkaloid, millingtonine (**239**) (Figure 3), which also naturally occurs as a mixture of diastereomers. The discrepancies of the optical rotation values between the isolated martinellid alkaloids and the synthesized enantiomers have resulted in several groups, suggesting that the martinella alkaloids also most likely are a close to racemic (or scalemic) mixture of enantiomers [30].

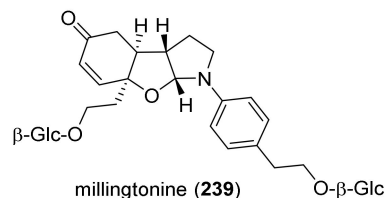
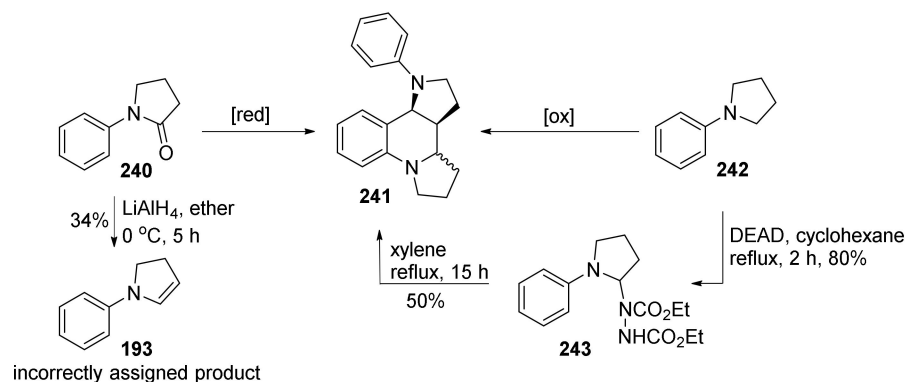


Figure 3. Millingtonine (**239**).

Interestingly, the dipyrroloquinoline scaffold was discovered in the laboratory decades before it was found in nature. The first synthesis of the dipyrroloquinoline was actually conducted in 1955 by Wittig and Sommer, in a lithium aluminium hydride (LiAlH₄) reduction reaction with lactam **240** (Scheme 39) [99]. The resulting product was incorrectly characterized to be pyrrole **193**, accompanied by a comment on how the properties of this product **193** was remarkably different from its stereoisomer, i.e., the corresponding 2,5-dihydropyrrole. The error was discovered in 1974 by Swan and Wilcock and Kerr and co-workers in two separate studies [100,101]. Both groups described that the product

formed under the Wittig and Sommer reaction conditions was in fact the dipyrroloquinoline **241** produced by dimerization of the enamine in equilibrium with the corresponding imine (Table 3, entry 1).



Scheme 39. Early work by Wittig and Sommer, followed by structural revision and additional reaction conditions reported by Swan, Wilcock, Kerr, and others to form the dipyrroloquinoline scaffold.

Table 3. Oxidative and reductive reaction conditions for formation of dipyrroloquinoline **241**.

Entry	Starting Material	Conditions	Yield ^a	Endo:Exo	Reference
1	240	LiAlH ₄ , ether, rt, 3.5 h	27%	38:36	[100]
2	242	O ₃ , <i>n</i> -hexane, 0 °C	41%	NR	[101]
3	242	1) DEAD, cyclohexane, reflux, 2 h, 80% 2) xylene, reflux, 15 h	50%	28:22	[101]
4	242	γ-irradiation, 17 d	9%	~1:1	[102]
5	242	di- <i>t</i> -butylperoxide, 140 °C, 44 h	NR	~1:1	[102]
6	242	Dibenzoyl peroxide, MeCN, 0 °C, 9 h	28%	1:0	[102]
7	242	<i>t</i> -BuOOH, NaOAc•3H ₂ O, cyclohexane 70 °C, 24 h	72%	1:0	[103]
8	242	Cu(OAc) ₂ , O ₂ , Et ₃ N	26%	11:15	[104]
9	240	PhMe ₂ SiLi, −78 to −20 °C	47%	31:16	[105]

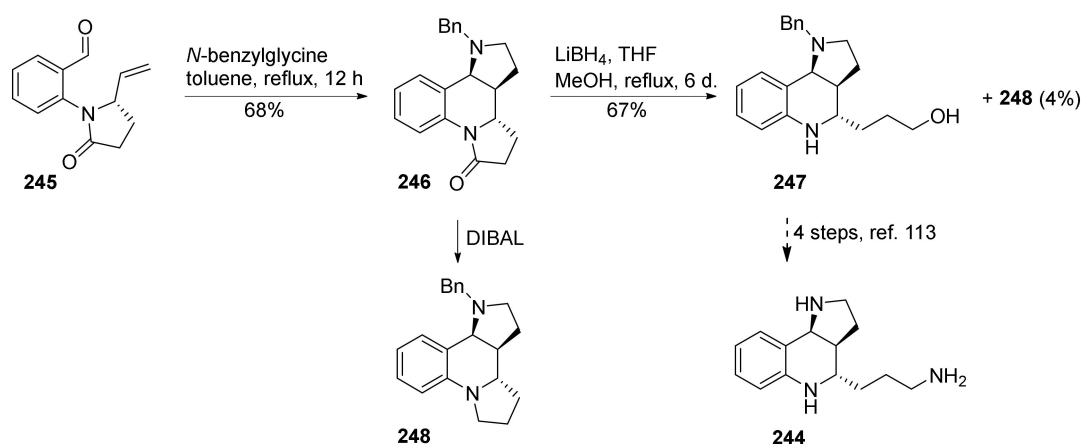
^a isolated combined yield of stereoisomers; NR = not reported.

Kerr and co-workers suggested that formation of the endo-product **241** as the major stereoisomer could support a concerted hetero Diels Alder dimerization mechanism [101]. In the same report, they also presented formation of the dimer **241** by oxidation of pyrrolidine **242** with ozone, or by using diethyl azodicarboxylate (DEAD) to form hydrazine **243**, followed by thermal decomposition [101] (Scheme 39, Table 3, entry 2 and 3). Swan and co-workers similarly presented oxidative formation of the dimer **241** from pyrrolidine **242** using gamma-rays or peroxides (Table 3, entry 4–6) [102]. They suggested that the intermediate enamine was, under these conditions, formed from the pyrrolidine radical. When treating pyrrolidine **242** with *t*-butylperoxide, a mixture of stereoisomeric dimers **241** was formed. However, with dibenzoyl peroxide, only the endo-stereoisomer **241** was isolated. This peculiarity was also observed by Rao and Periasamy when they treated pyrrolidine **242** with *t*-butyl hydroperoxide (HYDRO) in the presence of sodium acetate to form the endo-dimer **241** in 72% yield (Table 3, entry 7) [103].

Another approach towards dipyrroloquinoline **241** was presented by Minakata and co-workers in 1997 [104]. They described that oxidation of pyrrolidine **242** with catalytic copper(II) and triethyl amine as an additive under an oxygen atmosphere resulted in the formation of the dimer **241** in 26% yield (Table 3, entry 8). Interestingly, this method favored formation of the exo-stereoisomer **241** in a 15:11 ratio. Buswell and Fleming later showed that the dimer **241** could be made from lactam **240**, by treatment with dimethyl phenyl silyl lithium (PhMe₂SiLi) at −78 °C (Table 3, entry 9) [105]. Due to the high nucleophilicity of

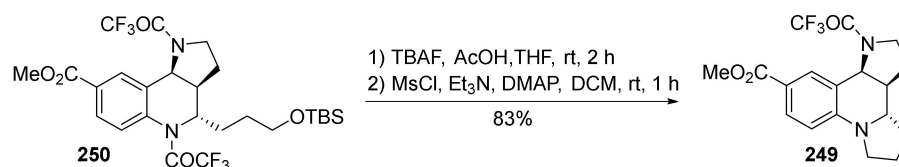
PhMe_2SiLi , Fleming suggested that the dimerization mechanism did not involve formation of an imine intermediate. Instead, he proposed that dimerization occurred between a pyrrolocarbene, formed from α -elimination of dimethyl phenyl silane oxide, and the corresponding dimethyl phenyl silane enolate. Formation of the dipyrroloquinoline **241** as a side product dimer when utilizing *N*-phenyl pyrrolidine in reactions with oxidative conditions is today a well-known issue [106–112].

In their synthesis of triamine **244**, Snider and co-workers prepared dipyrroloquinoline **245** as an intermediate (Scheme 40) [113]. A similar tetracycle **52** was also prepared by the Naito group in the RACE reaction previously mentioned (Scheme 7) [31]. Reduction of amide **246** with lithium borohydride afforded the desired alcohol **247** and minor amounts of pyrroline **248**. Moreover, Snider mentioned that reduction with lithium aluminium hydride gave tricycle **247** and tetracycle **248** in a 1:1 mixture, and that dipyrroloquinoline **248** was formed exclusively upon treatment with DIBAL.



Scheme 40. Snider and co-workers' synthesis of dipyrroloquinoline scaffold.

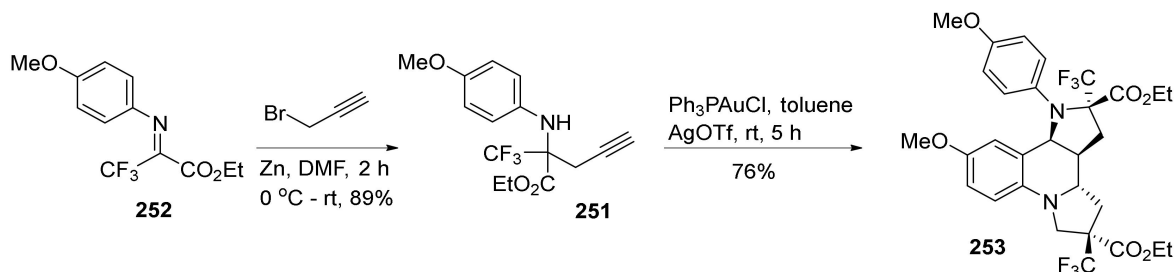
In a similar fashion to Snider, Ma and co-workers synthesized the dipyrroloquinoline **249** as a side product in their asymmetric total synthesis of martinellidic acid [29]. *N*-,*O*-deprotection of pyrroloquinoline **250** with TBAF followed by treatment of the corresponding alcohol with methanesulfonyl chloride provided dipyrroloquinoline **249** in a substitution reaction in 83% yield (Scheme 41). The X-ray structure of tetracycle **249** was used to confirm the exo-stereochemistry of the pyrroloquinoline scaffold **250** and consequently also the final product of the synthesis, namely (–)-martinellidic acid ((–)-**2**).



Scheme 41. Ma and coworkers' conversion of pyrroloquinoline **250** to dipyrroloquinoline **249**.

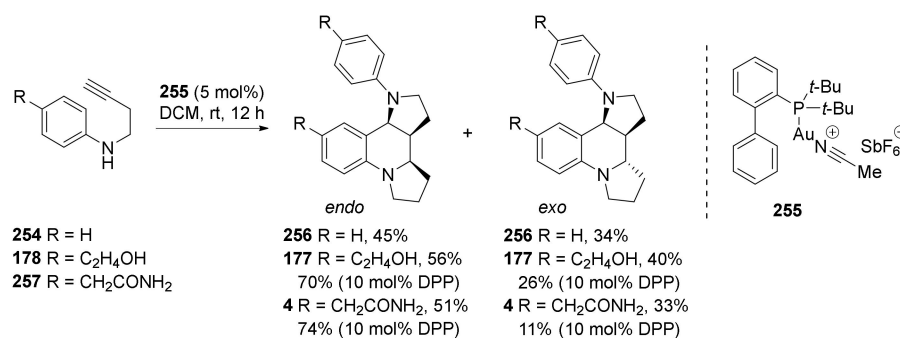
Fustero and co-workers developed a gold catalyzed stereoselective hydroamination of a propargylic amino ester, namely compound **251**, to form the dipyrroloquinoline scaffold as the exo-dia stereoisomer [114]. The reaction sequence commenced by treating iminoester **252** with propargylbromide in the presence of zinc providing propargylic amino ester **251** in good yield (Scheme 42). Hydroamination of the propargylic amino ester **251** to form the exo-dimer **253** was catalyzed by triphenylphosphine goldchloride (Ph_3PAuCl) and silver triflate (AgOTf) as an additive. During the optimization studies the group observed that solvents that were more polar than toluene, such as methanol and acetonitrile, resulted in the formation of more complex product mixtures and consequently lower yields of the desired product. As opposed to the choice of solvent, which had a large effect on the

outcome of the reaction, the use of different gold catalysts in the presence of AgOTf, and other additives such as AgNTf₂, AgSbF₆, and AgBF₄ in the presence of Ph₃PAuCl gave comparable results and yields (68–78%) to the ones obtained under the original conditions.



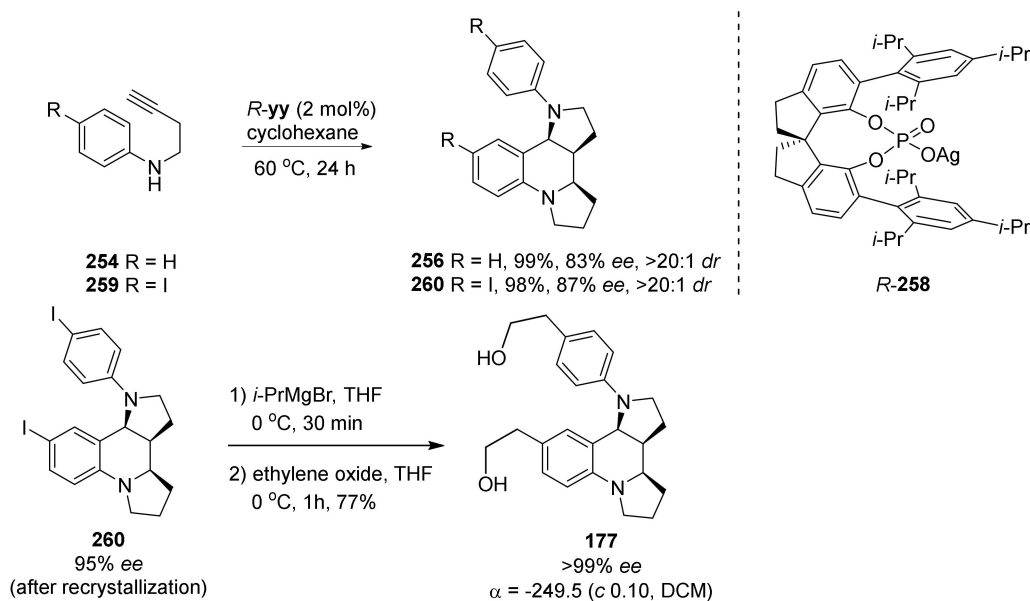
Scheme 42. Scaffold synthesis by Fustero and co-workers.

Another gold-catalyzed hydroamination of an aminoalkyne was described by the Liu group [115]. They presented the synthesis of the dipyrroloquinoline core from a 1,4-aminoalkyne **254** in a gold catalyzed tandem reaction with catalyst **255** (Scheme 43). The reaction sequence started with an intramolecular hydroamination reaction, followed by an aza-Diels Alder reaction, resulting in a 45:34 *endo*:*exo* mixture of diastereomer **256**. The reaction scope was further expanded to obtain the Incargranine B aglycon **177** (56:40, *endo*:*exo*), along with the natural product seneciobipyrrolidine (**4**, 51:33, *endo*:*exo*) from aminoalkynes **178** and **257**, respectively. *Endo*-diastereoselectivity was enhanced by addition of 10 mol% diphenylphosphate (DPP) to the reaction mixtures.



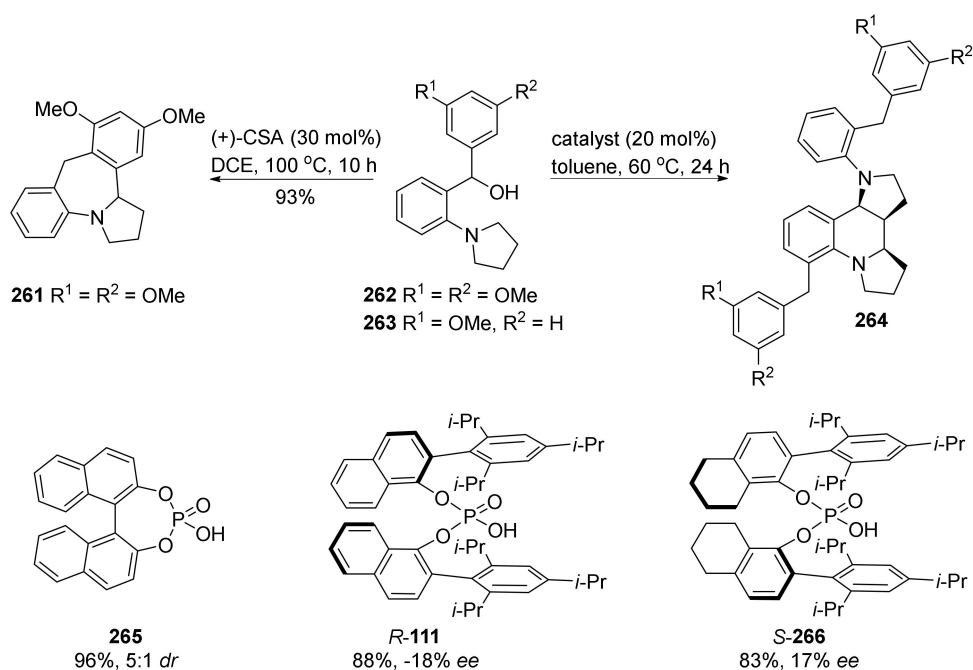
Scheme 43. Scaffold synthesis developed in the Liu group.

In their pursuit to enhance the stereochemical selectivity, the Liu group turned to silver catalysis [116]. When using a chiral silver-phosphate catalyst (*R*)-**258** instead of a gold catalyst, the reaction proceeded with a higher enantio- and diastereoselectivities and higher yields on a wide array of aniline-alkyne substrates, exemplified here by alkynes **254** and **259** (Scheme 44). The resulting iodo-*endo*-product **260** was further converted to the *epi*-incargranine B aglycon **177** by means of a Grignard reaction with ethylene oxide.



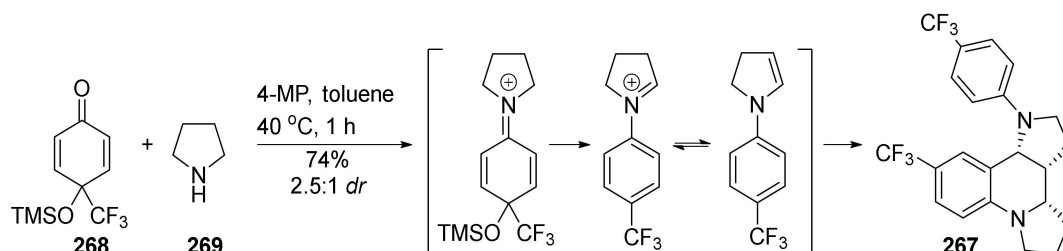
Scheme 44. The Liu group's synthesis of the aglycon moiety of incargranine B.

Xiao and co-workers were studying [1,5]-hydride transfer-cyclization reactions for the formation of benzazepines **261** from pyrrolidine **262** (Scheme 45) [117]. When investigating the scope of this reaction, they discovered that by reducing the number of methoxy substituents on the aromatic ring (the R-groups) from two to one (such as in compound **263**), benzazepines were no longer formed. Instead they obtained dipyrroloquinoline **264** in 20% yield. A study focusing on optimizing reaction conditions showed that by using the acid catalyst phenylphosphate **265** instead of (+)-10-camphorsulfonic acid ((+)-CSA) and conducting the reaction in toluene at 60 °C rather than in DCE at 100 °C gave dipyrroloquinoline **264** in 96% yield and 5:1 diastereomeric ratio, favoring formation of the endo-product (Scheme 45). The group further investigated the catalyst scope for the asymmetric synthesis of dimer **264**. From their collection of acid catalysts, the most efficient were phosphates (*R*)-**111** and (*S*)-**266**; however, these catalysts gave the exo- and endo-dimer **264** in only 18% and 17% ee, respectively.



Scheme 45. Scaffold synthesis by Xiao and co-workers.

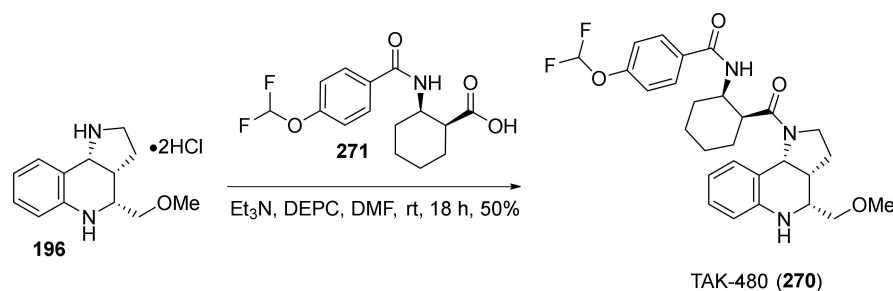
Liu and co-workers obtained the dipyrroloquinoline scaffold **267** in their study of in-situ formation of iminium ions generated from the condensation of 4-trifluoromethyl-*p*-quinols **268** with cyclic amines, such as pyrrolidine **269** (Scheme 46) [118]. Equal amounts of quinol **268** and amine **269** were stirred in toluene at elevated temperature, in the presence of 4-methoxyphenol (4-MP) as a proton donor, to afford the dipyrroloquinoline **267** in 74% yield and 2.5:1 *dr*.



Scheme 46. Scaffold synthesis by Liu and co-workers.

5. Elaborating Biological Properties

New and unusual scaffolds are as previously mentioned of great medicinal interest. Synthetic efforts to assemble the pyrroloquinoline scaffold have resulted in discovery of interesting biological activities. In 2005, Takeda Pharmaceutical company patented compounds with properties as NK₂ receptor antagonist for potential effectiveness in irritable bowel syndrome (IBS) patients [119–121]. Compounds in this patent, such as TAK-480 (**270**) (Scheme 47), were constructed around the pyrroloquinoline scaffold, which was assembled using the method developed in Takeda pharmaceutical company (Scheme 33) [92,93]. Drug candidate TAK-480 (**270**) is formed by linking the pyrroloquinoline **196** to the chiral cyclohexane carboxylic acid derivative **271**, using triethyl amine and diethyl cyanophosphonate (DEPC) in DMF (Scheme 47) [122].



Scheme 47. Coupling of pyrroloquinoline **196** and cyclohexane carboxylic acid **271** to form TAK-480 (**270**), a tachykinin NK₂ receptor antagonist, produced in Takeda Pharmaceutical company.

Another pharmaceutical compound built around the pyrroloquinoline scaffold is S-101479 (**272**), which has been produced by Kaken Pharmaceuticals (Figure 4). According to studies conducted by Furuya and co-workers, compound **272** exhibited a bone-anabolic effect in ovariectomized rats as a non-steroidal selective androgen receptor modulator (SARM) in osteoblastic cells [123,124]. The authors further suggest that, based on their results, the compound **272** could be a drug candidate for treatment of postmenopausal osteoporosis.

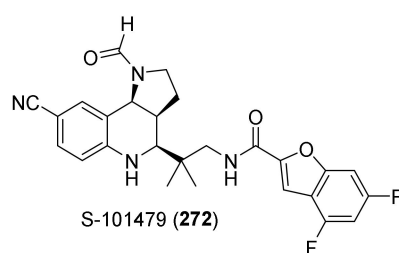


Figure 4. S-101479 (272), a drug candidate for treatment of postmenopausal osteoporosis from Kaken Pharmaceuticals.

The Broad institute diversity oriented synthesis (DOS) library, including the pyrroloquinoline-based DOS library developed by Marcaurrelle and co-workers, which was discussed previously, has in recent years been used for several high-throughput screenings of small molecules for specific biological activities [65]. Scherer and co-workers conducted a screening of the Broad Institute's small molecule collection (~100,000 compounds) against the Gram positive, anaerobic, spore-forming, opportunistic pathogen *Clostridium difficile*, a major cause of *C. difficile*-associated diarrhea (CDAD) [125]. With a high-throughput screening of the compound collection against *C. difficile*, a compound containing the pyrroloquinoline scaffold (BRD0761 (273)) displayed MIC ($\mu\text{g}/\text{mL}$) = 0.06–1 for a number of clinical *C. difficile* isolates (Figure 5). BRD0761 (273) showed greater potency, and more significantly, superior selectivity against *C. difficile* compared to the last resort antibiotic vancomycin, commonly used to treat patients with CDAD. Solubility and permeability (in Caco-2 cells) of compound BRD0761 suggested that oral dosing would be a suitable administration method. Thus, an efficacy study performed on a mouse model of CDAD was conducted with daily oral dosing of 25 mg/kg. BRD0761 (273) did reduce mortality rate as well as shedding of *C. difficile* CFU in feces, however not as efficiently as vancomycin.

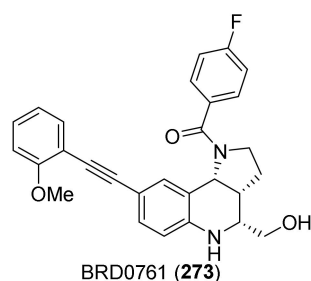


Figure 5. Inhibitor of *C. difficile* specific glutamate racemase.

Investigation of the mode of action for BRD0761 (273) via genomic analysis of resistant mutants and in silico studies revealed that the compound most likely targets cell wall biosynthesis via inhibition of glutamate racemase [125]. The enzyme is a known target in other Gram positive bacteria, such as *H. pylori* and *M. tuberculosis* [126,127]. This was, however, a novel target in *C. difficile*. Based on studies from Astra Zeneca that show species specific structure and activity of the glutamate racemase [128], Scherer and co-workers suggested that finding selective *C. difficile* glutamate reductase inhibitors may lead to identification of *C. difficile*-specific antibiotics.

The Broad institute DOS library was also included in a screening of 256,486 compounds for inhibitors of the aminotransferase BioA, an enzyme in the biotin biosynthetic pathway in *Mycobacterium tuberculosis* [129]. In an initial enzyme inhibition screening of the compound library, the pyrroloquinoline scaffold represented nearly 12% of all hits in the study, including pyrroloquinoline 274 as the screening's most potent hit (IC_{50} = 75 nM) (Figure 6). However, the activity of compound 274 dropped (MIC_{90} > 100) upon turning to whole cell screening.

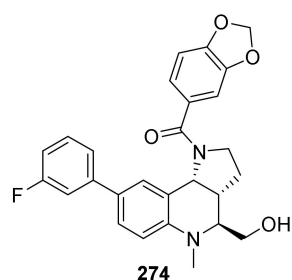


Figure 6. Inhibitor of the aminotransferase BioA.

As part of genome engineering technologies, control of the CRISPR-Cas9 activity, such as limiting off-target activity of the endonuclease Cas9, is essential. On this note, Choudhary and co-workers conducted a small molecule screen for stable, cell permeable, reversible inhibitors that disrupt the binding of the *Streptococcus pyogenes* endonuclease Cas9 (SpCas9) to DNA [130–132]. After an initial screening of representative compounds from the Broad institute DOS library, the “Povarov library”, which included a number of compounds with the pyrroloquinoline scaffold, was selected for further examination. BRD7087 (**275**) and BRD5779 (**276**) (Figure 7) were used to assess the inhibitory activity of the pyrroloquinoline scaffold. Both compounds displayed dose-dependent inhibition of SpCas9, were soluble in phosphate-buffered saline (PBS), and were non-cytotoxic.

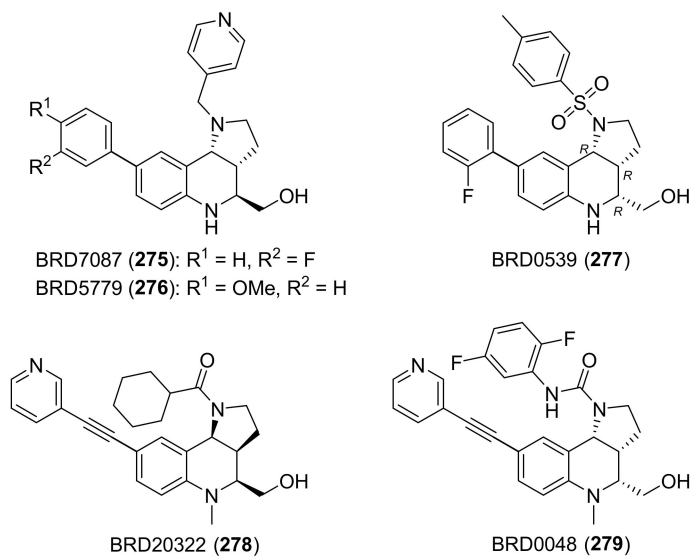


Figure 7. Inhibitors of DNA endonuclease Cas9 in *Streptococcus pyogenes* (**275–277**) and inhibitors of the transcription activation complex, comprised of dCas9:gRNA and transcription-activating SAM domains (**278–279**).

After further SpCas9 inhibitory testing of BRD7087 (**275**) analogues, one of the most promising hits, namely BRD0539 (**277**) (Figure 7), was analyzed in a structure–activity relationship (SAR) study of Cas9 inhibition potency. The study included examination of different *N*-linkages, replacement of the 2-fluorophenyl group, and evaluation of the scaffold stereochemistry. Sulfonamides on the pyrrolidine moiety displayed generally higher potency than corresponding amides. Displacement of the para-methyl group on the benzylic sulfonamide with para-fluoro, para-methoxy, or meta-methyl resulted in reduced inhibitory activity, as did introduction of heteroatoms (N and O) onto the aforementioned aromatic ring. Reduced activity was observed upon replacing the 2-fluorophenyl moiety with an alkenyl or a 3-*N,N*-dimethyl-carbamoyl-phenyl group, and also by introducing alkynyl spacers (such as seen in compounds **278** and **279**). Finally, elucidation of the four possible stereoisomers confirmed that the pyrroloquinoline **277**

with *R,R,R*-stereochemistry was the most potent inhibitor of SpCas9-DNA binding. In an equivalent approach to landing BRD0539 (277) as a functional potent SpCas9 inhibitor, BRD20322 (278) and BRD0048 (279) were identified as potent inhibitors of the transcription activation complex (Figure 7).

6. Concluding Remarks

Nature is an inexhaustible source of biologically interesting molecules that have benefitted humanity from its use as herbal medicine to isolation, characterization, and further synthetic manipulation of active ingredients. The biologically active martinella alkaloids in one such example. The chiral core structure found in the alkaloids, namely the hexahydropyrrolo-[3,2-*c*]-quinoline scaffold, has been an attractive synthetic target since its discovery in 1995. Exploration of the chemically diverse routes to this scaffold has laid the foundation for further elaboration of its potential medicinal benefits, aided by library syntheses and biological screening. As demonstrated by the Lawrence group, synthetic preparation of natural alkaloids also serves to control and revise the characterized structure of isolated natural products.

Though an excessive assembly of synthetic pathways towards the pyrroloquinoline scaffold has been prepared, much is yet to be discovered. The high biological activity found in the examination of the Broad Institute's DoS Povarov library together with the limited number of biological assays of compounds assembled around the pyrroloquinoline structure shows that this scaffold is still an underexplored source for biologically active compounds. For further exploration of the chemical utility of this scaffold, systematic approaches, such as library screens, are required. On the other hand, synthetically challenging compounds are usually excluded from such libraries and SAR-studies that delimit the selection of compounds to be synthesized follow certain rules, such as the Lipinski's rule of five. Therefore, fundamental curiosity-driven research is still needed for serendipitous discovery of compounds and their biological properties.

Author Contributions: Conceptualization: M.B.H. and M.O.S.; methodology: M.B.H. and M.O.S.; investigation: M.B.H.; resources: M.O.S.; data curation: M.B.H.; writing—Original draft preparation: M.B.H.; writing—Review and editing: M.B.H. and M.O.S.; supervision: M.O.S.; project administration: M.O.S.; funding acquisition: M.O.S. All authors have read and agreed to the published version of the manuscript.

Funding: This research was funded by the ToppForsk program at University of Stavanger.

Data Availability Statement: Supporting data for our results can be obtained by contacting the corresponding author.

Acknowledgments: Bjarte Holmelid, University of Bergen, is thanked for recording HRMS.

Conflicts of Interest: The authors declare no conflict of interest.

References

1. Guo, L.-D.; Chen, Y.; Xu, J. Total Synthesis of Daphniphyllum Alkaloids: From Bicycles to Diversified Caged Structures. *Acc. Chem. Res.* **2020**, *53*, 7390–7394. [[CrossRef](#)]
2. Baudoin, O. Multiple Catalytic C–H Bond Functionalization for Natural Product Synthesis. *Angew. Chem. Int. Ed.* **2020**, *59*, 17798–17809. [[CrossRef](#)]
3. Frontier, A.J.; Hernandez, J.J. New Twists in Nazarov Cyclization Chemistry. *Acc. Chem. Res.* **2020**, *53*, 1822–1832. [[CrossRef](#)] [[PubMed](#)]
4. Que, Y.; He, H. Advances in N-Heterocyclic Carbene Catalysis for Natural Product Synthesis. *Eur. J. Org. Chem.* **2020**, *2020*, 5917–5925. [[CrossRef](#)]
5. Mandal, S.; Thirupathi, B. Strategies for the construction of γ -spirocyclic butenolides in natural product synthesis. *Org. Biomol. Chem.* **2020**, *18*, 5287–5314. [[CrossRef](#)] [[PubMed](#)]
6. Zhang, Z.; Zhou, Y.-J.; Liang, X.-W. Total synthesis of natural products using photocycloaddition reactions of arenes. *Org. Biomol. Chem.* **2020**, *18*, 5558–5566. [[CrossRef](#)] [[PubMed](#)]
7. Kalita, S.J.; Cheng, F.; Huang, Y.Y. Recent advances of applying boron-reagents in asymmetric total syntheses of natural products and bio-active molecules. *Adv. Synth. Catal.* **2020**, *362*, 2778–2800. [[CrossRef](#)]

8. Fernandes, R.A.; Kumar, P.; Choudhary, P. Advances in catalytic and protecting-group-free total synthesis of natural products: A recent update. *Chem. Commun.* **2020**, *56*, 8569–8590. [[CrossRef](#)]
9. Hu, Y.-J.; Li, L.-X.; Han, J.-C.; Min, L.; Li, C.-C. Recent Advances in the Total Synthesis of Natural Products Containing Eight-Membered Carbocycles (2009–2019). *Chem. Rev.* **2020**, *120*, 5910–5953. [[CrossRef](#)]
10. Cragg, G.M.; Newman, D.J.; Snader, K.M. Natural Products in Drug Discovery and Development. *J. Nat. Prod.* **1997**, *60*, 52–60. [[CrossRef](#)]
11. Newman, D.J.; Cragg, G.M.; Snader, K.M. The influence of natural products upon drug discovery. *Nat. Prod. Rep.* **2000**, *17*, 215–234. [[CrossRef](#)] [[PubMed](#)]
12. Newman, D.J.; Cragg, G.M. Natural product scaffolds as leads to drugs. *Future Med. Chem.* **2009**, *1*, 1415–1427. [[CrossRef](#)] [[PubMed](#)]
13. Newman, D.J.; Cragg, G.M. Natural Products as Sources of New Drugs over the Last 25 Years. *J. Nat. Prod.* **2007**, *70*, 461–477. [[CrossRef](#)] [[PubMed](#)]
14. Newman, D.J.; Cragg, G.M. Natural Products as Sources of New Drugs over the 30 Years from 1981 to 2010. *J. Nat. Prod.* **2012**, *75*, 311–335. [[CrossRef](#)] [[PubMed](#)]
15. Newman, D.J.; Cragg, G.M. Natural Products as Sources of New Drugs from 1981 to 2014. *J. Nat. Prod.* **2016**, *79*, 629–661. [[CrossRef](#)]
16. Newman, D.J.; Cragg, G.M. Natural products as sources of new drugs over the nearly four decades from 01/1981 to 09/2019. *J. Nat. Prod.* **2020**, *83*, 770–803. [[CrossRef](#)]
17. Lovering, F.; Bikker, J.; Humblet, C. Escape from Flatland: Increasing Saturation as an Approach to Improving Clinical Success. *J. Med. Chem.* **2009**, *52*, 6752–6756. [[CrossRef](#)]
18. Monteleone, S.; Fuchs, J.E.; Liedl, K.R. Molecular connectivity predefines polypharmacology: Aliphatic rings, chirality, and sp³ centers enhance target selectivity. *Front. Pharmacol.* **2017**, *8*, 552. [[CrossRef](#)]
19. Witherup, K.M.; Ransom, R.W.; Graham, A.C.; Bernard, A.M.; Salvatore, M.J.; Lumma, W.C.; Anderson, P.S.; Pitzenberger, S.M.; Varga, S.L. Martinelline and martinellie acid, novel G-protein linked receptor antagonists from the tropical plant *Martinella iquitosensis* (Bignoniaceae). *J. Am. Chem. Soc.* **1995**, *117*, 6682–6685. [[CrossRef](#)]
20. Elvis-Offiah, U.B.; Bafor, E.E.; Eze, G.I.; Igbinumwen, O.; Viegelmann, C.; Edrada-Ebel, R. In vivo investigation of female reproductive functions and parameters in nonpregnant mice models and mass spectrometric analysis of the methanol leaf extract of *Emilia Coccinea* (Sims) G Dons. *Physiol. Rep.* **2016**, *4*, e13047. [[CrossRef](#)]
21. Zulfiker, A.H.M.; Sohrabi, M.; Qi, J.; Matthews, B.; Wei, M.Q.; Grice, I.D. Multi-constituent identification in Australian cane toad skin extracts using high-performance liquid chromatography high-resolution tandem mass spectrometry. *J. Pharm. Biomed. Anal.* **2016**, *129*, 260–272. [[CrossRef](#)] [[PubMed](#)]
22. Abhimannue, A.P.; Mohan, M.C.; Kumar, B.P. Inhibition of Tumor Necrosis Factor- α and Interleukin-1 β Production in Lipopolysaccharide-Stimulated Monocytes by Methanolic Extract of *Elephantopus scaber* Linn and Identification of Bioactive Components. *Appl. Biochem. Biotechnol.* **2016**, *179*, 427–443. [[CrossRef](#)] [[PubMed](#)]
23. Gentry, A.H.; Cook, K. *Martinella* (Bignoniaceae): A widely used eye medicine of South America. *J. Ethnopharmacol.* **1984**, *11*, 337–343. [[CrossRef](#)]
24. Ogunlesi, M.; Okie, W.; Ademoye, M. Medicinal Plants Used in Treating Eye Infections in Nigeria. In *A Textbook of Medicinal Plants from Nigeria*; Odugbemi, T., Ed.; University of Lagos Press: Lagos, Nigeria, 2008; p. 305.
25. Shen, Y.H.; Su, Y.Q.; Tian, J.M.; Lin, S.; Li, H.L.; Tang, J.; Zhang, W.D. A Unique Indolo-[1,7]naphthyridine Alkaloid from *Incarvillea mairei* var. *grandiflora* (Wehrh.) Grierson. *Helv. Chim. Acta* **2010**, *93*, 2393–2396. [[CrossRef](#)]
26. Brown, P.D.; Willis, A.C.; Sherburn, M.S.; Lawrence, A.L. Total synthesis and structural revision of the alkaloid incargranine B. *Angew. Chem. Int. Ed.* **2013**, *52*, 13273–13275. [[CrossRef](#)]
27. Tan, D.; Chou, G.; Wang, Z. Three New Alkaloids from *Senecio scandens*. *Chem. Nat. Compd.* **2014**, *50*, 329–332. [[CrossRef](#)]
28. Wang, D.; Huang, L.; Chen, S. *Senecio scandens* Buch.-Ham.: A review on its ethnopharmacology, phytochemistry, pharmacology, and toxicity. *J. Ethnopharmacol.* **2013**, *149*, 1–23. [[CrossRef](#)]
29. Ma, D.; Xia, C.; Jiang, J.; Zhang, J.; Tang, W. Aromatic nucleophilic substitution or CuI-catalyzed coupling route to martinellie acid. *J. Org. Chem.* **2003**, *68*, 442–451. [[CrossRef](#)]
30. Ikeda, S.; Shibuya, M.; Iwabuchi, Y. Asymmetric total synthesis of martinelline and martinellie acid. *Chem. Commun.* **2007**, 504–506. [[CrossRef](#)]
31. Shirai, A.; Miyata, O.; Tohnai, N.; Miyata, M.; Procter, D.J.; Sucunza, D.; Naito, T. Total Synthesis of (–)-Martinellie Acid via Radical Addition–Cyclization–Elimination Reaction. *J. Org. Chem.* **2008**, *73*, 4464–4475. [[CrossRef](#)]
32. Davies, S.G.; Fletcher, A.M.; Lee, J.A.; Lorkin, T.J.; Roberts, P.M.; Thomson, J.E. A diastereodivergent strategy for the asymmetric syntheses of (–)-martinellie acid and (–)-4-epi-martinellie acid. *Tetrahedron* **2013**, *69*, 9779–9803. [[CrossRef](#)]
33. Nyerges, M. Construction of pyrrolo [3,2-c] quinolines: Recent advances in the synthesis of the martinelline alkaloids. *Heterocycles* **2004**, *63*, 1685–1712. [[CrossRef](#)]
34. Lovely, C.J.; Bararinarayana, V. Synthetic studies toward the *Martinella* alkaloids. *Curr. Org. Chem.* **2008**, *12*, 1431–1453. [[CrossRef](#)]
35. Eichholzer, J.V.; Lewis, I.A.; Macleod, J.K.; Oelrichs, P.B.; Valley, P.J. Galegine and a new dihydroxyalkylacetamide from *Verbesina enceloiodes*. *Phytochemistry* **1982**, *21*, 97–99. [[CrossRef](#)]

36. Reuter, G. Arginin als Vorstufe von Galegin in *Galega officinalis* L. Zur Biochemie und Physiologie von Galegin in *Galega officinalis* L., III. Mitt. *Arch. Pharm.* **1963**, *296*, 516–522. [[CrossRef](#)]
37. Ma, D.; Xia, C.; Jiang, J.; Zhang, J. First total synthesis of martinellid acid, a naturally occurring bradykinin receptor antagonist. *Org. Lett.* **2001**, *3*, 2189–2191. [[CrossRef](#)]
38. Powell, D.A.; Batey, R.A. Total synthesis of the alkaloids martinellid and martinellid acid via a hetero Diels–Alder multicomponent coupling reaction. *Org. Lett.* **2002**, *4*, 2913–2916. [[CrossRef](#)]
39. Xia, C.; Heng, L.; Ma, D. Total synthesis of (±)-martinellid. *Tetrahedron Lett.* **2002**, *43*, 9405–9409. [[CrossRef](#)]
40. Davies, S.G.; Fletcher, A.M.; Lee, J.A.; Lorkin, T.J.; Roberts, P.M.; Thomson, J.E. Asymmetric synthesis of (–)-martinellid acid. *Org. Lett.* **2013**, *15*, 2050–2053. [[CrossRef](#)]
41. Rong, Z.; Li, Q.; Lin, W.; Jia, Y. Reagent-free synthesis of 2,3,4-polysubstituted tetrahydroquinolines: Application to the formal synthesis of (±)-martinellid acid and martinellid. *Tetrahedron Lett.* **2013**, *54*, 4432–4434. [[CrossRef](#)]
42. Yoshitomi, Y.; Arai, H.; Makino, K.; Hamada, Y. Enantioselective synthesis of martinellid chiral core and its diastereomer using asymmetric tandem Michael–aldol reaction. *Tetrahedron* **2008**, *64*, 11568–11579. [[CrossRef](#)]
43. He, Y.; Mahmud, H.; Moningka, R.; Lovely, C.J.; Dias, H.R. Cyclization reactions of *N*-acryloyl-2-aminobenzaldehyde derivatives: Formal total synthesis of martinellid acid. *Tetrahedron* **2006**, *62*, 8755–8769. [[CrossRef](#)]
44. Hadden, M.; Nieuwenhuyzen, M.; Osborne, D.; Stevenson, P.J.; Thompson, N.; Walker, A.D. Synthesis of the heterocyclic core of martinellid and martinellid acid. *Tetrahedron* **2006**, *62*, 3977–3984. [[CrossRef](#)]
45. Snider, B.B.; Ahn, Y.; O’Hare, S.M. Total synthesis of (±)-martinellid acid. *Org. Lett.* **2001**, *3*, 4217–4220. [[CrossRef](#)] [[PubMed](#)]
46. Hadden, M.; Nieuwenhuyzen, M.; Osborne, D.; Stevenson, P.J.; Thompson, N. Synthesis of the heterocyclic core of the alkaloids martinellid and martinellid acid. *Tetrahedron Lett.* **2001**, *42*, 6417–6419. [[CrossRef](#)]
47. Batey, R.A.; Powell, D.A. Multi-component coupling reactions: Synthesis of a guanidine containing analog of the hexahydropyrrolo [3,2-*c*] quinoline alkaloid martinellid. *Chem. Commun.* **2001**, *22*, 2362–2363. [[CrossRef](#)]
48. Davies, S.G.; Ichihara, O.; Walters, I. Asymmetric-synthesis of syn-*a*-alkyl-*b*-amino acids. *J. Chem. Soc. Perkin Trans.* **1994**, *9*, 1141–1147. [[CrossRef](#)]
49. Li, H.; Wang, J.; Xie, H.; Zu, L.; Jiang, W.; Duesler, E.N.; Wang, W. Chiral Diphenylprolinol TES Ether Promoted Conjugate Addition–Aldol-Dehydration Reactions between α , β -Unsaturated Aldehydes and 2-*N*-Protected Amino Benzaldehydes. *Org. Lett.* **2007**, *9*, 965–968. [[CrossRef](#)]
50. Hara, O.; Sugimoto, K.; Makino, K.; Hamada, Y. New synthesis of a pyrroloquinoline skeleton, the martinellid core, using a tandem Michael-aldol strategy. *Synlett* **2004**, *2004*, 1625–1627.
51. Pappoppula, M.; Aponick, A. Enantioselective Total Synthesis of (–)-Martinellid Acid. *Angew. Chem. Int. Ed.* **2015**, *54*, 15827–15830. [[CrossRef](#)]
52. Lackey, K.E. Compounds and Methods of Treatment. U.S. Patent 20080234267A1, 25 September 2008.
53. Behenna, D.C.; Stoltz, B.M. The enantioselective Tsuji allylation. *J. Am. Chem. Soc.* **2004**, *126*, 15044–15045. [[CrossRef](#)] [[PubMed](#)]
54. Ueda, M.; Kawai, S.; Hayashi, M.; Naito, T.; Miyata, O. Efficient entry into 2-substituted tetrahydroquinoline systems through alkylative ring expansion: Stereoselective formal synthesis of (±)-martinellid acid. *J. Org. Chem.* **2010**, *75*, 914–921. [[CrossRef](#)] [[PubMed](#)]
55. Batey, R.; Simoncic, P.; Smyj, R.; Lough, A. A three-component coupling protocol for the synthesis of substituted hexahydropyrrolo [3,2-*c*] quinolines. *Chem. Commun.* **1999**, *7*, 651–652. [[CrossRef](#)]
56. Kouznetsov, V.V. Recent synthetic developments in a powerful imino Diels-Alder reaction (Povarov reaction): Application to the synthesis of *N*-polyheterocycles and related alkaloids. *Tetrahedron* **2009**, *65*, 2721–2750. [[CrossRef](#)]
57. Fochi, M.; Caruana, L.; Bernardi, L. Catalytic asymmetric aza-Diels–Alder reactions: The Povarov cycloaddition reaction. *Synthesis* **2014**, *46*, 135–157. [[CrossRef](#)]
58. Hadden, M.; Stevenson, P.J. Regioselective synthesis of pyrroloquinolines—Approaches to Martinellid. *Tetrahedron Lett.* **1999**, *40*, 1215–1218. [[CrossRef](#)]
59. He, L.; Liu, H.-B.; Zhao, L.; Wang, D.-X.; Wang, M.-X. Lewis acid-catalyzed reaction between tertiary enamides and imines of salicylaldehydes: Expedient synthesis of novel 4-chromanamine derivatives. *Tetrahedron* **2015**, *71*, 523–531. [[CrossRef](#)]
60. Yu, J.; Jiang, H.-J.; Zhou, Y.; Luo, S.-W.; Gong, L.-Z. Sodium Salts of Anionic Chiral Cobalt(III) Complexes as Catalysts of the Enantioselective Povarov Reaction. *Angew. Chem. Int. Ed.* **2015**, *54*, 11209–11213. [[CrossRef](#)]
61. Liu, X.; Toy, P.H. Halogen Bond-Catalyzed Povarov Reactions. *Adv. Synth. Catal.* **2020**, *362*, 3437–3441. [[CrossRef](#)]
62. Reyes-Gutiérrez, P.E.; Amatov, T.T.; Švec, P.; Čisarová, I.; Šaman, D.; Pohl, R.; Teplý, F.; Pospíšil, L. Helquats as Promoters of the Povarov Reaction: Synthesis of 1,2,3,4-Tetrahydroquinoline Scaffolds Catalyzed by Helicene-Viologen Hybrids. *ChemPlusChem* **2020**, *85*, 2212–2218. [[CrossRef](#)]
63. Škopić, M.K.; Götte, K.; Gramse, C.; Dieter, M.; Pospich, S.; Raunser, S.; Weberskirch, R.; Brunschweiger, A. Micellar Brønsted Acid Mediated Synthesis of DNA-Tagged Heterocycles. *J. Am. Chem. Soc.* **2019**, *141*, 10546–10555. [[CrossRef](#)] [[PubMed](#)]
64. Xu, H.; Zuend, S.J.; Woll, M.G.; Tao, Y.; Jacobsen, E.N. Asymmetric Cooperative Catalysis of Strong Brønsted Acid–Promoted Reactions Using Chiral Ureas. *Science* **2010**, *327*, 986–990. [[CrossRef](#)] [[PubMed](#)]
65. Gerard, B.; O’Shea, M.W.; Donckele, E.; Kesavan, S.; Akella, L.B.; Xu, H.; Jacobsen, E.N.; Marcaurelle, L.A. Application of a catalytic asymmetric Povarov reaction using chiral ureas to the synthesis of a tetrahydroquinoline library. *ACS Comb. Sci.* **2012**, *14*, 621–630. [[CrossRef](#)]

66. Kinzel, T.; Zhang, Y.; Buchwald, S.L. A new palladium precatalyst allows for the fast Suzuki–Miyaura coupling reactions of unstable polyfluorophenyl and 2-heteroaryl boronic acids. *J. Am. Chem. Soc.* **2010**, *132*, 14073–14075. [[CrossRef](#)] [[PubMed](#)]
67. Lei, B.-L.; Ding, C.-H.; Yang, X.-F.; Wan, X.-L.; Hou, X.-L. Kinetic resolution of 2, 3-dihydro-2-substituted 4-quinolones by palladium-catalyzed asymmetric allylic alkylation. *J. Am. Chem. Soc.* **2009**, *131*, 18250–18251. [[CrossRef](#)]
68. Gigant, N.; Gillaizeau, I. Construction of nitrogen-fused tetrahydroquinolines via a domino reaction. *Org. Lett.* **2012**, *14*, 4622–4625. [[CrossRef](#)]
69. Song, Z.; Zhao, Y.-M.; Zhai, H. One-Step Construction of Tetrahydro-5 H-indolo [3,2-c] quinolines from Benzyl Azides and Indoles via a Cascade Reaction Sequence. *Org. Lett.* **2011**, *13*, 6331–6333. [[CrossRef](#)]
70. Desai, P.; Schildknegt, K.; Agrios, K.A.; Mossman, C.; Milligan, G.L.; Aube, J. Reactions of alkyl azides and ketones as mediated by Lewis acids: Schmidt and Mannich reactions using azide precursors. *J. Am. Chem. Soc.* **2000**, *122*, 7226–7232. [[CrossRef](#)]
71. Dagousset, G.; Retailleau, P.; Masson, G.; Zhu, J. Chiral phosphoric acid-catalyzed enantioselective three-component Povarov reaction using cyclic enethiouras as dienophiles: Stereocontrolled access to enantioenriched hexahydropyrroloquinolines. *Chem. Eur. J.* **2012**, *18*, 5869–5873. [[CrossRef](#)]
72. Roy, S.; Reiser, O. A Catalytic Multicomponent Approach for the Stereoselective Synthesis of cis-4,5-Disubstituted Pyrrolidinones and Tetrahydro-3H-pyrrolo[3,2-c]quinolines. *Angew. Chem. Int. Ed.* **2012**, *51*, 4722–4725. [[CrossRef](#)]
73. Wood, J.; Bagi, C.M.; Akuiche, C.; Bacchicocchi, A.; Baryza, J.; Blue, M.-L.; Brennan, C.; Campbell, A.-M.; Choi, S.; Cook, J.H.; et al. 4,5-Disubstituted cis-pyrrolidinones as inhibitors of type II 17 β -hydroxysteroid dehydrogenase. Part 3. Identification of lead candidate. *Bioorg. Med. Chem. Lett.* **2006**, *16*, 4965–4968. [[CrossRef](#)] [[PubMed](#)]
74. Hu, J.; Hirao, H.; Li, Y.; Zhou, J. Palladium-Catalyzed Asymmetric Intermolecular Cyclization. *Angew. Chem. Int. Ed.* **2013**, *52*, 8676–8680. [[CrossRef](#)] [[PubMed](#)]
75. Comesse, S.; Sanselme, M.; Daïch, A. New and expeditious tandem sequence aza-Michael/intramolecular nucleophilic substitution route to substituted γ -lactams: Synthesis of the tricyclic core of (\pm)-Martinellines. *J. Org. Chem.* **2008**, *73*, 5566–5569. [[CrossRef](#)] [[PubMed](#)]
76. Le Goff, R.; Lawson, A.M.; Daïch, A.; Comesse, S. Synthesis of highly functionalized pyrrolidines as tunable templates for the direct access to (\pm)-coerulescine and the tricyclic core of martinellines. *Org. Biomol. Chem.* **2013**, *11*, 1818–1821. [[CrossRef](#)]
77. Sun, M.; Zhang, T.; Bao, W. FeCl₃-Catalyzed Cascade Cyclization in One Pot: Synthesis of Ring-Fused Tetrahydroquinoline Derivatives from Arylamines and N-Substituted Lactams. *J. Org. Chem.* **2013**, *78*, 8155–8160. [[CrossRef](#)]
78. Yang, M.; Su, B.; Wang, Y.; Chen, K.; Jiang, X.; Zhang, Y.-F.; Zhang, X.-S.; Chen, G.; Cheng, Y.; Cao, Z.; et al. Silver-catalysed direct amination of unactivated C–H bonds of functionalized molecules. *Nat. Commun.* **2014**, *5*, 4707. [[CrossRef](#)]
79. Yang, Y.-J.; Zhang, H.-R.; Zhu, S.-Y.; Zhu, P.; Hui, X.-P. Highly stereoselective synthesis of functionalized pyrrolo [3, 2-c] quinolines via N-heterocyclic carbene catalyzed cascade sequence. *Org. Lett.* **2014**, *16*, 5048–5051. [[CrossRef](#)]
80. Wang, J.; Li, Y.; Sun, J.; Wang, H.; Jin, Z.; Chi, Y.R. Carbene-Catalyzed Enantioselective Addition of Benzylic Carbon to Unsaturated Acyl Azolium for Rapid Synthesis of Pyrrolo[3,2-c]quinolines. *ACS Catal.* **2018**, *8*, 9859–9864. [[CrossRef](#)]
81. Boomhoff, M.; Yadav, A.K.; Appun, J.; Schneider, C. Modular, flexible, and stereoselective synthesis of pyrroloquinolines: Rapid assembly of complex heterocyclic scaffolds. *Org. Lett.* **2014**, *16*, 6236–6239. [[CrossRef](#)]
82. Appun, J.; Stolz, F.; Naumov, S.; Abel, B.; Schneider, C. Modular Synthesis of Dipyrroloquinolines: A Combined Synthetic and Mechanistic Study. *J. Org. Chem.* **2018**, *83*, 1737–1744. [[CrossRef](#)]
83. Bakthadoss, M.; Kannan, D.; Srinivasan, J.; Vinayagam, V. Highly regio- and diastereo-selective synthesis of novel tri- and tetra-cyclic perhydroquinoline architectures via an intramolecular [3+2] cycloaddition reaction. *Org. Biomol. Chem.* **2015**, *13*, 2870–2874. [[CrossRef](#)] [[PubMed](#)]
84. Xiao, J.-A.; Li, J.; Xia, P.-J.; Zhou, Z.-F.; Deng, Z.-X.; Xiang, H.-Y.; Chen, X.-Q.; Yang, H. Diastereoselective Intramolecular [3+2]-Annulation of Donor–Acceptor Cyclopropane with Imine-Assembling Hexahydropyrrolo [3,2-c] quinolinone Scaffolds. *J. Org. Chem.* **2016**, *81*, 11185–11194. [[CrossRef](#)] [[PubMed](#)]
85. Pavlova, A.S.; Ivanova, O.A.; Chagarovskiy, A.O.; Stebunov, N.S.; Orlov, N.V.; Shumsky, A.N.; Budynina, E.M.; Rybakov, V.B.; Trushkov, I.V. Domino Staudinger/aza-Wittig/Mannich Reaction: An Approach to Diversity of Di- and Tetrahydropyrrole Scaffolds. *Chem. Eur. J.* **2016**, *22*, 17967–17971. [[CrossRef](#)] [[PubMed](#)]
86. Ivanov, K.L.; Villemson, E.V.; Budynina, E.M.; Ivanova, O.A.; Trushkov, I.V.; Melnikov, M.Y. Ring Opening of Donor–Acceptor Cyclopropanes with the Azide Ion: A Tool for Construction of N-Heterocycles. *Chem. Eur. J.* **2015**, *21*, 4975–4987. [[CrossRef](#)] [[PubMed](#)]
87. Wang, H.; Wang, C.; Huang, K.; Liu, L.; Chang, W.; Li, J. Copper-catalyzed cascade reaction via intramolecular hydroamination cyclization of homopropargylic amines and intermolecular Povarov reaction with imines. *Org. Lett.* **2016**, *18*, 2367–2370. [[CrossRef](#)]
88. Liu, L.; Wang, C.; Liu, Q.; Kong, Y.; Chang, W.; Li, J. Copper (II) Trifluoromethanesulfonate Catalyzed Hydroamination Cyclization–Dimerization Cascade Reaction of Homopropargylic Amines for the Construction of Complex Fused Nitrogen-Containing Tetracycles. *Eur. J. Org. Chem.* **2016**, *2016*, 3684–3690. [[CrossRef](#)]
89. Li, J.; Lin, N.; Yu, L.; Zhang, Y. Synthesis of β -prolinols via [3+2] cycloaddition and one-pot programmed reduction: Valuable building blocks for polyheterocycles. *Tetrahedron Lett.* **2016**, *57*, 5777–5780. [[CrossRef](#)]
90. Xie, H.; Gong, B.; Zhong, X.; Cui, H.; Xiang, J. Intramolecular Cycloaddition of Azomethine Ylides Activated by Aromatic Rings: Scope and Limitations. *Chem. Heterocyclic Comp.* **2016**, *52*, 484–492. [[CrossRef](#)]

91. Cai, J.; Li, F.; Deng, G.-J.; Ji, X.; Huang, H. The cyclopropylimine rearrangement/Povarov reaction cascade for the assembly of pyrrolo [3, 2-c] quinoline derivatives. *Green Chem.* **2016**, *18*, 3503–3506. [[CrossRef](#)]
92. Kondo, Y.; Nishikimi, Y. Process for Production of Optically Active Hexahydropyrroloquinoline and Intermediate for the Process. U.S. Patents WO 2010038434, 8 April 2010.
93. Tatsuta, K.; Kondo, Y. Process for Preparation of Hexahydropyrroloquinoline. U.S. Patents JP 2011256110A, 30 September 2011.
94. Yamada, M.; Usutani, H.; Ito, T.; Yamano, M. Construction of a (3aR, 4R, 9bR)-Hexahydropyrrolo-quinoline by Stereoselective Hydrogen-Mediated Domino Cyclization. *Org. Process Res. Dev.* **2019**, *23*, 535–547. [[CrossRef](#)]
95. Lindbäck, E.; Sydnes, M.O. Catalytic Enantioselective Synthesis of the Partially Reduced Tricyclic Pyrrolo [3,2-c] quinoline Core Structure of the Martinella Alkaloids. *ChemistrySelect* **2016**, *1*, 1837–1840. [[CrossRef](#)]
96. Kolb, H.C.; Andersson, P.G.; Sharpless, K.B. Toward an understanding of the high enantioselectivity in the osmium-catalyzed asymmetric dihydroxylation (AD). 1. Kinetics. *J. Am. Chem. Soc.* **1994**, *116*, 1278–1291. [[CrossRef](#)]
97. Reddy, J.S.; Rao, B.V. A short, efficient, and stereoselective total synthesis of a pyrrolidine alkaloid: (–)-codonopsinine. *J. Org. Chem.* **2007**, *72*, 2224–2227. [[CrossRef](#)] [[PubMed](#)]
98. Haarr, M.B.; Sydnes, M.O. Synthetic approach towards the martinella alkaloids. Unpublished work, 2020.
99. Wittig, G.; Sommer, H. Zum Verhalten ungesättigter Ammoniumsälze gegenüber Protonenacceptoren. *Justus Liebigs Ann. Chem.* **1955**, *594*, 1–14. [[CrossRef](#)]
100. Swan, G.A.; Wilcock, J.D. Reduction of some *N*-alkyl- and *N*-aryl-pyrrolidin-2-ones and-piperidin-2-ones by lithium aluminium hydride. *J. Chem. Soc. Perkin Trans.* **1974**, 885–891. [[CrossRef](#)]
101. Kerr, G.H.; Meth-Cohn, O.; Mullock, E.B.; Suschitzky, H. Reactions of *NN*-dialkylanilines with diethyl azodicarboxylate and with ozone. *J. Chem. Soc. Perkin Trans.* **1974**, 1614–1619. [[CrossRef](#)]
102. Khandelwal, G.D.; Swan, G.A.; Roy, R.B. Dehydrogenation of some aromatic tertiary amines by gamma radiation and by peroxides. *J. Chem. Soc. Perkin Trans.* **1974**, 891–896. [[CrossRef](#)]
103. Rao, G.A.; Periasamy, M. Cycloaddition of enamine and iminium ion intermediates formed in the reaction of *N*-arylpiperidines with T-HYDRO. *Synlett* **2015**, *26*, 2231–2236. [[CrossRef](#)]
104. Minakata, S.; Ohshima, Y.; Takemiya, A.; Ryu, I.; Komatsu, M.; Ohshiro, Y. Catalytic oxidation of amines utilizing binuclear copper (II) complex of 7-azaindole. *Chem. Lett.* **1997**, *26*, 311–312. [[CrossRef](#)]
105. Buswell, M.; Fleming, I. The reaction of phenyldimethylsilyllithium with *N*-phenylpyrrolidone. *Chem. Commun.* **2003**, 202–203. [[CrossRef](#)] [[PubMed](#)]
106. Min, C.; Sanchawala, A.; Seidel, D. Dual C–H Functionalization of *N*-Aryl Amines: Synthesis of Polycyclic Amines via an Oxidative Povarov Approach. *Org. Lett.* **2014**, *16*, 2756–2759. [[CrossRef](#)] [[PubMed](#)]
107. Ma, Y.; Yao, X.; Zhang, L.; Ni, P.; Cheng, R.; Ye, J. Direct Arylation of α -Amino C(sp³)-H Bonds by Convergent Paired Electrolysis. *Angew. Chem. Int. Ed.* **2019**, *58*, 16548–16552. [[CrossRef](#)] [[PubMed](#)]
108. Jia, Z.; Yang, Q.; Zhang, L.; Luo, S. Photoredox Mediated Acceptorless Dehydrogenative Coupling of Saturated *N*-Heterocycles. *ACS Catal.* **2019**, *9*, 3589–3594. [[CrossRef](#)]
109. Wang, L.; Liu, L.; Chang, W.; Li, J. The Divergent Cascade Reactions of Arylalkynols with Homopropargylic Amines or Electron-Deficient Olefins: Access to the Spiro-Isobenzofuran-b-pyrrolo-quinolines or Bridged-Isobenzofuran Polycycles. *J. Org. Chem.* **2018**, *83*, 7799–7813. [[CrossRef](#)] [[PubMed](#)]
110. Xu, G.-Q.; Xu, J.-T.; Feng, Z.-T.; Liang, H.; Wang, Z.-Y.; Qin, Y.; Xu, P.-F. Dual C(sp³)-H Bond Functionalization of *N*-Heterocycles through Sequential Visible-Light Photocatalyzed Dehydrogenation/ [2+2] Cycloaddition Reactions. *Angew. Chem. Int. Ed.* **2018**, *57*, 5110–5114. [[CrossRef](#)]
111. Kong, Y.; Liu, Y.; Wang, B.; Li, S.; Liu, L.; Chang, W.; Li, J. The Catalyst-Controlled Divergent Cascade Reactions of Homopropargylic Amines and Nitrones: Synthesis of Pyrrolo-Isloxazolidines and γ -Lactams. *Adv. Synth. Catal.* **2018**, *360*, 1240–1252. [[CrossRef](#)]
112. Wang, F.; He, Y.; Tian, M.; Zhang, X.; Fan, X. Synthesis of α -Formylated *N*-Heterocycles and Their 1,1-Diacetates from Inactivated Cyclic Amines Involving an Oxidative Ring Contraction. *Org. Lett.* **2018**, *20*, 864–867. [[CrossRef](#)]
113. Snider, B.B.; Ahn, Y.; Foxman, B.M. Synthesis of the tricyclic triamine core of martinelline and martinellinic acid. *Tetrahedron Lett.* **1999**, *40*, 3339–3342. [[CrossRef](#)]
114. Fustero, S.; Bello, P.; Miró, J.; Sánchez-Roselló, M.; Maestro, M.A.; Gonzalez, J.; del Pozo, C. Gold catalyzed stereoselective tandem hydroamination–formal aza-Diels–Alder reaction of propargylic amino esters. *Chem. Commun.* **2013**, *49*, 1336–1338. [[CrossRef](#)]
115. Ma, C.-L.; Li, X.-H.; Yu, X.-L.; Zhu, X.-L.; Hu, Y.-Z.; Dong, X.-W.; Tan, B.; Liu, X.-Y. Gold-catalyzed tandem synthesis of bioactive spiro-dipyrroloquinolines and its application in the one-step synthesis of incargranine B aglycone and seneciobipyrrolidine (I). *Org. Chem. Front.* **2016**, *3*, 324–329. [[CrossRef](#)]
116. Yu, X.-L.; Kuang, L.; Chen, S.; Zhu, X.-L.; Li, Z.-L.; Tan, B.; Liu, X.-Y. Counteranion-controlled unprecedented diastereo- and enantioselective tandem formal Povarov reaction for construction of bioactive octahydro-dipyrroloquinolines. *ACS Catal.* **2016**, *6*, 6182–6190. [[CrossRef](#)]
117. Li, S.-S.; Zhou, L.; Wang, L.; Zhao, H.; Yu, L.; Xiao, J. Organocatalytic C (sp³)-H functionalization via carbocation-initiated cascade [1,5]-hydride transfer/cyclization: Synthesis of dihydrodibenzo [b,e] azepines. *Org. Lett.* **2018**, *20*, 138–141. [[CrossRef](#)] [[PubMed](#)]
118. Shi, L.; Wang, M.; Pan, L.; Li, Y.; Liu, Q. Csp³-H bond functionalization of amines via tunable iminium ions: Divergent synthesis of trifluoromethylated arylamines. *Chem. Commun.* **2018**, *54*, 8721–8724. [[CrossRef](#)] [[PubMed](#)]

119. Kajino, M.; Hird, N.W.; Tarui, N.; Banno, H.; Kawano, Y.; Inatomi, N. Preparation of Fused Quinoline Derivatives as NK2 Receptor Antagonists for Functional Gastrointestinal Diseases. U.S. Patent WO 2005105802, 10 November 2005.
120. Tanaka, T.; Matsumoto-Okano, S.; Inatomi, N.; Fujioka, Y.; Kamiguchi, H.; Yamaguchi, M.; Imanishi, A.; Kawamoto, M.; Miura, K.; Nishikawa, Y. Establishment and validation of a rabbit model for in vivo pharmacodynamic screening of tachykinin NK2 antagonists. *J. Pharmacol. Sci.* **2012**, *118*, 487–495. [[CrossRef](#)]
121. Tanaka, T.; Tanaka, A.; Nakamura, A.; Matsushita, K.; Imanishi, A.; Matsumoto-Okano, S.; Inatomi, N.; Miura, K.; Toyoda, M.; Mizojiri, G. Effects of TAK-480, a Novel Tachykinin NK2-Receptor Antagonist, on Visceral Hypersensitivity in Rabbits and Ricinoleic Acid-Induced Defecation in Guinea Pigs. *J. Pharmacol. Sci.* **2012**, *120*, 15–25. [[CrossRef](#)]
122. Kajiwara, T.; Konishi, T.; Yamano, M. Asymmetric catalytic hydrogenation for large scale preparation of optically active 2-(N-benzoylamino) cyclohexanecarboxylic acid derivatives. *Catal. Sci. Technol.* **2012**, *2*, 2146–2152. [[CrossRef](#)]
123. Furuya, K.; Yamamoto, N.; Ohyabu, Y.; Makino, A.; Morikyu, T.; Ishige, H.; Kuzutani, K.; Endo, Y. The Novel Non-steroidal Selective Androgen Receptor Modulator S-101479 Has Additive Effects with Bisphosphonate, Selective Estrogen Receptor Modulator, and Parathyroid Hormone on the Bones of Osteoporotic Female Rats. *Biol. Pharm. Bull.* **2012**, *35*, 1096–1104. [[CrossRef](#)]
124. Furuya, K.; Yamamoto, N.; Ohyabu, Y.; Morikyu, T.; Ishige, H.; Albers, M.; Endo, Y. Mechanism of the tissue-specific action of the selective androgen receptor modulator S-101479. *Biol. Pharm. Bull.* **2013**, *36*, 442–451. [[CrossRef](#)]
125. Duvall, J.R.; Bedard, L.; Naylor-Olsen, A.M.; Manson, A.L.; Bittker, J.A.; Sun, W.; Fitzgerald, M.E.; He, Z.; Lee, M.D., IV; Marie, J.-C.; et al. Identification of highly specific diversity-oriented synthesis-derived inhibitors of *Clostridium difficile*. *ACS Infect. Dis.* **2017**, *3*, 349–359. [[CrossRef](#)]
126. Prosser, G.A.; Rodenburg, A.; Khoury, H.; de Chiara, C.; Howell, S.; Snijders, A.P.; de Carvalho, L.P.S. Glutamate racemase is the primary target of β -chloro-D-alanine in *Mycobacterium tuberculosis*. *Antimicrob. Agents Chemother.* **2016**, *60*, 6091–6099. [[CrossRef](#)] [[PubMed](#)]
127. Geng, B.; Basarab, G.; Comita-Prevoir, J.; Gowravaram, M.; Hill, P.; Kiely, A.; Loch, J.; MacPherson, L.; Morningstar, M.; Mullen, G. Potent and selective inhibitors of *Helicobacter pylori* glutamate racemase (MurI): Pyridodiazepine amines. *Bioorg. Med. Chem. Lett.* **2009**, *19*, 930–936. [[CrossRef](#)] [[PubMed](#)]
128. Lundqvist, T.; Fisher, S.L.; Kern, G.; Folmer, R.H.; Xue, Y.; Newton, D.T.; Keating, T.A.; Alm, R.A.; de Jonge, B.L. Exploitation of structural and regulatory diversity in glutamate racemases. *Nature* **2007**, *447*, 817–822. [[CrossRef](#)]
129. Park, S.W.; Casalena, D.E.; Wilson, D.J.; Dai, R.; Nag, P.P.; Liu, F.; Boyce, J.P.; Bittker, J.A.; Schreiber, S.L.; Finzel, B.C. Target-based identification of whole-cell active inhibitors of biotin biosynthesis in *Mycobacterium tuberculosis*. *Chem. Biol.* **2015**, *22*, 76–86. [[CrossRef](#)] [[PubMed](#)]
130. Maji, B.; Gangopadhyay, S.A.; Lee, M.; Shi, M.; Wu, P.; Heler, R.; Mok, B.; Lim, D.; Siriwardena, S.U.; Paul, B. A high-throughput platform to identify small-molecule inhibitors of CRISPR-Cas9. *Cell* **2019**, *177*, 1067–1079. [[CrossRef](#)]
131. Choudhary, A.; Fox, K.; Subramanian, H.; Franco, E. Compositions and Methods for Regulating Proteins and Nucleic Acids Activities. U.S. Patent 20200239879A1, 30 July 2020.
132. Choudhary, A.; Maji, B.; Gangopadhyay, S.A.; Lee, M.; Shi, M. Inhibitors of RNA-Guided Nuclease Target Binding and Uses Thereof. U.S. Patent WO 2020068304, 2 April 2020.

Paper III

Functionalized D- and L-Arabino-Pyrrolidines as Potent and Selective Glycosidase Inhibitors

*Marianne B. Haarr, Óscar López, José G. Fernández-Bolanõs, Emil
Lindbäck, and Magne O. Sydnes*

Manuscript in progress